Clinical Periodontology and Implant Dentistry

Fifth Edition

Edited by

Jan Lindhe
Niklaus P. Lang
Thorkild Karring

Associate Editors
Tord Berglundh
William V. Giannobile
Mariano Sanz

Blackwell
Munksgaard

HIGH DENT

PRODUCTS SERVICES TRAINING

همیار دندانسازان و دندانپزشکان در پروتز

مرکز تخصصی پروتزهای دندانی

های دنت

طراحی و ساخت انواع پروتزهای دندانی بویژه ایمپلنت

برگزار کننده دوره های آموزشی تخصصی وجامع دندانسازی و...

با ما همراه باشید...

WWW.HIGHDENT.IR

@highdent

@highdent

Volume 1
BASIC CONCEPTS

Edited by

Jan Lindhe
Niklaus P. Lang
Thorkild Karring

Blackwell Publishing editorial offices:
Blackwell Publishing Ltd, 9600 Garsington Road, Oxford OX4 2DQ, UK
Tel: +44 (0)1865 776868
Blackwell Publishing Professional, 2121 State Avenue, Ames, Iowa 50014-8300, USA
Tel: +1 515 292 0140
Blackwell Publishing Asia Pty Ltd, 550 Swanston Street, Carlton, Victoria 3053, Australia
Tel: +61 (0)3 8359 1011

First published 1983 by Munksgaard
Second edition published 1989
Third edition published 1997
Fourth edition published by Blackwell Munksgaard 2003
Reprinted 2003, 2005, 2006
Fifth edition 2008 by Blackwell Publishing Ltd

ISBN: 978-1-4051-6099-5

Library of Congress Cataloging-in-Publication Data
Clinical periodontology and implant dentistry / edited by Jan Lindhe,
Niklaus P. Lang, Thorkild Karring. — 5th ed.
p. ; cm.
Includes bibliographical references and index.
ISBN: 978-1-4051-6099-5 (hardback : alk. paper)
1. Periodontics. 2. Periodontal disease. 3. Dental implants. I. Lindhe, Jan.
II. Lang, Niklaus Peter. III. Karring, Thorkild.
[DNLM: 1. Periodontal Diseases. 2. Dental Implantation. 3. Dental Implants.
WU 240 C6415 2008]
RK361.C54 2008
617.6′32—dc22
2007037124

A catalogue record for this title is available from the British Library

Set in 9.5/12 pt Palatino by SNP Best-set Typesetter Ltd., Hong Kong
Printed and bound in Singapore by C.O.S. Printers Pte Ltd

The publisher's policy is to use permanent paper from mills that operate a sustainable forestry policy, and which has been manufactured from pulp processed using acid-free and elementary chlorine-free practices. Furthermore, the publisher ensures that the text paper and cover board used have met acceptable environmental accreditation standards.

For further information on Blackwell Publishing, visit our website:
www.blackwellmunksgaard.com

Contents

Part 4: Host–Parasite Interactions

Part 5: Trauma from Occlusion

Part 6: Periodontal Pathology

Part 7: Peri-implant Pathology

Part 8: Tissue Regeneration

Volume 2: CLINICAL CONCEPTS

Editors: Niklaus P. Lang and Jan Lindhe

Part 9: Examination Protocols

Part 18: Supportive Care

Part 19: Halitosis

Contributors

Martin Addy
Division of Restorative Dentistry (Periodontology)
Department of Oral and Dental Science
Bristol Dental School and Hospital
Bristol
UK

Maurício Araújo
Department of Dentistry
State University of Maringá
Maringá
Paraná
Brazil

Gary C. Armitage
Division of Periodontology
School of Dentistry
University of California San Francisco
San Francisco
CA
USA

Rolf Attström
Department of Periodontology
Centre for Oral Health Sciences
Malmö University
Malmö
Sweden

Robert A. Bagramian
Department of Periodontics and Oral Medicine
University of Michigan School of Dentistry
Ann Arbor
MI
USA

Hans-Rudolf Baur
Department of Internal Medicine
Spital Bern Tiefenau
Berne
Switzerland

Urs C. Belser
Department of Prosthetic Dentistry
School of Dental Medicine
University of Geneva
Geneva
Switzerland

Gunnar Bergenholtz
Department of Endodontology
Institute of Odontology
The Sahlgrenska Academy at Göteborg University
Göteborg
Sweden

Tord Berglundh
Department of Periodontology
Institute of Odontology
The Sahlgrenska Academy at Göteborg University
Göteborg
Sweden

Jean-Pierre Bernard
Department of Oral Surgery and Stomatology
School of Dental Medicine
University of Geneva
Geneva
Switzerland

Urs Brägger
Department of Periodontology and Fixed Prosthodontics
School of Dental Medicine
University of Berne
Berne
Switzerland

Rino Burkhardt
Private Practice
Zürich
Switzerland

Daniel Buser
Department of Oral Surgery and Stomatology
School of Dental Medicine
University of Berne
Berne
Switzerland

Gianfranco Carnevale
Private Practice
Rome
Italy

Delwyn Catley
Department of Psychology
University of Missouri – Kansas City
Kansas City
MO
USA

Noel Claffey
Dublin Dental School and Hospital
Trinity College
Dublin
Ireland

Lyndon F. Cooper
Department of Prosthodontics
University of North Carolina
Chapel Hill
NC
USA

Pierpaolo Cortellini
Private Practice
Florence
Italy

José J. Echeverría
Department of Periodontics
School of Dentistry
University of Barcelona
Barcelona
Spain

Ingvar Ericsson
Department of Prosthetic Dentistry
Faculty of Odontology
Malmö University
Malmö
Sweden

William V. Giannobile
Michigan Center for Oral Health Research
University of Michigan Clinical Center
Ann Arbor
MI
USA

Hans-Göran Gröndahl
Department of Oral and Maxillofacial Radiology
Institute of Odontology
The Sahlgrenska Academy at Göteborg University
Göteborg
Sweden

Kerstin Gröndahl
Department of Oral and Maxillofacial Radiology
Institute of Odontology
The Sahlgrenska Academy at Göteborg University
Göteborg
Sweden

Anne D. Haffajee
Department of Periodontology
The Forsyth Institute
Boston
MA
USA

Christoph H.F. Hämmerle
Clinic for Fixed and Removable Prosthodontics
Center for Dental and Oral Medicine and Cranio-Maxillofacial Surgery
University of Zürich
Zürich
Switzerland

Gunnar Hasselgren
Division of Endodontics
School of Dental and Oral Surgery
Columbia University College of Dental Medicine
New York
NY
USA

Lars Heijl
Department of Periodontology
Institute of Odontology
The Sahlgrenska Academy at Göteborg University
Göteborg
Sweden

David Herrera
Faculty of Odontology
University Complutense
Madrid
Spain

Palle Holmstrup
Department of Periodontology
School of Dentistry
University of Copenhagen
Copenhagen
Denmark

Reinhilde Jacobs
Oral Imaging Center
School of Dentistry, Oral Pathology and Maxillofacial Surgery
Catholic University of Leuven
Leuven
Belgium

Ronald E. Jung
Clinic for Fixed and Removable Prosthodontics
Center for Dental and Oral Medicine and Cranio-Maxillofacial Surgery
University of Zürich
Zürich
Switzerland

Thorkild Karring
Department of Periodontology and Oral Gerontology
Royal Dental College
University of Aarhus
Aarhus
Denmark

Denis F. Kinane
Oral Health and Systemic Disease Research Facility
School of Dentistry
University of Louisville
Louisville
KY
USA

Y. Joon Ko
Department of Prosthodontics
University of Iowa
Iowa City
IA
USA

Susan Krigel
Department of Psychology
University of Missouri – Kansas City
Kansas City
MO
USA

Marja L. Laine
Department of Oral Microbiology
Academic Centre for Dentistry Amsterdam (ACTA)
Amsterdam
The Netherlands

Niklaus P. Lang
Department of Periodontology and Fixed Prosthodontics
School of Dental Medicine
University of Berne
Berne
Switzerland

Ulf Lekholm
Department of Oral and Maxillofacial Surgery
Institute of Odontology
The Sahlgrenska Academy at Göteborg University
Göteborg
Sweden

Jan Lindhe
Department of Periodontology
Institute of Odontology
The Sahlgrenska Academy at Göteborg University
Göteborg
Sweden

Bruno G. Loos
Department of Periodontology
Academic Centre for Dentistry Amsterdam (ACTA)
Amsterdam
The Netherlands

Tord Lundgren
Department of Periodontics
School of Dentistry
Loma Linda University
Loma Linda
CA
USA

Angelo Mariotti
Section of Periodontology
Ohio State University College of Dentistry
Columbus
OH
USA

Andrea Mombelli
Department of Periodontology and Oral Pathophysiology
School of Dental Medicine
University of Geneva
Geneva
Switzerland

John Moran
Division of Restorative Dentistry (Periodontology)
Department of Oral and Dental Science
Bristol Dental School and Hospital
Bristol
UK

Sture Nyman
Deceased

Richard Palmer
Restorative Dentistry
King's College London Dental Institute
Guy's, King's and St Thomas' Hospitals
London
UK

Panos N. Papapanou
Division of Periodontics
Section of Oral and Diagnostic Sciences
Columbia University College of Dental Medicine
New York
NY
USA

David W. Paquette
Department of Periodontology
University of North Carolina School of Dentistry
Chapel Hill
NC
USA

Giovan P. Pini Prato
Department of Periodontology
University of Florence
Florence
Italy

Bjarni E. Pjetursson
Department of Periodontology and Fixed Prosthodontics
School of Dental Medicine
University of Berne
Berne
Switzerland

Ioannis Polyzois
Dublin Dental School and Hospital
Trinity College
Dublin
Ireland

Roberto Pontoriero
Private Practice
Milan
Italy

Marc Quirynen
Department of Periodontology
School of Dentistry
Catholic University of Leuven
Leuven
Belgium

Christoph A. Ramseier
Michigan Center for Oral Health Research
Department of Periodontics and Oral Medicine
University of Michigan School of Dentistry
Ann Arbor
MI
USA

Domenico Ricucci
Private Practice
Rome
Italy

Hector F. Rios
Department of Periodontics and Oral Medicine
University of Michigan School of Dentistry
Ann Arbor
MI
USA

Giovanni E. Salvi
Department of Periodontology
School of Dental Medicine
University of Berne
Berne
Switzerland

Mariano Sanz
Faculty of Odontology
University Complutense
Madrid
Spain

Marc A. Schätzle
Department of Orthodontics and Pediatric Dentistry
University of Zürich
Zürich
Switzerland

Sigmund S. Socransky
Department of Periodontology
The Forsyth Institute
Boston
MA
USA

Mena Soory
Restorative Dentistry
King's College London Dental Institute
Guy's, King's and St Thomas' Hospitals
London
UK

Clark M. Stanford
Dows Institute for Dental Research
University of Iowa
Iowa City
IA
USA

Ricardo P. Teles
Department of Periodontology
The Forsyth Institute
Boston
MA
USA

Maurizio S. Tonetti
Private Practice
Genoa
Italy

Leonardo Trombelli
Research Center for the Study of Periodontal Diseases
University of Ferrara
Ferrara
Italy

Ubele van der Velden
Department of Periodontology
Academic Centre for Dentistry Amsterdam (ACTA)
Amsterdam
The Netherlands

Fridus van der Weijden
Department of Periodontology
Academic Centre for Dentistry Amsterdam (ACTA)
Amsterdam
The Netherlands

Arie J. van Winkelhoff
Department of Oral Microbiology
Academic Centre for Dentistry Amsterdam (ACTA)
Amsterdam
The Netherlands

Hans-Peter Weber
Department of Restorative Dentistry and Biomaterials Science
Harvard School of Dental Medicine
Boston
MA
USA

Jan L. Wennström
Department of Periodontology
Institute of Odontology
The Sahlgrenska Academy at Göteborg University
Göteborg
Sweden

Jytte Westergaard
Department of Periodontology
School of Dentistry
University of Copenhagen
Copenhagen
Denmark

Ray C. Williams
Department of Periodontology
University of North Carolina School of Dentistry
Chapel Hill
NC
USA

Edwin G. Winkel
Department of Periodontology
Academic Centre for Oral Health
University Medical Centre Groningen
Groningen
The Netherlands

Björn U. Zachrisson
Department of Orthodontics
Dental Faculty
University of Oslo
Oslo
Norway

Giovanni Zucchelli
Department of Periodontology
Bologna University
Bologna
Italy

Preface

When the groundwork for the fifth edition of *Clinical Periodontology and Implant Dentistry* began in early 2007, it became clear that we had reached a fork in the road. It has always been my intention that each successive edition of this work should reflect the state of the art of clinical periodontology and, in doing such, should run the gamut of topics within this subject area. However, thorough coverage of an already large and now rapidly expanding specialty has resulted in a book of commensurate size and therefore for the fifth edition, the decision was taken to divide the book into two volumes: basic concepts and clinical concepts. The decision to make the split a purely physical one, and not an intellectual one, reflects the realization that over the past decade, implant dentistry has become a basic part of periodontology. The integrated structure of this latest edition of the textbook mirrors this merger.

In order for the student of dentistry, whatever his or her level, to learn how teeth and implants may function together as separate or connected units in the same dentition, a sound knowledge of the tissues that surround the natural tooth and the dental implant, as well as an understanding of the various lesions that may occur in the supporting tissues, is imperative. Hence, in both volumes of the textbook, chapters dealing with traditional periodontal issues, such as anatomy, pathology and treatment, are followed by similar topics related to tissues surrounding dental implants. In the first volume of the fifth edition, "basic concepts" as they relate to anatomy, microbiology and pathology, for example, are presented, while in the second volume ("clinical concepts"), various aspects of often evidence-based periodontal and restorative examination and treatment procedures are outlined.

It is my hope that the fifth edition of *Clinical Periodontology and Implant Dentistry* will challenge the reader intellectually, provide elucidation and clarity of information, and also impart an understanding of how the information presented in the text can, and should, be used in the practice of contemporary dentistry.

Jan Lindhe

Part 1: Anatomy

Chapter 1

The Anatomy of Periodontal Tissues

Jan Lindhe, Thorkild Karring, and Maurício Araújo

Introduction

This chapter includes a brief description of the characteristics of the normal periodontium. It is assumed that the reader has prior knowledge of oral embryology and histology. The periodontium (peri = around, odontos = tooth) comprises the following tissues (Fig. 1-1): (1) the *gingiva* (G), (2) the *periodontal ligament* (PL), (3) the *root cementum* (RC), and (4) the *alveolar bone* (AP). The alveolar bone consists of two components, the *alveolar bone proper* (ABP) and the alveolar process. The alveolar bone proper, also called "bundle bone", is continuous with the alveolar process and forms the thin bone plate that lines the alveolus of the tooth.

The main function of the periodontium is to attach the tooth to the bone tissue of the jaws and to maintain the integrity of the surface of the masticatory mucosa of the oral cavity. The periodontium, also called "the attachment apparatus" or "the supporting tissues of the teeth", constitutes a developmental, biologic, and functional unit which undergoes certain changes with age and is, in addition, subjected to morphologic changes related to functional alterations and alterations in the oral environment.

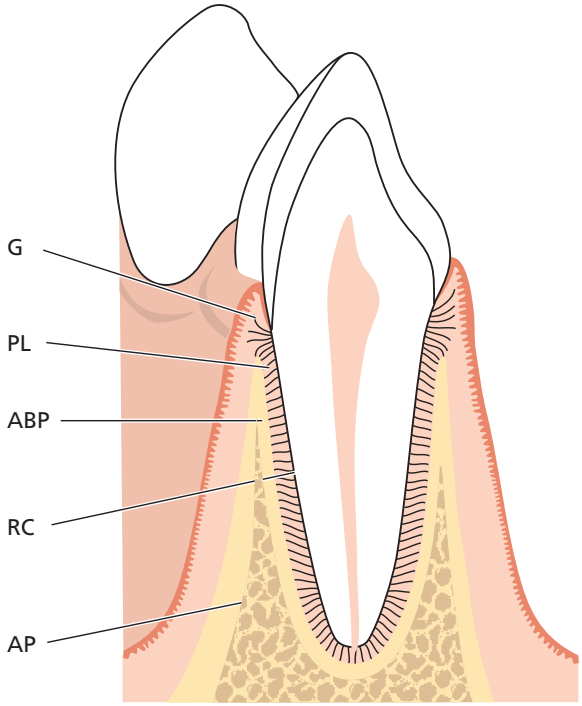

Fig. 1-1

The development of the periodontal tissues occurs during the development and formation of teeth. This process starts early in the embryonic phase when cells from the neural crest (from the neural tube of the embryo) migrate into the first branchial arch. In this position the neural crest cells form a band of *ectomesenchyme* beneath the epithelium of the stomatodeum (the primitive oral cavity). After the uncommitted neural crest cells have reached their location in the jaw space, the epithelium of the stomatodeum releases factors which initiate epithelial–ectomesenchymal interactions. Once these interactions have occurred, the ectomesenchyme takes the dominant role in the further development. Following the formation of the *dental lamina*, a series of processes are initiated (bud stage, cap stage, bell stage with root development) which result in the formation of a tooth and its surrounding periodontal tissues, including the alveolar bone proper. During the cap stage, condensation of ectomesenchymal cells appears in relation to the dental epithelium (the dental organ (DO)),

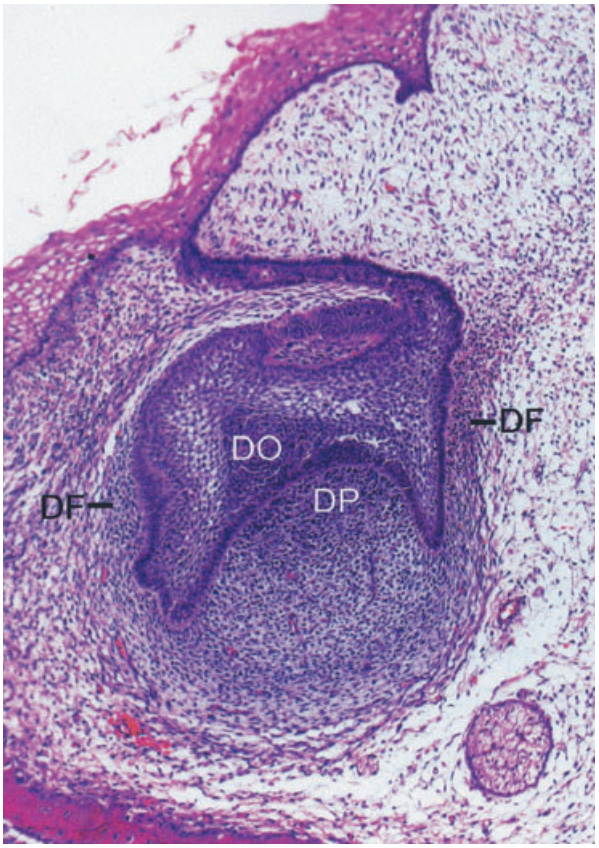

Fig. 1-2

forming the *dental papilla* (DP) that gives rise to the dentin and the pulp, and the *dental follicle* (DF) that gives rise to the periodontal supporting tissues (Fig. 1-2). The decisive role played by the ectomesenchyme in this process is further established by the fact that the tissue of the dental papilla apparently also determines the shape and form of the tooth.

If a tooth germ in the bell stage of development is dissected and transplanted to an ectopic site (e.g. the connective tissue or the anterior chamber of the eye), the tooth formation process continues. The crown and the root are formed, and the supporting structures, i.e. cementum, periodontal ligament, and a thin lamina of alveolar bone proper, also develop. Such experiments document that all information necessary for the formation of a tooth and its attachment apparatus obviously resides within the tissues of the dental organ and the surrounding ectomesenchyme. The dental organ is the formative organ of enamel, the dental papilla is the formative organ of the dentin–pulp complex, and the dental follicle is the formative organ of the attachment apparatus (the cementum, the periodontal ligament, and the alveolar bone proper).

The development of the root and the periodontal supporting tissues follows that of the crown. Epithelial cells of the external and internal dental epithelium (the dental organ) proliferate in an apical direction forming a double layer of cells named *Hertwig's epithelial root sheath* (RS). The odontoblasts (OB) forming the dentin of the root differentiate from ecto-

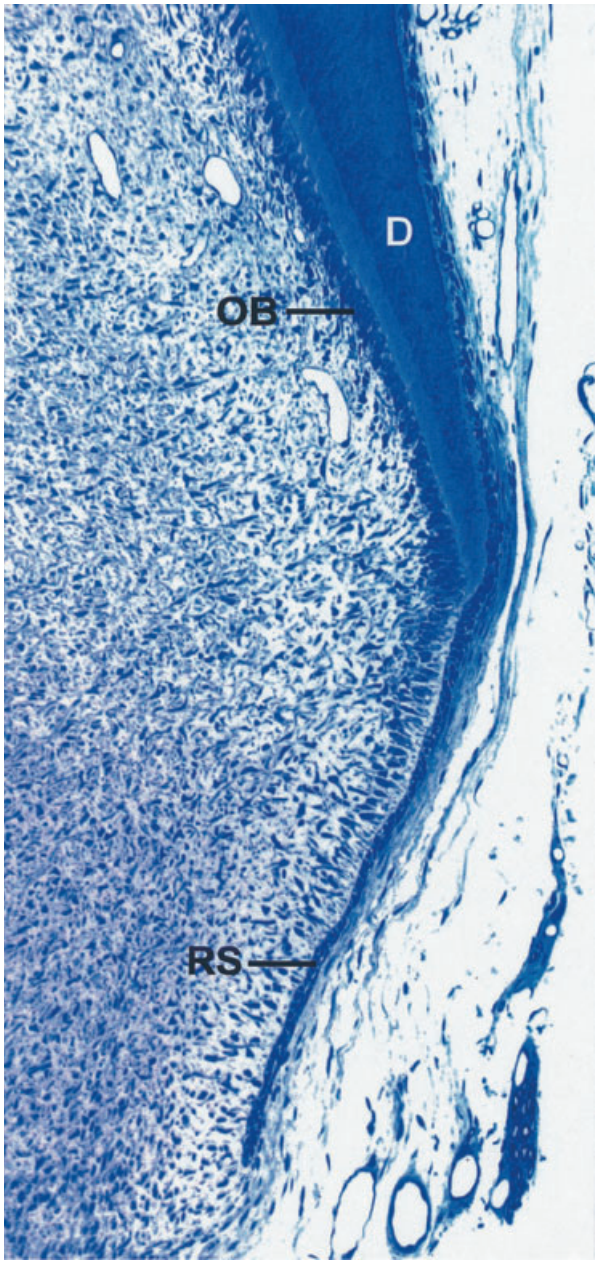

Fig. 1-3

mesenchymal cells in the dental papilla under inductive influence of the inner epithelial cells (Fig. 1-3). The dentin (D) continues to form in an apical direction producing the framework of the root. During formation of the root, the periodontal supporting tissues, including acellular cementum, develop. Some of the events in the cementogenesis are still unclear, but the following concept is gradually emerging.

At the start of dentin formation, the inner cells of Hertwig's epithelial root sheath synthesize and secrete enamel-related proteins, probably belonging to the amelogenin family. At the end of this period, the epithelial root sheath becomes fenestrated and ectomesenchymal cells from the dental follicle penetrate through these fenestrations and contact the root surface. The ectomesenchymal cells in contact with the enamel-related proteins differentiate into cementoblasts and start to form cementoid. This cementoid

Fig. 1-4

Fig. 1-5

represents the organic matrix of the cementum and consists of a ground substance and collagen fibers, which intermingle with collagen fibers in the not yet fully mineralized outer layer of the dentin. It is assumed that the cementum becomes firmly attached to the dentin through these fiber interactions. The formation of the cellular cementum, which covers the apical third of the dental roots, differs from that of acellular cementum in that some of the cementoblasts become embedded in the cementum.

The remaining parts of the periodontium are formed by ectomesenchymal cells from the dental follicle lateral to the cementum. Some of them differentiate into periodontal fibroblasts and form the fibers of the periodontal ligament while others become osteoblasts producing the alveolar bone proper in which the periodontal fibers are anchored. In other words, the primary alveolar wall is also an ectomesenchymal product. It is likely, but still not conclusively documented, that ectomesenchymal cells remain in the mature periodontium and take part in the turnover of this tissue.

Gingiva

Macroscopic anatomy

The oral mucosa (mucous membrane) is continuous with the skin of the lips and the mucosa of the soft palate and pharynx. The oral mucosa consists of (1) the *masticatory mucosa*, which includes the gingiva and the covering of the hard palate, (2) the *specialized mucosa*, which covers the dorsum of the tongue, and (3) the remaining part, called the *lining mucosa*.

Fig. 1-4 The gingiva is that part of the masticatory mucosa which covers the alveolar process and surrounds the cervical portion of the teeth. It consists of an epithelial layer and an underlying connective tissue layer called the *lamina propria*. The gingiva obtains its final shape and texture in conjunction with eruption of the teeth.

In the coronal direction the coral pink gingiva terminates in the *free gingival margin*, which has a scalloped outline. In the apical direction the gingiva is continuous with the loose, darker red *alveolar mucosa* (lining mucosa) from which the gingiva is separated by a usually easily recognizable borderline called

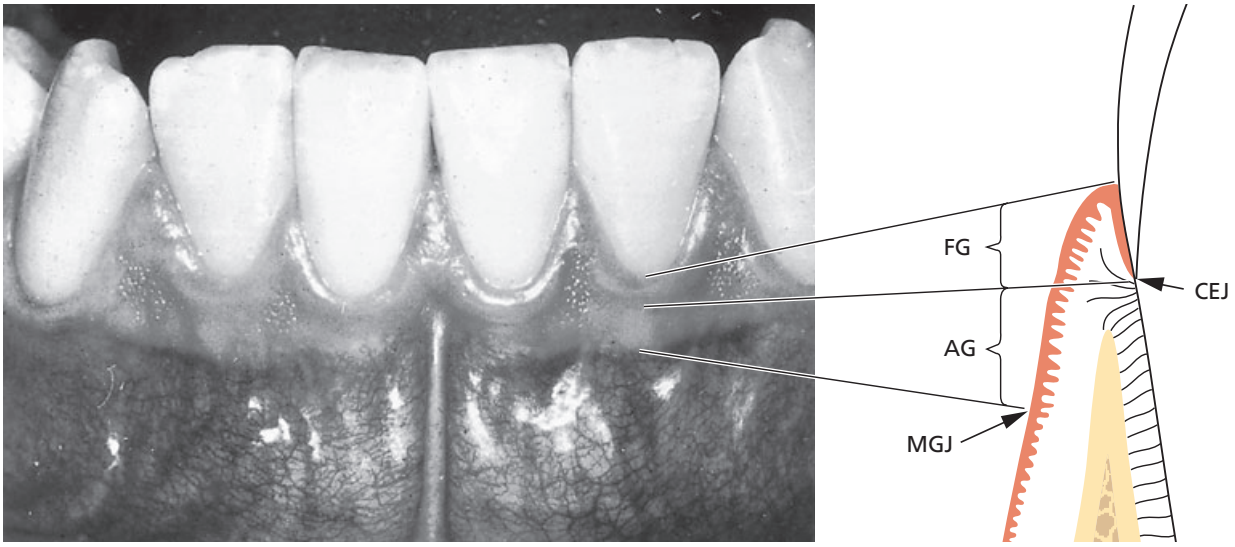

Fig. 1-6

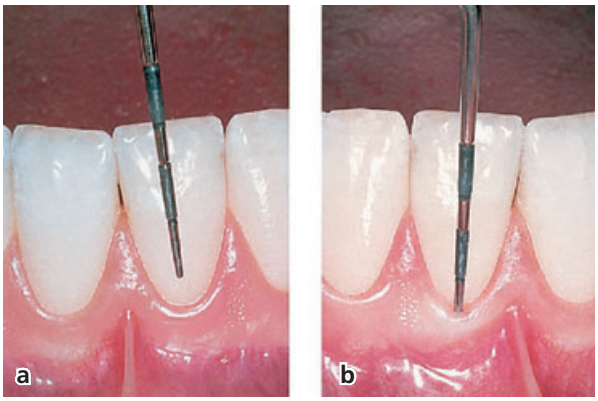

Fig. 1-7

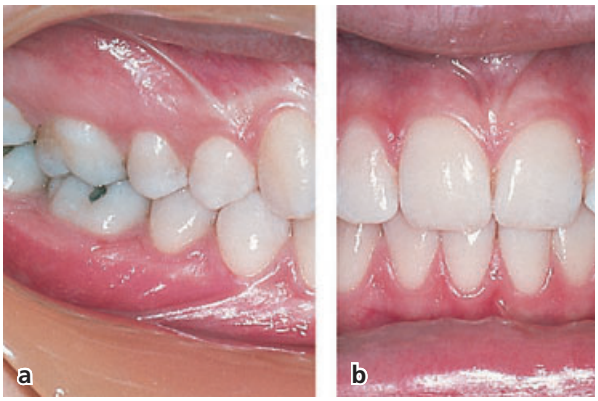

Fig. 1-8

either the mucogingival junction (arrows) or the mucogingival line.

Fig. 1-5 There is no mucogingival line present in the palate since the hard palate and the maxillary alveolar process are covered by the same type of masticatory mucosa.

Fig. 1-6 Two parts of the gingiva can be differentiated:

1. The free gingiva (FG)
2. The attached gingiva (AG).

The free gingiva is coral pink, has a dull surface and firm consistency. It comprises the gingival tissue at the vestibular and lingual/palatal aspects of the teeth, and the *interdental gingiva* or the *interdental papillae*. On the vestibular and lingual side of the teeth, the free gingiva extends from the gingival margin in apical direction to the *free gingival groove* which is positioned at a level corresponding to the level of the *cemento-enamel junction* (CEJ). The attached gingiva is demarcated by the mucogingival junction (MGJ) in the apical direction.

Fig. 1-7 The free gingival margin is often rounded in such a way that a small invagination or sulcus is formed between the tooth and the gingiva (Fig. 1-7a).

When a periodontal probe is inserted into this invagination and, further apically, towards the cemento-enamel junction, the gingival tissue is separated from the tooth, and a "*gingival pocket*" or "*gingival crevice*" is artificially opened. Thus, in normal or clinically healthy gingiva there is in fact no "gingival pocket" or "gingival crevice" present but the gingiva is in close contact with the enamel surface. In the illustration to the right (Fig. 1-7b), a periodontal probe has been inserted in the tooth/gingiva interface and a "gingival crevice" artificially opened approximately to the level of the cemento-enamel junction.

After completed tooth eruption, the free gingival margin is located on the enamel surface approximately 1.5–2 mm coronal to the cemento-enamel junction.

Fig. 1-8 The shape of the interdental gingiva (the interdental papilla) is determined by the contact relationships between the teeth, the width of the approximal tooth surfaces, and the course of the cemento-enamel junction. In anterior regions of the

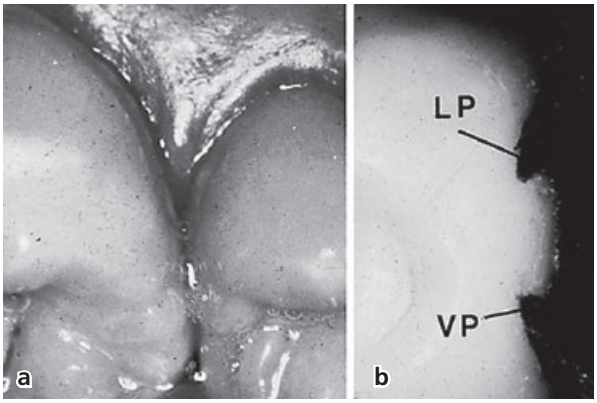

Fig. 1-9

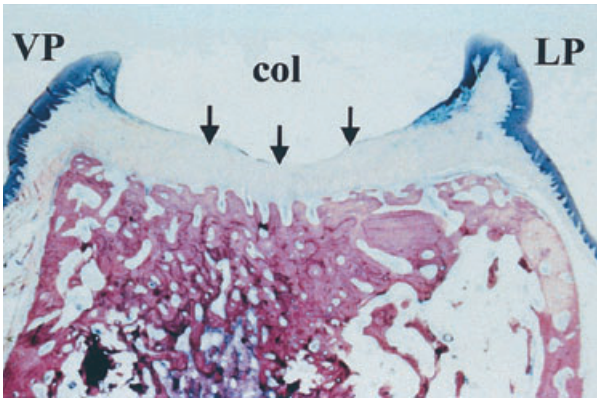

Fig. 1-9c

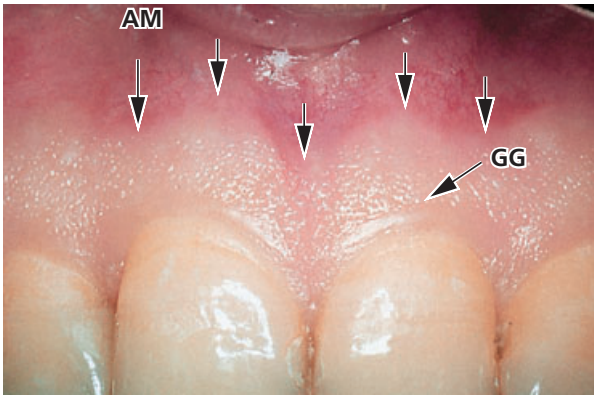

Fig. 1-10

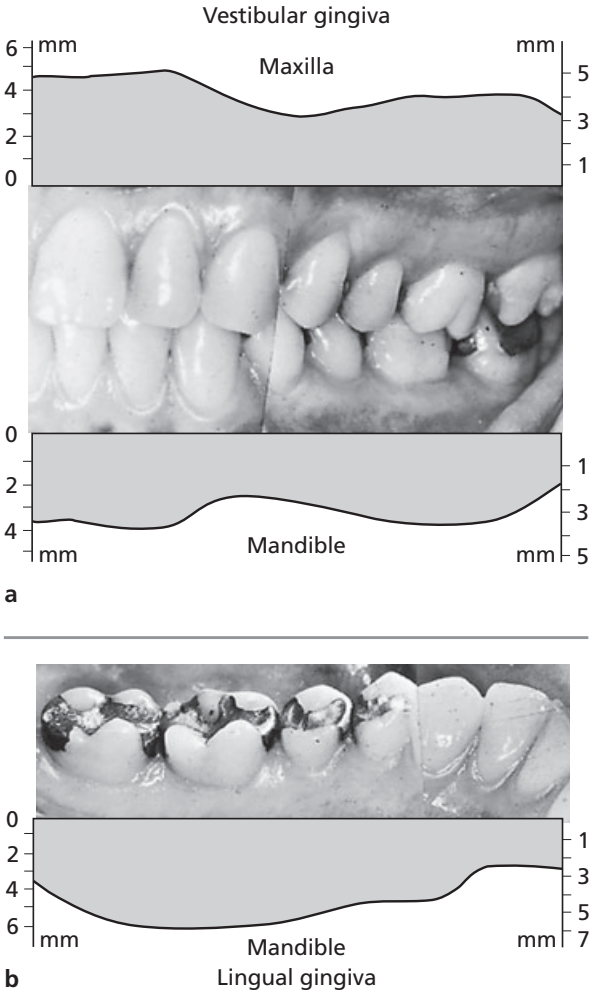

Fig. 1-11

dentition, the interdental papilla is of pyramidal form (Fig. 1-8b) while in the molar regions, the papillae are more flattened in the buccolingual direction (Fig. 1-8a). Due to the presence of interdental papillae, the free gingival margin follows a more or less accentuated, scalloped course through the dentition.

Fig. 1-9 In the premolar/molar regions of the dentition, the teeth have approximal contact surfaces (Fig. 1-9a) rather than contact points. Since the interdental papilla has a shape in conformity with the outline of the interdental contact surfaces, a concavity – *a col* – is established in the premolar and molar regions, as demonstrated in Fig. 1-9b, where the distal tooth has been removed. Thus, the interdental papillae in these areas often have one vestibular (VP) and one lingual/palatal portion (LP) separated by the col region. The col region, as demonstrated in the histological section (Fig. 1-9c), is covered by a thin non-keratinized epithelium (arrows). This epithelium has many features in common with the junctional epithelium (see Fig. 1-34).

Fig. 1-10 The attached gingiva is demarcated in the coronal direction, by the free gingival groove (GG) or, when such a groove is not present, by a horizontal plane placed at the level of the cemento-enamel junction. In clinical examinations it was observed that a free gingival groove is only present in about 30–40% of adults.

The free gingival groove is often most pronounced on the vestibular aspect of the teeth, occurring most frequently in the incisor and premolar regions of the mandible, and least frequently in the mandibular molar and maxillary premolar regions.

The attached gingiva extends in the apical direction to the mucogingival junction (arrows), where it becomes continuous with the alveolar (lining) mucosa (AM). It is of firm texture, coral pink in color, and often shows small depressions on the surface. The depressions, named “stippling”, give the appearance

Fig. 1-12

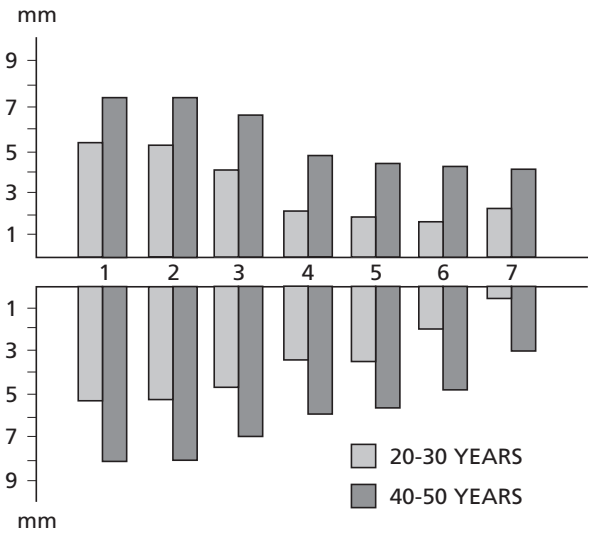

Fig. 1-13

of orange peel. It is firmly attached to the underlying alveolar bone and cementum by connective tissue fibers, and is, therefore, comparatively immobile in relation to the underlying tissue. The darker red alveolar mucosa (AM) located apical to the mucogingival junction, on the other hand, is loosely bound to the underlying bone. Therefore, in contrast to the attached gingiva, the alveolar mucosa is mobile in relation to the underlying tissue.

Fig. 1-11 describes how the width of the gingiva varies in different parts of the mouth. In the maxilla (Fig. 1-11a) the vestibular gingiva is generally widest in the area of the incisors and most narrow adjacent to the premolars. In the mandible (Fig. 1-11b) the gingiva on the lingual aspect is particularly narrow in the area of the incisors and wide in the molar region. The range of variation is 1–9 mm.

Fig. 1-12 illustrates an area in the mandibular premolar region where the gingiva is extremely narrow. The arrows indicate the location of the mucogingival junction. The mucosa has been stained with an iodine solution in order to distinguish more accurately between the gingiva and the alveolar mucosa.

Fig. 1-13 depicts the result of a study in which the width of the attached gingiva was assessed and related to the age of the patients examined. It was found that the gingiva in 40–50-year-olds was significantly wider than that in 20–30-year-olds. This observation indicates that the width of the gingiva tends to increase with age. Since the mucogingival junction remains stable throughout life in relation to the lower border of the mandible, the increasing width of the gingiva may suggest that the teeth, as a result of occlusal wear, erupt slowly throughout life.

Microscopic anatomy

Oral epithelium

Fig. 1-14a A schematic drawing of a histologic section (see Fig. 1-14b) describing the composition of the gingiva and the contact area between the gingiva and the enamel (E).

Fig 1-14b The free gingiva comprises all epithelial and connective tissue structures (CT) located coronal to a horizontal line placed at the level of the cemento-enamel junction (CEJ). The epithelium covering the free gingiva may be differentiated as follows:

- *Oral epithelium* (OE), which faces the oral cavity
- *Oral sulcular epithelium* (OSE), which faces the tooth without being in contact with the tooth surface
- *Junctional epithelium* (JE), which provides the contact between the gingiva and the tooth.

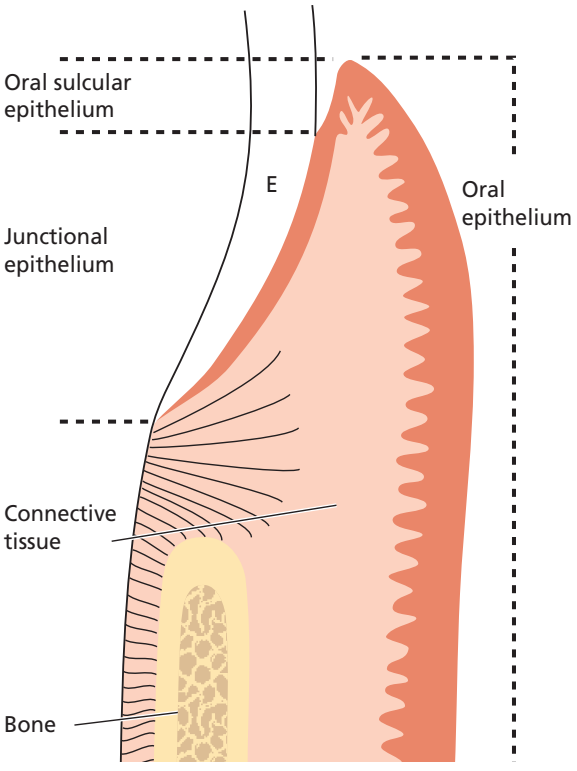

Fig. 1-14a

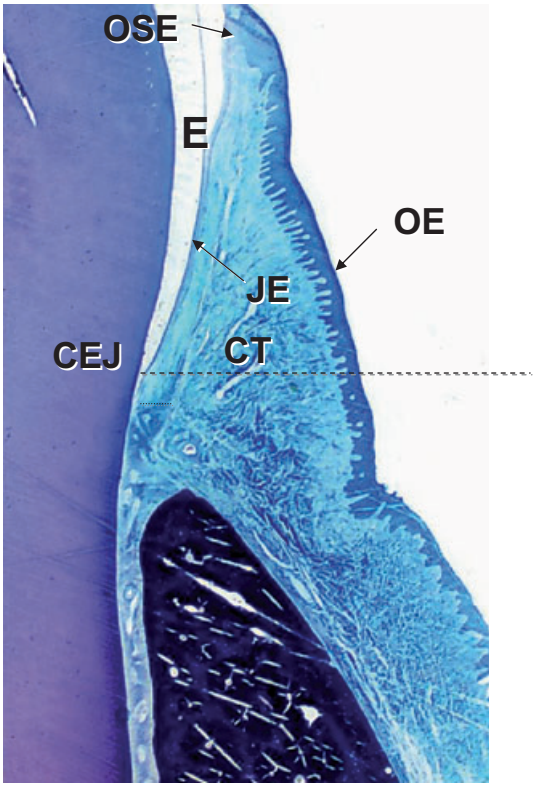

Fig. 1-14b

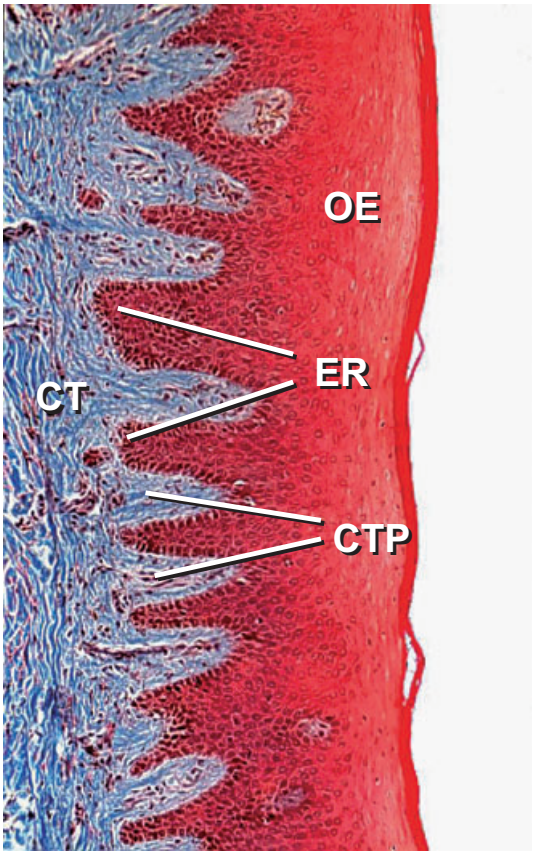

Fig. 1-14c

Fig. 1-15

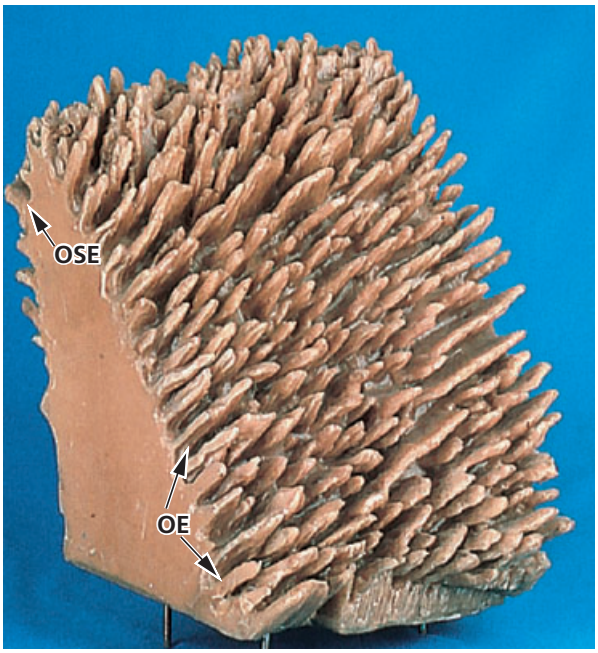

Fig. 1-16

Fig. 1-14c The boundary between the oral epithelium (OE) and underlying connective tissue (CT) has a wavy course. The connective tissue portions which project into the epithelium are called *connective tissue papillae* (CTP) and are separated from each other by

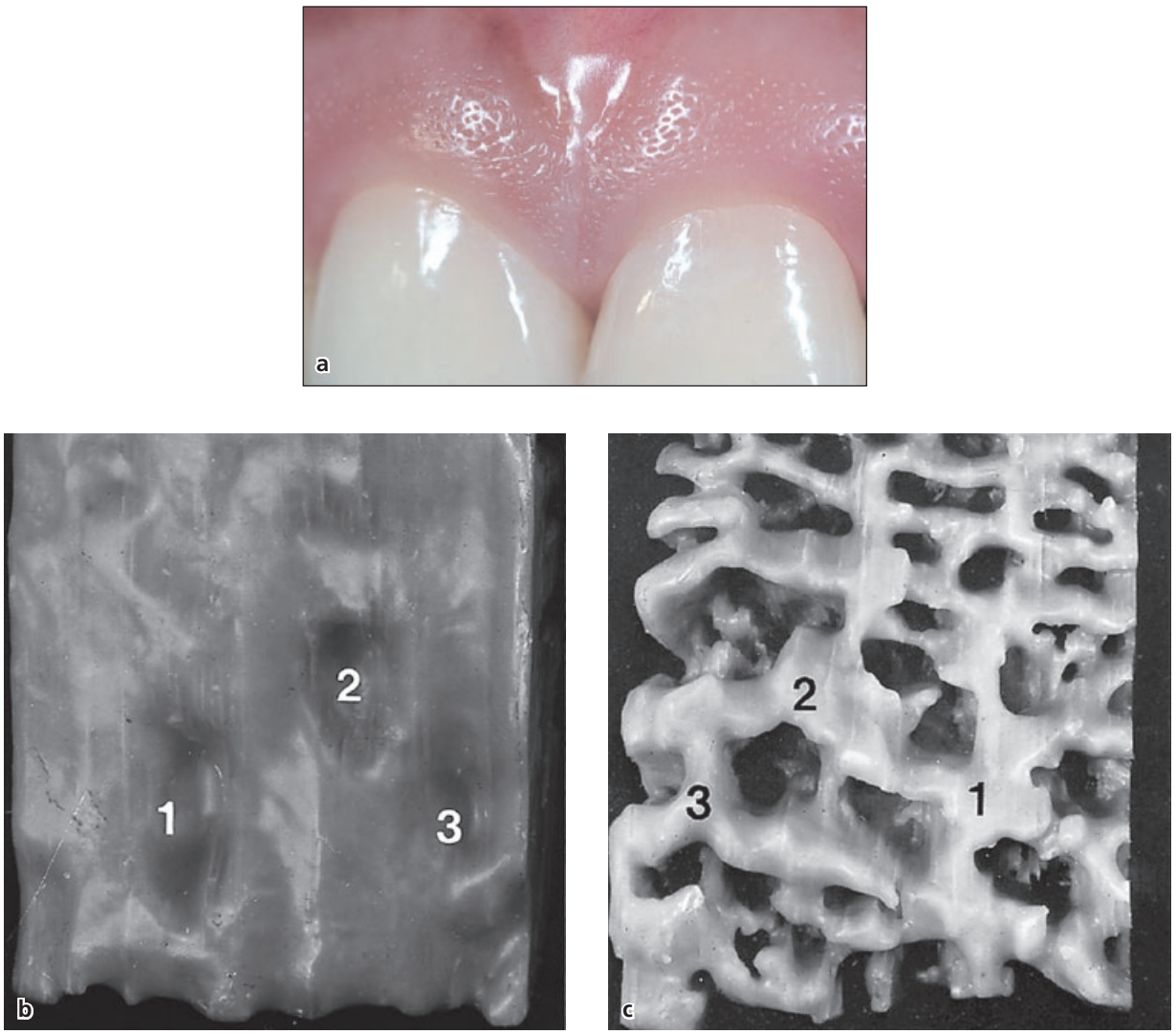

Fig. 1-17

epithelial ridges – so-called *rete pegs* (ER). In normal, non-inflamed gingiva, rete pegs and connective tissue papillae are lacking at the boundary between the junctional epithelium and its underlying connective tissue (Fig. 1-14b). Thus, a characteristic morphologic feature of the oral epithelium and the oral sulcular epithelium is the presence of rete pegs, while these structures are lacking in the junctional epithelium.

Fig. 1-15 presents a model, constructed on the basis of magnified serial histologic sections, showing the subsurface of the oral epithelium of the gingiva after the connective tissue has been removed. The subsurface of the oral epithelium (i.e. the surface of the epithelium facing the connective tissue) exhibits several depressions corresponding to the connective tissue papillae (in Fig. 1-16) which project into the epithelium. It can be seen that the epithelial projections, which in histologic sections separate the connective tissue papillae, constitute a continuous system of epithelial ridges.

Fig. 1-16 presents a model of the connective tissue, corresponding to the model of the epithelium shown in Fig. 1-15. The epithelium has been removed, thereby making the vestibular aspect of the gingival connective tissue visible. Notice the connective tissue papillae which project into the space that was occupied by the oral epithelium (OE) in Fig. 1-15 and by the oral sulcular epithelium (OSE) on the back of the model.

Fig. 1-17a In 40% of adults the attached gingiva shows a stippling on the surface. The photograph shows a case where this stippling is conspicuous (see also Fig. 1-10).

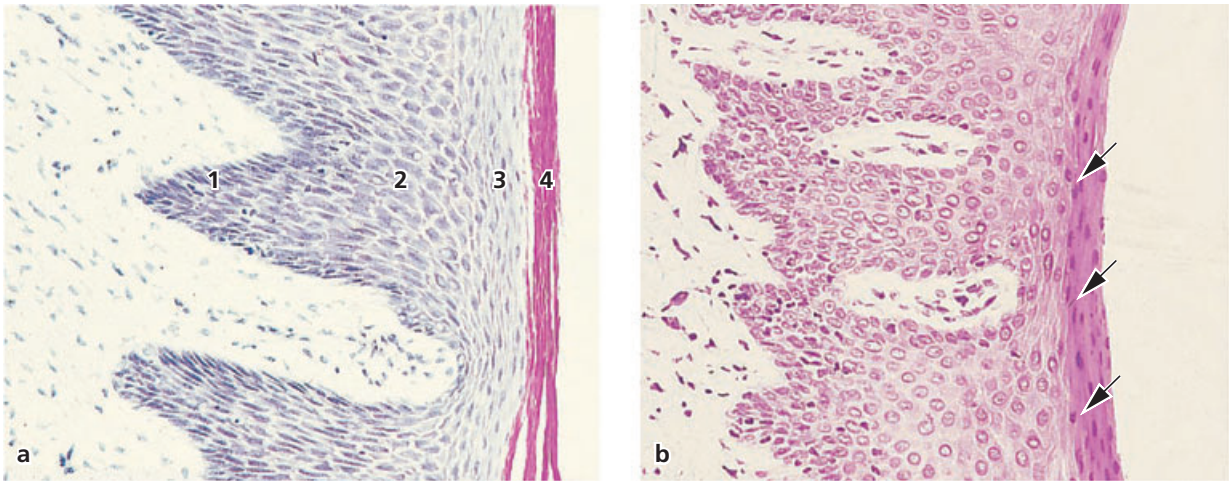

Fig. 1-18

Fig. 1-17b presents a magnified model of the outer surface of the oral epithelium of the attached gingiva. The surface exhibits the minute depressions (1–3) which, when present, give the gingiva its characteristic stippled appearance.

Fig. 1-17c shows a photograph of the subsurface (i.e. the surface of the epithelium facing the connective tissue) of the same model as that shown in Fig. 1-17b. The subsurface of the epithelium is characterized by the presence of epithelial ridges which merge at various locations (1–3). The depressions (1–3) seen on the outer surface of the epithelium (shown in Fig. 1-17b) correspond with the fusion sites (1–3) between epithelial ridges. Thus, the depressions on the surface of the gingiva occur in the areas of fusion between various epithelial ridges.

Fig. 1-18 (a) A portion of the oral epithelium covering the free gingiva is illustrated in this photomicrograph. The oral epithelium is a *keratinized*, *stratified*, *squamous epithelium* which, on the basis of the degree to which the keratin-producing cells are differentiated, can be divided into the following cell layers:

1. *Basal layer* (stratum basale or stratum germinativum)
2. *Prickle cell layer* (stratum spinosum)
3. *Granular cell layer* (stratum granulosum)
4. *Keratinized cell layer* (stratum corneum).

It should be observed that in this section, cell nuclei are lacking in the outer cell layers. Such an epithelium is denoted *orthokeratinized*. Often, however, the cells of the stratum corneum of the epithelium of human gingiva contain remnants of the nuclei (arrows) as seen in Fig. 1-18b. In such a case, the epithelium is denoted *parakeratinized*.

Fig. 1-19 In addition to the keratin-producing cells which comprise about 90% of the total cell population, the oral epithelium contains the following types of cell:

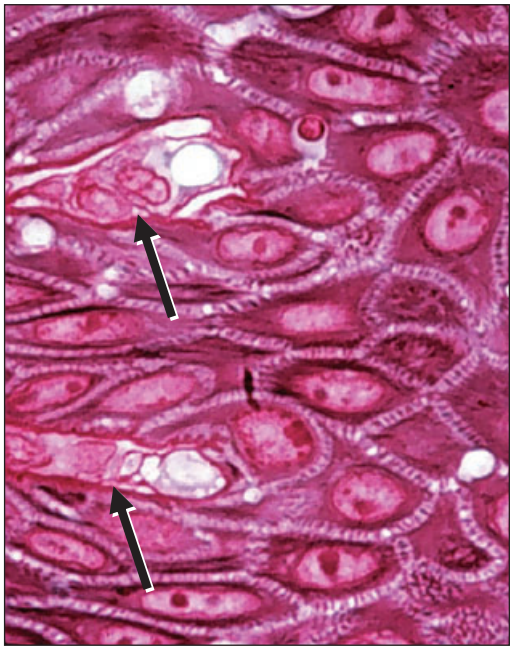

Fig. 1-19

- *Melanocytes*
- *Langerhans cells*
- *Merkel's cells*
- *Inflammatory cells.*

These cell types are often stellate and have cytoplasmic extensions of various size and appearance. They are also called "clear cells" since in histologic sections, the zone around their nuclei appears lighter than that in the surrounding keratin-producing cells.

The photomicrograph shows "clear cells" (arrows) located in or near the stratum basale of the oral epithelium. Except the Merkel's cells, these "clear cells", which do not produce keratin, lack desmosomal attachment to adjacent cells. The melanocytes are

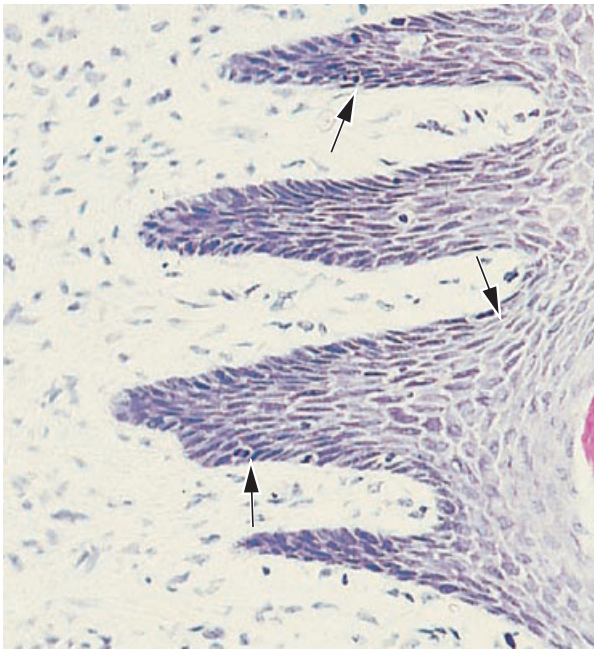

Fig. 1-20

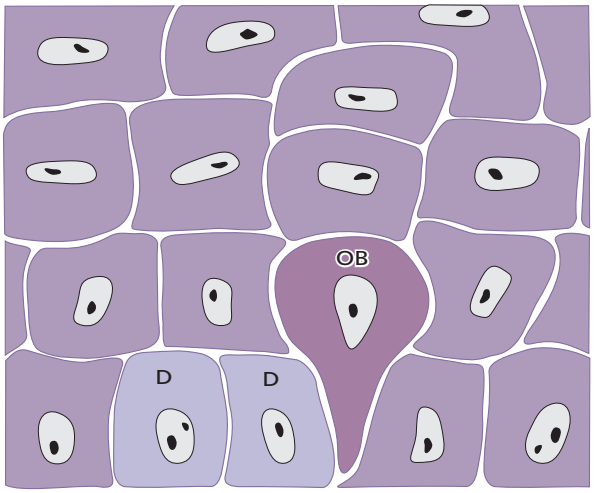

Fig. 1-21

pigment-synthesizing cells and are responsible for the melanin pigmentation occasionally seen on the gingiva. However, both lightly and darkly pigmented individuals present melanocytes in the epithelium.

The Langerhans cells are believed to play a role in the defense mechanism of the oral mucosa. It has been suggested that the Langerhans cells react with antigens which are in the process of penetrating the epithelium. An early immunologic response is thereby initiated, inhibiting or preventing further antigen penetration of the tissue. The Merkel's cells have been suggested to have a sensory function.

Fig. 1-20 The cells in the basal layer are either cylindric or cuboid, and are in contact with the *basement membrane* that separates the epithelium and the connective tissue. The basal cells possess the ability to divide, i.e. undergo mitotic cell division. The cells marked with arrows in the photomicrograph are in the process of dividing. It is in the basal layer that the epithelium is renewed. Therefore, this layer is also termed *stratum germinativum*, and can be considered the *progenitor cell compartment* of the epithelium.

Fig. 1-21 When two daughter cells (D) have been formed by cell division, an adjacent "older" basal cell (OB) is pushed into the spinous cell layer and starts, as a *keratinocyte*, to traverse the epithelium. It takes approximately 1 month for a keratinocyte to reach the outer epithelial surface, where it becomes shed from the stratum corneum. Within a given time, the number of cells which divide in the basal layer equals the number of cells which become shed from the surface. Thus, under normal conditions there is complete equilibrium between cell renewal and cell loss so that the epithelium maintains a constant thickness. As the basal cell migrates through the epithelium, it becomes flattened with its long axis parallel to the epithelial surface.

Fig. 1-22 The basal cells are found immediately adjacent to the connective tissue and are separated from this tissue by the basement membrane, probably produced by the basal cells. Under the light microscope this membrane appears as a structureless zone approximately 1–2 µm wide (arrows) which reacts positively to a PAS stain (periodic acid-Schiff stain). This positive reaction demonstrates that the basement membrane contains carbohydrate (glycoproteins). The epithelial cells are surrounded by an extracellular substance which also contains protein–polysaccharide complexes. At the ultrastructural level, the basement membrane has a complex composition.

Fig. 1-23 is an electronmicrograph (magnification ×70 000) of an area including part of a basal cell, the basement membrane, and part of the adjacent connective tissue. The basal cell (BC) occupies the upper portion of the picture. Immediately beneath the basal cell an approximately 400 Å wide electron-lucent zone can be seen which is called *lamina lucida* (LL). Beneath the lamina lucida an electron-dense zone of approximately the same thickness can be observed. This zone is called *lamina densa* (LD). From the lamina densa so-called *anchoring fibers* (AF) project in a fan-shaped fashion into the connective tissue. The anchoring fibers are approximately 1 µm in length and terminate freely in the connective tissue. The basement membrane, which appeared as an entity under the light microscope, thus, in the electronmicrograph, appears to comprise one lamina lucida and one lamina densa with adjacent connective tissue fibers (anchoring fibers). The cell membrane of the epithelial cells facing the lamina lucida harbors a number of electron-dense, thicker zones appearing at various intervals along the cell membrane. These structures are called *hemidesmosomes* (HD). The cytoplasmic

Fig. 1-22

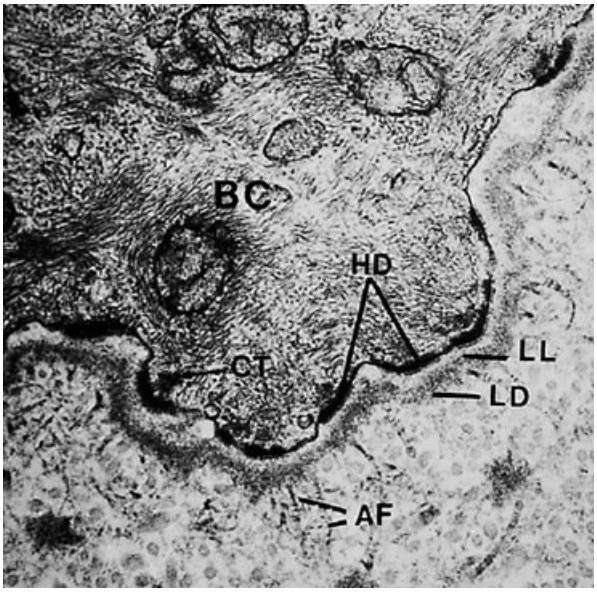

Fig. 1-23

tonofilaments (CT) in the cell converge towards the hemidesmosomes. The hemidesmosomes are involved in the attachment of the epithelium to the underlying basement membrane.

Fig. 1-24 illustrates an area of stratum spinosum in the gingival oral epithelium. Stratum spinosum consists of 10–20 layers of relatively large, polyhedral cells, equipped with short cytoplasmic processes resembling spines. The cytoplasmic processes (arrows) occur at regular intervals and give the cells a prickly appearance. Together with intercellular protein–carbohydrate complexes, cohesion between the cells is provided by numerous "desmosomes" (pairs of hemidesmosomes) which are located between the cytoplasmic processes of adjacent cells.

Fig. 1-25 shows an area of stratum spinosum in an electronmicrograph. The dark-stained structures between the individual epithelial cells represent the *desmosomes* (arrows). A desmosome may be considered to be two hemidesmosomes facing one another. The presence of a large number of desmosomes indicates that the cohesion between the epithelial cells is solid. The light cell (LC) in the center of the illustration harbors no hemidesmosomes and is, therefore, not a keratinocyte but rather a "clear cell" (see also Fig. 1-19).

Fig. 1-26 is a schematic drawing describing the composition of a desmosome. A desmosome can be

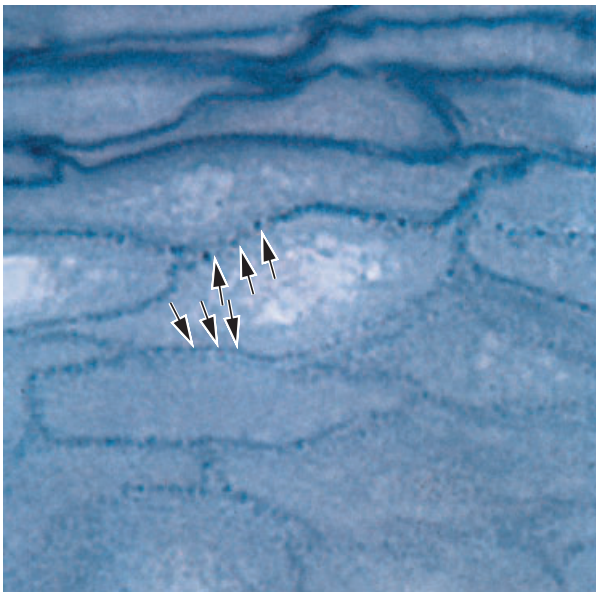

Fig. 1-24

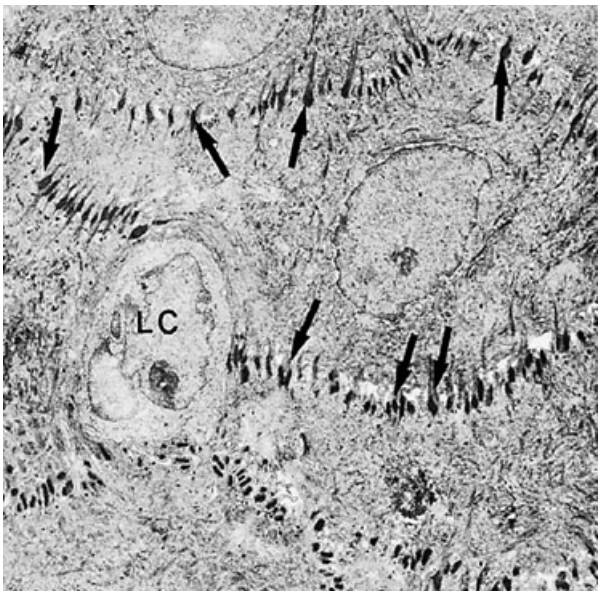

Fig. 1-25

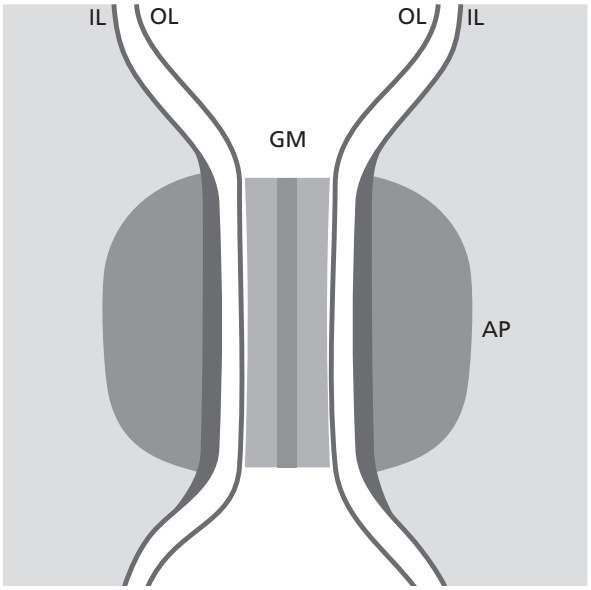

Fig. 1-26

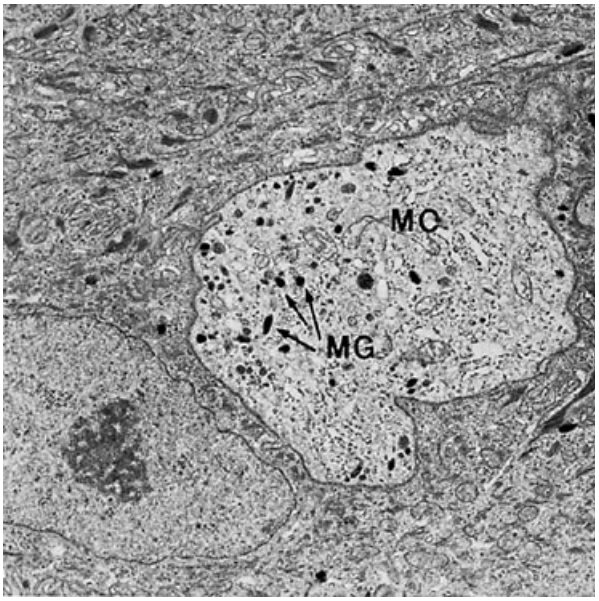

Fig. 1-27

considered to consist of two adjoining hemidesmosomes separated by a zone containing electron-dense granulated material (GM). Thus, a desmosome comprises the following structural components: (1) the *outer leaflets* (OL) of the cell membrane of two adjoining cells, (2) the thick *inner leaflets* (IL) of the cell membranes and (3) the *attachment plaques* (AP), which represent granular and fibrillar material in the cytoplasm.

Fig. 1-27 As mentioned previously, the oral epithelium also contains melanocytes, which are responsible for the production of the pigment melanin. Melanocytes are present in individuals with marked pigmentation of the oral mucosa as well as in individuals where no clinical signs of pigmentation can be seen. In this electronmicrograph a melanocyte (MC) is present in the lower portion of the stratum spinosum. In contrast to the keratinocytes, this cell contains melanin granules (MG) and has no tonofilaments or hemidesmosomes. Note the large amount of tonofilaments in the cytoplasm of the adjacent keratinocytes.

Fig. 1-28 When traversing the epithelium from the basal layer to the epithelial surface, the keratinocytes undergo continuous differentiation and specialization. The many changes which occur during this process are indicated in this diagram of a keratinized stratified squamous epithelium. From the basal layer (stratum basale) to the granular layer (stratum granulosum) both the number of tonofilaments (F) in the cytoplasm and the number of desmosomes (D) increase. In contrast, the number of organelles, such as mitochondria (M), lamellae of rough endoplasmic reticulum (E) and Golgi complexes (G), decrease in the keratinocytes on their way from the basal layer towards the surface. In the stratum granulosum, electron-dense *keratohyalin bodies* (K) and clusters of

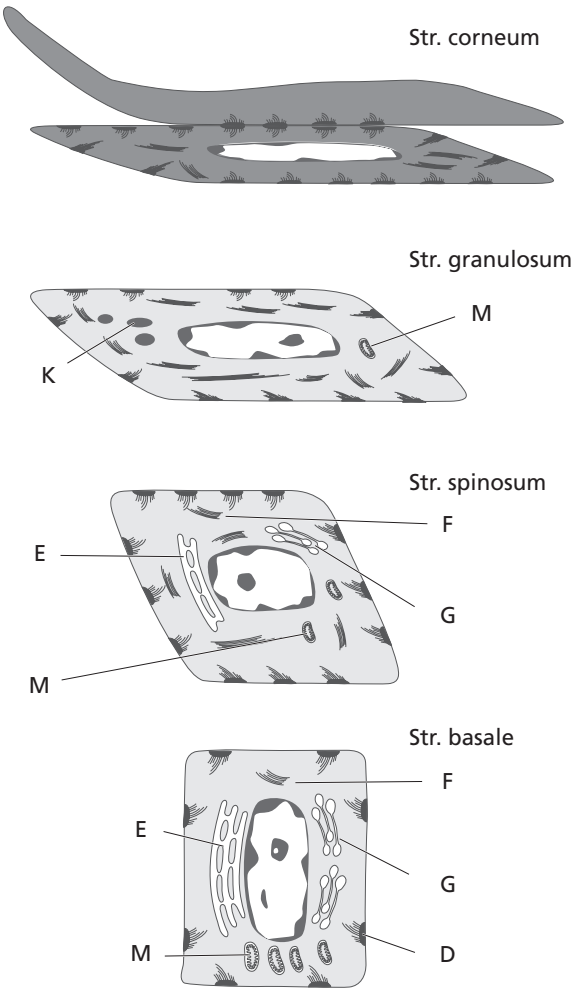

Fig. 1-28

glycogen-containing granules start to occur. Such granules are believed to be related to the synthesis of keratin.

Fig. 1-29 is a photomicrograph of the stratum granulosum and stratum corneum. Keratohyalin granules (arrows) are seen in the stratum granulosum. There is an abrupt transition of the cells from the stratum granulosum to the stratum corneum. This is indicative of a very sudden keratinization of the cytoplasm of the keratinocyte and its conversion into a horny squame. The cytoplasm of the cells in the stratum corneum (SC) is filled with keratin and the entire apparatus for protein synthesis and energy production, i.e. the nucleus, the mitochondria, the endoplasmic reticulum, and the Golgi complex, is lost. In a parakeratinized epithelium, however, the cells of the stratum corneum contain remnants of nuclei. Keratinization is considered a process of differentiation rather than degeneration. It is a process of protein synthesis which requires energy and is dependent on functional cells, i.e. cells containing a nucleus and a normal set of organelles.

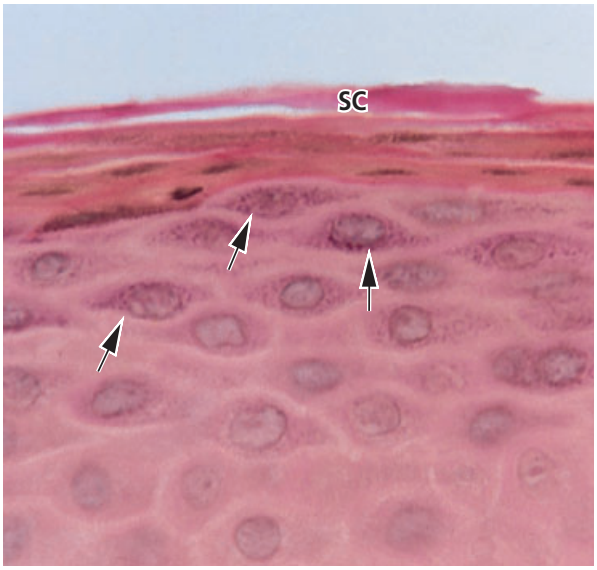

Fig. 1-29

Summary: The keratinocyte undergoes continuous differentiation on its way from the basal layer to the surface of the epithelium. Thus, once the keratinocyte has left the basement membrane it can no longer divide but maintains a capacity for production of protein (tonofilaments and keratohyalin granules). In the granular layer, the keratinocyte is deprived of its energy- and protein-producing apparatus (probably by enzymatic breakdown) and is abruptly converted into a keratin-filled cell which, via the stratum corneum, is shed from the epithelial surface.

Fig. 1-30 illustrates a portion of the epithelium of the alveolar (lining) mucosa. In contrast to the epithelium of the gingiva, the lining mucosa has no stratum corneum. Notice that cells containing nuclei can be identified in all layers, from the basal layer to the surface of the epithelium.

Fig. 1-30

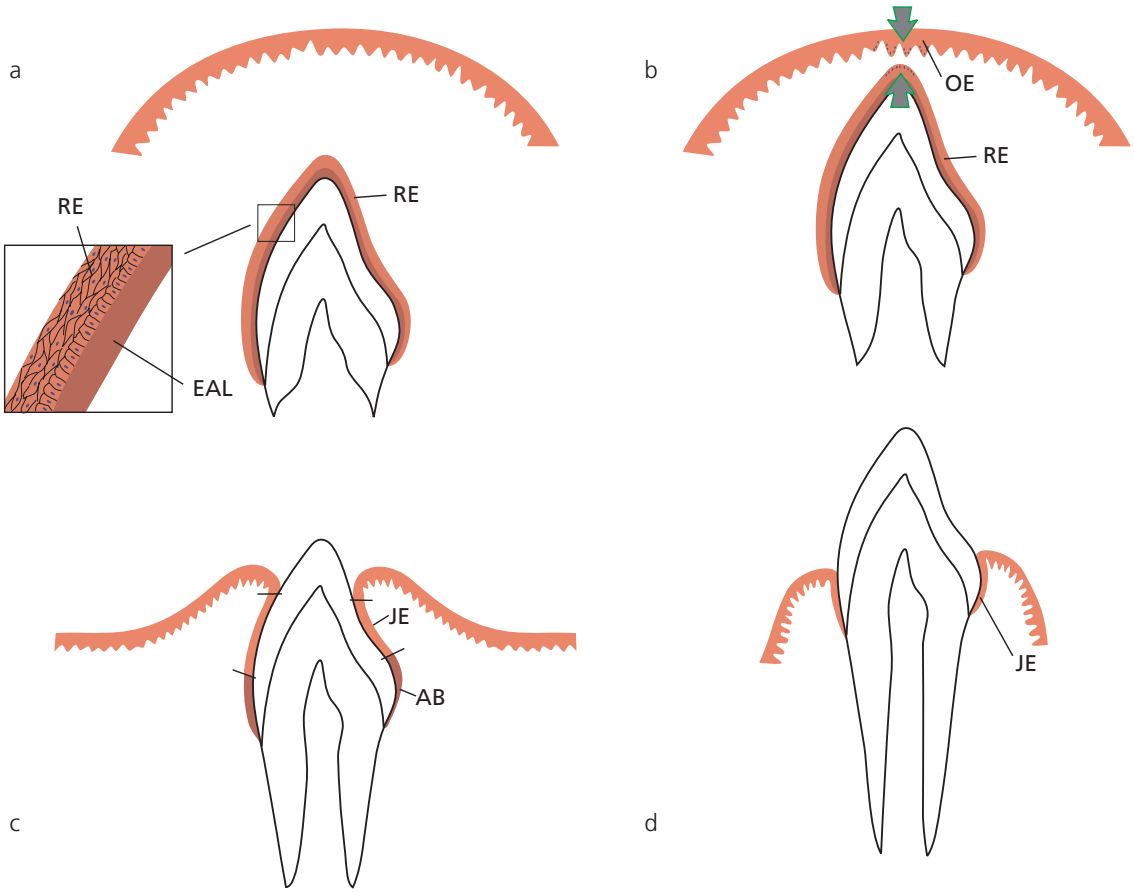

Fig. 1-31

Dento-gingival epithelium

The tissue components of the dento-gingival region achieve their final structural characteristics in conjunction with the eruption of the teeth. This is illustrated in Fig. 1-31a–d.

Fig. 1-31a When the enamel of the tooth is fully developed, the enamel-producing cells (ameloblasts) become reduced in height, produce a basal lamina and form, together with cells from the outer enamel epithelium, the so-called reduced dental epithelium (RE). The basal lamina (epithelial attachment lamina: EAL) lies in direct contact with the enamel. The contact between this lamina and the epithelial cells is maintained by hemidesmosomes. The reduced enamel epithelium surrounds the crown of the tooth from the moment the enamel is properly mineralized until the tooth starts to erupt.

Fig. 1-31b As the erupting tooth approaches the oral epithelium, the cells of the outer layer of the reduced dental epithelium (RE), as well as the cells of the basal layer of the oral epithelium (OE), show increased mitotic activity (arrows) and start to migrate into the underlying connective tissue. The migrating epithelium produces an epithelial mass between the oral epithelium and the reduced dental epithelium so that the tooth can erupt without bleeding. The former ameloblasts do not divide.

Fig. 1-31c When the tooth has penetrated into the oral cavity, large portions immediately apical to the incisal area of the enamel are covered by a junctional epithelium (JE) containing only a few layers of cells. The cervical region of the enamel, however, is still covered by ameloblasts (AB) and outer cells of the reduced dental epithelium.

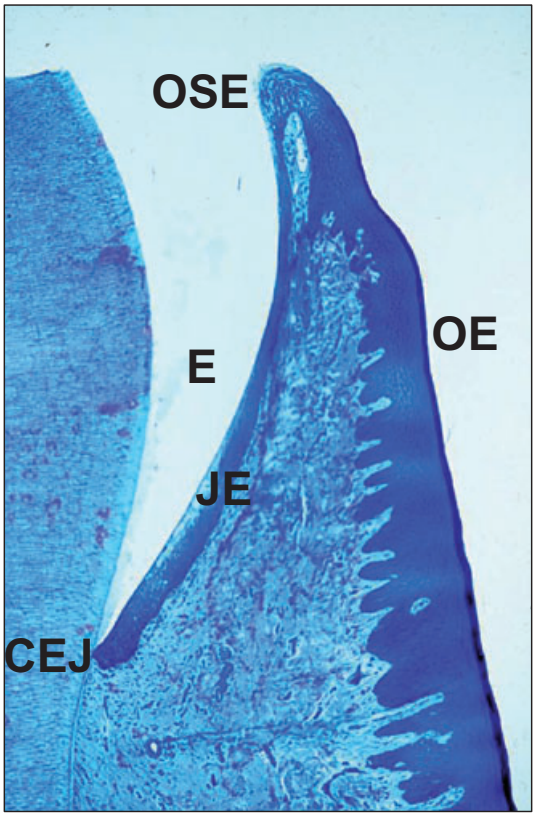

Fig. 1-32

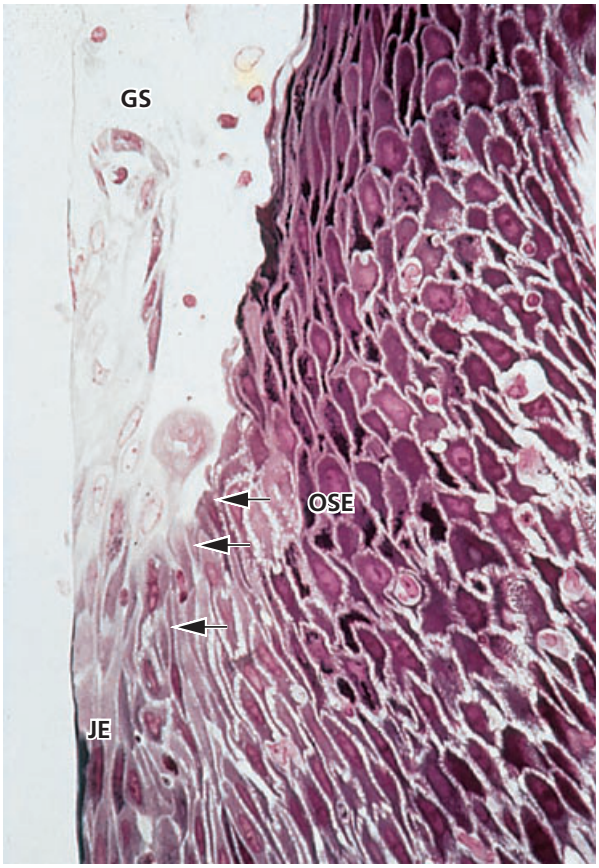

Fig. 1-33

Fig. 1-31d During the later phases of tooth eruption, all cells of the reduced enamel epithelium are replaced by a junctional epithelium. This epithelium is continuous with the oral epithelium and provides the attachment between the tooth and the gingiva. If the free gingiva is excised after the tooth has fully erupted, a new junctional epithelium, indistinguishable from that found following tooth eruption, will develop during healing. The fact that this new junctional epithelium has developed from the oral epithelium indicates that the cells of the oral epithelium possess the ability to differentiate into cells of junctional epithelium.

Fig. 1-32 is a histologic section cut through the border area between the tooth and the gingiva, i.e. the *dentogingival region*. The enamel (E) is to the left. To the right are the *junctional epithelium* (JE), the *oral sulcular epithelium* (OSE), and the *oral epithelium* (OE). The oral sulcular epithelium covers the shallow groove, the gingival sulcus, located between the enamel and the top of the free gingiva. The junctional epithelium differs morphologically from the oral sulcular epithelium and oral epithelium, while the two latter are structurally very similar. Although individual variation may occur, the junctional epithelium is usually widest in its coronal portion (about 15–20 cell layers), but becomes thinner (3–4 cells) towards the cementoenamel junction (CEJ). The borderline between the junctional epithelium and the underlying connective tissue does not present epithelial rete pegs except when inflamed.

Fig. 1-33 The junctional epithelium has a free surface at the bottom of the *gingival sulcus* (GS). Like the oral sulcular epithelium and the oral epithelium, the junctional epithelium is continuously renewed through cell division in the basal layer. The cells migrate to the base of the gingival sulcus from where they are shed. The border between the junctional epithelium (JE) and the oral sulcular epithelium (OSE) is indicated by arrows. The cells of the oral sulcular epithelium are cuboidal and the surface of this epithelium is keratinized.

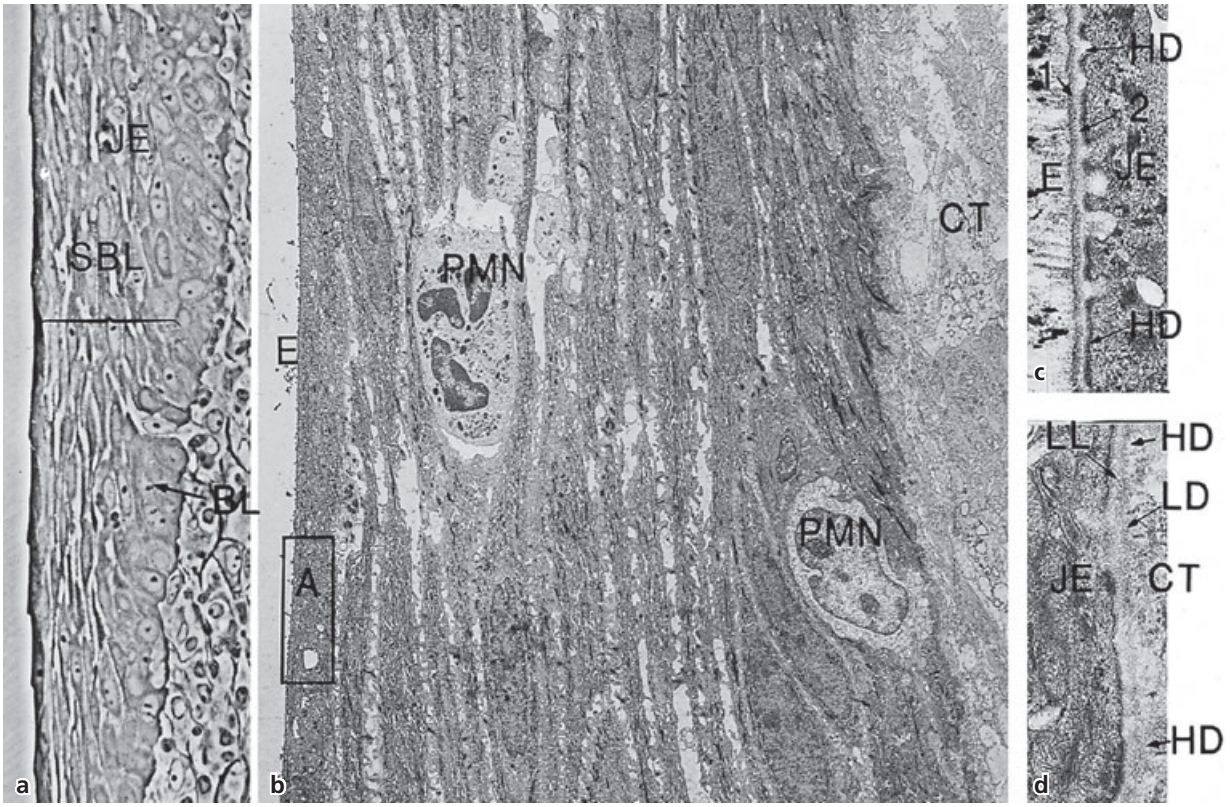

Fig. 1-34

Fig. 1-34 illustrates different characteristics of the junctional epithelium. As can be seen in Fig. 1-34a, the cells of the junctional epithelium (JE) are arranged into one basal layer (BL) and several suprabasal layers (SBL). Fig. 1-34b demonstrates that the basal cells as well as the suprabasal cells are flattened with their long axis parallel to the tooth surface. (CT = connective tissue, E = enamel space.)

There are distinct differences between the oral sulcular epithelium, the oral epithelium and the junctional epithelium:

1. The size of the cells in the junctional epithelium is, relative to the tissue volume, larger than in the oral epithelium.
2. The intercellular space in the junctional epithelium is, relative to the tissue volume, comparatively wider than in the oral epithelium.
3. The number of desmosomes is smaller in the junctional epithelium than in the oral epithelium.

Note the comparatively wide intercellular spaces between the oblong cells of the junctional epithelium, and the presence of two neutrophilic granulocytes (PMN) which are traversing the epithelium.

The framed area (A) is shown in a higher magnification in Fig. 1-34c, from which it can be seen that the basal cells of the junctional epithelium are not in direct contact with the enamel (E). Between the enamel and the epithelium (JE) one electron-dense zone (1) and one electron-lucent zone (2) can be seen. The electron-lucent zone is in contact with the cells of the junctional epithelium (JE). These two zones have a structure very similar to that of the lamina densa (LD) and lamina lucida (LL) in the basement membrane area (i.e. the epithelium (JE)–connective tissue (CT) interface) described in Fig. 1-23. Furthermore, as seen in Fig. 1-34d, the cell membrane of the junctional epithelial cells harbors hemidesmosomes (HD) towards the enamel as it does towards the connective tissue. Thus, the interface between the enamel and the junctional epithelium is similar to the interface between the epithelium and the connective tissue.

Fig. 1-35 is a schematic drawing of the most apically positioned cell in the junctional epithelium. The enamel (E) is depicted to the left in the drawing. It can be seen that the electron-dense zone (1) between the junctional epithelium and the enamel can be considered a continuation of the lamina densa (LD) in the basement membrane of the connective tissue side. Similarly, the electron-lucent zone (2) can be considered a continuation of the lamina lucida (LL). It should be noted, however, that at variance with the epithelium–connective tissue interface, there are no anchoring fibers (AF) attached to the lamina densa-like structure (1) adjacent to the enamel. On the other hand, like the basal cells adjacent to the basement membrane (at the connective tissue interface), the cells of the junctional epithelium facing the lamina lucida-like structure (2) harbor hemidesmosomes. Thus, the interface between the junctional epithelium and the enamel is structurally very similar to the

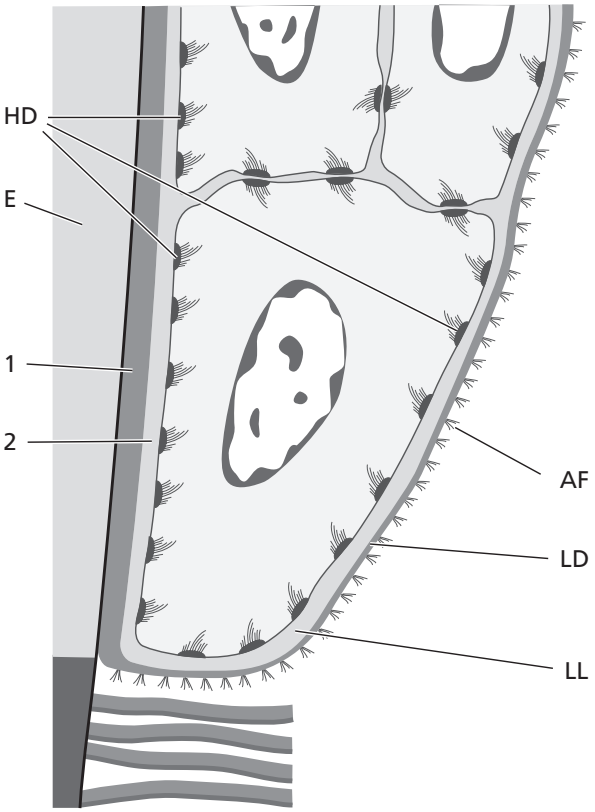

Fig. 1-35

epithelium–connective tissue interface, which means that the junctional epithelium is not only in contact with the enamel but is actually physically attached to the tooth via hemidesmosomes.

Lamina propria

The predominant tissue component of the gingiva is the connective tissue (lamina propria). The major components of the connective tissue are *collagen fibers* (around 60% of connective tissue volume), *fibroblasts* (around 5%), *vessels and nerves* (around 35%) which are embedded in an amorphous ground substance (matrix).

Fig. 1-36 The drawing illustrates a fibroblast (F) residing in a network of connective tissue fibers (CF). The intervening space is filled with matrix (M), which constitutes the "environment" for the cell.

Cells

The different types of cell present in the connective tissue are: (1) *fibroblasts*, (2) *mast cells*, (3) *macrophages*, and (4) *inflammatory cells*.

Fig. 1-37 The *fibroblast* is the predominant connective tissue cell (65% of the total cell population). The fibroblast is engaged in the production of various types of fibers found in the connective tissue, but is also instrumental in the synthesis of the connective tissue matrix. The fibroblast is a spindle-shaped or stellate cell with an oval-shaped nucleus containing one or

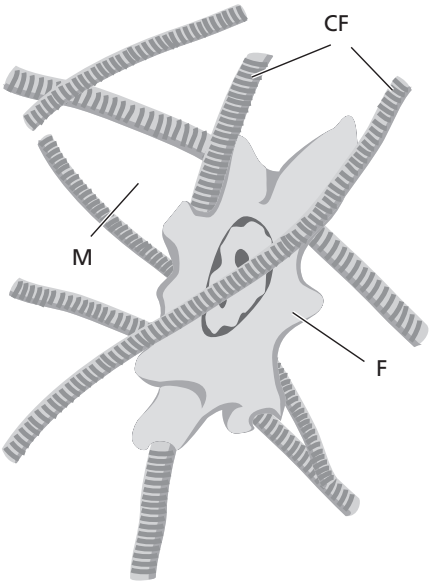

Fig. 1-36

more nucleoli. A part of a fibroblast is shown in electron microscopic magnification. The cytoplasm contains a well developed granular endoplasmic reticulum (E) with ribosomes. The Golgi complex (G) is usually of considerable size and the mitochondria (M) are large and numerous. Furthermore, the cytoplasm contains many fine tonofilaments (F). Adjacent to the cell membrane, all along the periphery of the cell, a large number of vesicles (V) can be found.

Fig. 1-38 The *mast cell* is responsible for the production of certain components of the matrix. This cell also produces vasoactive substances, which can affect the function of the microvascular system and control the flow of blood through the tissue. A mast cell is presented in electron microscopic magnification. The cytoplasm is characterized by the presence of a large number of vesicles (V) of varying size. These vesicles

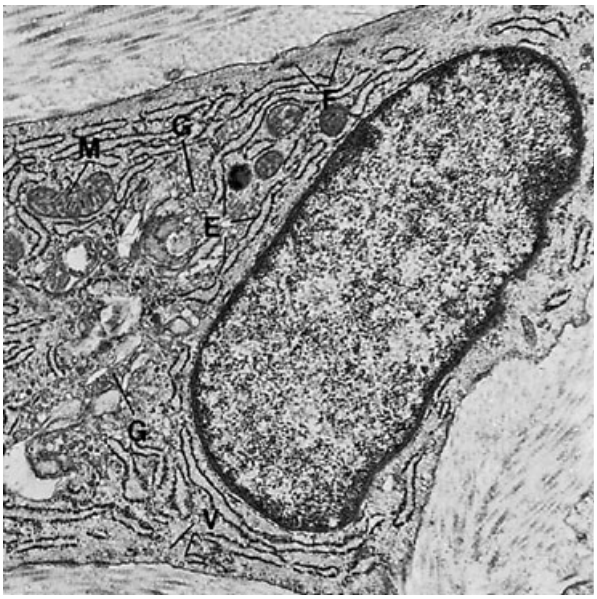

Fig. 1-37

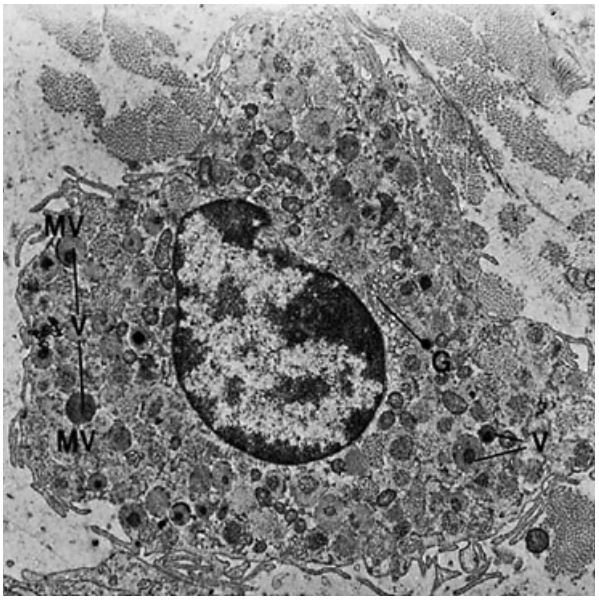

Fig. 1-38

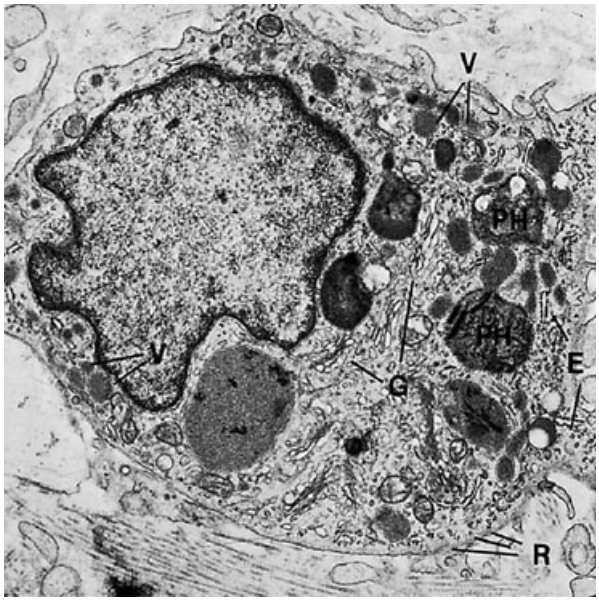

Fig. 1-39

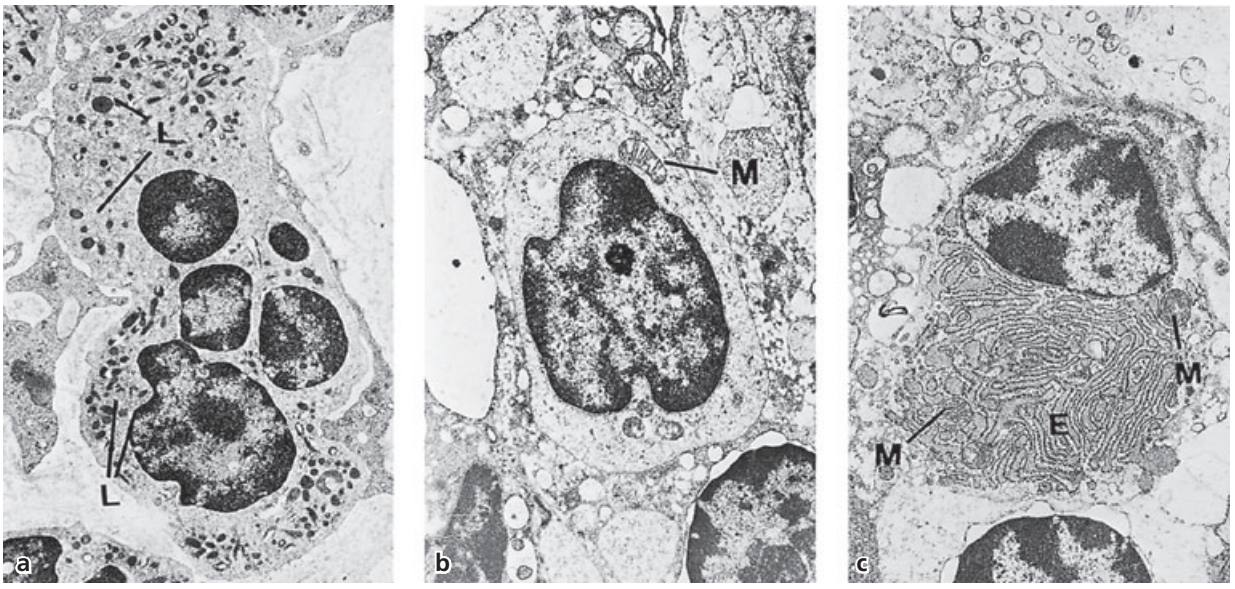

Fig. 1-40

contain biologically active substances such as proteolytic enzymes, histamine and heparin. The Golgi complex (G) is well developed, while granular endoplasmic reticulum structures are scarce. A large number of small cytoplasmic projections, i.e. microvilli (MV), can be seen along the periphery of the cell.

Fig. 1-39 The *macrophage* has a number of different phagocytic and synthetic functions in the tissue. A macrophage is shown in electron microscopic magnification. The nucleus is characterized by numerous invaginations of varying size. A zone of electron-dense chromatin condensations can be seen along the periphery of the nucleus. The Golgi complex (G) is well developed and numerous vesicles (V) of varying size are present in the cytoplasm. Granular endoplasmic reticulum (E) is scarce, but a certain number of free ribosomes (R) are evenly distributed in the cytoplasm. Remnants of phagocytosed material are often found in lysosomal vesicles: phagosomes (PH). In the periphery of the cell, a large number of microvilli of varying size can be seen. Macrophages are particularly numerous in inflamed tissue. They are derived from circulating blood monocytes which migrate into the tissue.

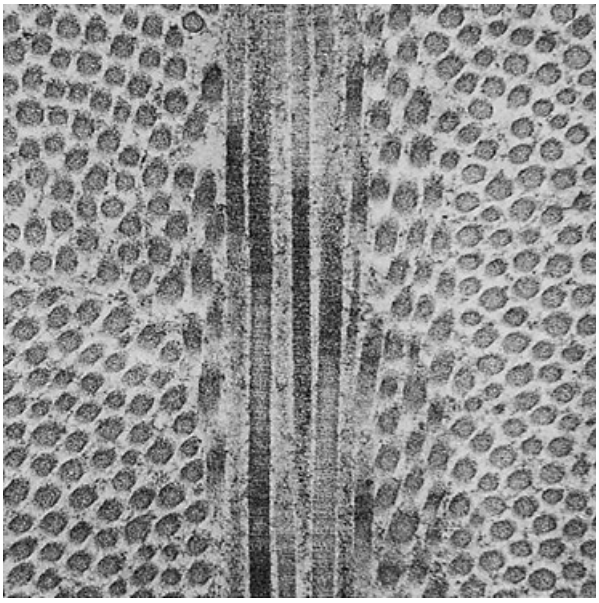

Fig. 1-41

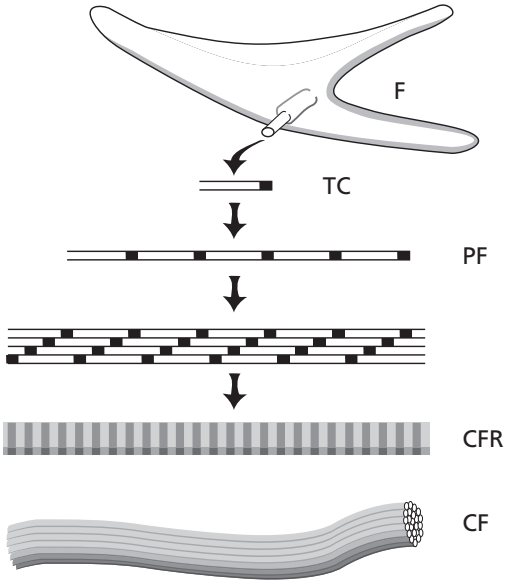

Fig. 1-42

Fig. 1-40 Besides fibroblasts, mast cells and macrophages, the connective tissue also harbors *inflammatory cells* of various types, for example neutrophilic granulocytes, lymphocytes, and plasma cells.

The *neutrophilic granulocytes*, also called *polymorphonuclear leukocytes*, have a characteristic appearance (Fig. 1-40a). The nucleus is lobulate and numerous lysosomes (L), containing lysosomal enzymes, are found in the cytoplasm.

The *lymphocytes* (Fig. 1-40b) are characterized by an oval to spherical nucleus containing localized areas of electron-dense chromatin. The narrow border of cytoplasm surrounding the nucleus contains numerous free ribosomes, a few mitochondria (M), and, in localized areas, endoplasmic reticulum with fixed ribosomes. Lysosomes are also present in the cytoplasm.

The *plasma cells* (Fig. 1-40c) contain an eccentrically located spherical nucleus with radially deployed electron-dense chromatin. Endoplasmic reticulum (E) with numerous ribosomes is found randomly distributed in the cytoplasm. In addition, the cytoplasm contains numerous mitochondria (M) and a well developed Golgi complex.

Fibers

The connective tissue fibers are produced by the fibroblasts and can be divided into: (1) *collagen fibers*, (2) *reticulin fibers*, (3) *oxytalan fibers*, and (4) *elastic fibers*.

Fig. 1-41 The *collagen fibers* predominate in the gingival connective tissue and constitute the most essential components of the periodontium. The electronmicrograph shows cross sections and longitudinal sections of collagen fibers. The collagen fibers have a characteristic cross-banding with a periodicity of 700 Å between the individual dark bands.

Fig. 1-42 illustrates some important features of the synthesis and the composition of collagen fibers produced by fibroblasts (F). The smallest unit, the collagen molecule, is often referred to as *tropocollagen*. A tropocollagen molecule (TC) which is seen in the upper portion of the drawing is approximately 3000 Å long and has a diameter of 15 Å. It consists of three polypeptide chains intertwined to form a helix. Each chain contains about 1000 amino acids. One third of these are glycine and about 20% proline and hydroxyproline, the latter being found practically only in collagen. Tropocollagen synthesis takes place inside the fibroblast from which the tropocollagen molecule is secreted into the extracellular space. Thus, the polymerization of tropocollagen molecules to collagen fibers takes place in the extracellular compartment. First, tropocollagen molecules are aggregated longitudinally to *protofibrils* (PF), which are subsequently laterally aggregated parallel to *collagen fibrils* (CFR), with an overlapping of the tropocollagen molecules by about 25% of their length. Due to the fact that special refraction conditions develop after staining at the sites where the tropocollagen molecules adjoin, a cross-banding with a periodicity of approximately 700 Å occurs under light microscopy. The *collagen fibers* (CF) are bundles of collagen fibrils, aligned in such a way that the fibers also exhibit a cross-banding with a periodicity of 700 Å. In the tissue, the fibers are usually arranged in bundles. As the collagen fibers mature, covalent crosslinks are formed between the tropocollagen molecules, resulting in an age-related reduction in collagen solubility.

Cementoblasts and *osteoblasts* are cells which also possess the ability to produce collagen.

Fig. 1-43

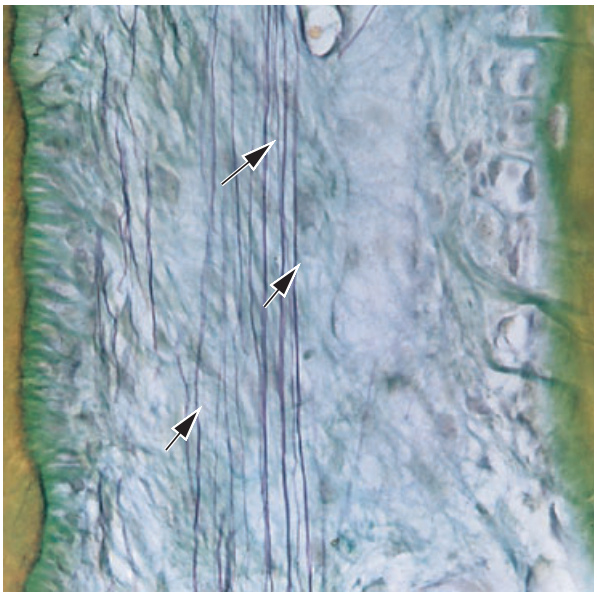

Fig. 1-44

Fig. 1-43 *Reticulin fibers*, as seen in this photomicrograph, exhibit argyrophilic staining properties and are numerous in the tissue adjacent to the basement membrane (arrows). However, reticulin fibers also occur in large numbers in the loose connective tissue surrounding the blood vessels. Thus, reticulin fibers are present at the epithelium–connective tissue and the endothelium–connective tissue interfaces.

Fig 1-44 *Oxytalan fibers* are scarce in the gingiva but numerous in the periodontal ligament. They are composed of long thin fibrils with a diameter of approximately 150 Å. These connective tissue fibers can be demonstrated light microscopically only after previous oxidation with peracetic acid. The photomicrograph illustrates oxytalan fibers (arrows) in the periodontal ligament, where they have a course mainly parallel to the long axis of the tooth. The function of these fibers is as yet unknown. The cementum is seen to the left and the alveolar bone to the right.

Fig. 1-45 *Elastic fibers* in the connective tissue of the gingiva and periodontal ligament are only present in association with blood vessels. However, as seen in this photomicrograph, the lamina propria and submucosa of the alveolar (lining) mucosa contain numerous elastic fibers (arrows). The gingiva (G) seen coronal to the mucogingival junction (MGJ) contains no elastic fibers except in association with the blood vessels.

Fig. 1-46 Although many of the collagen fibers in the gingiva and the periodontal ligament are irregularly or randomly distributed, most tend to be arranged in groups of bundles with a distinct orientation. According to their insertion and course in the tissue, the oriented bundles in the gingiva can be divided into the following groups:

1. *Circular fibers* (CF) are fiber bundles which run their course in the free gingiva and encircle the tooth in a cuff- or ring-like fashion.
2. *Dento-gingival fibers* (DGF) are embedded in the cementum of the supra-alveolar portion of the root and project from the cementum in a fan-like configuration out into the free gingival tissue of the facial, lingual and interproximal surfaces.
3. *Dento-periosteal fibers* (DPF) are embedded in the same portion of the cementum as the dento-gingival fibers, but run their course apically over the vestibular and lingual bone crest and terminate in the tissue of the attached gingiva. In the border area between the free and attached gingiva, the epithelium often lacks support by underlying oriented collagen fiber bundles. In this area the free gingival groove (GG) is often present.
4. *Trans-septal fibers* (TF), seen on the drawing to the right, extend between the supra-alveolar cementum of approximating teeth. The trans-septal fibers run straight across the interdental septum and are embedded in the cementum of adjacent teeth.

Fig. 1-47 illustrates in a histologic section the orientation of the trans-septal fiber bundles (arrows) in the supra-alveolar portion of the interdental area. It should be observed that, besides connecting the cementum (C) of adjacent teeth, the trans-septal fibers also connect the supra-alveolar cementum (C) with the crest of the alveolar bone (AB). The four groups

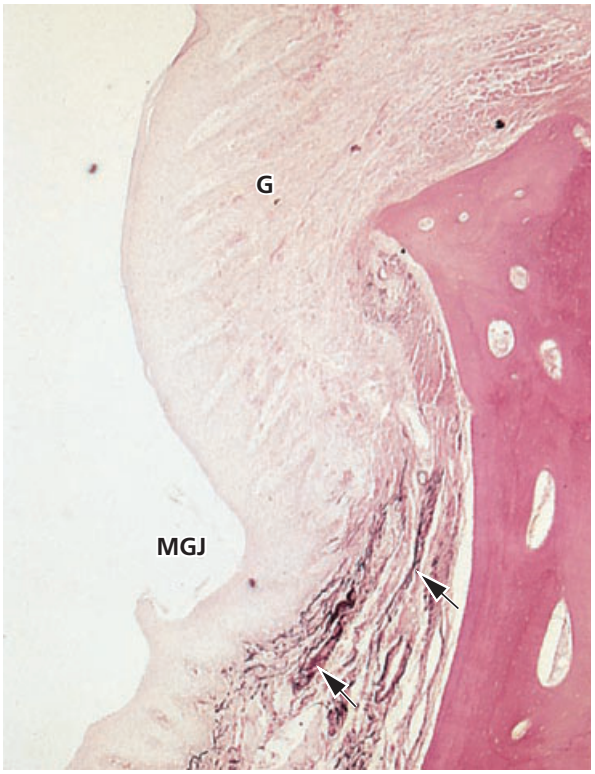

Fig. 1-45

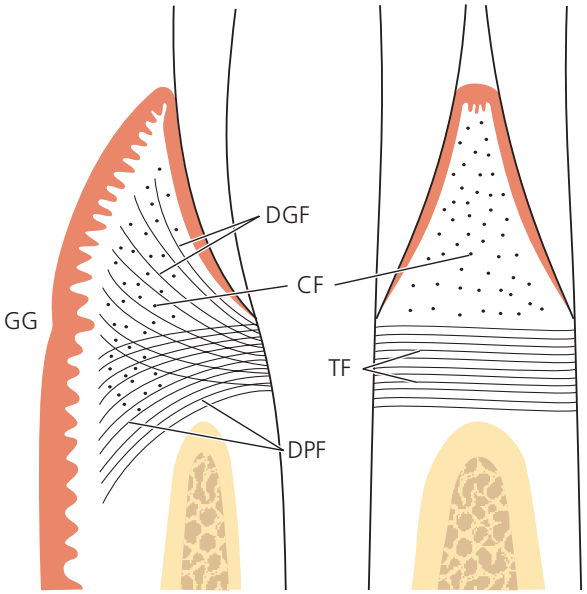

Fig. 1-46

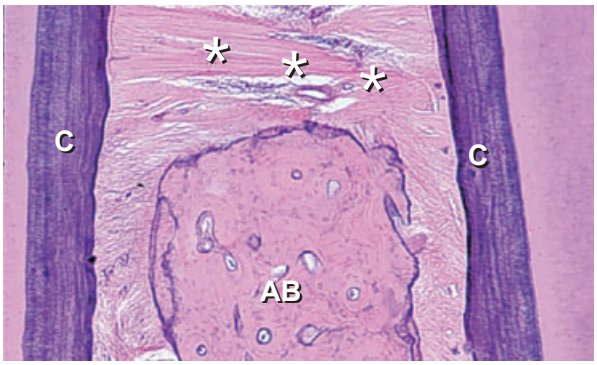

Fig. 1-47

of collagen fiber bundles presented in Fig. 1-46 reinforce the gingiva and provide the resilience and tone which is necessary for maintaining its architectural form and the integrity of the dento-gingival attachment.

Matrix

The *matrix* of the connective tissue is produced mainly by the fibroblasts, although some constituents are produced by mast cells, and other components are derived from the blood. The matrix is the medium in which the connective tissue cells are embedded and it is essential for the maintenance of the normal function of the connective tissue. Thus, the transportation of water, electrolytes, nutrients, metabolites, etc., to and from the individual connective tissue cells occurs within the matrix. The main constituents of the connective tissue matrix are protein–carbohydrate macromolecules. These complexes are normally divided into *proteoglycans* and *glycoproteins*. The proteoglycans contain *glycosaminoglycans* as the carbohydrate units (hyaluronan sulfate, heparan sulfate, etc.), which are attached to one or more protein chains via covalent bonds. The carbohydrate component is always predominant in the proteoglycans. The glycosaminoglycan called hyaluronan or "hyaluronic acid" is probably not bound to protein. The glycoproteins (fibronectin, osteonectin, etc.) also contain polysaccharides, but these macromolecules are different from glycosaminoglycans. The protein component is predominating in glycoproteins. In the macromolecules, mono- or oligosaccharides are connected to one or more protein chains via covalent bonds.

Fig. 1-48 Normal function of the connective tissue depends on the presence of proteoglycans and gly-

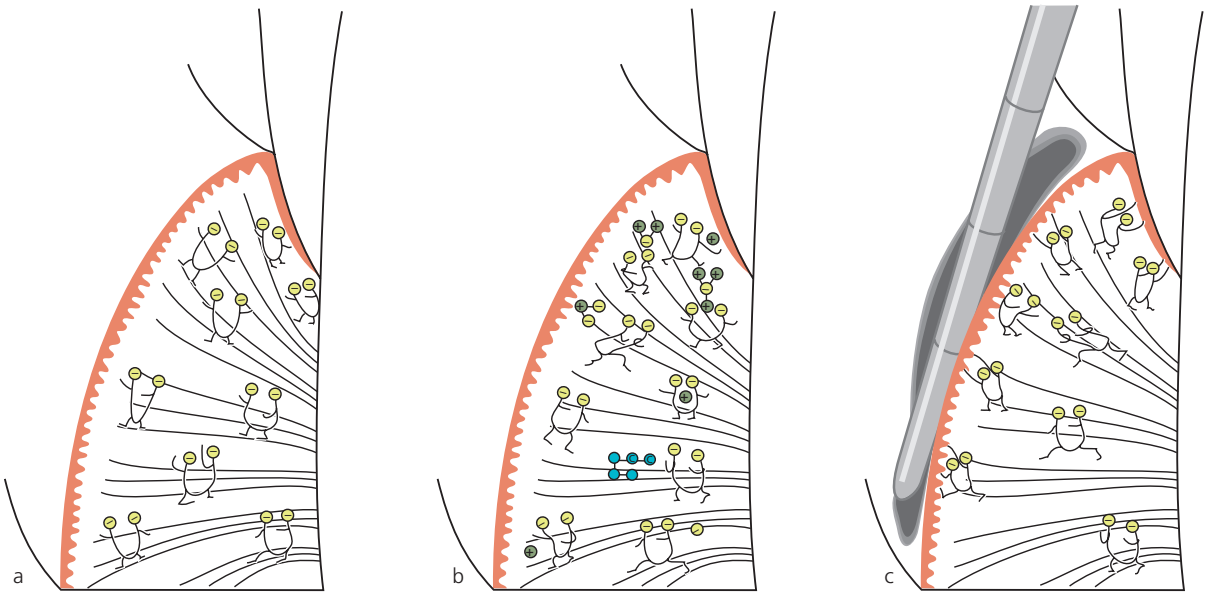

Fig. 1-48

cosaminoglycans. The carbohydrate moiety of the proteoglycans, the glycosaminoglycans (), are large, flexible, chain formed, negatively charged molecules, each of which occupies a rather large space (Fig. 1-48a). In such a space, smaller molecules, e.g. water and electrolytes, can be incorporated while larger molecules are prevented from entering (Fig. 1-48b). The proteoglycans thereby regulate diffusion and fluid flow through the matrix and are important determinants for the fluid content of the tissue and the maintenance of the osmotic pressure. In other words, the proteoglycans act as a molecule filter and, in addition, play an important role in the regulation of cell migration (movements) in the tissue. Due to their structure and hydration, the macromolecules exert resistance towards deformation, thereby serving as regulators of the consistency of the connective tissue (Fig. 1-48c). If the gingiva is suppressed, the macromolecules become deformed. When the pressure is eliminated, the macromolecules regain their original form. Thus, the macromolecules are important for the resilience of the gingiva.

Epithelial mesenchymal interaction

There are many examples of the fact that during the embryonic development of various organs, a mutual inductive influence occurs between the epithelium and the connective tissue. The development of the teeth is a characteristic example of such phenomena. The connective tissue is, on the one hand, a determining factor for normal development of the tooth bud while, on the other, the enamel epithelia exert a definite influence on the development of the mesenchymal components of the teeth.

It has been suggested that tissue differentiation in the adult organism can be influenced by environmental factors. The skin and mucous membranes, for instance, often display increased keratinization and hyperplasia of the epithelium in areas which are exposed to mechanical stimulation. Thus, the tissues seem to adapt to environmental stimuli. The presence of keratinized epithelium on the masticatory mucosa has been considered to represent an adaptation to mechanical irritation released by mastication. However, research has demonstrated that the char-

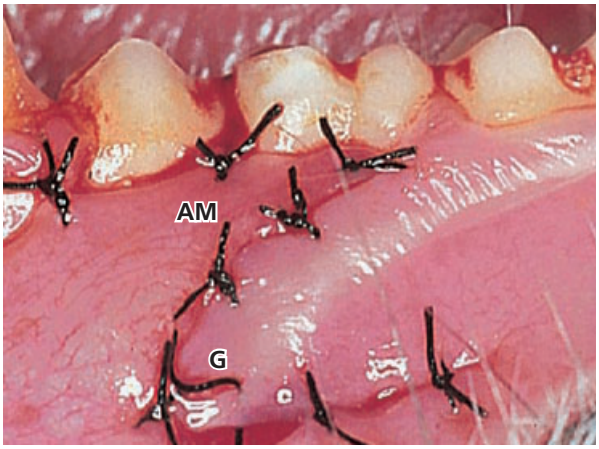

Fig. 1-49

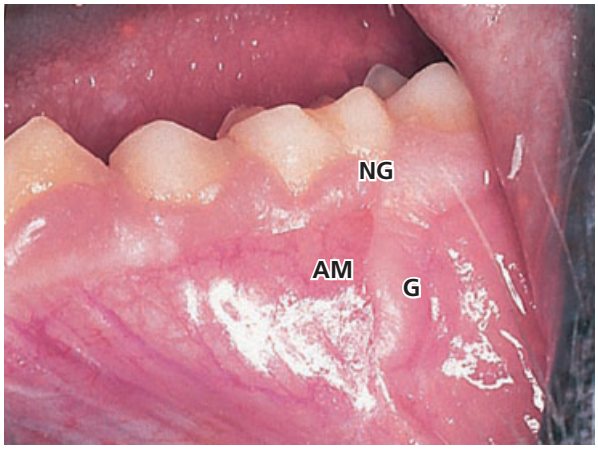

Fig. 1-50

Fig. 1-51

Fig. 1-52

acteristic features of the epithelium in such areas are genetically determined. Some pertinent observations are reported in the following:

Fig. 1-49 shows an area in a monkey where the gingiva (G) and the alveolar mucosa (AM) have been transposed by a surgical procedure. The alveolar mucosa is placed in close contact with the teeth while the gingiva is positioned in the area of the alveolar mucosa.

Fig. 1-50 shows the same area, as seen in Fig. 1-49, 4 months later. Despite the fact that the transplanted gingiva (G) is mobile in relation to the underlying bone, like the alveolar mucosa, it has retained its characteristic, morphologic features of a masticatory mucosa. However, a narrow zone of new keratinized gingiva (NG) has regenerated between the transplanted alveolar mucosa (AM) and the teeth.

Fig. 1-51 presents a histologic section cut through the transplanted gingiva seen in Fig. 1-50. Since elastic fibers are lacking in the gingival connective tissue (G), but are numerous (small arrows) in the connective tissue of the alveolar mucosa (AM), the transplanted gingival tissue can readily be identified. The epithelium covering the transplanted gingival tissue exhibits a distinct keratin layer (between large arrows) on the surface, and also the configuration of the epithelium–connective tissue interface (i.e. rete pegs and connective tissue papillae) is similar to that of normal non-transplanted gingiva. Thus, the heterotopically located gingival tissue has maintained its original specificity. This observation demonstrates that the characteristics of the gingiva are genetically determined rather than being the result of functional adaptation to environmental stimuli.

Fig. 1-52 shows a histologic section cut through the coronal portion of the area of transplantation (shown in Fig. 1-50). The transplanted gingival tissue (G) shown in Fig. 1-51 can be seen in the lower portion of the photomicrograph. The alveolar mucosa transplant (AM) is seen between the large arrows in the middle of the illustration. After surgery, the alveolar mucosa transplant was positioned in close contact with the teeth as seen in Fig. 1-49. After healing, a narrow zone of keratinized gingiva (NG) developed coronal to the alveolar mucosa transplant (see Fig. 1-50). This new zone of gingiva (NG), which can be seen in the upper portion of the histologic section, is covered by keratinized epithelium and the connective tissue contains no purple-stained elastic fibers. In addition, it is important to notice that the junction between keratinized and non-keratinized epithelium (large arrows) corresponds exactly to the junction between "elastic" and "inelastic" connective tissue (small arrows). The connective tissue of the new gingiva has regenerated from the connective tissue of the supra-alveolar and periodontal ligament compartments and has separated the alveolar mucosal transplant (AM) from the tooth (see Fig. 1-53). However, it is most likely that the epithelium which covers the new gingiva has migrated from the adjacent epithelium of the alveolar mucosa.

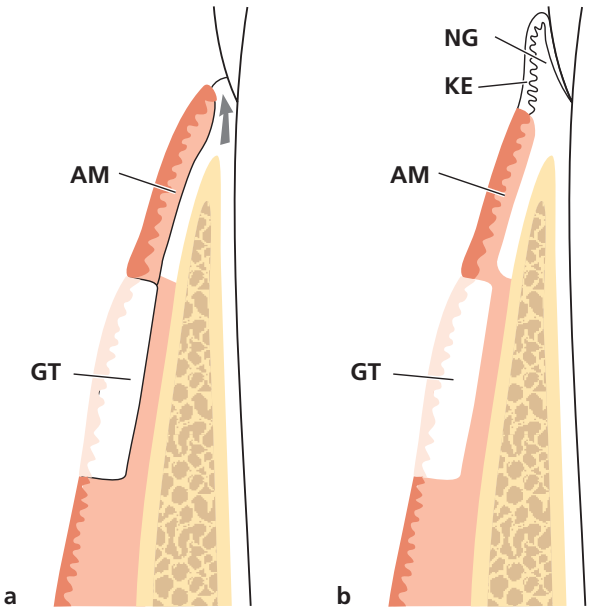

Fig. 1-53

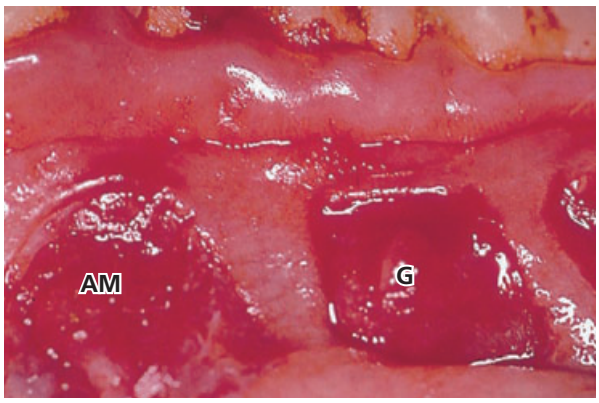

Fig. 1-54

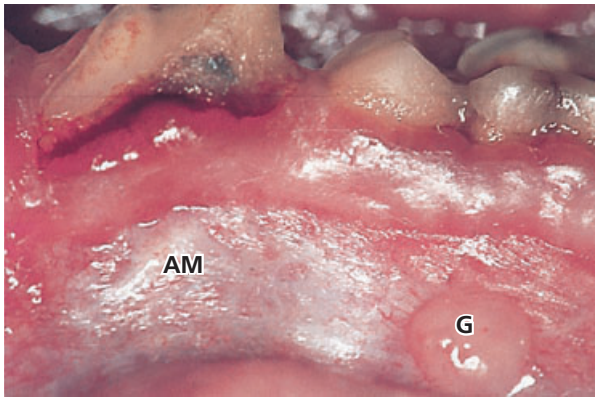

Fig. 1-55

Fig. 1-53 presents a schematic drawing of the development of the new, narrow zone of keratinized gingiva (NG) seen in Figs. 1-50 and 1-52.

Fig. 1-53a Granulation tissue has proliferated coronally along the root surface (arrow) and has separated the alveolar mucosa transplant (AM) from its original contact with the tooth surface.

Fig. 1-53b Epithelial cells have migrated from the alveolar mucosal transplant (AM) on to the newly formed gingival connective tissue (NG). Thus, the newly formed gingiva has become covered with a keratinized epithelium (KE) which originated from the non-keratinized epithelium of the alveolar mucosa (AM). This implies that the newly formed gingival connective tissue (NG) possesses the ability to induce changes in the differentiation of the epithelium originating from the alveolar mucosa. This epithelium, which is normally non-keratinized, apparently differentiates to keratinized epithelium because of stimuli arising from the newly formed gingival connective tissue (NG). (GT: gingival transplant.)

Fig. 1-54 illustrates a portion of gingival connective tissue (G) and alveolar mucosal connective tissue (AM) which, after transplantation, has healed into wound areas in the alveolar mucosa. Epithelialization of these transplants can only occur through migration of epithelial cells from the surrounding alveolar mucosa.

Fig. 1-55 shows the transplanted gingival connective tissue (G) after re-epithelialization. This tissue portion has attained an appearance similar to that of the normal gingiva, indicating that this connective tissue is now covered by keratinized epithelium. The transplanted connective tissue from the alveolar mucosa (AM) is covered by non-keratinized epithelium, and has the same appearance as the surrounding alveolar mucosa.

Fig. 1-56 presents two histologic sections through the area of the transplanted gingival connective tissue. The section shown in Fig. 1-56a is stained for elastic fibers (arrows). The tissue in the middle without elastic fibers is the transplanted gingival connective tissue (G). Fig. 1-56b shows an adjacent section stained with hematoxylin and eosin. By comparing Figs. 1-56a and 1-56b it can be seen that:

1. The transplanted gingival connective tissue is covered by keratinized epithelium (between arrowheads)
2. The epithelium–connective tissue interface has the same wavy course (i.e. rete pegs and connective tissue papillae) as seen in normal gingiva.

The photomicrographs seen in Figs. 1-56c and 1-56d illustrate, at a higher magnification, the border area between the alveolar mucosa (AM) and the transplanted gingival connective tissue (G). Note the distinct relationship between keratinized epithelium (arrow) and "inelastic" connective tissue (arrowheads), and between non-keratinized epithelium and

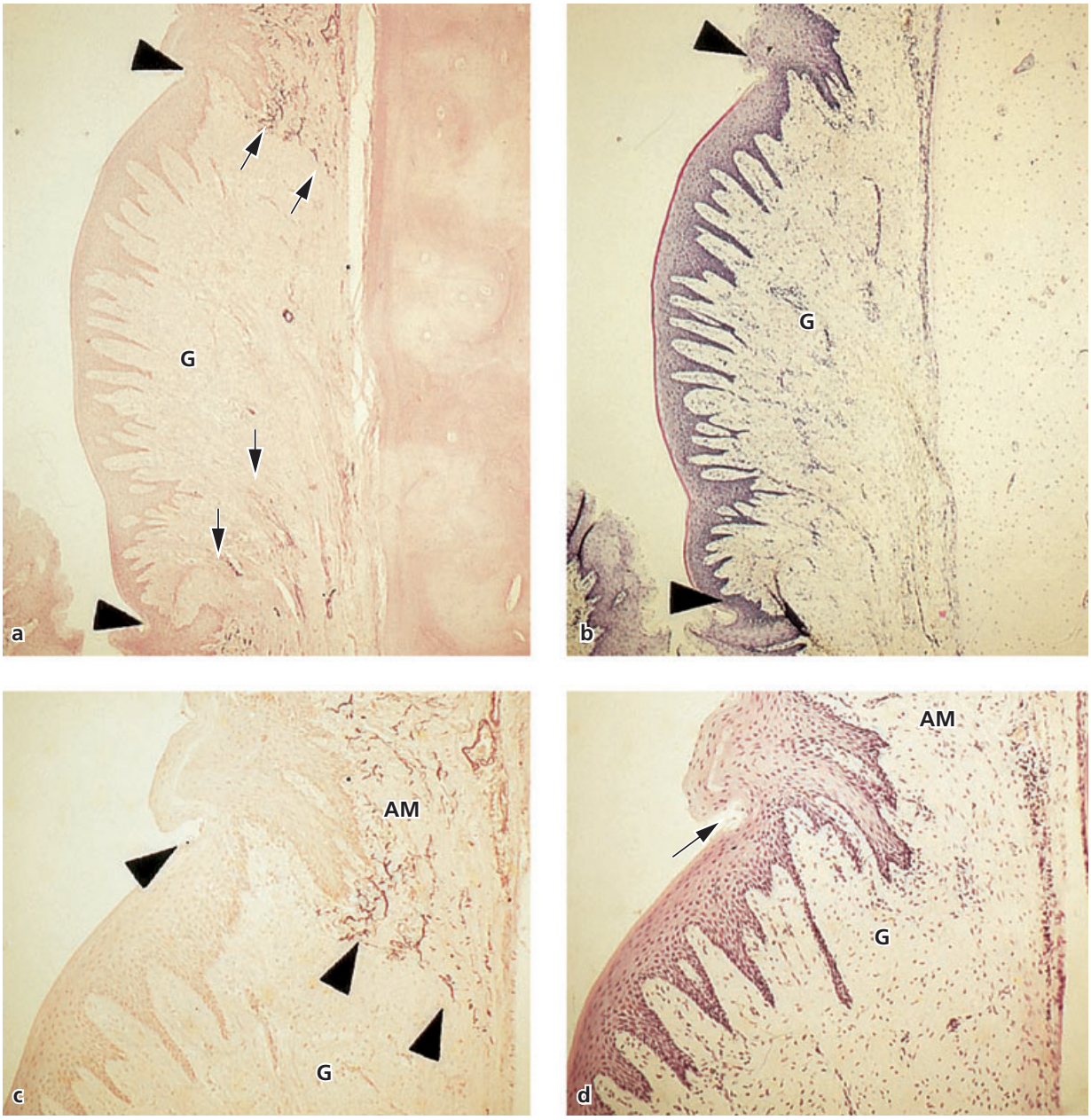

Fig. 1-56

"elastic" connective tissue. The establishment of such a close relationship during healing implies that the transplanted gingival connective tissue possesses the ability to alter the differentiation of epithelial cells as previously suggested (Fig. 1-53). From being non-keratinizing cells, the cells of the epithelium of the alveolar mucosa have evidently become keratinizing cells. This means that the specificity of the gingival epithelium is determined by genetic factors inherent in the connective tissue.

Periodontal ligament

The periodontal ligament is the soft, richly vascular and cellular connective tissue which surrounds the roots of the teeth and joins the root cementum with the socket wall. In the coronal direction, the periodontal ligament is continuous with the lamina propria of the gingiva and is demarcated from the gingiva by the collagen fiber bundles which connect the alveolar bone crest with the root (the alveolar crest fibers).

Fig. 1-57 is a radiograph of a mandibular premolar–molar region. In radiographs two types of alveolar bone can be distinguished:

1. The part of the alveolar bone which covers the alveolus, called "lamina dura" (arrows)
2. The portion of the alveolar process which, in the radiograph, has the appearance of a meshwork. This is called the "spongy bone".

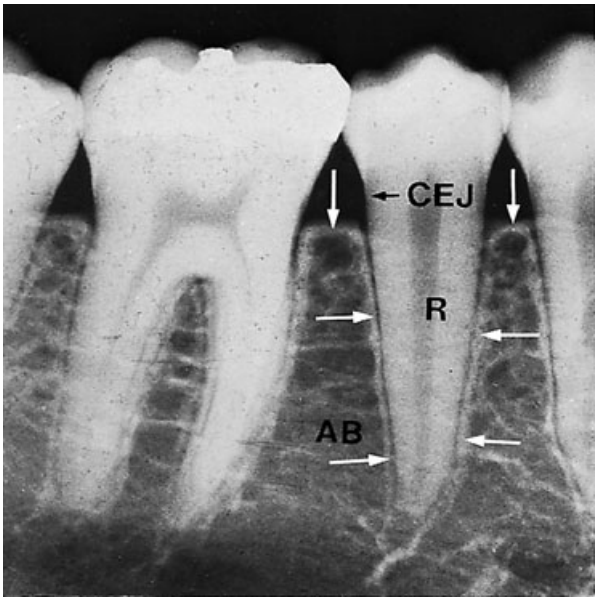

Fig. 1-57

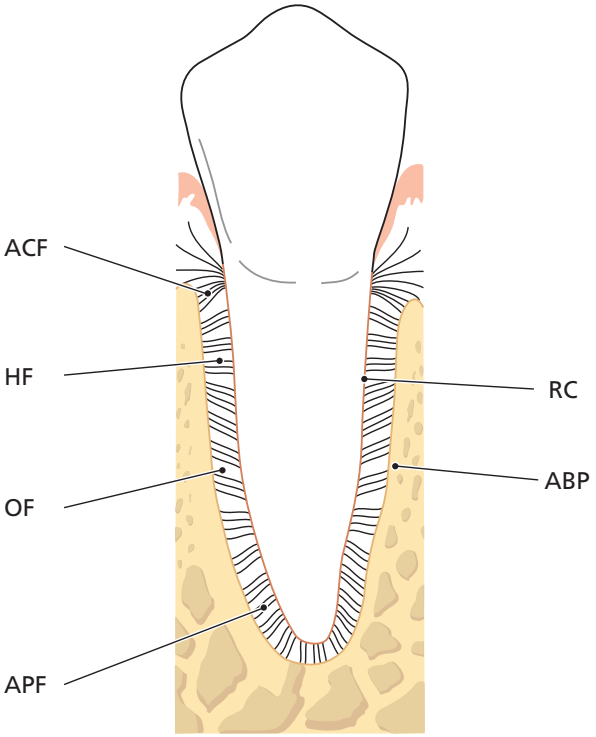

Fig. 1-58

The periodontal ligament is situated in the space between the roots (R) of the teeth and the lamina dura or the alveolar bone proper (arrows). The alveolar bone (AB) surrounds the tooth to a level approximately 1 mm apical to the cemento-enamel junction (CEJ). The coronal border of the bone is called the *alveolar crest* (arrows).

The periodontal ligament space has the shape of an hourglass and is narrowest at the mid-root level. The width of the periodontal ligament is approximately 0.25 mm (range 0.2–0.4 mm). The presence of a periodontal ligament permits forces, elicited during masticatory function and other tooth contacts, to be distributed to and resorbed by the alveolar process via the alveolar bone proper. The periodontal ligament is also essential for the mobility of the teeth. Tooth mobility is to a large extent determined by the width, height, and quality of the periodontal ligament (see Chapters 14 and 51).

Fig. 1-58 illustrates in a schematic drawing how the periodontal ligament is situated between the alveolar bone proper (ABP) and the root cementum (RC). The tooth is joined to the bone by bundles of collagen fibers which can be divided into the following main groups according to their arrangement:

1. *Alveolar crest fibers* (ACF)
2. *Horizontal fibers* (HF)
3. *Oblique fibers* (OF)
4. *Apical fibers* (APF).

Fig. 1-59 The periodontal ligament and the root cementum develop from the loose connective tissue (the follicle) which surrounds the tooth bud. The schematic drawing depicts the various stages in the organization of the periodontal ligament which forms concomitantly with the development of the root and the eruption of the tooth.

Fig. 1-59a The tooth bud is formed in a crypt of the bone. The collagen fibers produced by the fibroblasts in the loose connective tissue around the tooth bud are embedded, during the process of their maturation, into the newly formed cementum immediately apical to the cemento-enamel junction (CEJ). These fiber bundles oriented towards the coronal portion of the bone crypt will later form the dento-gingival fiber group, the dento-periosteal fiber group and the transseptal fiber group which belong to the oriented fibers of the gingiva (see Fig. 1-46).

Fig. 1-59b The true periodontal ligament fibers, the *principal fibers*, develop in conjunction with the eruption of the tooth. First, fibers can be identified entering the most marginal portion of the alveolar bone.

Fig. 1-59c Later, more apically positioned bundles of oriented collagen fibers are seen.

Fig. 1-59d The orientation of the collagen fiber bundles alters continuously during the phase of tooth eruption. First, when the tooth has reached contact in occlusion and is functioning properly, the fibers of the periodontal ligament associate into groups of

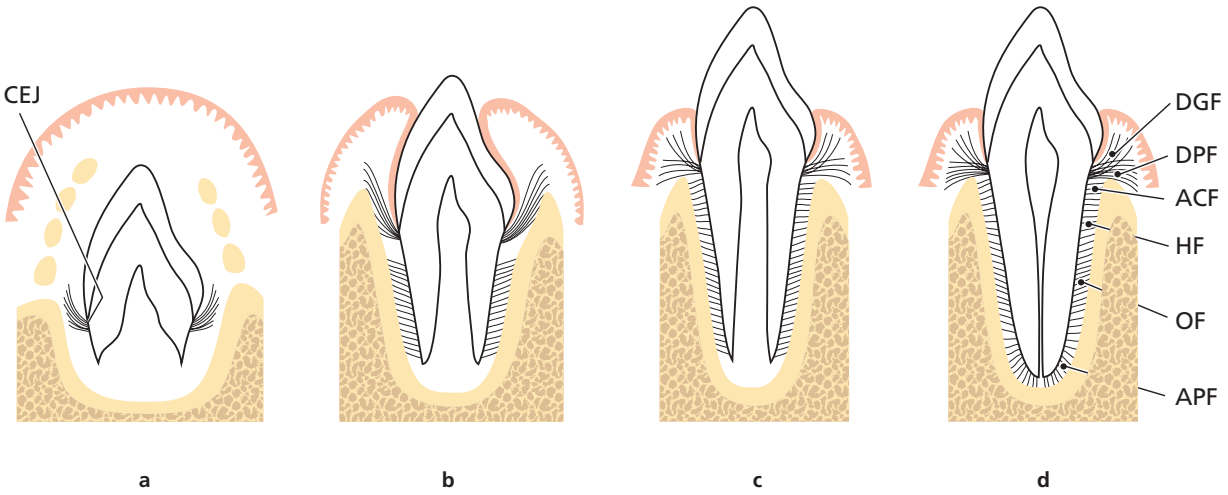

Fig. 1-59

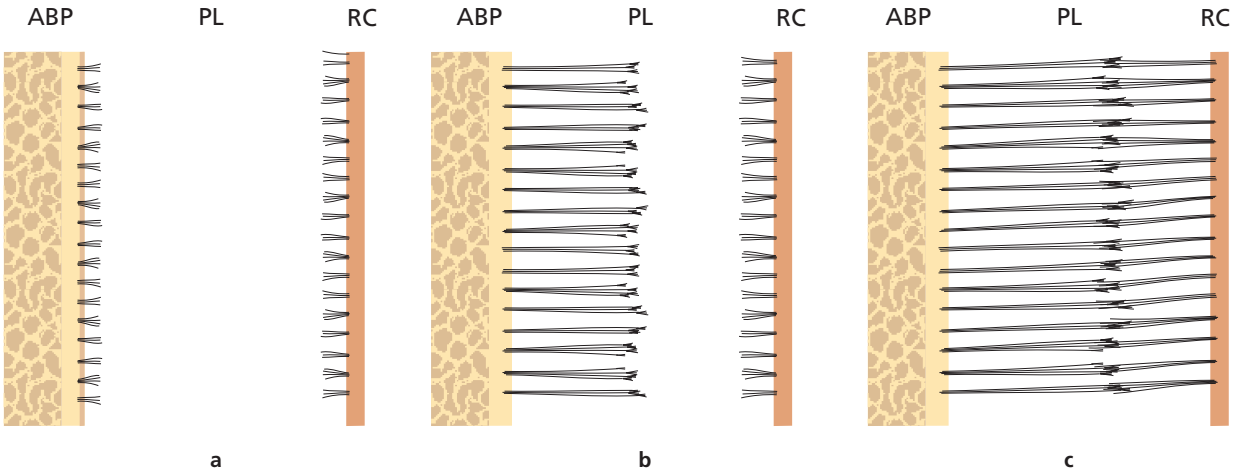

Fig. 1-60

well oriented dentoalveolar collagen fibers demonstrated in Fig. 1-58. These collagen structures undergo constant remodeling (i.e. resorption of old fibers and formation of new ones).

Fig. 1-60 This schematic drawing illustrates the development of the principal fibers of the periodontal ligament. The alveolar bone proper (ABP) is seen to the left, the periodontal ligament (PL) is depicted in the center and the root cementum (RC) is seen to the right.

Fig. 1-60a First, small, fine, brush-like fibrils are detected arising from the root cementum and projecting into the PL space. At this stage the surface of the bone is covered by osteoblasts. From the surface of the bone only a small number of radiating, thin collagen fibrils can be seen.

Fig. 1-60b Later on, the number and thickness of fibers entering the bone increase. These fibers radiate towards the loose connective tissue in the mid-portion of the periodontal ligament area (PL), which contains more or less randomly oriented collagen fibrils. The fibers originating from the cementum are still short while those entering the bone gradually become longer. The terminal portions of these fibers carry finger-like projections.

Fig. 1-60c The fibers originating from the cementum subsequently increase in length and thickness and fuse in the periodontal ligament space with the fibers originating from the alveolar bone. When the tooth, following eruption, reaches contact in occlusion and starts to function, the principal fibers become organized in bundles and run continuously from the bone to the cementum.

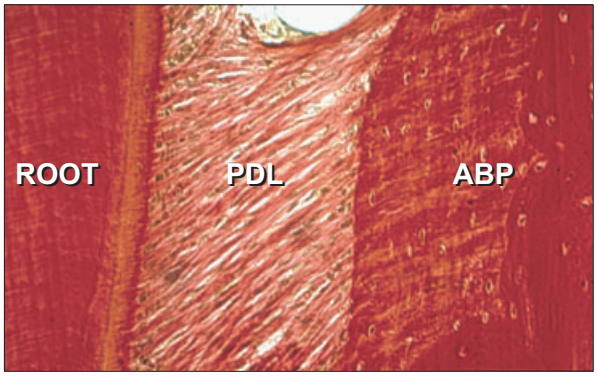

Fig. 1-61a

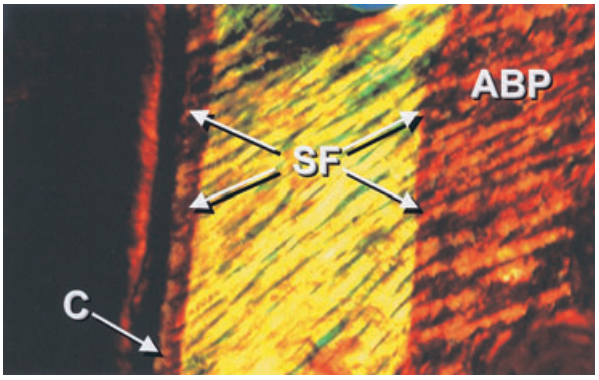

Fig. 1-61b

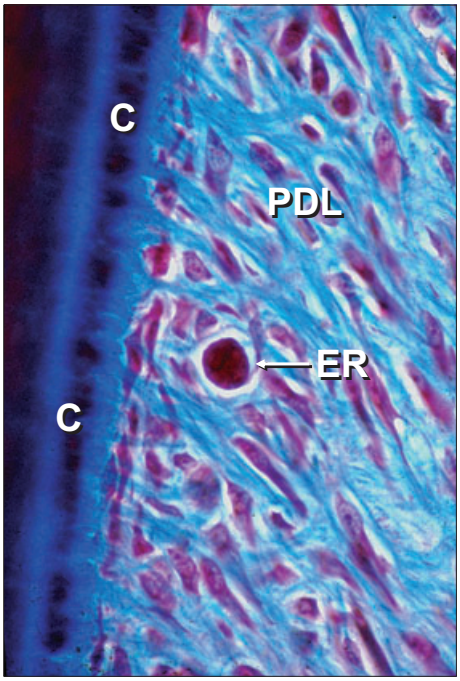

Fig. 1-62a

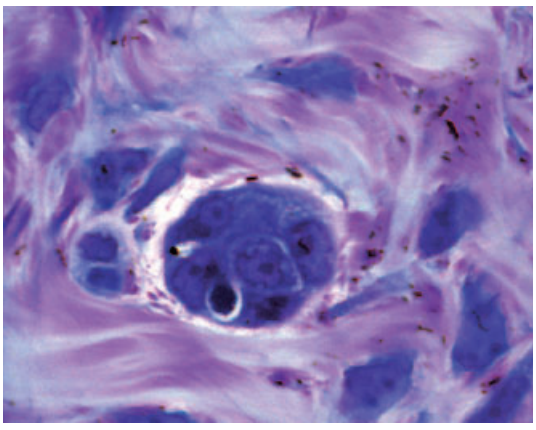

Fig. 1-62b

Fig. 1-61a illustrates how the principal fibers of the periodontal ligament (PDL) run continuously from the root cementum to the alveolar bone proper (ABP). The principal fibers embedded in the cementum (Sharpey's fibers) have a smaller diameter but are more numerous than those embedded in the alveolar bone proper (Sharpey's fibers).

Fig. 1-61b presents a polarized version of Fig. 1-61a. In this illustration the Sharpey's fibers (SF) can be seen penetrating not only the cementum (C) but also the entire width of the alveolar bone proper (ABP). The periodontal ligament also contains a few elastic fibers associated with the blood vessels. Oxytalan fibers (see Fig. 1-44) are also present in the periodontal ligament. They have a mainly apico-occlusal orientation and are located in the ligament closer to the tooth than to the alveolar bone. Very often they insert into the cementum. Their function has not been determined.

The cells of the periodontal ligament are: *fibroblasts*, *osteoblasts*, *cementoblasts*, *osteoclasts*, as well as *epithelial cells* and *nerve fibers*. The fibroblasts are aligned along the principal fibers, while cementoblasts line the surface of the cementum, and the osteoblasts line the bone surface.

Fig. 1-62a shows the presence of clusters of epithelial cells (ER) in the periodontal ligament (PDL). These cells, called the *epithelial cell rests of Mallassez*, represent remnants of the Hertwig's epithelial root sheath. The epithelial cell rests are situated in the periodontal ligament at a distance of 15–75 µm from the cementum (C) on the root surface. A group of such epithelial cell rests is seen in a higher magnification in Fig. 1-62b.

Fig. 1-63 Electron microscopically it can be seen that the epithelial cell rests are surrounded by a basement membrane (BM) and that the cell membranes of the epithelial cells exhibit the presence of desmosomes (D) as well as hemidesmosomes (HD). The epithelial cells contain only few mitochondria and have a poorly developed endoplasmic reticulum. This means that they are vital, but resting, cells with minute metabolism.

Fig. 1-64 is a photomicrograph of a periodontal ligament removed from an extracted tooth. This

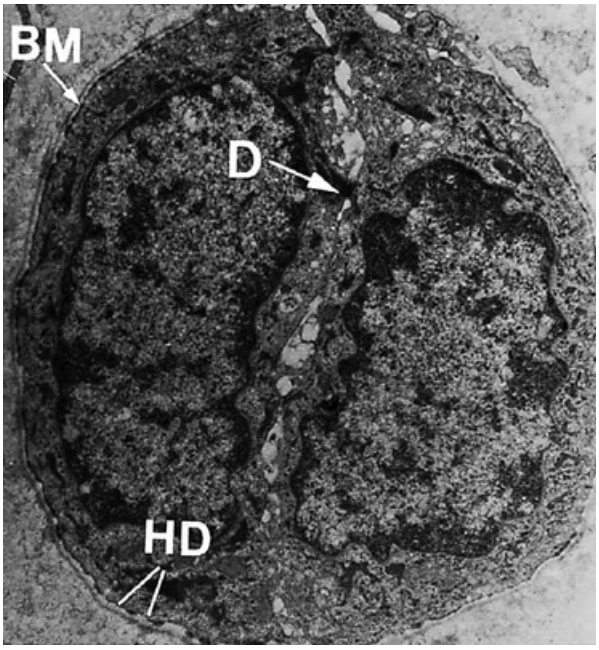

Fig. 1-63

specimen, prepared tangential to the root surface, shows that the epithelial cell rests of Mallassez, which in ordinary histologic sections appear as isolated groups of epithelial cells, in fact form a continuous network of epithelial cells surrounding the root. Their function is unknown at present.

Root cementum

The cementum is a specialized mineralized tissue covering the root surfaces and, occasionally, small portions of the crown of the teeth. It has many features in common with bone tissue. However, the cementum contains no blood or lymph vessels, has no innervation, does not undergo physiologic resorption or remodeling, but is characterized by continuing deposition throughout life. Like other mineralized tissues, it contains collagen fibers embedded in an organic matrix. Its mineral content, which is mainly hydroxyapatite, is about 65% by weight; a little more than that of bone (i.e. 60%). Cementum serves different functions. It attaches the periodontal ligament fibers to the root and contributes to the process of repair after damage to the root surface.

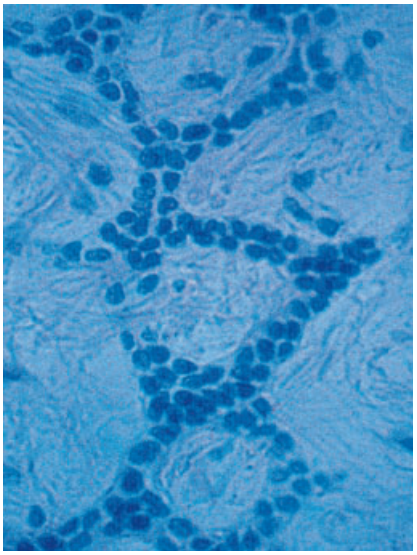

Fig. 1-64

Different forms of cementum have been described:

1. *Acellular, extrinsic fiber cementum* (AEFC) is found in the coronal and middle portions of the root and contains mainly bundles of Sharpey's fibers. This type of cementum is an important part of the attachment apparatus and connects the tooth with the alveolar bone proper.
2. *Cellular, mixed stratified cementum* (CMSC) occurs in the apical third of the roots and in the furcations. It contains both extrinsic and intrinsic fibers as well as cementocytes.
3. *Cellular, intrinsic fiber cementum* (CIFC) is found mainly in resorption lacunae and it contains intrinsic fibers and cementocytes.

Fig. 1-65a shows a portion of a root with adjacent periodontal ligament (PDL). A thin layer of acellular, extrinsic fiber cementum (AEFC) with densely packed extrinsic fibers covers the peripheral dentin. Cementoblasts and fibroblasts can be observed adjacent to the cementum.

Fig. 1-65b represents a scanning electron micrograph of AEFC. Note that the extrinsic fibers attach to the dentin (left) and are continous with the collagen fiber

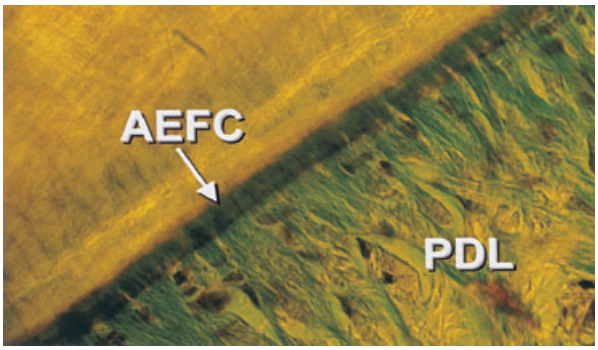

Fig. 1-65a

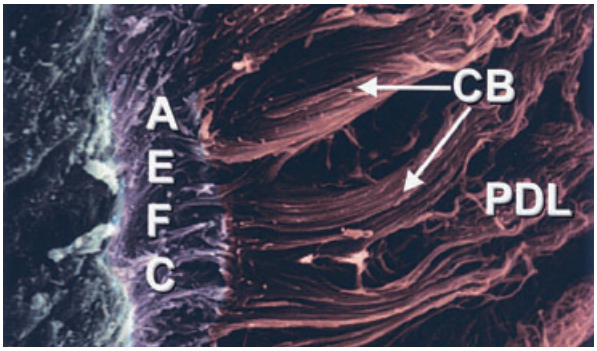

Fig. 1-65b

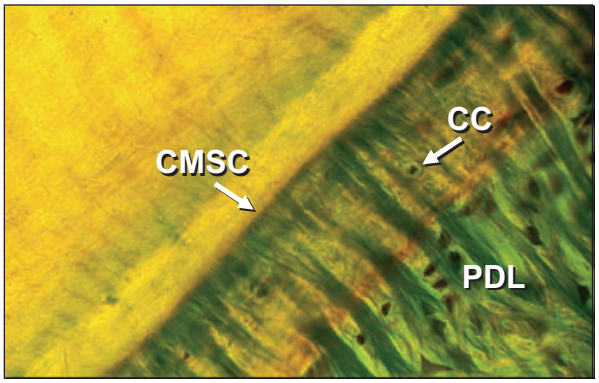

Fig. 1-66

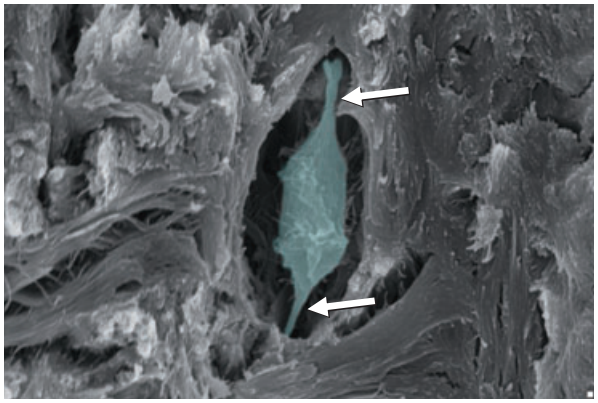

Fig. 1-67

bundles (CB) of the periodontal ligament (PDL). The AEFC is formed concomitantly with the formation of the root dentin. At a certain stage during tooth formation, the epithelial sheath of Hertwig, which lines the newly formed predentin, is fragmented. Cells from the dental follicle then penetrate the epithelial sheath of Hertwig and occupy the area next to the predentin. In this position, the ectomesenchymal cells from the dental follicle differentiate into cementoblasts and begin to produce collagen fibers at right angles to the surface. The first cementum is deposited on the highly mineralized superficial layer of the mantle dentin called the "hyaline layer" which contains enamel matrix proteins and the initial collagen fibers of the cementum. Subsequently, cementoblasts drift away from the surface resulting in increased thickness of the cementum and incorporation of principal fibers.

Fig. 1-66 demonstrates the structure of cellular, mixed stratified cementum (CMSC) which, in contrast to AEFC, contains cells and intrinsic fibers. The CMSC is laid down throughout the functional period of the tooth. The various types of cementum are produced by cementoblasts or periodontal ligament (PDL) cells lining the cementum surface. Some of these cells become incorporated into the cementoid, which subsequently mineralizes to form cementum. The cells which are incorporated in the cementum are called *cementocytes* (CC).

Fig. 1-67 illustrates how cementocytes (blue cell) reside in lacunae in CMSC or CIFC. They communicate with each other through a network of cytoplasmic processes (arrows) running in canaliculi in the cementum. The cementocytes also communicate with

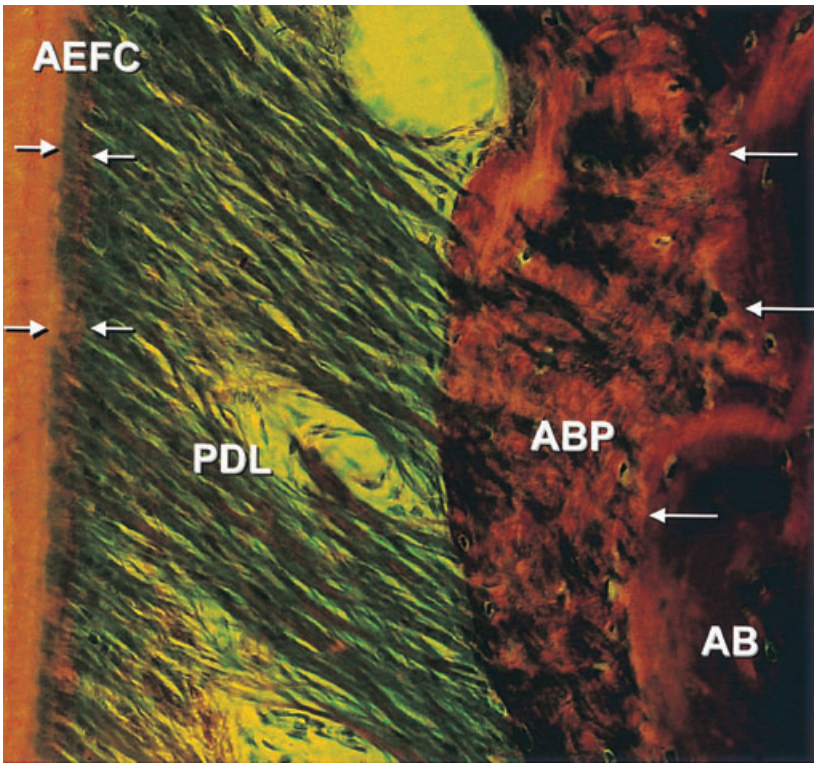

Fig. 1-68a

the cementoblasts on the surface through cytoplasmic processes. The presence of cementocytes allows transportation of nutrients through the cementum, and contributes to the maintenance of the vitality of this mineralized tissue.

Fig. 1-68a is a photomicrograph of a section through the periodontal ligament (PDL) in an area where the root is covered with acellular, extrinsic fiber cementum (AEFC). The portions of the principal fibers of the periodontal ligament which are embedded in the root cementum (arrows) and in the alveolar bone proper (ABP) are called *Sharpey's fibers*. The arrows to the right indicate the border between ABP and the alveolar bone (AB). In AEFC the Sharpey's fibers have a smaller diameter and are more densely packed than their counterparts in the alveolar bone. During the continuous formation of AEFC, portions of the periodontal ligament fibers (principal fibers) adjacent to the root become embedded in the mineralized tissue. Thus, the Sharpey's fibers in the cementum are a direct continuation of the principal fibers in the periodontal ligament and the supra-alveolar connective tissue.

Fig. 1-68b The Sharpey's fibers constitute the *extrinsic fiber system* (E) of the cementum and are produced by fibroblasts in the periodontal ligament. The *intrinsic fiber system* (I) is produced by cementoblasts and is composed of fibers oriented more or less parallel to the long axis of the root.

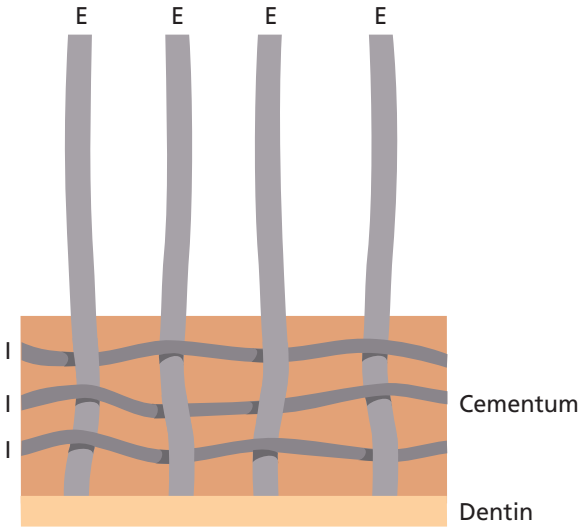

Fig. 1-68b

Fig. 1-69 shows extrinsic fibers penetrating acellular, extrinsic fiber cementum (AEFC). The characteristic cross-banding of the collagen fibers is masked in the cementum because apatite crystals have become deposited in the fiber bundles during the process of mineralization.

Fig. 1-70 In contrast to the bone, the cementum (C) does not exhibit alternating periods of resorption and apposition, but increases in thickness throughout life by deposition of successive new layers. During this

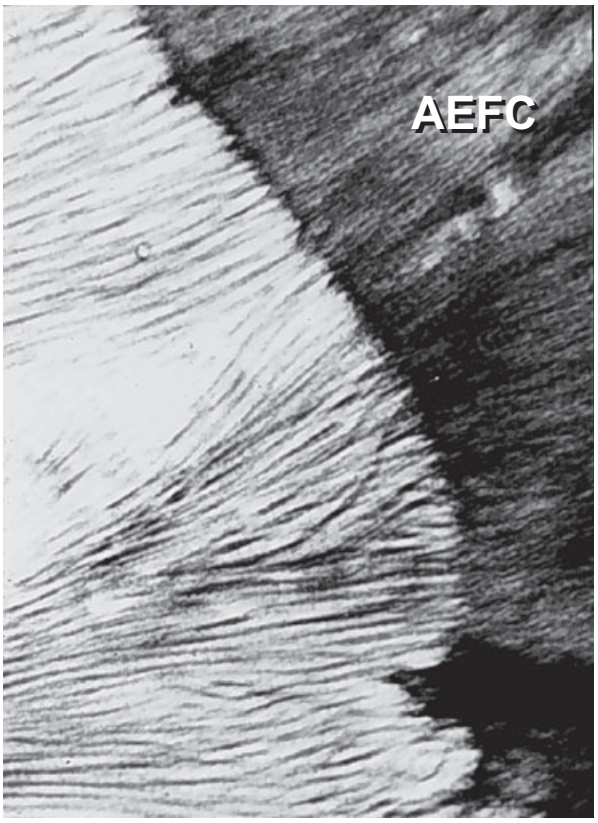

Fig. 1-69

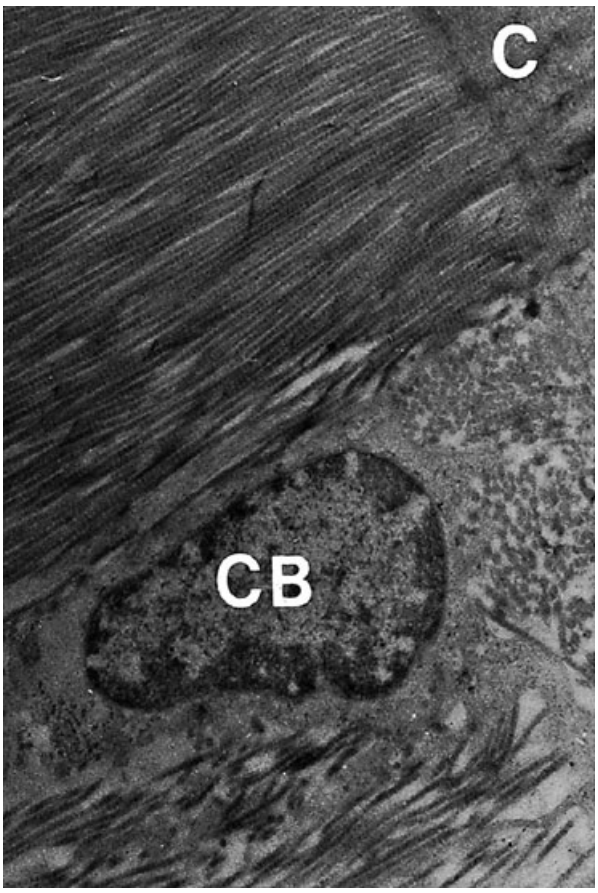

Fig. 1-70

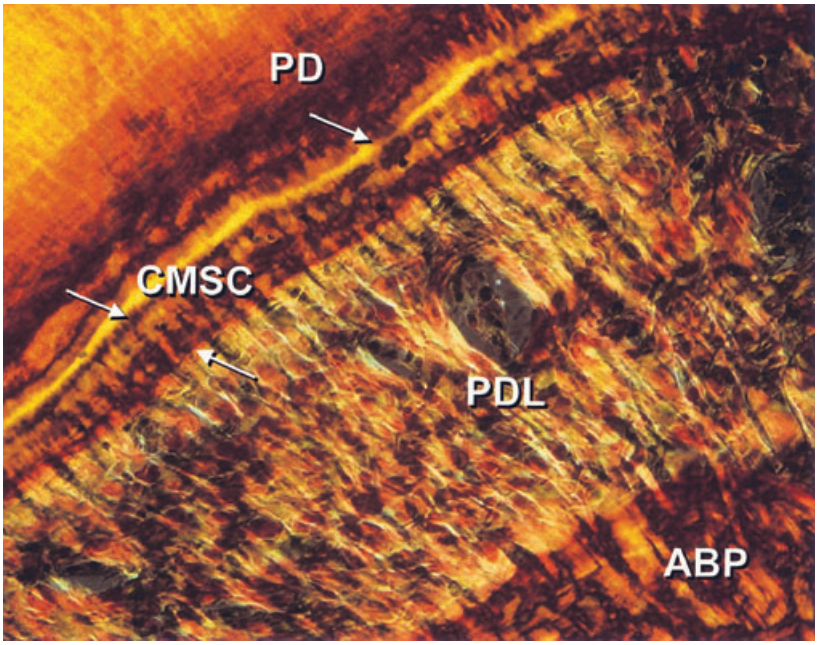

Fig. 1-71

process of gradual apposition, the particular portion of the principal fibers which resides immediately adjacent to the root surface becomes mineralized. Mineralization occurs by the deposition of hydroxyapatite crystals, first within the collagen fibers, later upon the fiber surface, and finally in the interfibrillar matrix. The electronphotomicrograph shows a cementoblast (CB) located near the surface of the cementum (C) and between two inserting principal fiber bundles. Generally, the AEFC is more mineralized than CMSC and CIFC. Sometimes only the periphery of the Sharpey's fibers of the CMSC is mineralized, leaving an unmineralized core within the fiber.

Fig. 1-71 is a photomicrograph of the periodontal ligament (PDL) which resides between the cementum (CMSC) and the alveolar bone proper (ABP). The CMSC is densely packed with collagen fibers oriented parallel to the root surface (intrinsic fibers) and Sharpey's fibers (extrinsic fibers), oriented more or less perpendicularly to the cementum–dentin junction (predentin (PD)). The various types of cementum increase in thickness by gradual apposition throughout life. The cementum becomes considerably wider in the apical portion of the root than in the cervical portion, where the thickness is only 20–50 µm. In the apical root portion the cementum is often 150–250 µm wide. The cementum often contains incremental lines indicating alternating periods of formation. The CMSC is formed after the termination of tooth eruption, and after a response to functional demands.

Alveolar bone

The alveolar process is defined as the parts of the maxilla and the mandible that form and support the sockets of the teeth. The alveolar process develops in conjunction with the development and eruption of the teeth. The alveolar process consists of bone which is formed both by cells from the dental follicle (alveolar bone proper) and cells which are independent of tooth development. Together with the root cementum and the periodontal membrane, the alveolar bone constitutes the attachment apparatus of the teeth, the main function of which is to distribute and resorb forces generated by, for example, mastication and other tooth contacts.

Fig. 1-72 illustrates a cross section through the alveolar process (pars alveolaris) of the maxilla at the mid-root level of the teeth. Note that the bone which covers the root surfaces is considerably thicker at the palatal than at the buccal aspect of the jaw. The walls of the sockets are lined by *cortical bone* (arrows), and the area between the sockets and between the compact jaw bone walls is occupied by *cancellous bone*. The cancellous bone occupies most of the interdental septa but only a relatively small portion of the buccal and palatal bone plates. The cancellous bone contains *bone trabeculae*, the architecture and size of which are partly genetically determined and partly the result of the forces to which the teeth are exposed during function. Note how the bone on the buccal and palatal aspects of the alveolar process varies in thickness from one region to another. The bone plate is thick at the palatal aspect and on the buccal aspect of the molars but thin in the buccal anterior region.

Fig. 1-73 shows cross sections through the mandibular alveolar process at levels corresponding to the coronal (Fig. 1-73a) and apical (Fig. 1-73b) thirds of the roots. The bone lining the wall of the sockets (alveolar bone proper) is often continuous with the compact or cortical bone at the lingual (L) and buccal

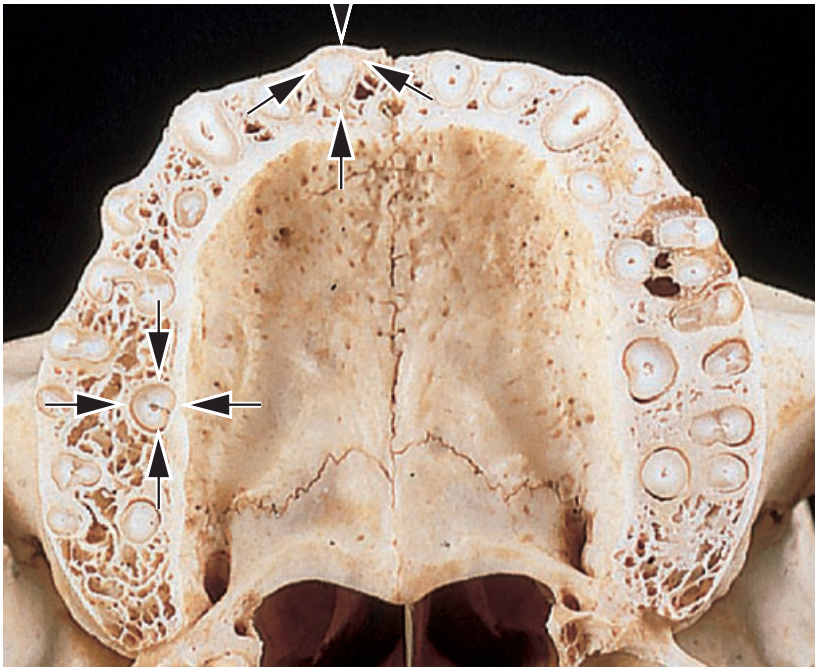

Fig. 1-72

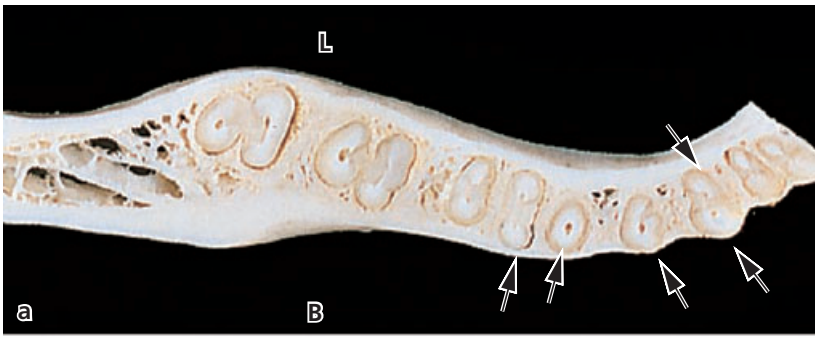

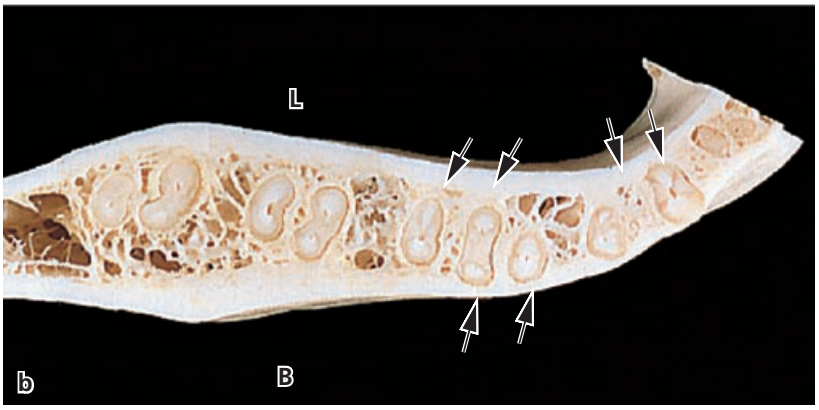

Fig. 1-73

(B) aspects of the alveolar process (arrows). Note how the bone on the buccal and lingual aspects of the alveolar process varies in thickness from one region to another. In the incisor and premolar regions, the bone plate at the buccal aspects of the teeth is considerably thinner than at the lingual aspect. In the molar region, the bone is thicker at the buccal than at the lingual surfaces.

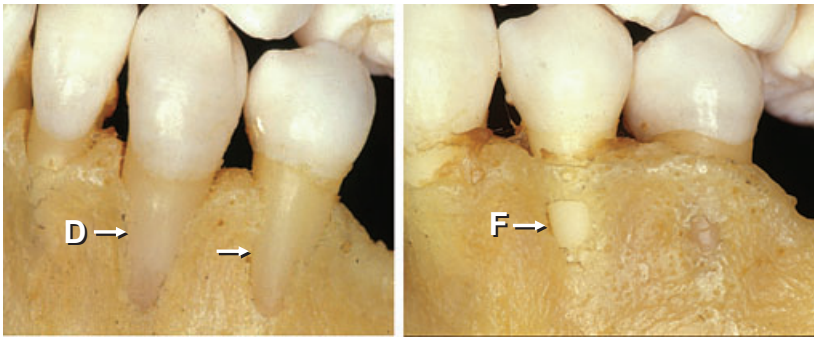

Fig. 1-74

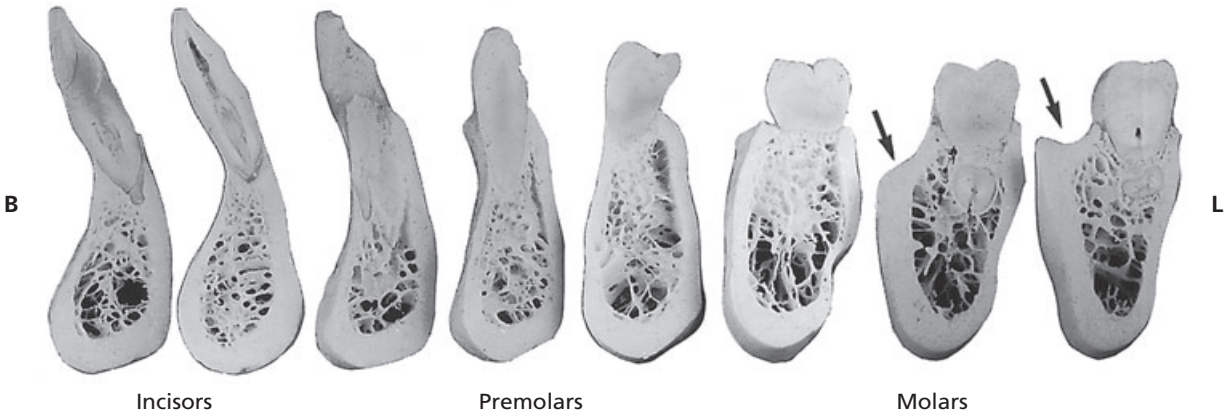

Fig. 1-75

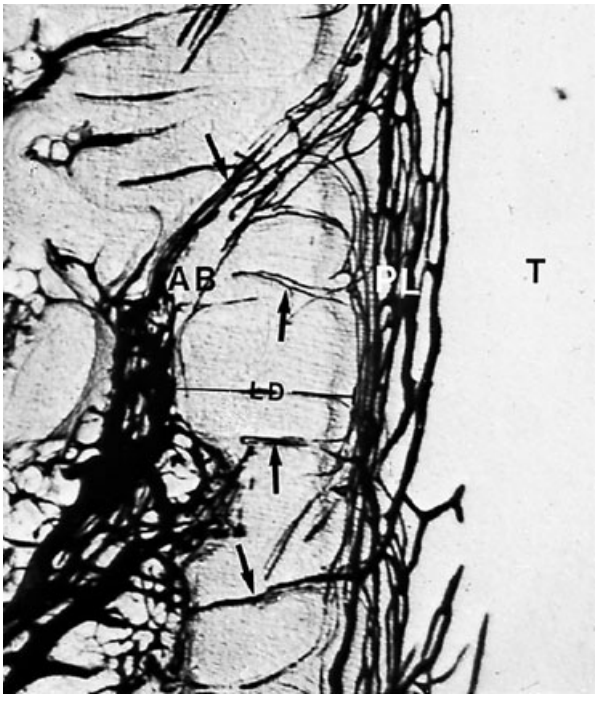

Fig. 1-76

Fig. 1-74 At the buccal aspect of the jaws, the bone coverage is sometimes missing at the coronal portion of the roots, forming a so-called *dehiscence* (D). If some bone is present in the most coronal portion of such an area the defect is called a *fenestration* (F). These defects often occur where a tooth is displaced out of the arch and are more frequent over anterior than posterior teeth. The root in such defects is covered only by periodontal ligament and the overlying gingiva.

Fig. 1-75 presents vertical sections through various regions of the mandibular dentition. The bone wall at the buccal (B) and lingual (L) aspects of the teeth varies considerably in thickness, e.g. from the premolar to the molar region. Note, for instance, how the presence of the oblique line (*linea obliqua*) results in a shelf-like bone process (arrows) at the buccal aspect of the second and third molars.

Fig. 1-76 shows a section through the periodontal ligament (PL), tooth (T), and the alveolar bone (AB). The blood vessels in the periodontal ligament and the alveolar bone appear black because the blood system was perfused with ink. The compact bone (alveolar bone proper) which lines the tooth socket, and in a radiograph (Fig. 1-57) appears as "lamina dura" (LD), is perforated by numerous *Volkmann's canals* (arrows) through which blood vessels, lymphatics, and nerve fibers pass from the alveolar bone (AB) to the periodontal ligament (PL). This layer of bone into which the principal fibers are inserted (Sharpey's fibers) is sometimes called "bundle bone". From a functional and structural point of view, this "bundle bone" has many features in common with the cementum layer on the root surfaces.

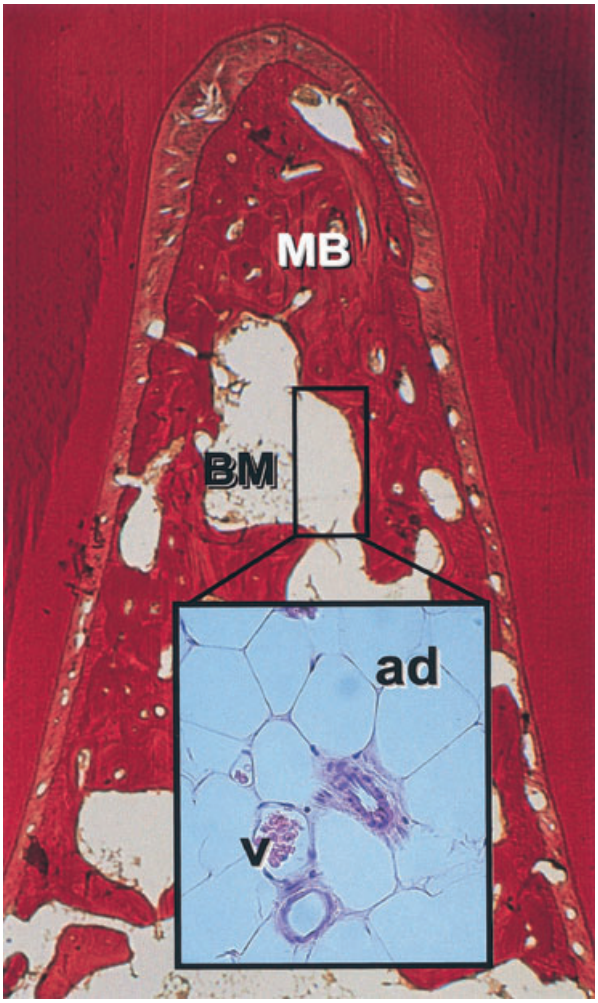

Fig. 1-77

Fig. 1-77 The alveolar process starts to form early in fetal life, with mineral deposition at small foci in the mesenchymal matrix surrounding the tooth buds. These small mineralized areas increase in size, fuse, and become resorbed and remodeled until a continuous mass of bone has formed around the fully erupted teeth. The mineral content of bone, which is mainly hydroxyapatite, is about 60% on a weight basis. The photomicrograph illustrates the bone tissue within the furcation area of a mandibular molar. The bone tissue can be divided into two compartments: mineralized bone (MB) and bone marrow (BM). The mineralized bone is made up of lamellae – lamellar bone – while the bone marrow contains adipocytes (ad), vascular structures (v), and undifferentiated mesenchymal cells (see insertion).

Fig. 1-78 The mineralized, lamellar bone includes two types of bone tissue: the bone of the alveolar process (AB) and the alveolar bone proper (ABP), which covers the alveolus. The ABP or the bundle bone has a varying width and is indicated with white arrows. The alveolar bone (AB) is a tissue of mesenchymal origin and it is not considered as part of the genuine attachment apparatus. The alveolar bone proper (ABP), on the other hand, together with the periodontal ligament (PDL) and the cementum (C), is responsible for the attachment between the tooth and the skeleton. AB and ABP may, as a result of altered functional demands, undergo adaptive changes.

Fig. 1-79 describes a portion of lamellar bone. The lamellar bone at this site contains *osteons* (white

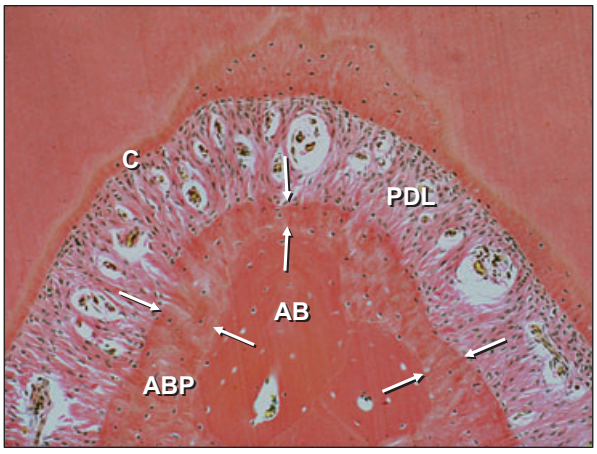

Fig. 1-78

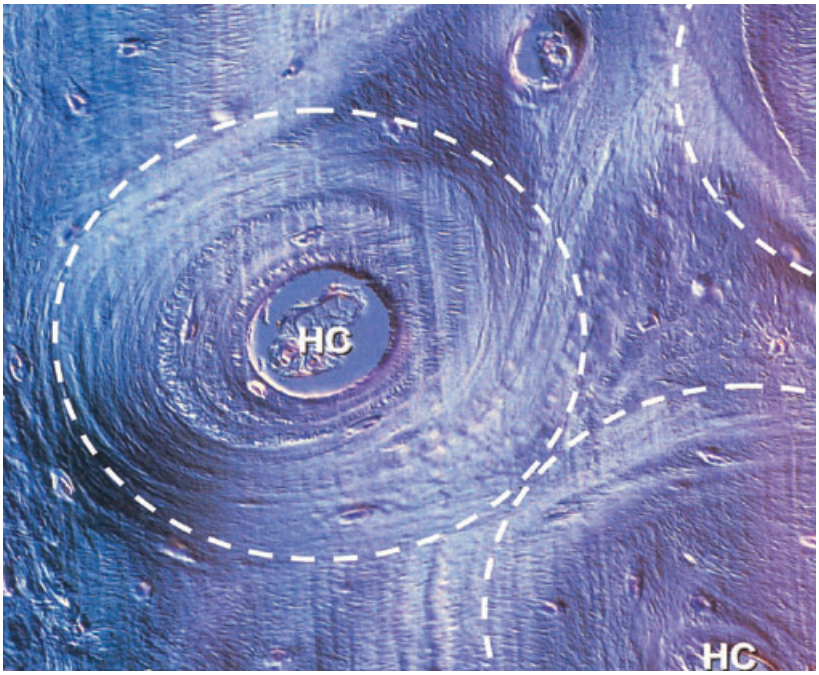

Fig. 1-79

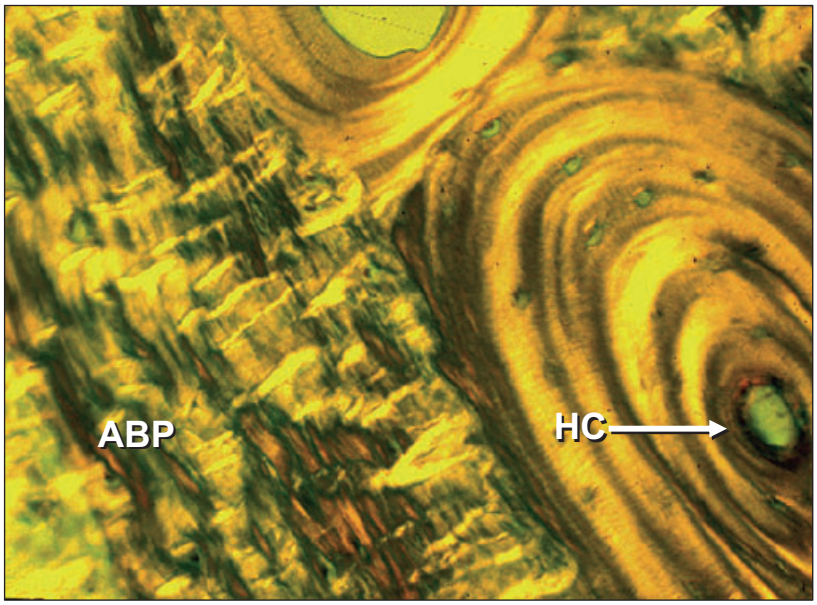

Fig. 1-80a

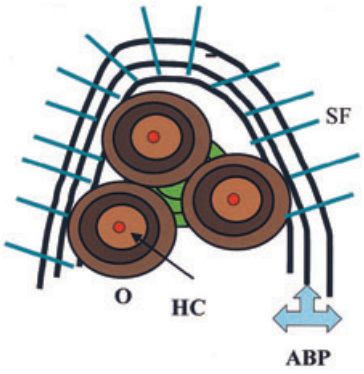

Fig. 1-80b

circles) each of which harbors a blood vessel located in a Haversian canal (HC). The blood vessel is surrounded by concentric, mineralized lamellae to form the osteon. The space between the different osteons is filled with so-called interstitial lamellae. The osteons in the lamellar bone are not only structural units but also metabolic units. Thus, the nutrition of the bone is secured by the blood vessels in the Haversian canals and connecting vessels in the Volkmann canals.

Fig. 1-80 The histologic section (Fig. 1-80a) shows the borderline between the alveolar bone proper (ABP) and lamellar bone with an osteon. Note the presence of the Haversian canal (HC) in the center of the osteon. The alveolar bone proper (ABP) includes circumferential lamellae and contains Sharpey's fibers which extend into the periodontal ligament. The schematic drawing (Fig. 1-80b) is illustrating three active osteons (brown) with a blood vessel (red) in the Haversian canal (HC). Interstitial lamella (green) is located between the osteons (O) and represents an old and partly remodelled osteon. The alveolar bone proper (ABP) is presented by the dark lines into which the Sharpey's fibers (SF) insert.

Fig. 1-81 illustrates an osteon with osteocytes (OC) residing in osteocyte lacunae in the lamellar bone. The osteocytes connect via canaliculi (can) which

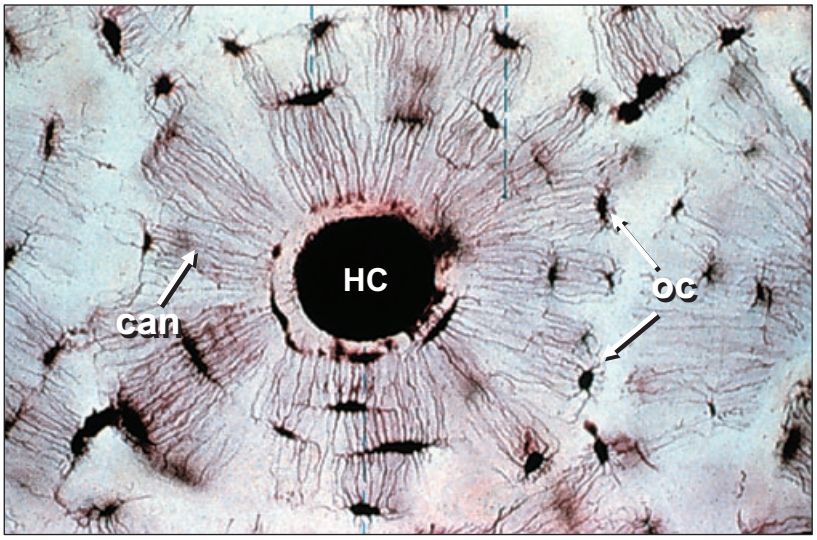

Fig. 1-81

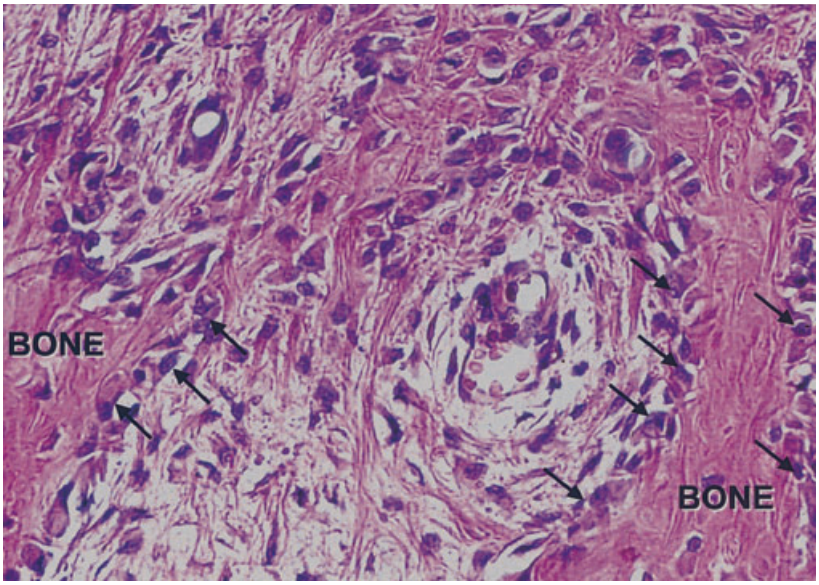

Fig. 1-82

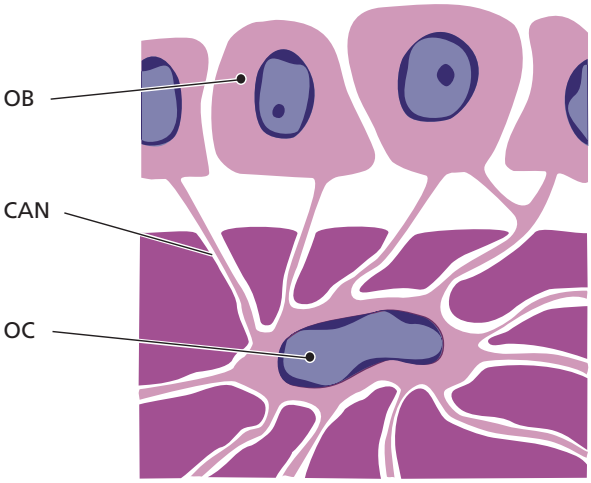

Fig. 1-83

contain cytoplasmatic projections of the osteocytes. A Haversian canal (HC) is seen in the middle of the osteon.

Fig. 1-82 illustrates an area of the alveolar bone in which bone formation occurs. The osteoblasts (arrows), the bone-forming cells, are producing bone matrix (osteoid) consisting of collagen fibers, glycoproteins, and proteoglycans. The bone matrix or the osteoid undergoes mineralization by the deposition of minerals such as calcium and phosphate, which are subsequently transformed into hydroxyapatite.

Fig. 1-83 The drawing illustrates how osteocytes, present in the mineralized bone, communicate with osteoblasts on the bone surface through canaliculi.

Fig. 1-84

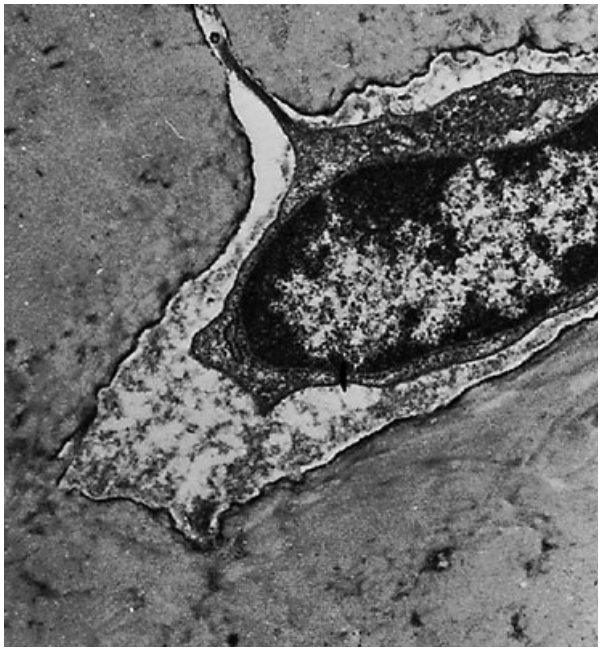

Fig. 1-85

Fig. 1-84 All active bone-forming sites harbor osteoblasts. The outer surface of the bone is lined by a layer of such osteoblasts which, in turn, are organized in a periosteum (P) that contains densely packed collagen fibers. On the "inner surface" of the bone, i.e. in the bone marrow space, there is an endosteum (E), which presents similar features as the periosteum.

Fig. 1-85 illustrates an osteocyte residing in a lacuna in the bone. It can be seen that cytoplasmic processes radiate in different directions.

Fig. 1-86 illustrates osteocytes (OC) and how their long and delicate cytoplasmic processes communicate through the canaliculi (CAN) in the bone. The resulting canalicular–lacunar system is essential for cell metabolism by allowing diffusion of nutrients and waste products. The surface between the osteocytes with their cytoplasmic processes on the one

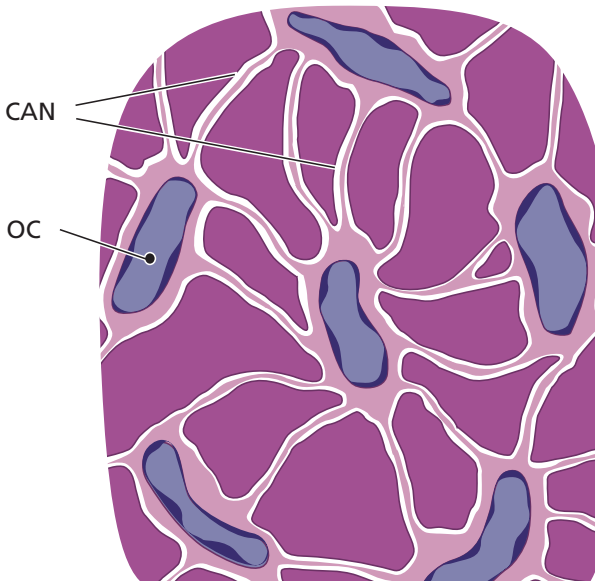

Fig. 1-86

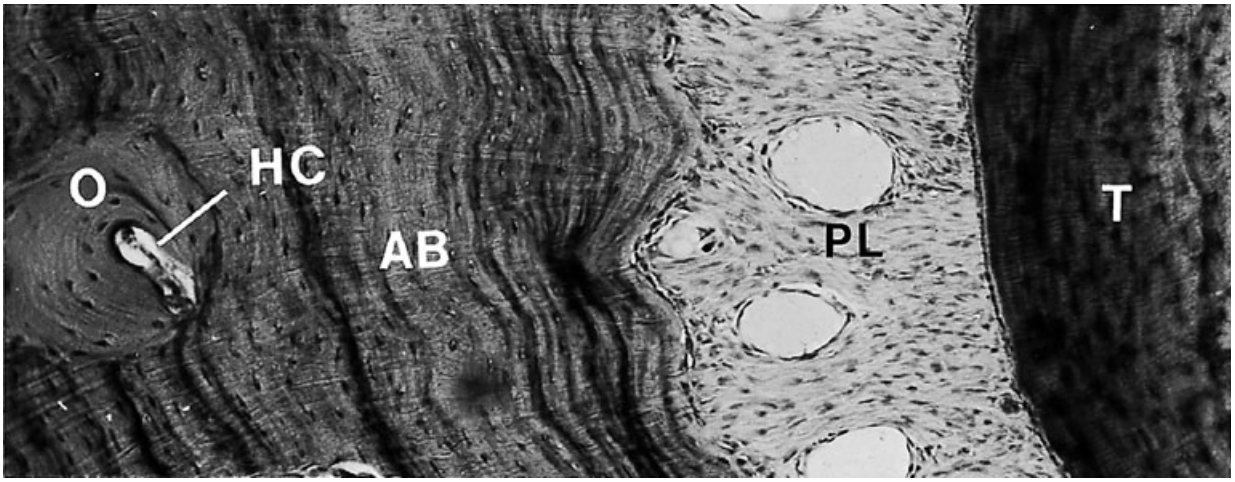

Fig. 1-87

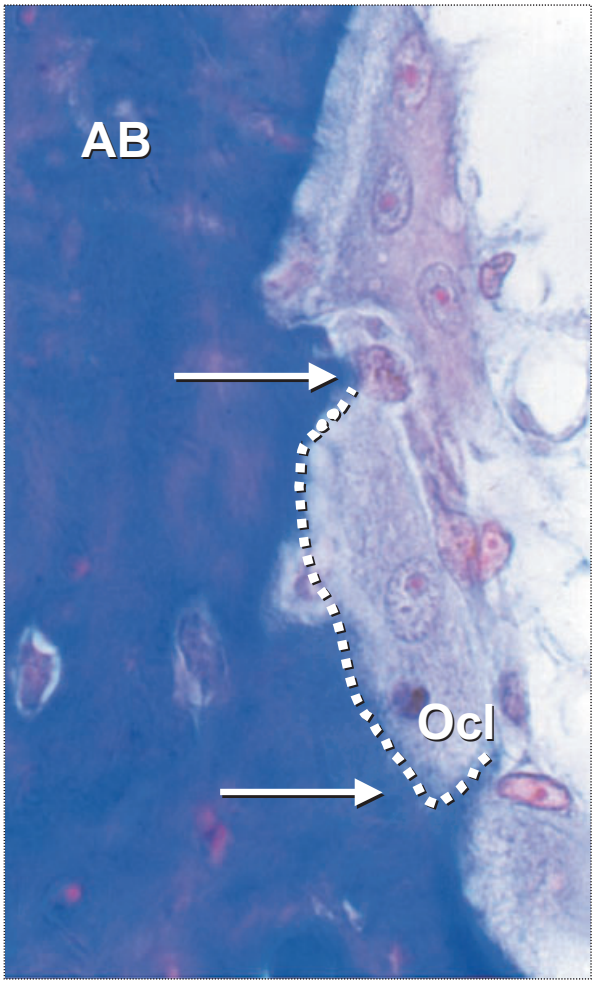

Fig. 1-88

side, and the mineralized matrix on the other, is very large. It has been calculated that the interface between cells and matrix in a cube of bone, 10 × 10 × 10 cm, amounts to approximately 250 m^2. This enormous surface of exchange serves as a regulator, e.g. for serum calcium and serum phosphate levels via hormonal control mechanisms.

Fig. 1-87 The alveolar bone is constantly renewed in response to functional demands. The teeth erupt and migrate in a mesial direction throughout life to compensate for attrition. Such movement of the teeth implies remodeling of the alveolar bone. During the process of remodeling, the bone trabeculae are continuously resorbed and reformed and the cortical bone mass is dissolved and replaced by new bone. During breakdown of the cortical bone, resorption canals are formed by proliferating blood vessels. Such canals, which contain a blood vessel in the center, are subsequently refilled with new bone by the formation of lamellae arranged in concentric layers around the blood vessel. A new Haversian system (O) is seen in the photomicrograph of a horizontal section through the alveolar bone (AB), periodontal ligament (PL), and tooth (T).

Fig. 1-88 The resorption of bone is always associated with *osteoclasts* (Ocl). These cells are giant cells specialized in the breakdown of mineralized matrix (bone, dentin, cementum) and are probably developed from blood monocytes. The resorption occurs by the release of acid substances (lactic acid, etc.) which form an acidic environment in which the mineral salts of the bone tissue become dissolved. Remaining organic substances are eliminated by enzymes and osteoclastic phagocytosis. Actively resorbing osteoclasts adhere to the bone surface and produce lacunar pits called *Howship's lacunae* (dotted line). They are mobile and capable of migrating over the bone surface. The photomicrograph demonstrates osteoclastic activity at the surface of alveolar bone (AB).

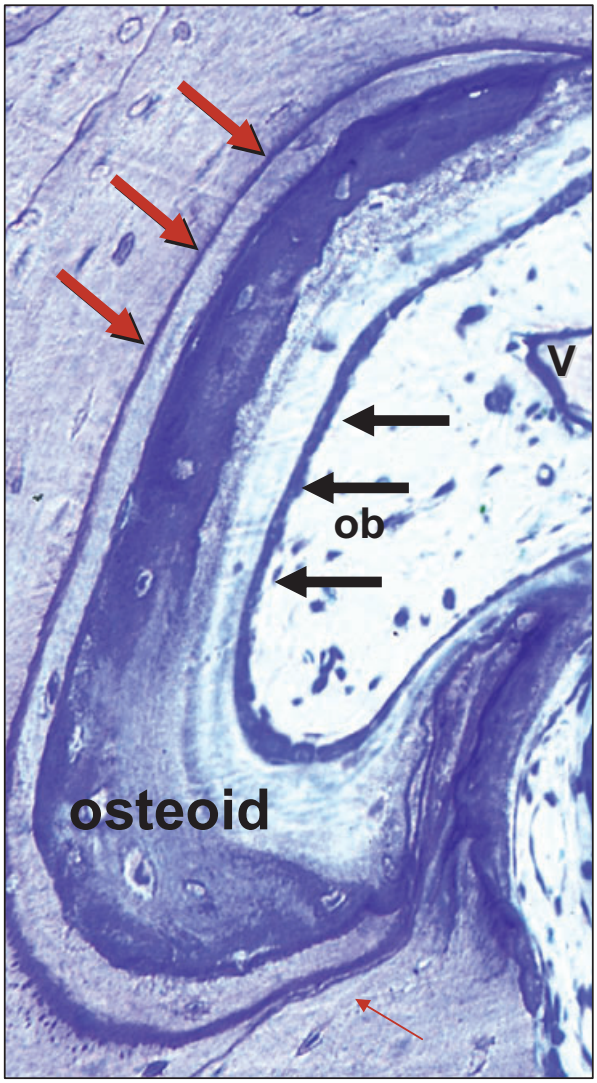

Fig. 1-89

Fig. 1-89 illustrates a so-called bone multicellular unit (BMU), which is present in bone tissue undergoing active remodeling. The reversal line, indicated by red arrows, demonstrates the level to which bone resorption has occurred. From the reversal line new bone has started to form and has the character of osteoid. Note the presence of osteoblasts (ob) and vascular structures (v). The osteoclasts resorb organic as well as inorganic substances.

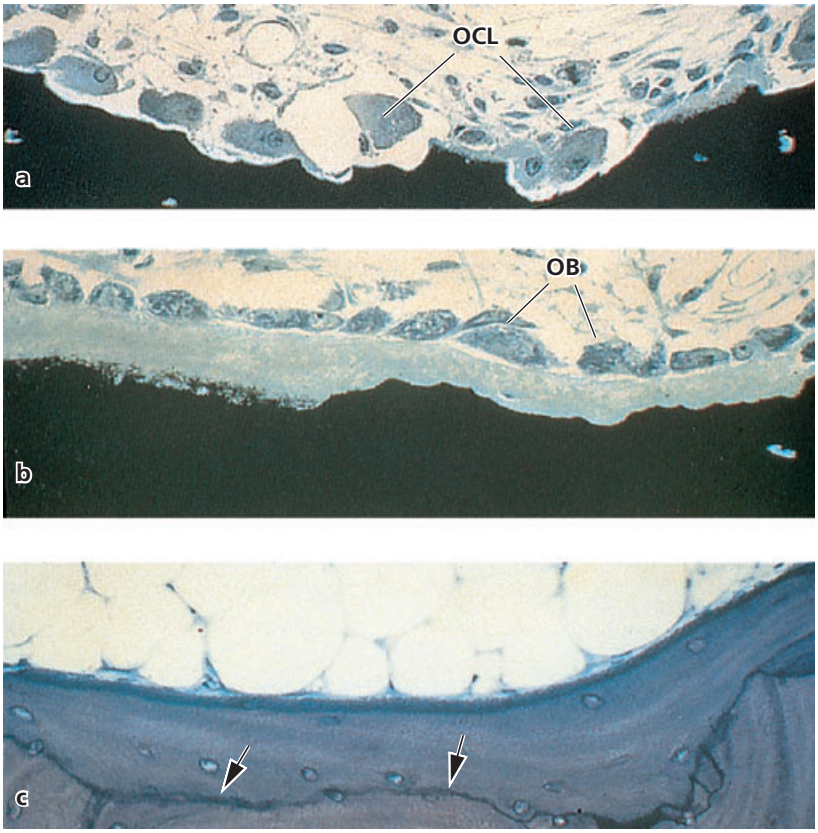

Fig. 1-90

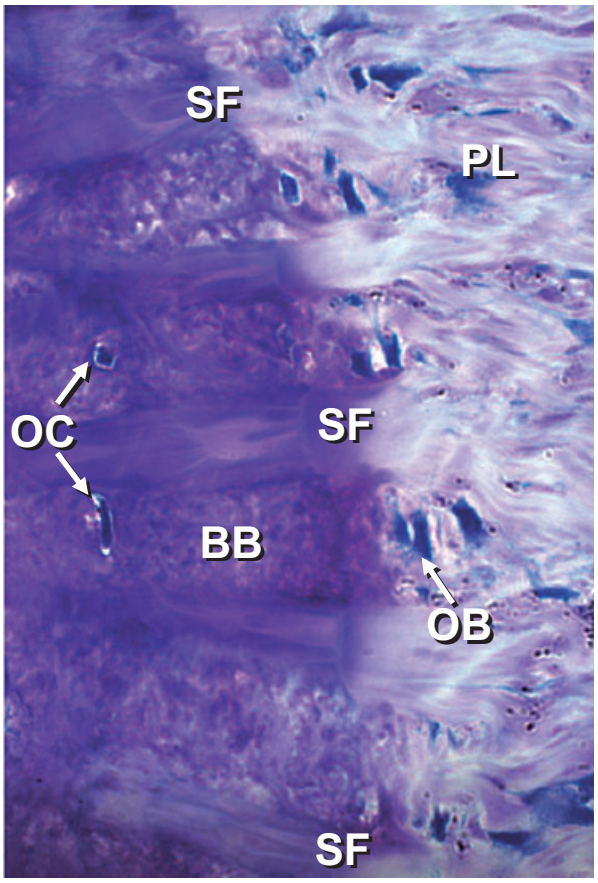

Fig. 1-91

Fig. 1-90 Both the cortical and cancellous alveolar bone are constantly undergoing remodeling (i.e. resorption followed by formation) in response to tooth drifting and changes in functional forces acting on the teeth. Remodeling of the trabecular bone starts with resorption of the bone surface by osteoclasts (OCL) as seen in Fig. 1-90a. After a short period, osteoblasts (OB) start depositing new bone (Fig. 1-90b) and finally a new bone multicellular unit is formed, clearly delineated by a reversal line (arrows) as seen in Fig. 1-90c.

Fig. 1-91 Collagen fibers of the periodontal ligament (PL) insert in the mineralized bone which lines the wall of the tooth socket. This bone, called alveolar bone proper or bundle bone (BB), has a high turnover rate. The portions of the collagen fibers which are inserted inside the bundle bone are called Sharpey's fibers (SF). These fibers are mineralized at their periphery, but often have a non-mineralized central core. The collagen fiber bundles inserting in the bundle bone generally have a larger diameter and are less numerous than the corresponding fiber bundles in the cementum on the opposite side of the periodontal ligament. Individual bundles of fibers can be followed all the way from the alveolar bone to the cementum. However, despite being in the same bundle of fibers, the collagen adjacent to the bone is always less mature than that adjacent to the cementum. The collagen on the tooth side has a low turnover rate. Thus, while the collagen adjacent to the bone is renewed relatively rapidly, the collagen adjacent to the root surface is renewed slowly or not at all. Note the occurrence of osteoblasts (OB) and osteocytes (OC).

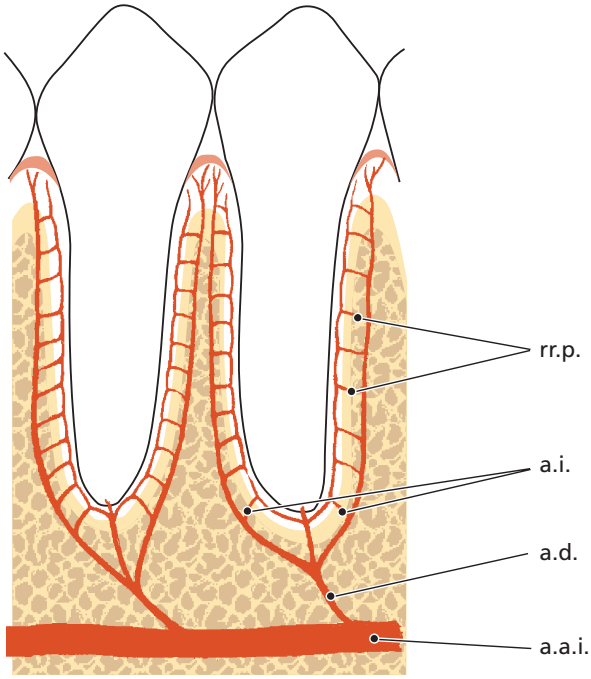

Fig. 1-92

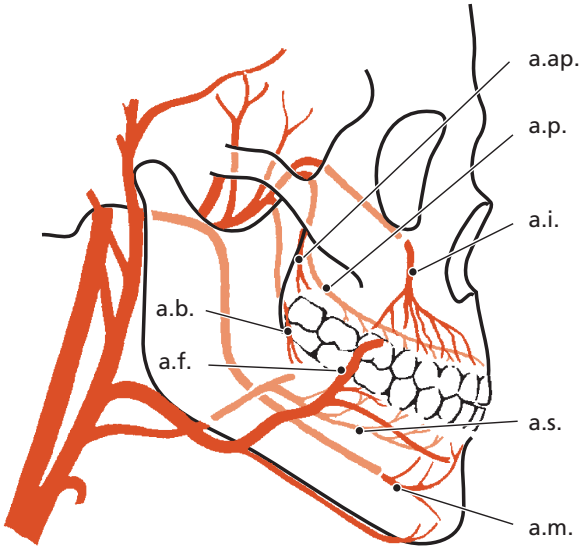

Fig. 1-93

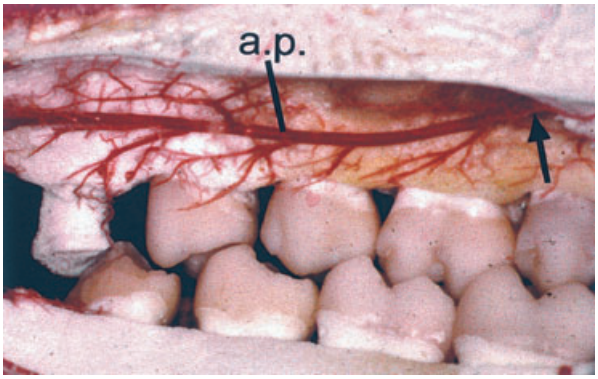

Fig. 1-94

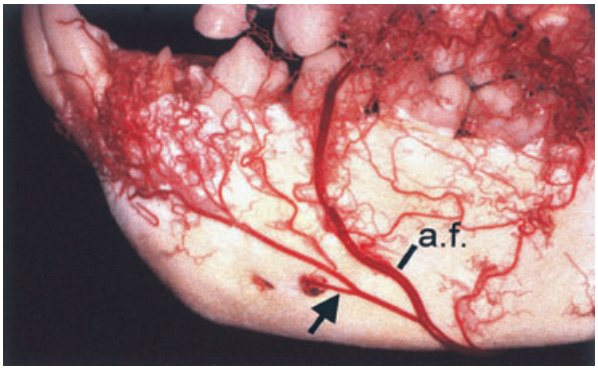

Fig. 1-95

Blood supply of the periodontium

Fig. 1-92 The schematic drawing depicts the blood supply to the teeth and the periodontal tissues. The *dental artery* (a.d.), which is a branch of the *superior* or *inferior* alveolar artery (a.a.i.), dismisses the *intraseptal artery* (a.i.) before it enters the tooth socket. The terminal branches of the *intraseptal artery* (*rami perforantes*, rr.p.) penetrate the alveolar bone proper in canals at all levels of the socket (see Fig. 1-76). They anastomose in the periodontal ligament space, together with blood vessels originating from the apical portion of the periodontal ligament and with other terminal branches, from the intraseptal artery (a.i.). Before the dental artery (a.d.) enters the root canal it puts out branches which supply the apical portion of the periodontal ligament.

Fig. 1-93 The gingiva receives its blood supply mainly through *supraperiosteal* blood vessels which are terminal branches of the *sublingual artery* (a.s.), the *mental artery* (a.m.), the *buccal artery* (a.b.), the *facial artery* (a.f.), the *greater palatine artery* (a.p.), the *infra orbital artery* (a.i.), and the *posterior superior dental artery* (a.ap.).

Fig. 1-94 depicts the course of the greater palatine artery (a.p.) in a specimen of a monkey which was perfused with plastic at sacrifice. Subsequently, the soft tissue was dissolved. The greater palatine artery (a.p.), which is a terminal branch of the *ascending palatine artery* (from the *maxillary*, "internal maxillary", artery), runs through the *greater palatine canal* (arrow) to the palate. As this artery runs in a frontal direction it puts out branches which supply the gingiva and the masticatory mucosa of the palate.

Fig. 1-95 The various arteries are often considered to supply certain well defined regions of the dentition. In reality, however, there are numerous anastomoses

Fig. 1-96

present between the different arteries. Thus, the *entire system of blood vessels*, rather than individual groups of vessels, should be regarded as the unit supplying the soft and hard tissue of the maxilla and the mandible, e.g. in this figure there is an anastomosis (arrow) between the *facial artery* (a.f.) and the blood vessels of the mandible.

Fig. 1-96 illustrates a vestibular segment of the maxilla and mandible from a monkey which was perfused with plastic at sacrifice. Notice that the vestibular gingiva is supplied with blood mainly through *supraperiosteal* blood vessels (arrows).

Fig. 1-97

Fig. 1-97 As can be seen, blood vessels (arrows) originating from vessels in the periodontal ligament pass the alveolar bone crest and contribute to the blood supply of the free gingiva.

Fig. 1-98 shows a specimen from a monkey which was perfused with ink at the time of sacrifice. Subsequently, the specimen was treated to make the tissue transparent (cleared specimen). To the right, the supraperiosteal blood vessels (sv) can be seen. During

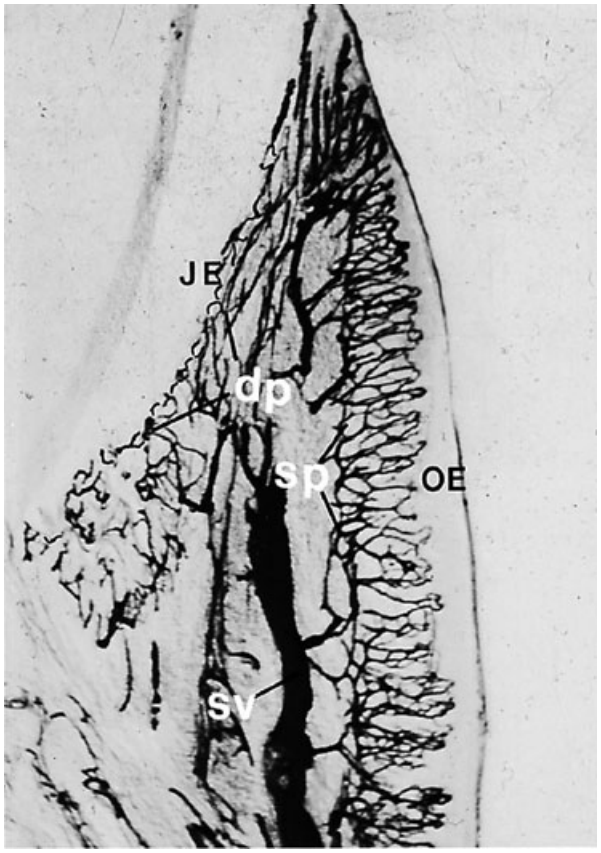

Fig. 1-98

Fig. 1-99

their course towards the free gingiva they put forth numerous branches to the *subepithelial plexus* (sp), located immediately beneath the oral epithelium of the free and attached gingiva. This subepithelial plexus in turn yields thin *capillary loops* to each of the connective tissue papillae projecting into the oral epithelium (OE). The number of such capillary loops is constant over a very long time and is not altered by application of epinephrine or histamine to the gingival margin. This implies that the blood vessels of the lateral portions of the gingiva, even under normal circumstances, are fully utilized and that the blood flow to the free gingiva is regulated entirely by velocity alterations. In the free gingiva, the supraperiosteal blood vessels (sv) anastomose with blood vessels from the periodontal ligament and the bone. Beneath the junctional epithelium (JE) seen to the left, is a plexus of blood vessels termed the *dento-gingival plexus* (dp). The blood vessels in this plexus have a thickness of approximately 40 µm, which means that they are mainly venules. In healthy gingiva, no capillary loops occur in the dento-gingival plexus.

Fig. 1-99 This specimen illustrates how the subepithelial plexus (sp), beneath the oral epithelium of the free and attached gingiva, yields thin capillary loops to each connective tissue papilla. These capillary loops have a diameter of approximately 7 µm, which means they are the size of true capillaries.

Fig. 1-100 illustrates the dento-gingival plexus in a section cut parallel to the subsurface of the junctional epithelium. As can be seen, the dento-gingival plexus consists of a fine-meshed network of blood vessels. In the upper portion of the picture, capillary loops can be detected belonging to the subepithelial plexus beneath the oral sulcular epithelium.

Fig. 1-101 is a schematic drawing of the blood supply to the free gingiva. As stated above, the main blood supply of the free gingiva derives from the *supraperiosteal* blood vessels (SV) which, in the gingiva, anastomose with blood vessels from the *alveolar bone* (ab) and *periodontal ligament* (pl). To the right in the drawing, the oral epithelium (OE) is depicted with its underlying subepithelial plexus of vessels (sp). To the left beneath the junctional epithelium (JE), the dento-gingival plexus (dp) can be seen, which, under normal conditions, comprises a fine-meshed network without capillary loops.

Fig. 1-100

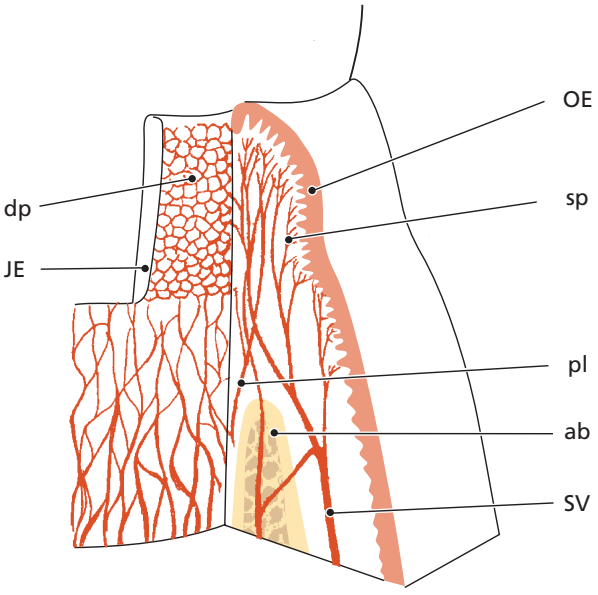

Fig. 1-101

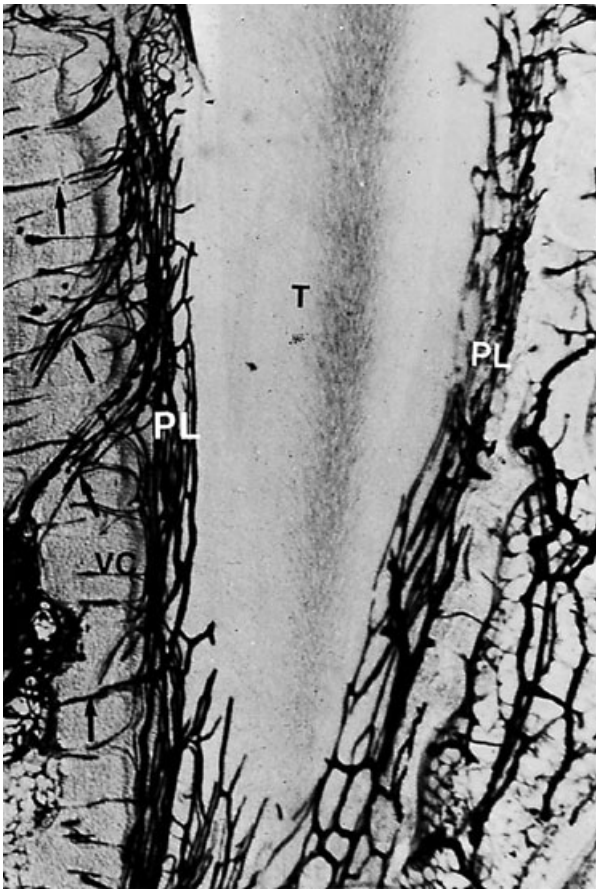

Fig. 1-102

Fig. 1-103

Fig. 1-102 shows a section prepared through a tooth (T) with its periodontium. Blood vessels (perforating rami; arrows) arising from the intraseptal artery in the alveolar bone run through canals (Volkmann's canals) in the socket wall (VC) into the periodontal ligament (PL), where they anastomose.

Fig. 1-103 shows blood vessels in the periodontal ligament in a section cut parallel to the root surface. After entering the periodontal ligament, the blood vessels (perforating rami; arrows) anastomose and form a polyhedral network which surrounds the root like a stocking. The majority of the blood vessels in the periodontal ligament are found close to the alveolar bone. In the coronal portion of the periodontal ligament, blood vessels run in coronal direction, passing the alveolar bone crest, into the free gingiva (see Fig. 1-97).

Fig. 1-104 is a schematic drawing of the blood supply of the periodontium. The blood vessels in the periodontal ligament form a polyhedral network surrounding the root. Note that the free gingiva receives its blood supply from (1) supraperiosteal blood vessels, (2) the blood vessels of the periodontal ligament, and (3) the blood vessels of the alveolar bone.

Fig. 1-105 illustrates schematically the so-called *extravascular* circulation through which nutrients and other substances are carried to the individual cells and metabolic waste products are removed from the tissue. In the arterial (A) end of the capillary, to the left in the drawing, a hydraulic pressure of approximately 35 mmHg is maintained as a result of the pumping function of the heart. Since the hydraulic pressure is higher than the osmotic pressure (OP) in the tissue (which is approximately 30 mmHg), transportation of substances will occur from the blood vessels to the extravascular space (ES). In the venous (V) end of the capillary system, to the right in the drawing, the hydraulic pressure has decreased to approximately 25 mmHg (i.e. 5 mmHg lower than the osmotic pressure in the tissue). This allows transportation of substances from the extravascular space to the blood vessels. Thus, the difference between the hydraulic pressure and the osmotic pressure (OP) results in transportation of substances from the blood vessels to the extravascular space in the arterial part of the capillary while, in the venous part, transportation of substances occurs from the extravascular space to the blood vessels. An extravascular circulation is hereby established (small arrows).

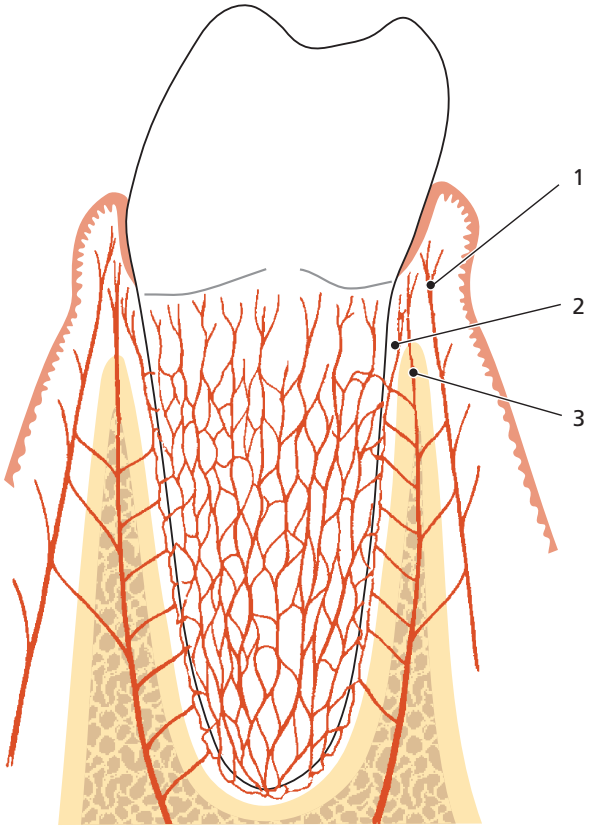

Fig. 1-104

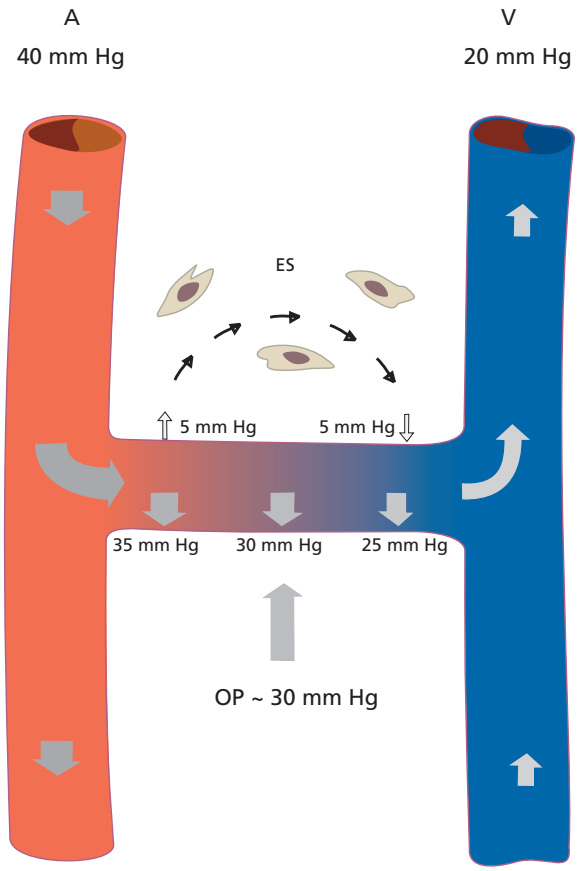

Fig. 1-105

Lymphatic system of the periodontium

Fig. 1-106 The smallest lymph vessels, the *lymph capillaries*, form an extensive network in the connective tissue. The wall of the lymph capillary consists of a single layer of endothelial cells. For this reason such capillaries are difficult to identify in an ordinary histologic section. The lymph is absorbed from the tissue fluid through the thin walls into the lymph capillaries. From the capillaries, the lymph passes into larger lymph vessels which are often in the vicinity of corresponding blood vessels. Before the lymph enters the blood stream it passes through one or more *lymph nodes* in which the lymph is filtered and supplied with lymphocytes. The lymph vessels are like veins provided with valves. The lymph from the periodontal tissues drains to the lymph nodes of the head and the neck. The labial and lingual gingiva of the mandibular incisor region is drained to the *submental lymph nodes* (sme). The palatal gingiva of the maxilla is drained to the *deep cervical lymph nodes* (cp). The buccal gingiva of the maxilla and the buccal and lingual gingiva in the mandibular premolar–molar region are drained to *submandibular lymph nodes* (sma). Except for the third molars and mandibular incisors, all teeth with their adjacent periodontal tissues are drained to the submandibular lymph nodes (sma). The third molars are drained to the *jugulodigastric lymph node* (jd) and the mandibular incisors to the *submental lymph nodes* (sme).

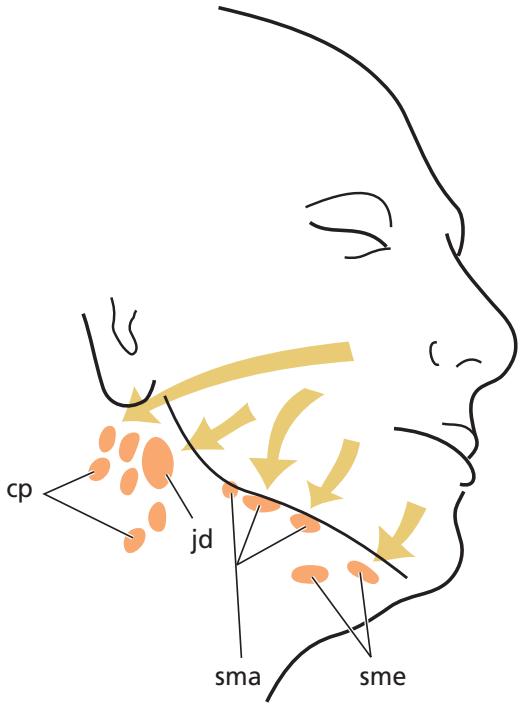

Fig. 1-106

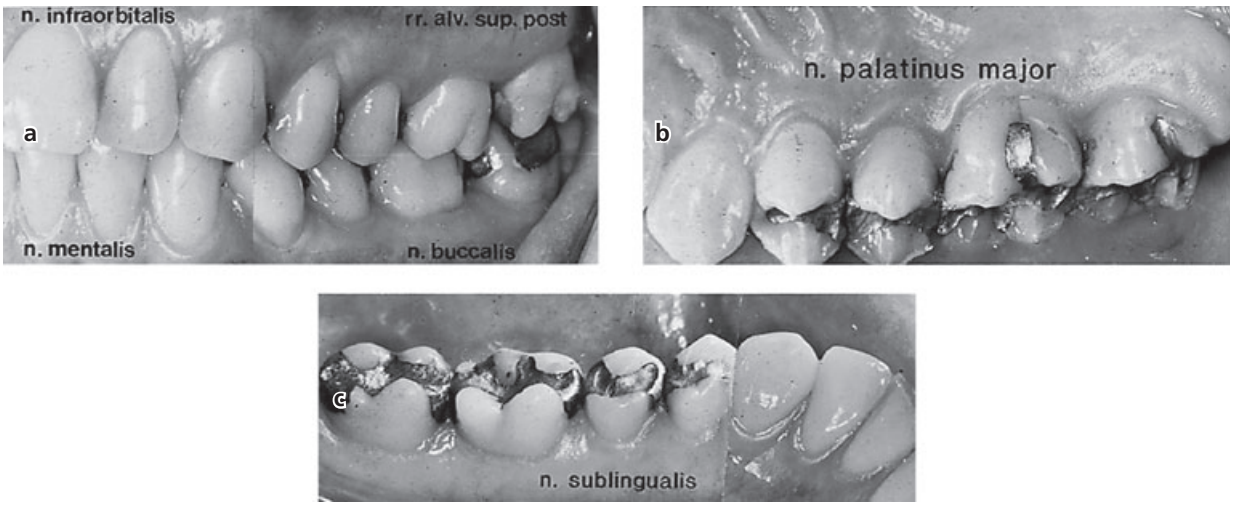

Fig. 1-107

Nerves of the periodontium

Like other tissues in the body, the periodontium contains receptors which record pain, touch, and pressure (*nociceptors* and *mechanoreceptors*). In addition to the different types of sensory receptors, nerve components are found innervating the blood vessels of the periodontium. Nerves recording pain, touch, and pressure have their trophic center in the *semilunar ganglion* and are brought to the periodontium via the *trigeminal nerve* and its end branches. Owing to the presence of receptors in the periodontal ligament, small forces applied on the teeth may be identified. For example, the presence of a very thin (10–30 µm) metal foil strip placed between the teeth during occlusion can readily be identified. It is also well known that a movement which brings the teeth of the mandible in contact with the occlusal surfaces of the maxillary teeth is arrested reflexively and altered into an opening movement if a hard object is detected in the chew. Thus, the receptors in the periodontal ligament, together with the proprioceptors in muscles and tendons, play an essential role in the regulation of chewing movements and chewing forces.

Fig. 1-107 shows the various regions of the gingiva which are innervated by end branches of the trigeminal nerve. The gingiva on the labial aspect of maxillary incisors, canines, and premolars is innervated by *superior labial branches* from the *infraorbital nerve* (n. infraorbitalis) (Fig. 1-107a). The buccal gingiva in the maxillary molar region is innervated by branches from the *posterior superior dental nerve* (rr. alv. sup. post) (Fig. 1-107a). The palatal gingiva is innervated by the *greater palatal nerve* (n. palatinus major) (Fig. 1-107b), except for the area of the incisors, which is innervated by the *long sphenopalatine nerve* (n. pterygopalatini). The lingual gingiva in the mandible is innervated by the *sublingual nerve* (n. sublingualis) (Fig. 1-107c), which is an end branch of the *lingual nerve*. The gingiva at the labial aspect of mandibular

Fig. 1-108

incisors and canines is innervated by the *mental nerve* (n. mentalis), and the gingiva at the buccal aspect of the molars by the *buccal nerve* (n. buccalis) (Fig. 1-107a). The innervation areas of these two nerves frequently overlap in the premolar region. The teeth in the mandible, including their periodontal ligament, are innervated by the *inferior alveolar nerve* (n. alveolaris inf.), while the teeth in the maxilla are innervated by the *superior alveolar plexus* (n. alveolares sup).

Fig. 1-108 The small nerves of the periodontium follow almost the same course as the blood vessels. The nerves to the gingiva run in the tissue superficial to the periosteum and put out several branches to the oral epithelium on their way towards the free gingiva. The nerves enter the periodontal ligament through the perforations (Volkmann's canals) in the socket wall (see Fig. 1-102). In the periodontal ligament, the nerves join larger bundles which take a course parallel to the long axis of the tooth. The photomicrograph illustrates small nerves (arrows) which have emerged from larger bundles of ascending nerves in order to supply certain parts of the periodontal ligament tissue. Various types of neural terminations such as free nerve endings and Ruffini's corpuscles have been identified in the periodontal ligament.

Acknowledgment

We thank the following for contributing to the illustrations in Chapter 1: M. Listgarten, R.K. Schenk, H.E. Schroeder, K.A. Selvig, and K. Josephsen.

References

Ainamo, J. & Talari, A. (1976). The increase with age of the width of attached gingiva. *Journal of Periodontal Research* **11**, 182–188.

Anderson, D.T., Hannam, A.G. & Matthews, G. (1970). Sensory mechanisms in mammalian teeth and their supporting structures. *Physiological Review* **50**, 171–195.

Bartold, P.M. (1995). Turnover in periodontal connective tissue: dynamic homeostasis of cells, collagen and ground substances. *Oral Diseases* **1**, 238–253.

Beertsen, W., McCulloch, C.A.G. & Sodek, J. (1997). The periodontal ligament: a unique, multifunctional connective tissue. *Periodontology 2000* **13**, 20–40.

Bosshardt, D.D. & Schroeder, H.E. (1991). Establishment of acellular extrinsic fiber cementum on human teeth. A light- and electron-microscopic study. *Cell Tissue Research* **263**, 325–336.

Bosshardt, D.D. & Selvig, K.A. (1997). Dental cementum: the dynamic tissue covering of the root. *Periodontology 2000* **13**, 41–75.

Carranza, E.A., Itoiz, M.E., Cabrini, R.L. & Dotto, C.A. (1966). A study of periodontal vascularization in different laboratory animals. *Journal of Periodontal Research* **1**, 120–128.

Egelberg, J. (1966). The blood vessels of the dentogingival junction. *Journal of Periodontal Research* **1**, 163–179.

Fullmer, H.M., Sheetz, J.H. & Narkates, A.J. (1974). Oxytalan connective tissue fibers. A review. *Journal of Oral Pathology* **3**, 291–316.

Hammarström, L. (1997). Enamel matrix, cementum development and regeneration. *Journal of Clinical Periodontology* **24**, 658–677.

Karring, T. (1973). Mitotic activity in the oral epithelium. *Journal of Periodontal Research, Suppl.* **13**, 1–47.

Karring, T. & Löe, H. (1970). The three-dimensional concept of the epithelium-connective tissue boundary of gingiva. *Acta Odontologica Scandinavia* **28**, 917–933.

Karring, T., Lang, N.R. & Löe, H. (1974). The role of gingival connective tissue in determining epithelial differentiation. *Journal of Periodontal Research* **10**, 1–11.

Karring, T., Ostergaard, E. & Löe, H. (1971). Conservation of tissue specificity after heterotopic transplantation of gingiva and alveolar mucosa. *Journal of Periodontal Research* **6**, 282–293.

Kvam, E. (1973). Topography of principal fibers. *Scandinavian Journal of Dental Research* **81**, 553–557.

Lambrichts, I., Creemers, J. & van Steenberghe, D. (1992). Morphology of neural endings in the human periodontal ligament: an electron microscopic study. *Journal of Periodontal Research* **27**, 191–196.

Listgarten, M.A. (1966). Electron microscopic study of the gingivo-dental junction of man. *American Journal of Anatomy* **119**, 147–178.

Listgarten, M.A. (1972). Normal development, structure, physiology and repair of gingival epithelium. *Oral Science Review* **1**, 3–67.

Lozdan, J. & Squier, C.A. (1969). The histology of the mucogingival junction. *Journal of Periodontal Research* **4**, 83–93.

Melcher, A.H. (1976). Biological processes in resorption, deposition and regeneration of bone. In: Stahl, S.S., ed. *Periodontal Surgery, Biologic Basis and Technique*. Springfield: C.C. Thomas, pp. 99–120.

Page, R.C., Ammons, W.F., Schectman, L.R. & Dillingham, L. A. (1974). Collagen fiber bundles of the normal marginal gingiva in the marmoset. *Archives of Oral Biology* **19**, 1039–1043.

Palmer, R.M. & Lubbock, M.J. (1995). The soft connective tissue of the gingiva and periodontal ligament: are they unique? *Oral Diseases* **1**, 230–237.

Saffar, J.L., Lasfargues, J.J. & Cherruah, M. (1997). Alveolar bone and the alveolar process: the socket that is never stable. *Periodontology 2000* **13**, 76–90.

Schenk, R.K. (1994). Bone regeneration: Biologic basis. In: Buser, D., Dahlin, C. & Schenk, R. K., eds. *Guided Bone Regeneration in Implant Dentistry*. Berlin: Quintessence Publishing Co.

Schroeder, H.E. (1986). The periodontium. In: Schroeder, H. E., ed. *Handbook of Microscopic Anatomy.* Berlin: Springer, pp. 47–64.

Schroeder, H.E. & Listgarten, M.A. (1971). *Fine Structure of the Developing Epithelial Attachment of Human Teeth*, 2nd edn. Basel: Karger, p. 146.

Schroeder, H.E. & Listgarten, M.A. (1997). The gingival tissues: the architecture of periodontal protection. *Periodontology 2000* **13**, 91–120.

Schroeder, H.E. & Münzel-Pedrazzoli, S. (1973). Correlated morphometric and biochemical analysis of gingival tissue. Morphometric model, tissue sampling and test of stereologic procedure. *Journal of Microscopy* **99**, 301–329.

Schroeder, H.E. & Theilade, J. (1966). Electron microscopy of normal human gingival epithelium. *Journal of Periodontal Research* **1**, 95–119.

Selvig, K.A. (1965). The fine structure of human cementum. *Acta Odontologica Scandinavica* **23**, 423–441.

Valderhaug, J.R. & Nylen, M.U. (1966). Function of epithelial rests as suggested by their ultrastructure. *Journal of Periodontal Research* **1**, 67–78.

Chapter 2

The Edentulous Alveolar Ridge

Maurício Araújo and Jan Lindhe

Clinical considerations

The alveolar process forms in harmony with the development and eruption of the teeth and it gradually regresses when the teeth are lost. In other words, the formation as well as the continued preservation of the alveolar process is dependent on the continued presence of teeth. Furthermore, the morphologic characteristics of the alveolar process are related to the size and shape of the teeth, events occurring during tooth eruption as well as the inclination of the erupted teeth. Thus, subjects with long and narrow teeth, compared with subjects who have short and wide teeth, appear to have a more delicate alveolar process and, in particular, a thin, sometimes fenestrated buccal bone plate (Fig. 2-1).

The tooth and its surrounding attachment tissues – the root cementum, the periodontal ligament and the bundle bone – establish a functional unit (Fig. 2-2). Hence, forces elicited, for example during mastication, are transmitted from the crown of the tooth via the root and the attachment tissues to the load-carrying hard tissue structures in the alveolar process, where they are dispersed. The loss of teeth, and the loss or change of function within and around the socket will result in a series of adaptive alterations of the now edentulous portion of the ridge. Thus, it is well documented that following *multiple tooth* extractions and the subsequent restoration with removable dentures, the size of the alveolar ridge will become markedly reduced, not only in the horizontal but also in the vertical dimension (Figs. 2-3, 2-4); in addition, the arch will be shortened (Atwood 1962, 1963; Johnson 1963, 1969; Carlsson *et al*. 1967).

Also following the removal of *single* teeth the alveolar ridge will be markedly diminished (Fig. 2-5). The magnitude of this change was studied and reported in a publication by Pietrokovski and Massler (1967). The authors had access to 149 dental cast models (72 maxillary and 77 mandibular) in which one tooth was missing (and not replaced) on one side of the jaw. The outer contours of the buccal and lingual (palatal) portions of the ridge at a tooth site and at

Fig. 2-1 Buccal aspect of adult skull preparations illustrating a dentate maxilla of one subject with a thick (a) and another subject with a thin (b) periodontal biotype.

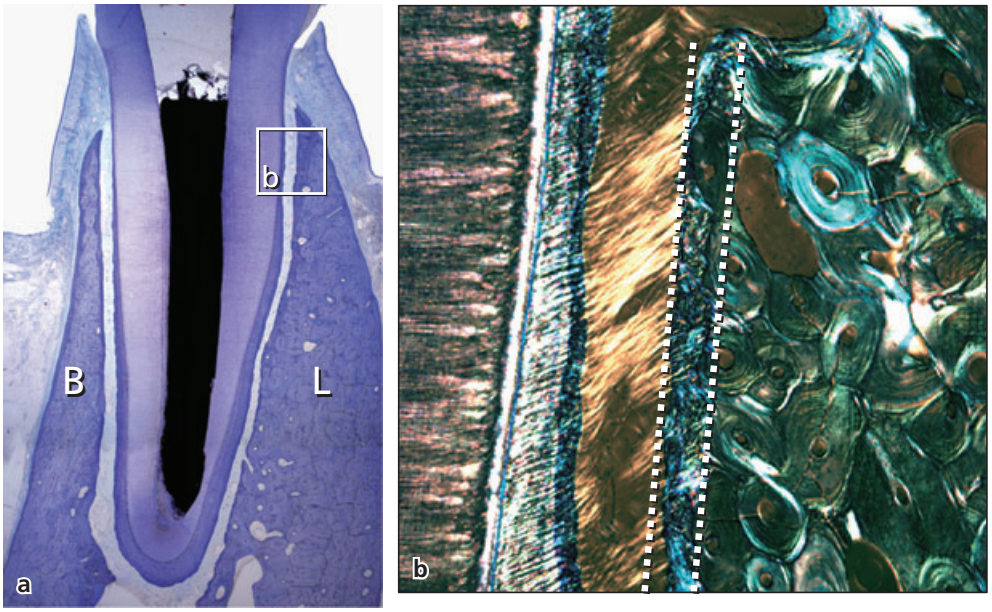

Fig. 2-2 Buccal–lingual section of a dentate portion of the alveolar process. B = buccal aspect; L = lingual aspect. (a) The tooth is surrounded by its attachment tissues. (b) Larger magnification of the attachment tissues. Note that the dentin is connected to the alveolar bone via the root cementum, the periodontal ligament and the alveolar bone. The inner portion of the alveolar bone (dotted line) is called the alveolar bone proper or the bundle bone.

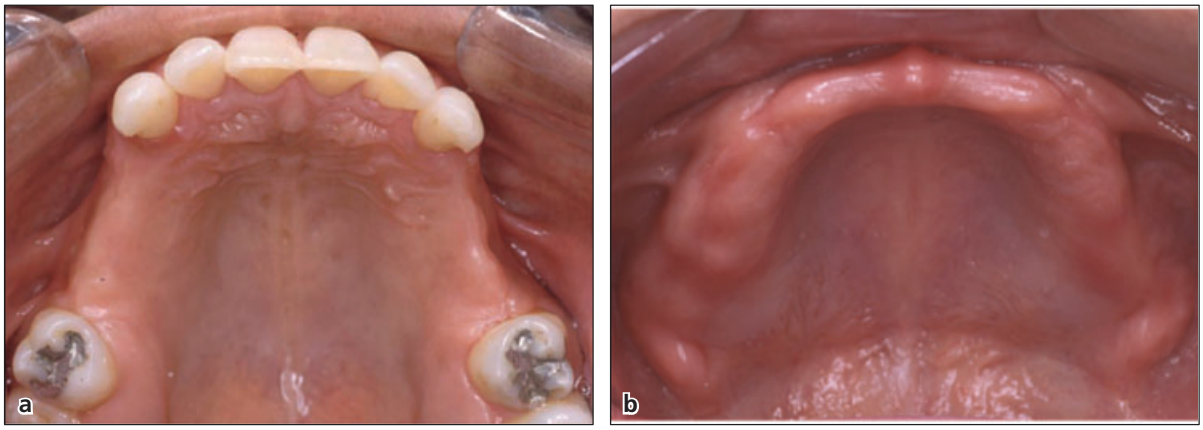

Fig. 2-3 (a) Clinical view of a partially edentulous maxilla. Note that the crest of the edentulous portions of the ridge is narrow in the buccal–palatal direction. (b) Clinical view of a fully edentulous and markedly resorbed maxilla. Note that *papilla incisiva* is located in the center of the ridge. This indicates that the entire buccal but also a substantial portion of the palatal ridge are missing.

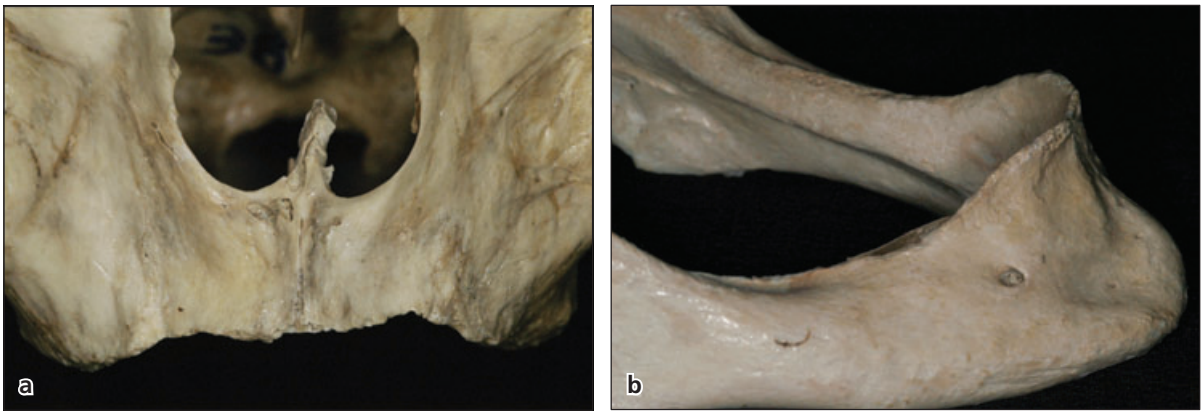

Fig. 2-4 Buccal aspect of a skull preparation illustrating a fully edentulous maxilla (a) and mandible (b). The small segments of the alveolar ridge that still remain are extremely thin in the buccal–palatal/lingual direction.

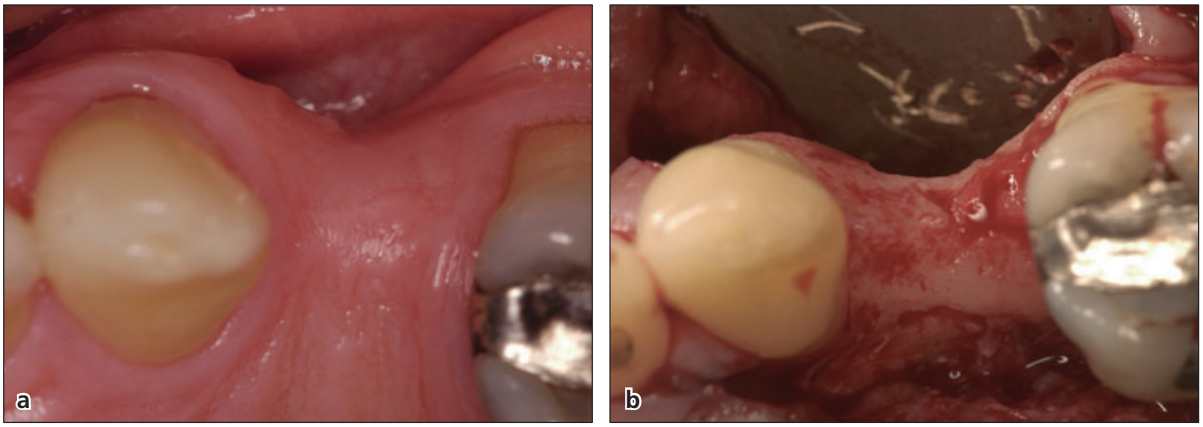

Fig. 2-5 Clinical view of an edentulous ridge in the maxillary premolar region. The premolar was extracted several years before the clinical documentation was made. (a) Note the presence of a buccal invagination of the ridge. (b) Following flap elevation, the crest region of the severely resorbed buccal portion of alveolar process is disclosed.

the contralateral edentulous site were determined by the use of a profile stylus and an imaging technique. Their findings are reported in Table 2-1.

It was concluded that the amount of tissue resorption (hard and soft tissues combined) following the loss of a single tooth was substantial and that the reduction of the ridge was greater along the buccal surface than along the lingual and palatal surfaces in every specimen examined, although the absolute amounts and differences varied from one group of teeth to the next. As a result of this tissue modeling, the center of the edentulous site shifted toward the lingual or palatal aspect of the ridge. The observations made by Pietrokovski and Massler (1967) were supported by recent findings presented by Schropp *et al*. (2003). They studied bone and soft tissue volume changes that took place during a 12-month period following the extraction of single premolars and molars. Clinical as well as cast model measurements were made immediately after tooth extraction and subsequently after 3, 6, and 12 months of healing. It was observed that the buccal–lingual/palatal dimension during the first 3 months was reduced about 30%, and after 12 months the edentulous site had lost at least 50% of its original width. Furthermore, the height of the buccal bone plate was reduced and after 12 months of healing the buccal prominence was located 1.2 mm apical of its lingual/palatal counterpart.

Conclusion: The extraction of single as well as multiple teeth induces a series of adaptive changes in the soft and hard tissues that result in an overall regress of the edentulous site(s). Resorption appears to be more pronounced at the buccal than at lingual/palatal aspects of the ridge.

In this context it should be observed that the alveolar process might also undergo change as the result of tooth-related disease processes, such as aggressive, chronic and necrotizing forms of marginal periodontitis as well as periapical periodontitis. Furthermore, traumatic injuries may cause marked alterations of the maxilla and mandible including their alveolar processes.

Table 2-1 Average amount of resorption of tooth extraction in different tooth areas*

Tooth	Average amount of resorption (mm)		Difference
	Buccal surface	Lingual/palatal surface	
Mandibular teeth			
Central incisor	2.08	0.91	1.17
Lateral incisor	3.54	1.41	2.13
Canine	3.25	1.59	1.66
First premolar	3.45	1.40	2.05
Second premolar	3.28	0.75	2.53
First molar	4.69	2.79	1.90
Second molar	4.30	3.00	1.30
Maxillary teeth			
Central incisor	3.03	1.46	1.57
Lateral incisor	3.47	0.86	2.61
Canine	3.33	1.91	1.42
First premolar	3.33	2.04	1.29
Second premolar	2.58	1.62	0.96
First molar	5.25	3.12	2.13

* "The amount of resorption was greater along the buccal surface than along the lingual or palatal surface in every specimen examined, although the absolute amounts and differences varied very widely. This caused a shift in the center of the edentulous ridge toward the lingual or palatal side of the ridge with a concomitant *decrease* in arch length in the mandible as well as the maxillae." (Pietrokovski & Massler 1967)

Remaining bone in the edentulous ridge

In the publication by Schropp *et al*. (2003) bone tissue formation in extraction sockets was studied by means of subtraction radiography. Thus, radiographs of the study sites were obtained using a standardized technique immediately after tooth extraction and then

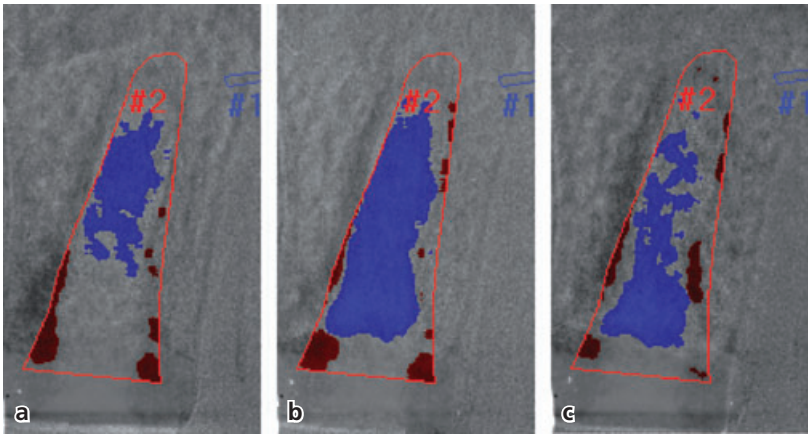

Fig. 2-6 Radiographic (subtraction radiography) images of an extraction site obtained after (a) 3 months, (b) 6 months, and (c) 12 months of healing. The blue color represents areas of new bone formation. During the first 6 months, the deposition of new bone was intense. Between 6 and 12 months, some of the newly formed bone was remodeled. (Courtesy of Dr. L. Schropp.)

after 3, 6, and 12 months of healing (Fig. 2-6). It was observed that in the first few months some bone loss (height) took place in the alveolar crest region. Most of the bone gain in the socket occurred in the first 3 months. There was additional gain of bone in the socket between 3 and 6 months. In the interval between 6 and 12 months, the newly formed bone obviously remodeled and the amount of mineralized tissue was reduced. In other words, towards the end of socket healing small amounts of mineralized tissue may have remained in the center of the edentulous site.

Classification of remaining bone

Based on the volume of remaining mineralized bone, the edentulous sites may, according to Lekhom and Zarb (1985), be classified into five different groups (Fig. 2-7). In groups A and B substantial amounts of the alveolar process still remain, whereas in groups C, D, and E, there are only minute remnants of the alveolar process present. Lekholm and Zarb (1985) also classified the "quality" of the bone in the edentulous site. Class 1 and class 2 characterized a location in which the walls – the cortical plates – of the site are thick and the volume of bone marrow is small. Sites that belong to class 3 and class 4, however, are bordered by relatively thin walls of cortical bone, while the amount of cancellous bone (spongiosa), including trabeculae of lamellar bone and marrow, is large.

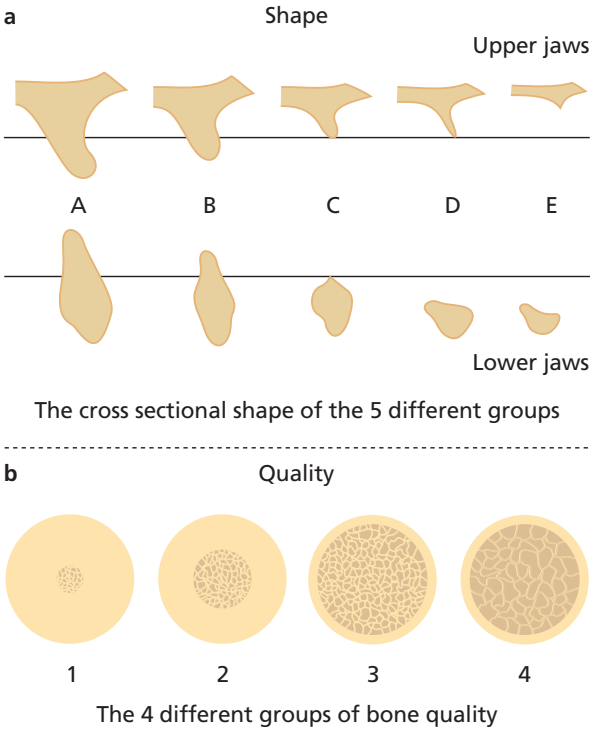

Fig. 2-7 Schematic drawings showing (a) a classification of residual jaw shape, and (b) jaw bone quality, according to Lekholm and Zarb (1985).

Topography of the alveolar process

The dentate alveolar process is defined as the portion of the mandible or maxilla that contains the sockets of the teeth (Fig. 2-8). There is, however, no distinct boundary between the alveolar process and the basal bone of the jaws.

The alveolar process (Fig. 2-9) is comprised of the outer walls – buccal and lingual/palatal cortical plates – and a central portion of spongy bone (anatomic term) – or trabecular bone (radiographic term) or cancellous bone (histologic term) – that contains bone trabeculae as well as marrow. The cortical plates are continuous with the bone that lines the sockets, i.e. the alveolar bone proper (Fig. 2-10). The alveolar bone proper can also be identified as the cribriform plate (anatomic term; Fig. 2-11), or the lamina dura dentes (radiographic term; Fig. 2-12) or the bundle bone (histologic term; Fig. 2-2b). The bundle bone is the tissue in which the extrinsic collagen fiber bundles of the periodontal ligament are embedded.

The cortical plates (the outer walls) of the alveolar process meet the alveolar bone proper at the crest of the interdental septum (Fig. 2-10); at sites with a normal periodontium this is located about 1–2 mm apical of the cemento-enamel junction of adjacent teeth. In some portions of the anterior dentition, the spongy bone of the alveolar process may be absent.

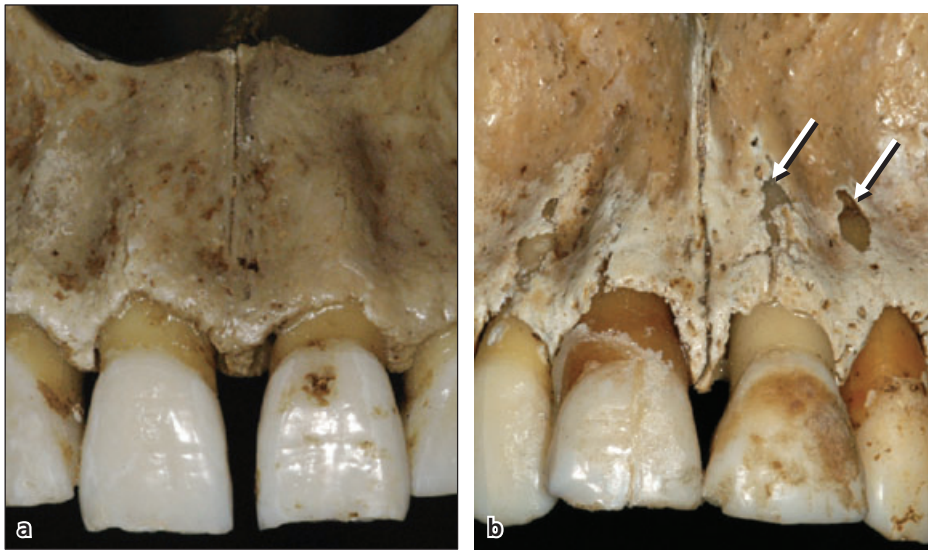

Fig. 2-8 Buccal aspect of the maxillary incisor region of a skull preparation illustrating one subject with a thick (a) and another subject with a thin (b) periodontal biotype. Arrows indicate the presence of fenestrations in the buccal bone.

Fig. 2-9 A buccal–lingual section from a human skull preparation illustrating the outer buccal and lingual cortical plates of the alveolar process, as well as the spongy bone in the center of the ridge.

The cortical plates in such locations are continuous with the alveolar bone proper of the socket.

The cortical plate is made up of lamellar bone. Lamellar bone contains both concentric and interstitial lamellae (see Chapter 1). The spongy bone contains trabeculae of lamellar bone; in the adult these are surrounded by a marrow that is rich in adipocytes and pluripotent, mesenchymal stroma cells (Fig. 2-13). Such cells may be induced to form bone, but also to support the differentiation of hemapoietic cells and thereby the differentiation of osteoclasts.

Fig. 2-10 The empty alveolus of a second maxillary premolar is illustrated in the skull preparation. The buccal and palatal cortical plates are continuous with the alveolar bone proper and the bone tissue of the interdental septum. The perforations in the crest region represent the Volkman's canals.

The trabeculae of the spongy bone are orientated in directions that allow them to take up and distribute stress that occurs during mastication and other tooth contacts.

Alterations of the alveolar process following tooth extraction

The alterations that occur in the alveolar ridge following the extraction of single teeth can, for didactic reasons, be divided in two interrelated series of events, namely *intra-alveolar processes* and *extra-alveolar processes.*

Intra-alveolar processes

The healing of extraction sockets in human volunteers was studied by e.g. Amler (1969) and Evian

Fig. 2-11 A mandibular molar region of a human skull preparation. The second molar was removed in the skull preparation. In such an anatomic section, the alveolar bone proper (on the inside of the alveolus) is often termed the *cribriform plate*. This is due to the numerous perforations (Volkman's canals) that are present on the bone surface.

Fig. 2-13 Histologic section presenting the mesio-distal aspect of a fresh extraction socket bordered by two neighboring roots. Note that the alveolar bone from the tooth sites is continuous with the walls of the empty socket. The interdental septum contains cancellous bone including trabeculae of lamellar bone and marrow.

Fig. 2-12 Radiograph obtained from the specimen illustrated in Fig. 2-11. In the radiograph the alveolar bone proper is often identified as lamina dura (dentes).

et al. (1982). Although the biopsy technique used by Amler only allowed the study of healing in the marginal portions of the empty socket, his findings are often referred to. A copy of the drawing included in Amler's publication "The time sequence of tissue regeneration in human extraction wounds" is presented in Fig. 2-14.

Amler stated that following tooth extraction, the first 24 hours are characterized by the formation of a *blood clot* in the socket. Within 2–3 days the blood clot is gradually being replaced with *granulation tissue*. After 4–5 days, the *epithelium* from the margins of the soft tissue starts to proliferate to cover the granulation tissue in the socket. One week after extraction, the socket contains granulation tissue, *young connective tissue*, and *osteoid* formation is ongoing in the apical portion of the socket. After 3 weeks, the socket contains connective tissue and there are signs of mineralization of the osteoid. The *epithelium* covers the wound. After 6 weeks of healing, bone formation in the socket is pronounced and trabeculae of newly formed bone can be seen.

Amler's study was of short duration, so it could only evaluate events that took place in the marginal portion of the healing socket. His experimental data did not include the important later phase of socket healing that involves the processes of modeling and remodeling of the newly formed tissue in various parts of the alveolus. Thus, the tissue composition of the fully healed extraction site was not documented in the study.

The results from a recent, long-term experiment in the dog (Cardaropoli *et al*. 2003) will therefore be used to describe more in detail the various phases of socket healing including processes of both modeling and remodeling. Following the elevation of buccal and lingual full-thickness flaps, the distal roots of mandibular premolars were extracted (Fig. 2-15a). The mucosal flaps were managed to provide soft tissue coverage of the fresh extraction wound (Fig. 2-15b). Healing of the extraction sites was monitored

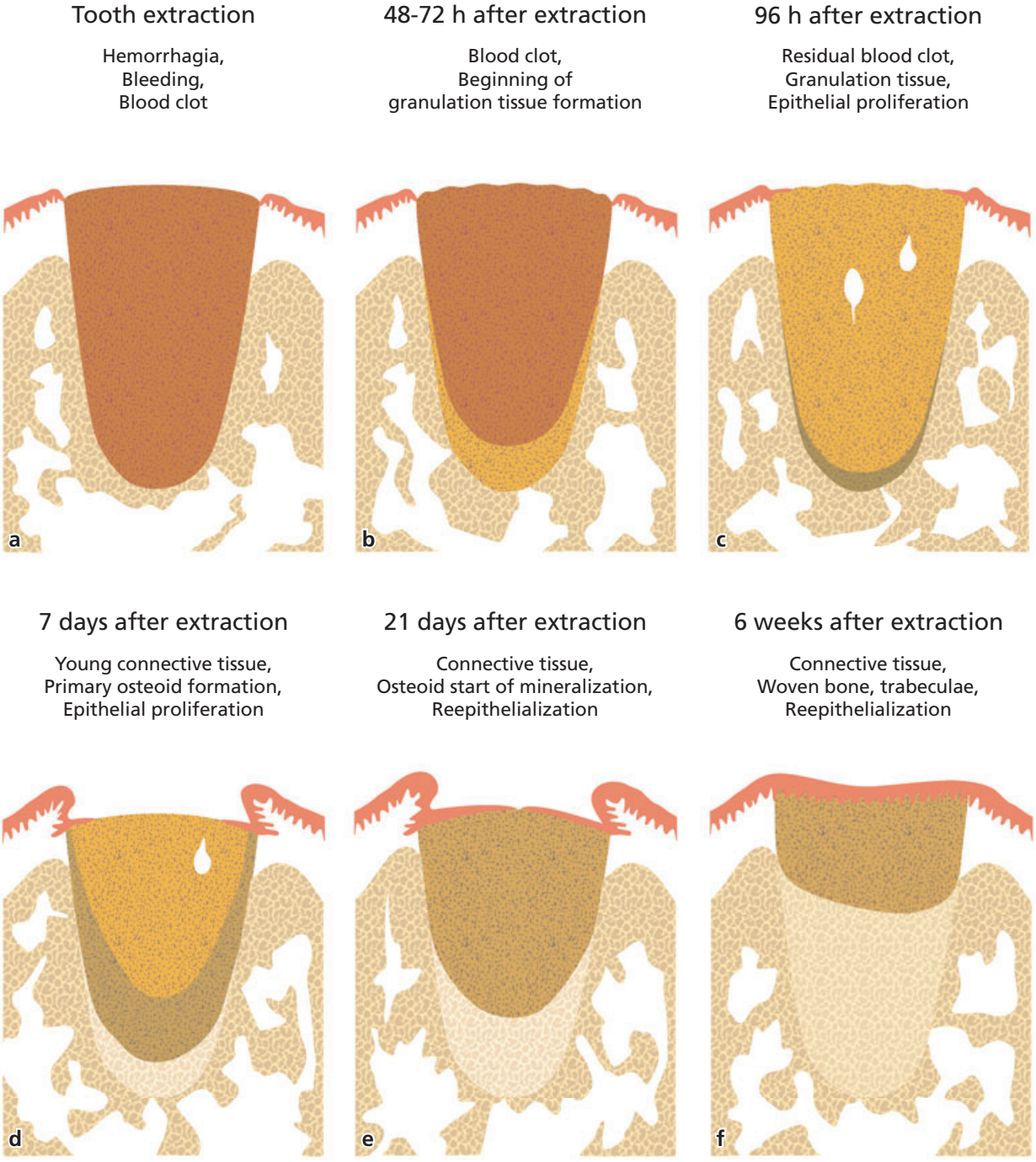

Fig. 2-14 Healing of the alveolar socket after tooth extraction according to Amler (1969). (a) Bleeding and formation of a blood clot immediately after tooth extraction. Blood vessels are closed by trombi and a fibrin network is formed. (b) Already, during the first 48 hours, neutrophilic granulocytes, monocytes and fibroblasts begin to migrate within the fibrin network. (c) The blood clot is slowly replaced by granulation tissue. (d) Granulation tissue forms predominantly in the apical third of the alveolus. There is increased density of fibroblasts. After 4 days, contraction of the clot and proliferation of the oral epithelium is seen. Osteoclasts are visible at the margin of the alveolus. Osteoblasts and osteoids seem to appear in the bottom of the alveolus. (e) Reorganization of the granulation tissue through formation of osteoid trabeculae. Epithelial proliferation from the wound margins on the top of the young connective tissue. Again, the formation of osteoid trabeculae is evident from the wall of the alveolus in a coronal direction. After 3 weeks some of the trabeculae start to mineralize. (f) Radiographically, bone formation may be visible. The soft tissue wound is closed and epithelialized after 6 weeks. However, bone fill in the alveolus takes up to 4 months and does not seem to reach the level of the neighboring teeth.

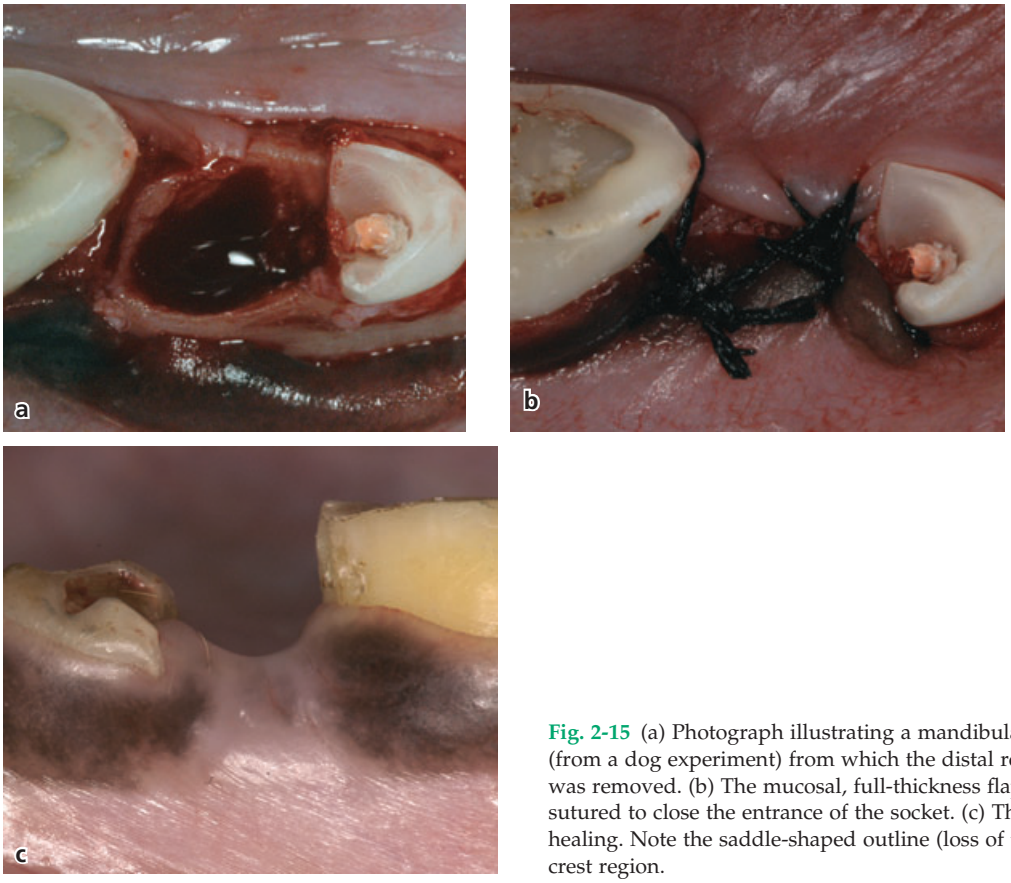

Fig. 2-15 (a) Photograph illustrating a mandibular premolar site (from a dog experiment) from which the distal root of the 4th premolar was removed. (b) The mucosal, full-thickness flaps were replaced and sutured to close the entrance of the socket. (c) The site after 6 months of healing. Note the saddle-shaped outline (loss of tissue) of the alveolar crest region.

in biopsy specimens obtained at time intervals between 1 day and 6 months (Fig. 2-15c).

Overall pattern of socket healing

Figure 2-13 presents a mesio-distal section of a fresh extraction socket bordered by adjacent roots. The socket is filled with a coagulum. The socket walls are continuous with the alveolar bone proper of the neighboring teeth. The tissue inside the interdental (inter-radicular) septa is made up of cancellous bone and includes trabeculae of lamellar bone within bone marrow.

The empty socket is first filled with blood and a *coagulum* (clot) forms (Fig. 2-16a). Inflammatory cells (polymorphonuclear leukocytes and monocytes/macrophages) migrate into the coagulum and start to phagocytose elements of necrotic tissue. The process of wound cleansing is initiated (Fig. 2-16b). Sprouts of newly formed vessels and mesenchymal cells (from the severed periodontal ligament) enter the coagulum and *granulation tissue* is formed. The granulation tissue is gradually replaced with *provisional connective tissue* (Fig. 2-16c) and subsequently immature bone (*woven bone*) is laid down (Fig. 2-16d). The hard tissue walls of the socket – the alveolar bone proper or the bundle bone – are resorbed and the socket wound becomes filled with woven bone (Fig. 2-16e). The initial phases of the healing process are now completed. In subsequent phases the woven bone in the socket is gradually remodeled into lamellar bone and marrow (Fig. 2-16f, g, h).

Important events in socket healing

Blood clotting

Immediately after tooth extraction, blood from the severed blood vessels will fill the cavity. Proteins derived from vessels and damaged cells initiate a series of events that lead to the formation of a fibrin network (Fig. 2-17). *Platelets* form aggregates and interact with the fibrin network to produce a *blood clot* (a coagulum) that effectively plugs the severed vessels and stops bleeding. The blood clot acts as a physical matrix that directs cellular movements and it contains substances that are of importance for the forthcoming healing process. Thus, the clot contains substances that (1) influence mesenchymal cells (i.e. *growth factors*) and (2) enhance the activity of inflammatory cells. Such substances will thus induce and amplify the migration of various types of cells into the socket wound, as well as their proliferation, differentiation and synthetic activity within the coagulum.

Although the blood clot is crucial in the initial phase of wound healing, its removal is mandatory to allow the formation of new tissue. Thus, within a few days after the tooth extraction, the blood clot will start to break down, i.e. the process of "fibrinolysis" is initiated (Fig. 2-18).

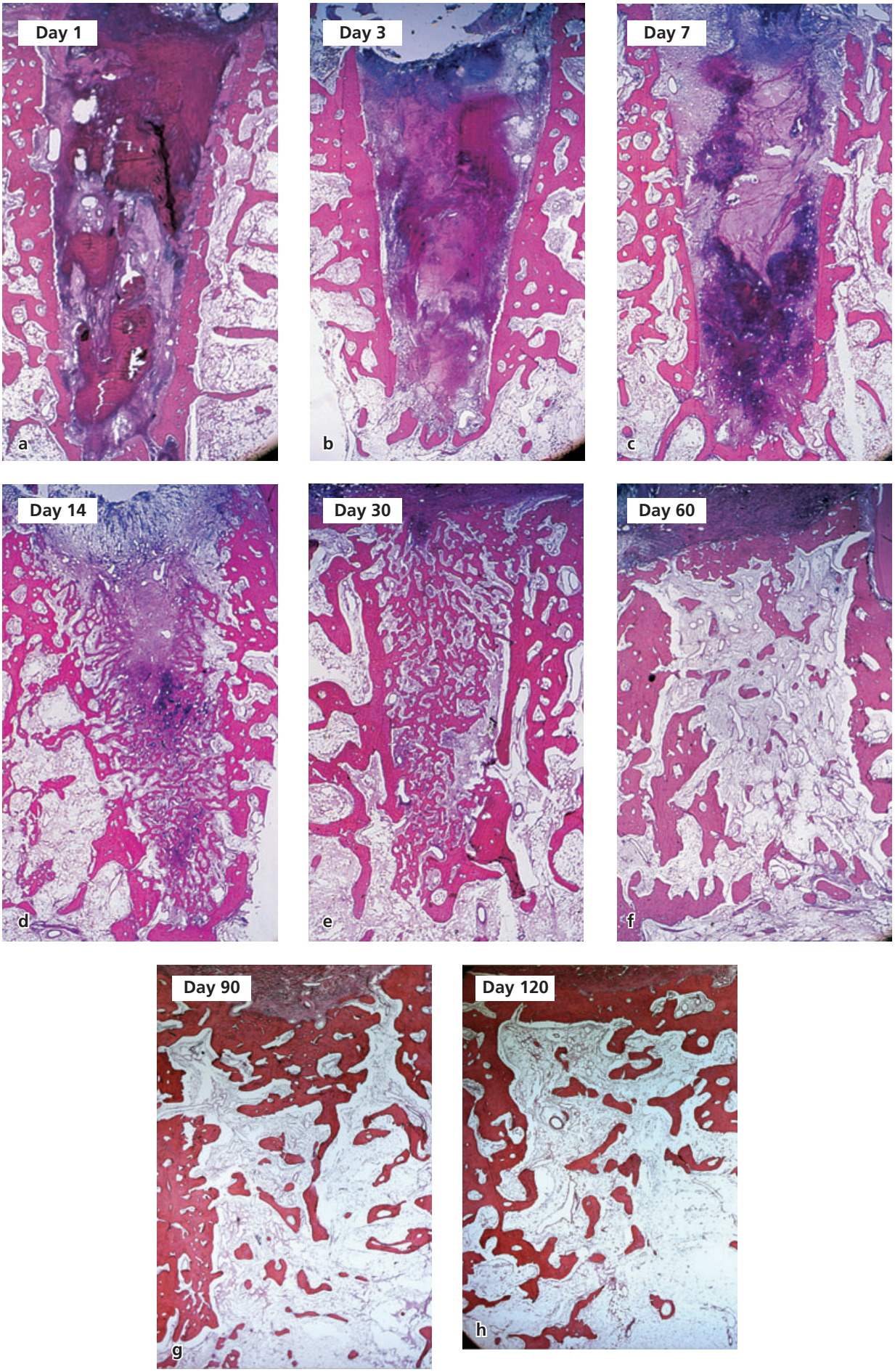

Fig. 2-16 Overall pattern of bone formation in an extraction socket. For details see text.

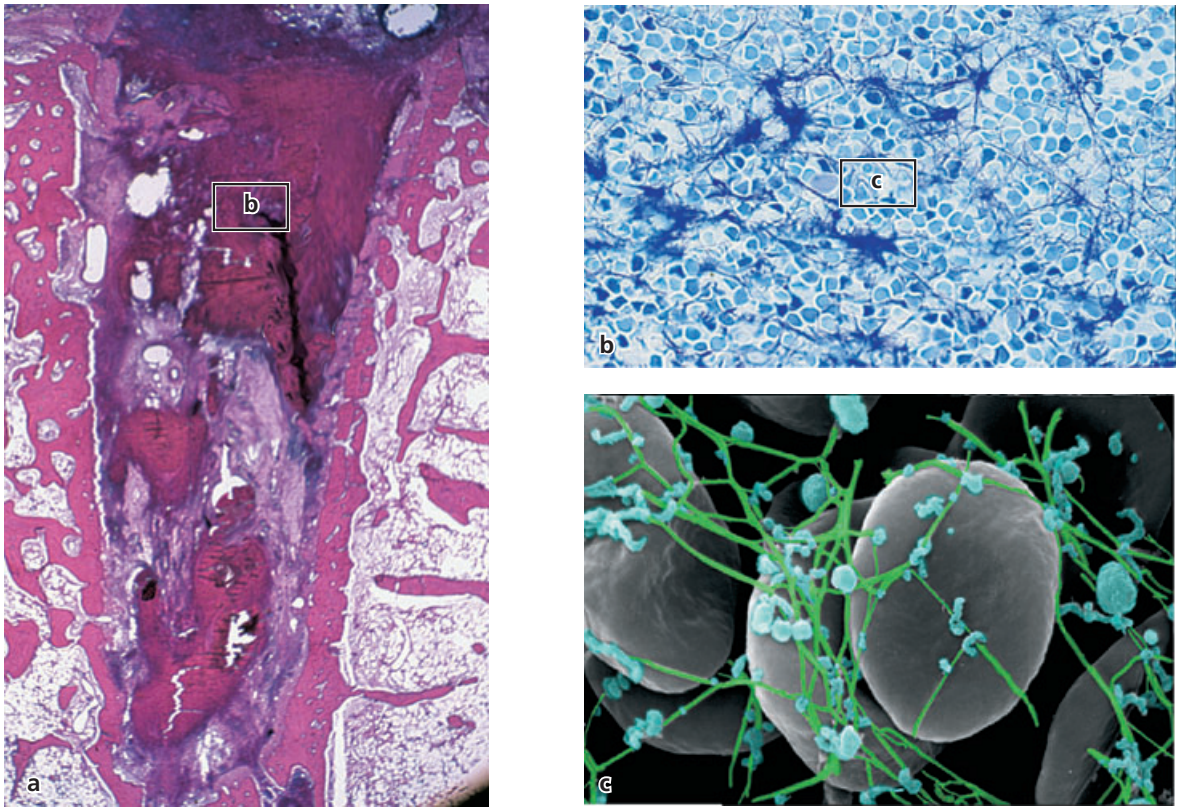

Fig. 2-17 Histologic section (mesio-distal aspect) representing 1 day of healing (a). The socket is occupied with a blood clot that contains large numbers of erythrocytes (b) entrapped in a fibrin network, as well as platelets (blue in (c)).

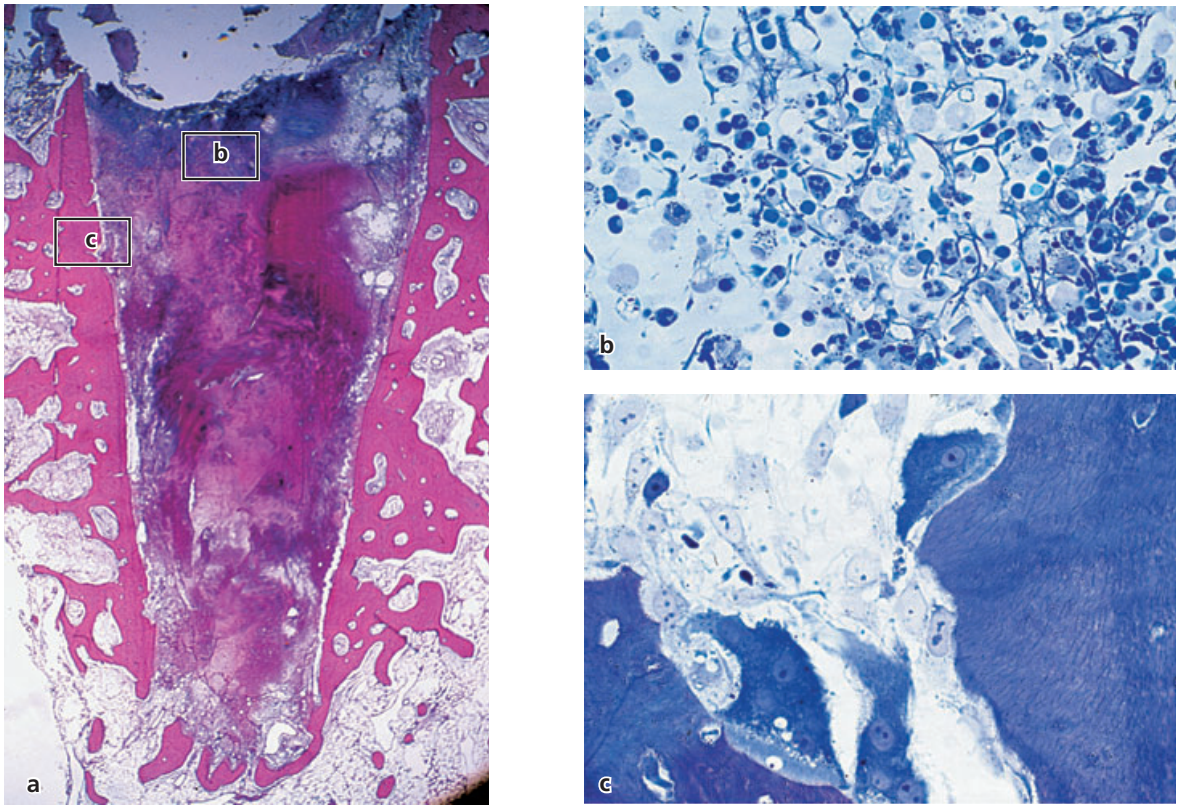

Fig. 2-18 (a) Histologic section (mesio-distal aspect) representing 3 days of healing. (b) Note the presence of neutrophils and macrophages that are engaged in wound cleansing and the break down of the blood clot. (c) Osteoclastic activity occurs on the surface of the old bone in the socket walls.

Wound cleansing

Neutrophils and macrophages migrate into the wound, engulf bacteria and damaged tissue (Fig. 2-18) and clean the site before the formation of new tissue can start. The neutrophils enter the wound early while macrophages appear somewhat later. The macrophages are not only involved in the cleaning of the wound but they also release growth factors and cytokines that further promote the migration, proliferation and differentiation of mesenchymal cells. Once the debris has been removed and the wound has become "sterilized", the neutrophils undergo a programmed cell death (*apoptosis*) and are removed from the site through the action of macrophages. The macrophages subsequently withdraw from the wound.

Tissue formation

Sprouts of vascular structures (from the severed periodontal ligament) as well as mesenchymal, fibroblast-like cells (from the periodontal ligament and from adjacent bone marrow regions) enter the socket. The mesenchymal cells start to proliferate and deposit matrix components in an extracellular location (Fig. 2-19a,b,c); a new tissue, i.e. *granulation tissue*, will gradually replace the blood clot. The granulation tissue eventually contains macrophages, and a large number of fibroblast-like cells as well as numerous newly formed blood vessels. The fibroblast-like cells continue (1) to release growth factors, (2) to proliferate, and (3) to deposit a new extra cellular matrix that guides the ingrowth of additional cells and allows the further differentiation of the tissue. The newly formed vessels provide the oxygen and nutrients that are needed for the increasing number of cells that occur in the new tissue. The intense synthesis of matrix components exhibited by the mesenchymal cells is called *fibroplasia*, while the formation of new vessels is called *angiogenesis*. A *provisional connective tissue* is established through the combination of fibroplasia and angiogenesis (Fig. 2-20).

The transition of the provisional connective tissue into bone tissue occurs along the vascular structures. Thus, osteoprogenitor cells (e.g. pericytes) migrate and gather in the vicinity of the vessels. They differentiate into osteoblasts that produce a matrix of collagen fibers, which takes on a woven pattern. The *osteoid* is formed. The process of mineralization is initiated within the osteoid. The osteoblasts continue to lay down osteoid and occasionally such cells are trapped in the matrix and become osteocytes. This newly formed bone is called *woven bone* (Fig. 2-21).

The woven bone is the first type of bone to be formed and is characterized by (1) its rapid deposition as fingerlike projections along the route of vessels, (2) the poorly organized collagen matrix, (3) the large number of osteoblasts that are trapped in its mineralized matrix, and (4) its low load-bearing capacity. Trabeculae of woven bone are shaped around and encircle the vessel. The trabeculae become

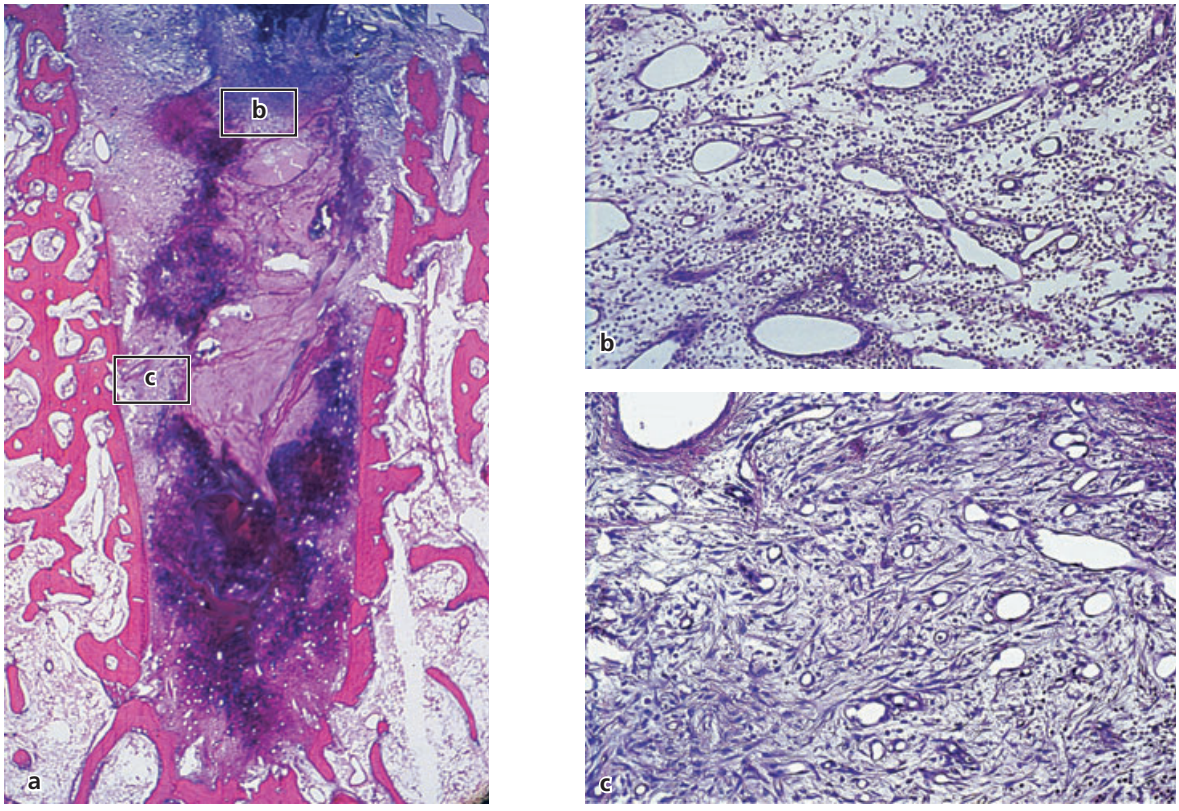

Fig. 2-19 (a) Histologic section (mesio-distal aspect) representing 7 days of healing. (b) Note the presence of a richly vascularized early granulation tissue with large numbers of inflammatory cells in the upper portion of the socket. (c) In more apical areas, a tissue including large numbers of fibroblast-like cells is present, i.e. late granulation tissue.

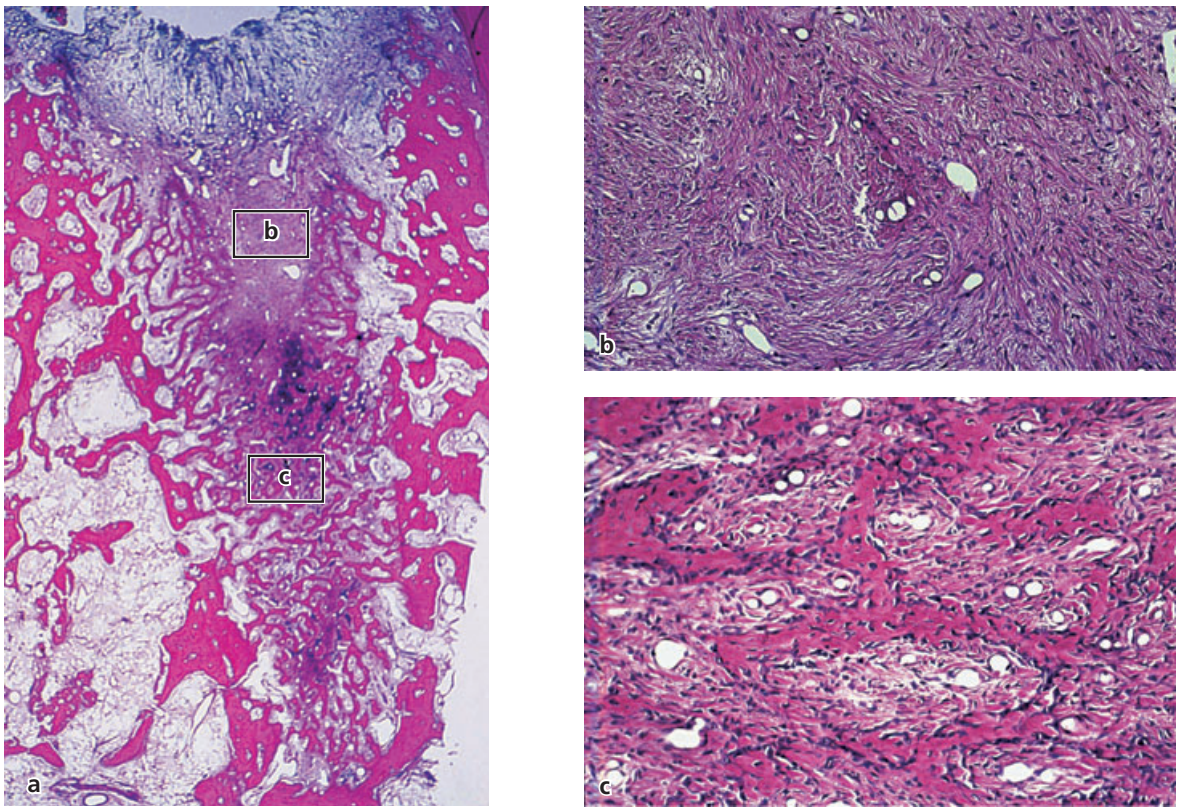

Fig. 2-20 (a) Histologic section (mesio-distal aspect) representing 14 days of healing. (b) In the marginal portion of the wound, a provisional connective tissue rich in fibroblast-like cells is present. (c) The formation of woven bone has at this time interval already begun in apical and lateral regions of the socket.

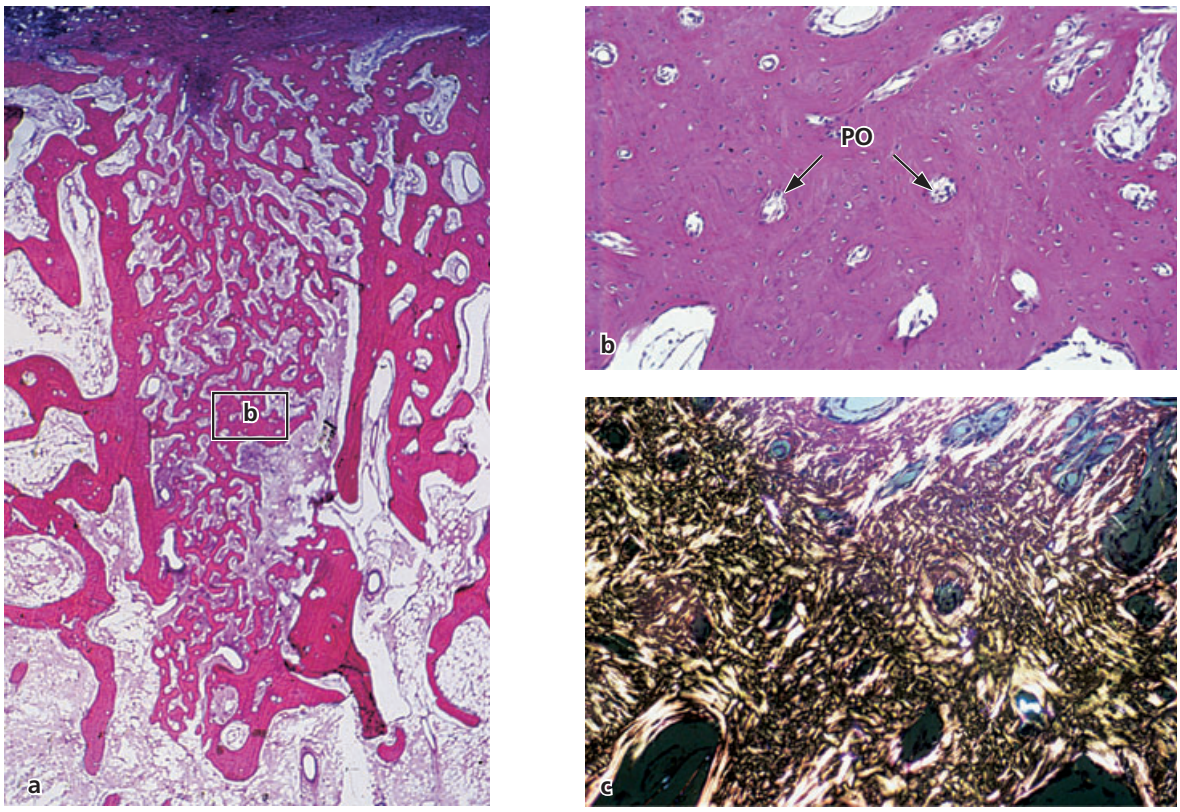

Fig. 2-21 (a) Histologic section (mesio-distal aspect) representing 30 days of healing. The socket is filled with woven bone. (b) This woven bone contains a large number of cells and primary osteons (PO). (c) The woven pattern of the collagen fibers of this type of bone is illustrated (polarized light).

thicker through the deposition of additional woven bone. Cells (osteocytes) become entrapped in the bone tissue and the first set of osteons, the *primary osteons*, are organized. The woven bone is occasionally reinforced by the deposition of so called *parallel-fibered bone*, that has its collagen fibers organized not in a woven but in a concentric pattern.

It is important to realize that during this early phase of healing the bone tissue in the walls of the socket (the bundle bone) is removed and replaced with woven bone.

Tissue modeling and remodeling

The initial bone formation is a fast process. Within a few weeks, the entire extraction socket will become filled with woven bone or, as this tissue is also called, *primary bone spongiosa*. The woven bone offers (1) a stable scaffold, (2) a solid surface, (3) a source of osteoprogenitor cells, and (4) ample blood supply for cell function and matrix mineralization.

The woven bone with its primary osteons is gradually replaced with lamellar bone and bone marrow (Fig. 2-22). In this process, the primary osteons are replaced with *secondary osteons*. The woven bone is first resorbed to a certain level. This level of the resorption front will establish a so-called *reversal line*, which is also the level from which new bone with secondary osteons will form (Fig. 2-23). Although this remodeling may start early during socket healing it will take several months until all woven bone in the extraction socket has been replaced with lamellar bone and marrow.

An important part of socket healing involves the formation of a *hard tissue cap* that will close the marginal entrance to the socket. This cap is initially comprised of woven bone (Fig. 2-24a) but is subsequently remodeled and replaced with lamellar bone that becomes continuous with the cortical plate at the periphery of the edentulous site (Fig. 2-24b). This process is called corticalization.

The wound is now healed, but the tissues in the site will continue to adapt to functional demands. Since there is no stress from forces elicited during mastication and other occlusal contacts there is no demand on mineralized bone in the areas previously occupied by the tooth. Thus, the socket apical of the hard tissue cap will remodel mainly into marrow. Indeed, in many edentulous patients the entire alveolar ridge will regress as a result of continuous adaptation to lack of function.

Extra-alveolar processes

In an experiment in the dog (Araújo & Lindhe 2005) alterations in the profile of the edentulous ridge that occurred following tooth extraction were carefully examined. In this study the 3rd and 4th mandibular

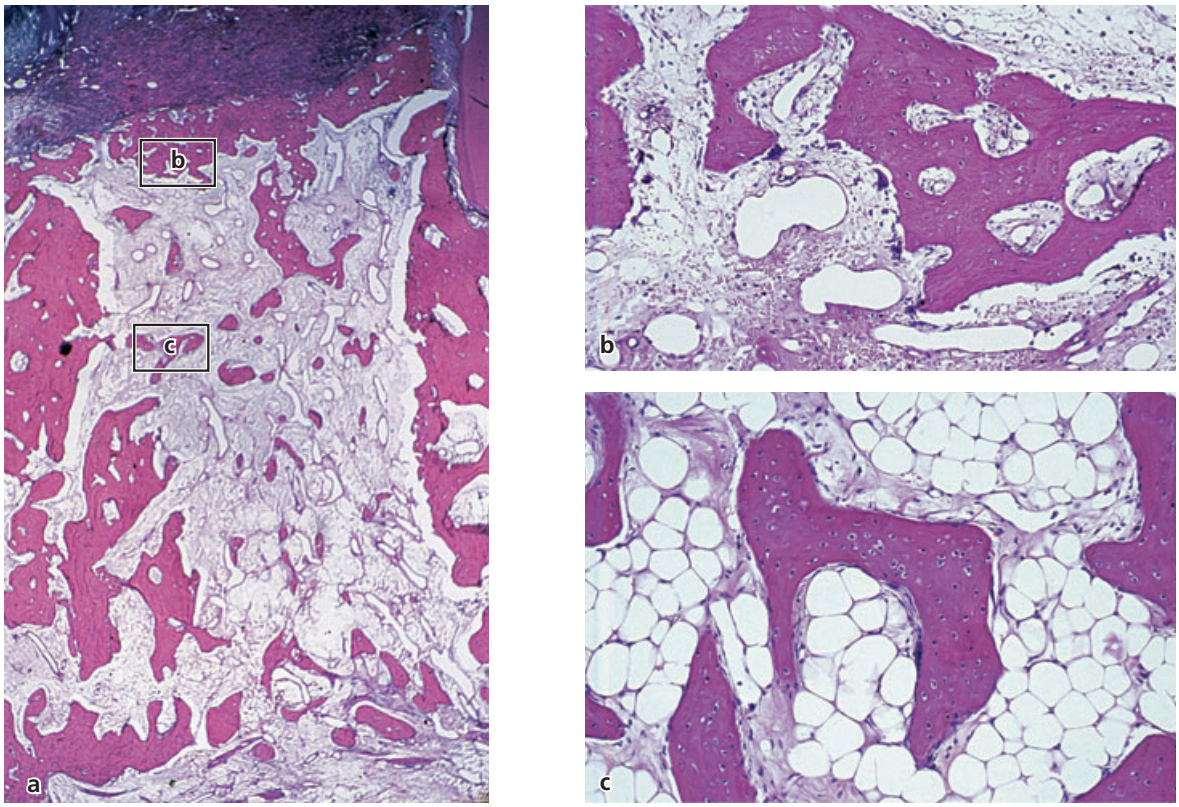

Fig. 2-22 (a) Histologic section (mesio-distal aspect) representing 60 days of healing. (b) A large portion of the woven bone has been replaced with bone marrow. (c) Note the presence of a large number of adipocytes residing in a tissue that still contains woven bone.

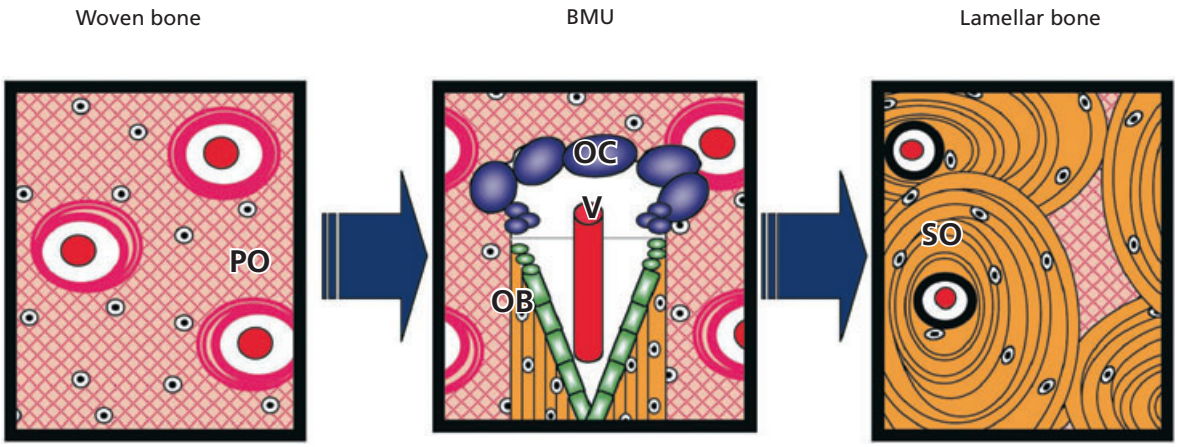

Fig. 2-23 Schematic drawing that describes how woven bone is replaced by lamellar bone. Woven bone with primary osteons is substituted by lamellar bone in a process that involves the presence of bone multicellular units (BMUs). The BMU contains osteoclasts (OC), as well as vascular structures (V) and osteoblasts (OB). Thus, the osteoblasts in the BMU produce bone tissue in a concentric fashion around the vessel, and lamellar bone with secondary osteons is formed.

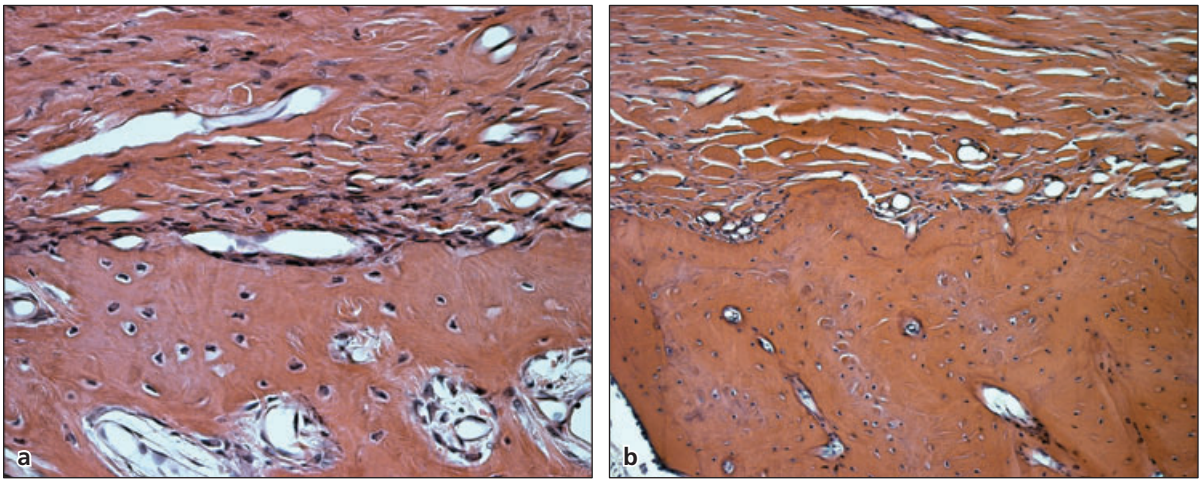

Fig. 2-24 Histologic sections (mesio-distal aspect) describing the hard tissue that has formed at the entrance of a healing extraction socket and the process of corticalization. (a) Woven bone with primary osteons occupies the socket entrance after 60 days of healing. (b) After 180 days the woven bone has been replaced with mainly lamellar bone.

premolars were hemi-sected. Buccal and lingual full-thickness flaps were raised; the distal roots were carefully removed. The flaps were replaced and sutured to cover the fresh extraction socket (Fig. 2-25). Biopsy specimens, including an individual extraction socket and adjacent roots, were obtained after 1, 2, 4, and 8 weeks of healing. The blocks were sectioned in the *buccal–lingual* plane.

Figure 2-26 illustrates a buccal–lingual section of the distal root of an intact 3rd premolar with surrounding soft and hard tissues. The lingual hard tissue wall is substantially wider than its buccal counterpart. The marginal portion of the lingual wall is presented in a higher magnification in Fig. 2-26a. A layer of bundle bone occupies the inner portion of the lingual bone wall. A thin layer of bundle bone is also present at the top of the ridge. Figure 2-26b illustrates the corresponding portion of the buccal bone wall. Note that all the mineralized tissue in the marginal 1–2 mm of the buccal ridge is comprised of bundle bone. In this context, it must be remembered that bundle bone is part of the attachment tissues for the tooth; this tissue has no obvious function following the removal of the tooth and will thus eventually be resorbed and disappear.

- *1 week after tooth extraction* (Fig. 2-27). At this interval the socket is occupied by a coagulum. Furthermore, a large number of osteoclasts can be seen on the outside as well as on the inside of the buccal and lingual bone walls. The presence of osteoclasts on the inner surface of the socket walls indicates that the bundle bone is being resorbed.
- *2 weeks after tooth extraction* (Fig. 2-28). Newly formed immature bone (woven bone) resides in the apical and lateral parts of the socket, while more central and marginal portions are occupied by a provisional connective tissue. In the marginal

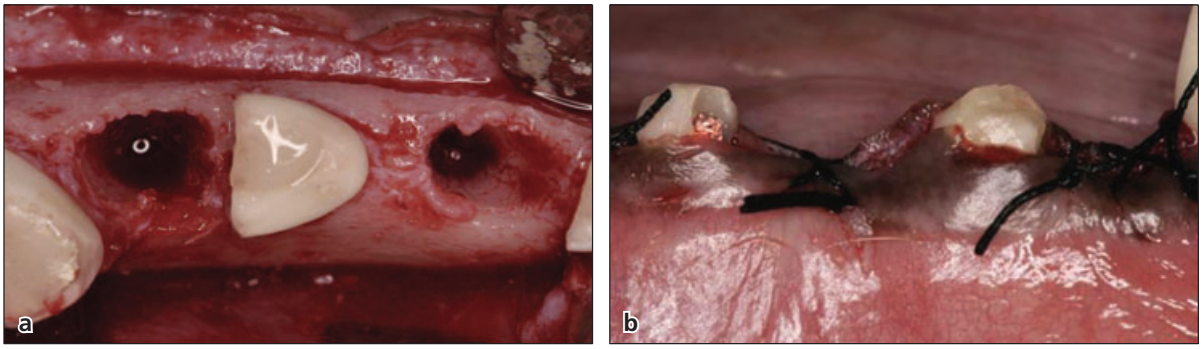

Fig. 2-25 (a) Photograph illustrating mandibular premolar sites (from a dog experiment) from which the distal roots of the 4th and 3rd premolars were extracted. (b) The mucosal, full-thickness flaps were replaced and sutured to close the entrance of the socket.

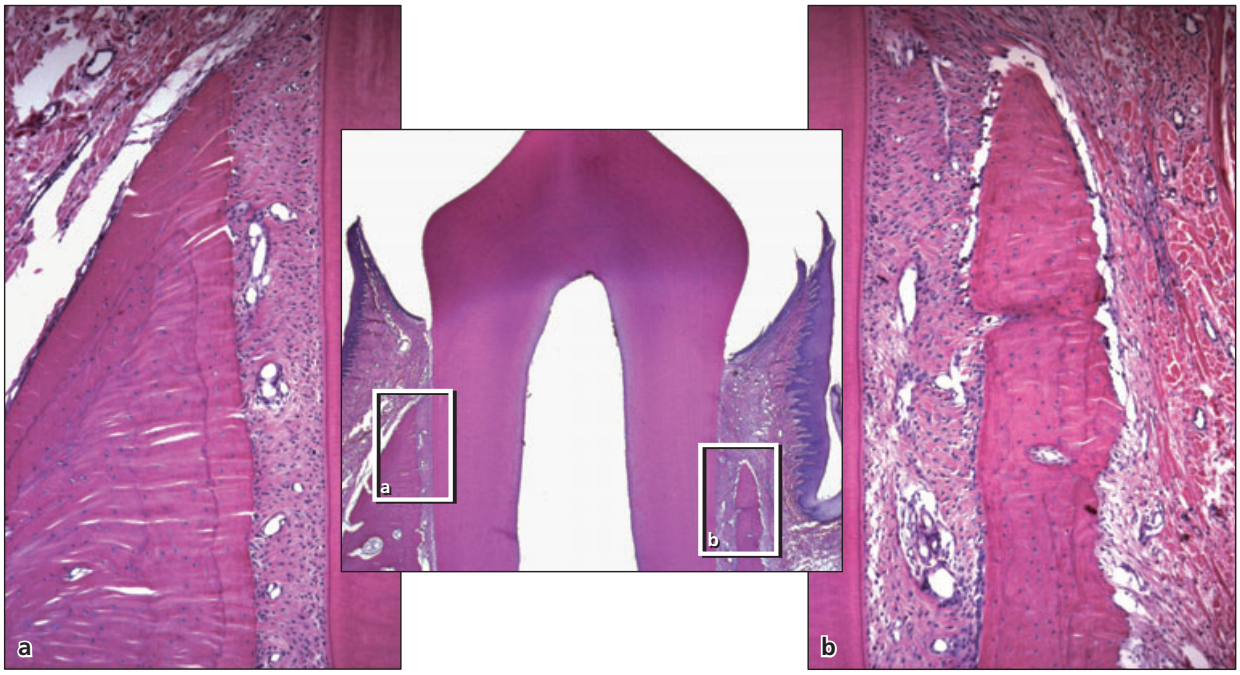

Fig. 2-26 Histologic section (buccal–lingual aspect) of the distal root of an intact 3rd premolar in the dog. Note the wide lingual and thinner buccal bone wall. Higher magnification of the crestal bone of the lingual wall (a) and buccal wall (b). B = buccal bone; L = lingual bone.

and outer portions of the socket walls numerous osteoclasts can be seen. In several parts of the socket walls the bundle bone has been replaced with woven bone.

- *4 weeks after tooth extraction* (Fig. 2-29). The entire socket is occupied with woven bone at this stage of healing. Large numbers of osteoclasts are present in the outer and marginal portions of the hard tissue walls. Osteoclasts also line the trabeculae of woven bone present in the central and lateral aspects of the socket. In other words the newly formed woven bone is being replaced with a more mature type of bone.
- *8 weeks after tooth extraction* (Fig. 2-30). A layer of cortical bone covers the entrance to the extraction site. Corticalization has occurred. The woven bone that was present in the socket at the 4-week interval is replaced with bone marrow and some trabeculae of lamellar bone in the 8-week specimens. On the outside and on the top of the buccal and lingual bone wall there are signs of ongoing hard tissue resorption. The crest of the buccal bone wall is located apical of its lingual counterpart.

The relative change in the location of the crest of the buccal and lingual bone walls that took place during the 8 weeks of healing is illustrated in Fig. 2-31. While the level of the margin of the lingual wall remained reasonably unchanged, the margin of the buccal wall shifted several millimeters in an apical direction.

There are at least two reasons why, in this animal model, more bone loss occurred in the buccal than in the lingual wall during socket healing. First, prior to tooth extraction, the marginal 1–2 mm

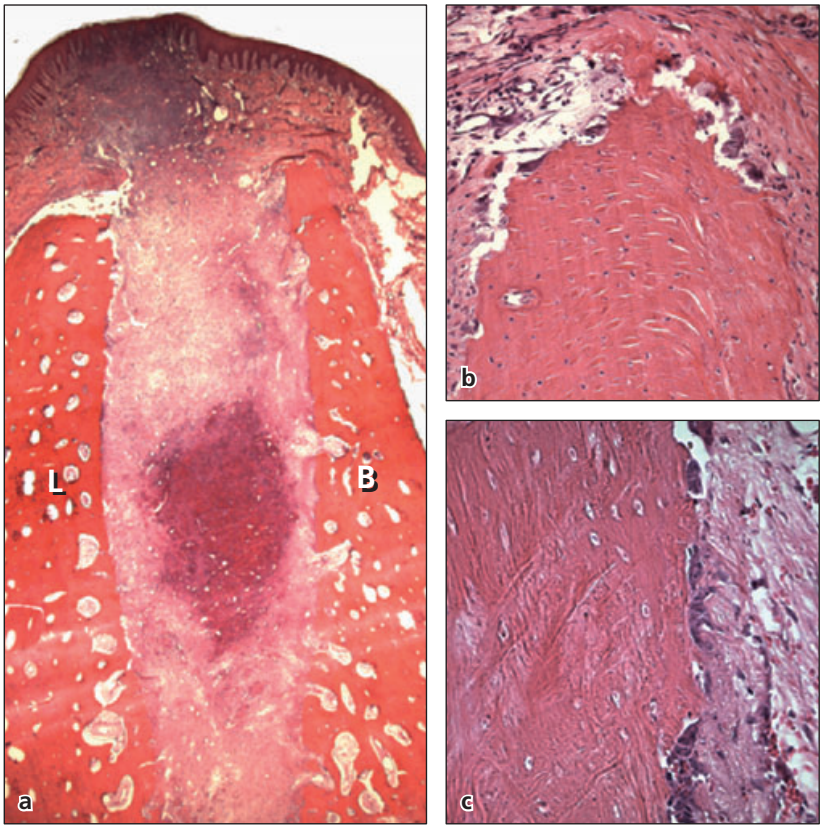

Fig. 2-27 (a) Histologic section (buccal–lingual aspect) of the socket after 1 week of healing. Note the presence of a large number of osteoclasts on the crestal portion (b) and inner portion (c) of the buccal wall. B = buccal bone; L = lingual bone.

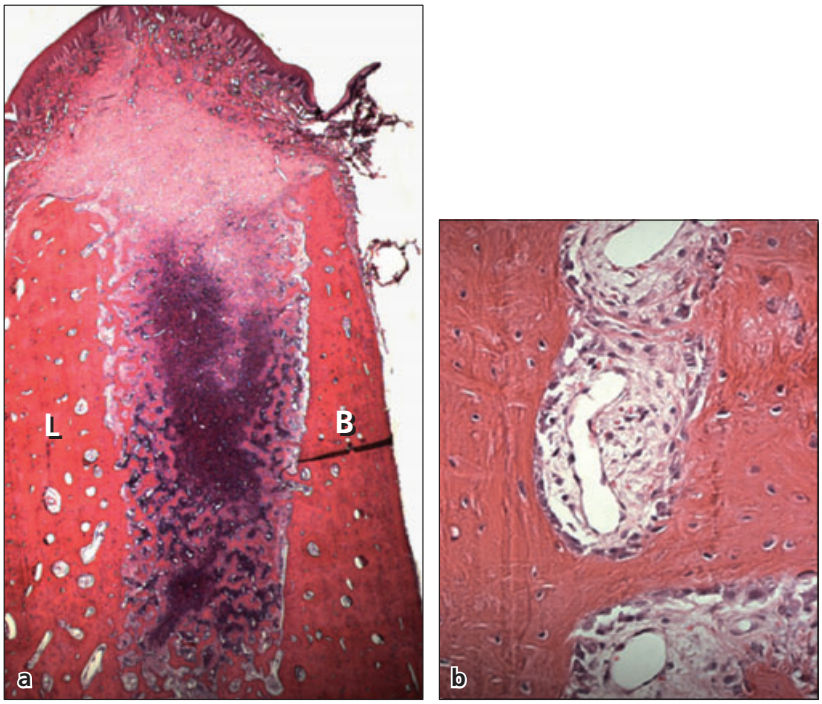

Fig. 2-28 (a) Histologic section (buccal–lingual aspect) of the socket after 2 weeks of healing. (b) Note that the bundle bone in the lingual aspect of the socket is being replaced with woven bone. B = buccal bone; L = lingual bone.

of the crest of the buccal bone wall was occupied by bundle bone. Only a minor fraction of the crest of the lingual wall contained bundle bone. Bundle bone, as stated above, is a tooth-dependent tissue and will gradually disappear after tooth extraction. Thus, since there is relatively more bundle bone in the crest region of the buccal than of the lingual wall, hard tissue loss will become most pronounced in the buccal wall. Secondly, the lingual bone wall of the socket is markedly wider than that of the buccal wall. It is well known from the periodontal literature (e.g. Wilderman *et al*. 1960; Wilderman 1963; Tavtigian 1970; Wood *et al*. 1972; Araújo *et al*. 2005) that flap elevation and the separation of the perios-

teum from the bone tissue will result in surface resorption; this will result in more vertical height reduction of the thin buccal than of the wider lingual bone wall.

Topography of the edentulous ridge

As described previously in this chapter, the processes of modeling and remodeling that occur following tooth extraction (loss) result in pronounced resorption of the various components of the alveolar ridge. The resorption of the buccal bone wall is more pronounced than the resorption of the lingual/palatal wall and hence the center of the ridge will move in lingual/palatal direction. In the extreme case, the entire alveolar process may be lost following tooth loss and in such situations only the bone of the base of the mandible and the base of the maxilla remains.

Figure 2-32 presents a buccal–lingual section of an edentulous site prepared from a biopsy of a dog obtained 2–3 years after tooth extraction. The ridge

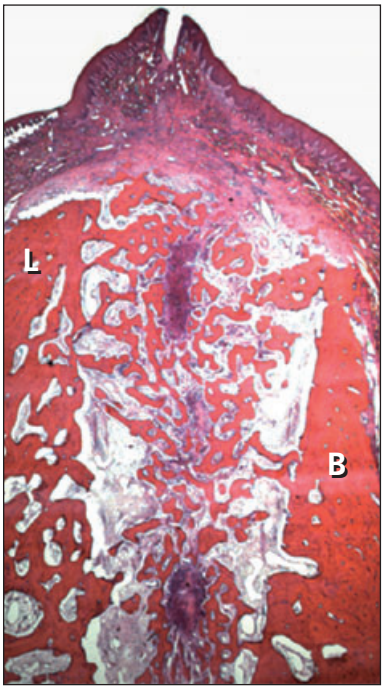

Fig. 2-29 Histologic section (buccal–lingual aspect) of the socket after 4 weeks of healing. The extraction socket is filled with woven bone. On the top of the buccal wall the old bone in the crest region is being resorbed and replaced with either connective tissue or woven bone. B = buccal bone; L = lingual bone.

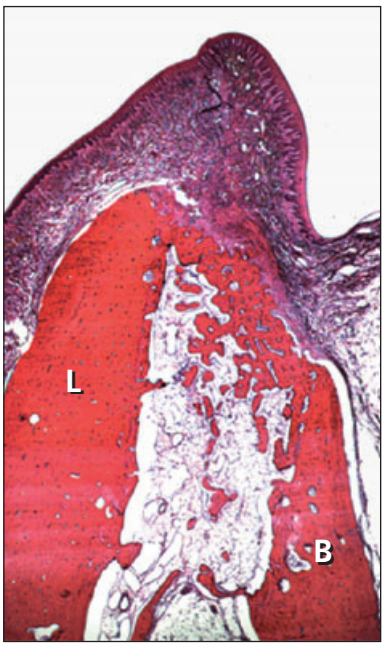

Fig. 2-30 Histologic section (buccal–lingual aspect) of the socket after 8 weeks of healing. The entrance of the socket is sealed with a cap of newly formed mineralized bone. Note that the crest of the buccal wall is located apical of the crest of the lingual wall. B = buccal bone; L = lingual bone.

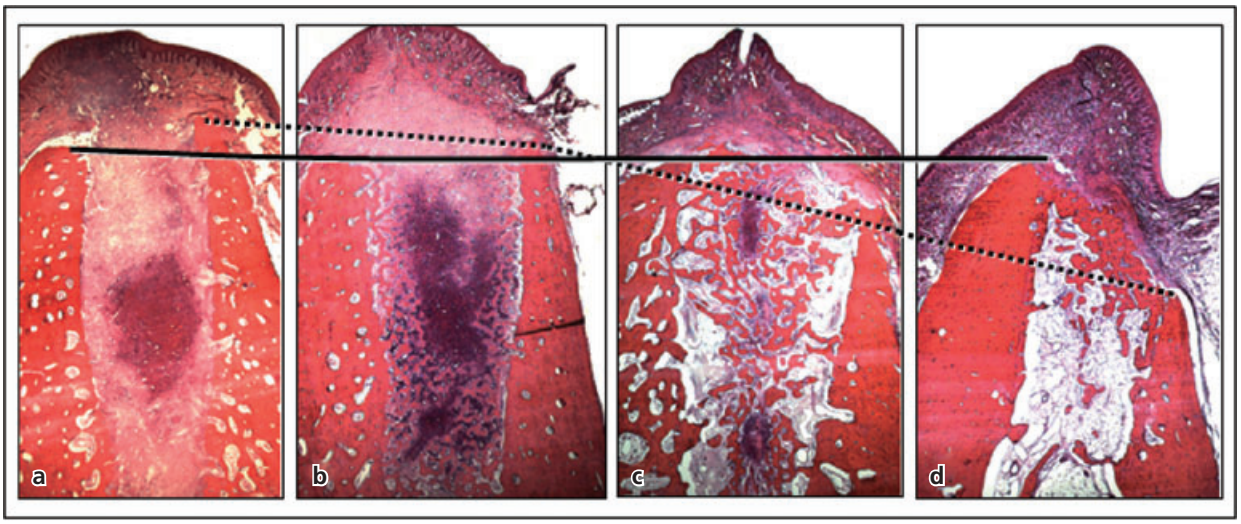

Fig. 2-31 Histologic sections (buccal–lingual aspects) describing the profile of the edentulous region in the dog after (a) 1, (b) 2, (c) 4, and (d) 8 weeks of healing following tooth extraction. While the marginal level of the lingual wall was maintained during the process of healing (solid line), the crest of the buccal wall was replaced >2 mm in the apical direction (dotted line).

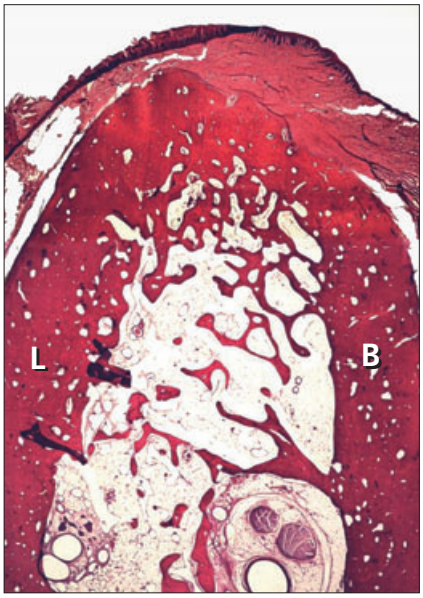

Fig. 2-32 Histologic section (buccal–lingual aspect) describing an edentulous mandibular site (from a dog experiment) 2 years after the extraction of the tooth. Note that the crest is higher at the lingual than at the buccal aspect of the site. B = buccal bone; L = lingual bone.

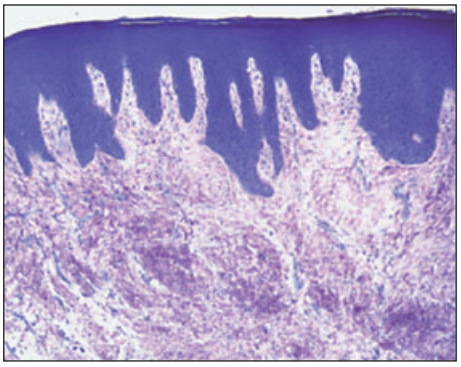

Fig. 2-33 Histologic section illustrating the mucosa residing over the bone crest. The mucosa has a well keratinized epithelium and a connective tissue densely packed with collagen fibers.

is covered by a mucosa (Fig. 2-33) that in this particular case is about 2–3 mm high and is comprised of keratinized epithelium and dense connective tissue that is attached via the periosteum to the cortical bone. Depending on factors such as the biotype, the jaw (maxilla or mandible), the location (anterior, posterior) in the jaw, location of the muco-gingival junction, depth of the buccal and lingual vestibule, and the amount of hard tissue resorption, the edentulous site may be lined with either masticatory, keratinized mucosa or lining, non-keratinized mucosa.

The outer walls of the remaining portion of the alveolar process are comprised of lamellar bone. The buccal bone plate is comparatively thin and the lingual/palatal plate comparatively thick. The cortical plates enclose the cancellous bone that harbors trabeculae of lamellar bone and marrow. The bone marrow contains numerous vascular structures as well as adipocytes and pluripotent mesenchymal cells. As a rule the ridge of the edentulous site in the maxilla contains comparatively more cancellous bone than a site in the mandible.

References

Amler, M.H. (1969). The time sequence of tissue regeneration in human extraction wounds. *Oral Surgery, Oral Medicine and Oral Pathology* **27**, 309–318.

Araújo, M.G. & Lindhe, J. (2005). Dimensional ridge alterations following tooth extraction. An experimental study in the dog. *Journal of Clinical Periodontology* **32**, 212–218.

Araújo, M.G., Sukekava, F., Wennström, J.L. & Lindhe, J. (2005). Ridge alterations following implant placement in fresh extraction sockets; an experimental study in the dog. *Journal of Clinical Periodontology* **32**, 645–652.

Atwood, D.A. (1962). Some clinical factors related to the rate of resorption of residual ridges. *Journal of Prosthetic Dentistry* **12**, 441–450.

Atwood, D.A. (1963). Postextraction changes in the adult mandible as illustrated by microradiographs of midsagittal section and serial cephalometric roentgenograms. *Journal of Prosthetic Dentistry* **13**, 810–816.

Cardaropoli, G., Araújo, M. & Lindhe, J. (2003). Dynamics of bone tissue formation in tooth extraction sites. An experimental study in dogs. *Journal of Clinical Periodontology* **30**, 809–818.

Carlsson, G.E., Thilander, H. & Hedegård, B. (1967). Histological changes in the upper alveolar process after extraction with or without insertion of an immediate full denture. *Acta Odontologica Scandinavica* **25**, 21–43.

Evian, C.I., Rosenberg, E.S., Cosslet, J.G. & Corn, H. (1982). The osteogenic activity of bone removed from healing extraction sockets in human. *Journal of Periodontology* **53**, 81–85.

Friedenstein, A.G. (1973). Determined and inducible osteogenic precursor cells. In: *Hand Tissue Growth Repair and Remineralization*. Aba Foundation Symposium 11, pp. 169–181.

Johnson, K. (1963). A study of the dimensional changes occurring in the maxilla after tooth extraction. Part I. Normal healing. *Australian Dental Journal* **8**, 241–244.

Johnson, K. (1969). A study of the dimensional changes occurring in the maxilla following tooth extraction. *Australian Dental Journal* **14**, 428–433.

Lekholm, U. & Zarb, G.A. (1985). Patient selection. In: Brånemark, P-I., Zarb, G.A. & Albreksson, T., eds. *Tissue Integrated Prostheses. Osseointegrationin Clinical Dentistry*. Chicago: Quintessence, pp. 199–209.

Pietrokovski, J. & Massler, M. (1967). Alveolar ridge resorption following tooth extraction. *Journal of Prosthetic Dentistry* **17**, 21–27.

Schropp, L., Wenzel, A., Kostopoulos, L. & Karring, T. (2003). Bone healing and soft tissue contour changes following single-tooth extraction: a clinical and radiograhic 12-month prospective study. *International Journal of Periodontics & Restorative Dentistry* **23**, 313–323.

Tavtigian, R. (1970). The height of the facial radicular alveolar crest following apically positioned flap operations. *Journal of Periodontology* **41**, 412–418.

Wilderman, M.N. (1963). Repair after a periosteal retention procedure. *Journal of Periodontology* **34**, 487–503.

Wilderman, M.N., Wentz, F. & Orban, B.J. (1960). Histogenesis of repair after mucogingival surgery. *Journal of Periodontology* **31**, 283–299.

Wood, D.L., Hoag, P.M., Donnenfeld, W.O. & Rosenfeld, L.D. (1972). Alveolar crest reduction following full and partial thickness flaps. *Journal of Periodontology* **42**, 141–144.

Chapter 3

The Mucosa at Teeth and Implants

Jan Lindhe, Jan L. Wennström, and Tord Berglundh

The gingiva

Biologic width

A term frequently used to describe the dimensions of the soft tissues that face the teeth is *the biologic width of the soft tissue attachment*. The development of the *biologic width concept* was based on studies and analyses by, among others, Gottlieb (1921), Orban and Köhler (1924), and Sicher (1959), who documented that the soft tissue attached to the teeth was comprised of two parts, one fibrous tissue and one attachment of epithelium. In a publication by Gargiulo *et al.* (1961) called "Dimensions and relations of the dentogingival junction in humans", sections from autopsy block specimens that exhibited different degree of "passive tooth eruption" (i.e. periodontal tissue breakdown) were examined. Histometric assessments were made to describe the length of the sulcus (not part of the attachment), the epithelial attachment (today called junctional epithelium), and of the connective tissue attachment (Fig. 3-1). It was observed that the length of the connective tissue attachment varied within narrow limits (1.06–1.08 mm) while the length of the attached epithelium was about 1.4 mm at sites with normal periodontium, 0.8 mm at sites with moderate and 0.7 mm at sites with advanced periodontal tissue breakdown. In other words, (1) the biologic width of the attachment varied between about 2.5 mm in the normal case and 1.8 mm in the advanced disease case, and (2) the most variable part of the attachment was the length of the epithelial attachment (junctional epithelium).

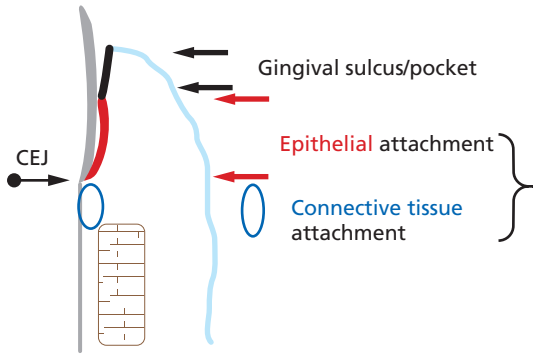

Fig. 3-1 Drawing describing the "biologic width" of the soft tissue attachment at the buccal surface of a tooth with healthy periodontium. The combined length of the junctional epithelium (epithelial attachment) and the connective tissue attachment is considered to represent the "biologic width" of the soft tissue attachment. Note the gingival sulcus is NOT part of the attachment.

Dimensions of the buccal tissue

The morphologic characteristics of the gingiva are related to the dimension of the alveolar process, the form (anatomy) of the teeth, events that occur during tooth eruption, and the eventual inclination and position of the fully erupted teeth (Wheeler 1961; O'Connor & Biggs 1964; Weisgold 1977). Ochenbein

Fig. 3-2 Clinical photograph of a subject that belongs to the "pronounced scalloped" gingival biotype. The crowns of the teeth are comparatively long and slender. The papillae are comparatively long, the gingival margin is thin and the zone of attached gingiva is short.

Fig. 3-3 Clinical photograph of a subject that belongs to the "flat" gingival biotype. The crowns of the teeth are comparatively short but wide. The papillae are comparatively short but voluminous and the zone of attached gingiva is wide.

and Ross (1969) and Becker *et al*. (1997) proposed (1) that the anatomy of the gingiva is related to the contour of the osseous crest, and (2) that two basic types of gingival architecture may exist, namely the "*pronounced scalloped*" and the "*flat*" biotype.

Subjects who belong to the "*pronounced scalloped*" biotype have long and slender teeth with tapered crown form, delicate cervical convexity and minute interdental contact areas that are located close to the incisal edge (Fig. 3-2). The maxillary front teeth of such individuals are surrounded with a thin free gingiva, the buccal margin of which is located at or apical of the cemento-enamel junction. The zone of gingiva is narrow, and the outline of the gingival margin is highly scalloped (Olsson *et al*. 1993). On the other hand, subjects who belong to the "*flat*" gingival biotype have incisors with squared crown form with pronounced cervical convexity (Fig. 3-3). The gingiva of such individuals is wider and more voluminous, the contact areas between the teeth are large and more apically located, and the interdental papillae are short. It was reported that subjects with pronounced scalloped gingiva often exhibited more advanced soft tissue recession in the anterior maxilla than subjects with a flat gingiva (Olsson & Lindhe 1991).

Kan *et al*. (2003) measured the dimension of the gingiva – as determined by bone sounding – at the buccal-mesial and buccal-distal aspects of maxillary anterior teeth. Bone sounding determines the distance between the soft tissue margin and the crest of the bone and, hence, provides an estimate that is about 1 mm greater than that obtained in a regular probing pocket depth measurement. The authors reported that the thickness of the gingiva varied between subjects of different gingival biotypes. Thus, the height of the gingiva at the buccal-approximal surfaces in subjects who belonged to the flat biotype was, on average, 4.5 mm, while in subjects belonging to the pronounced scalloped biotype the corresponding dimension (3.8 mm) was significantly smaller. This indicates that subjects who belong to the flat biotype have more voluminous soft buccal/approximal tissues than subjects who belong to the pronounced scalloped biotype.

Pontoriero and Carnevale (2001) performed evaluations of the reformation of the gingival unit at the buccal aspect of teeth exposed to crown lengthening procedures using a denudation technique. At the 1-year follow-up examination after surgery the regain of soft tissue – measured from the level of the denuded osseous crest – was greater in patients with a thick (flat) biotype than in those with a thin (pronounced scalloped) biotype (3.1 mm versus 2.5 mm). No assessment was made of the bone level change that had occurred between the baseline and the follow-up examination. It must, however, be anticipated that some bone resorption had taken place during healing and that the biologic width of the new connective tissue attachment had been re-established coronal to the level of the resected osseous crest.

The dimensions of the buccal gingiva may also be affected by the buccal–lingual position of the tooth within the alveolar process. A change of the tooth position in buccal direction results in reduced dimensions of the buccal gingiva, while an increase is observed following a lingual tooth movement (Coatoam *et al*. 1981; Andlin-Sobocki & Brodin 1993). In fact, Müller and Könönen (2005) demonstrated in a study of the variability of the thickness of the buccal gingiva of young adults that most of the variation in gingival thickness was due to the tooth position and that the contribution of subject variability (i.e. flat and pronounced scalloped) was minimal.

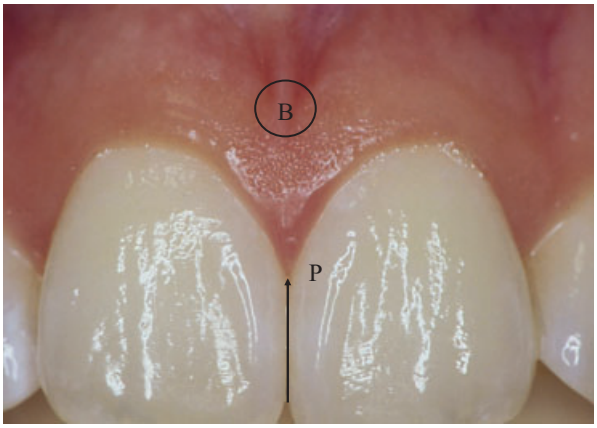

Fig. 3-4 Tarnow *et al.* (1992) measured the distance between the contact point (P) between the crowns of the teeth and the bone crest (B) using sounding (transgingival probing).

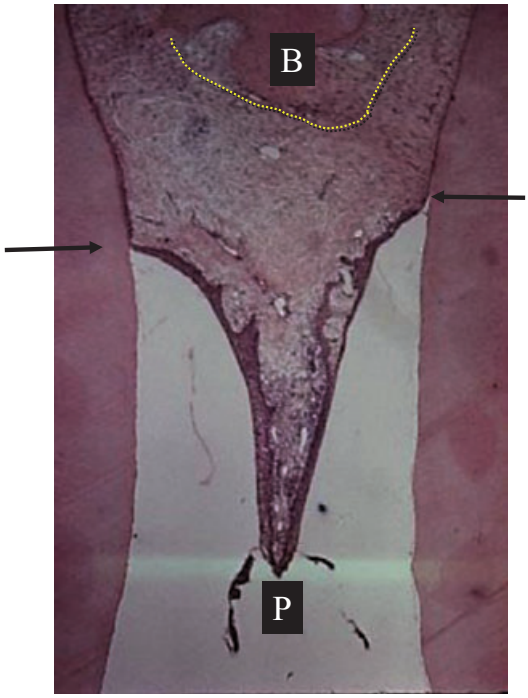

Fig. 3-5 Mesio-distal section of the interproximal area between the two central incisors. Arrows indicate the location of the cemento-enamel junction. Dotted line indicates the outline of the marginal bone crest. The distance between the contact point (P) between the crowns of the teeth and the bone crest (B) indicates the height of the papilla.

Dimensions of the interdental papilla

The interdental papilla in a normal, healthy dentition has one buccal and one lingual/palatal component that are joined in the col region (Chapter 1; Figs. 1-1–1-9). Experiments performed in the 1960s (Kohl & Zander 1961; Matherson & Zander 1963) revealed that the shape of the papilla in the col region was not determined by the outline of the bone crest but by the shape of the contact relationship that existed between adjacent teeth.

Tarnow *et al*. (1992) studied whether the distance between the contact point (area) between teeth and the crest of the corresponding inter-proximal bone could influence the degree of papilla fill that occurred at the site. Presence or absence of a papilla was determined visually in periodontally healthy subjects. If there was no space visible apical of the contact point, the papilla was considered complete. If a "black space" was visible at the site, the papilla was considered incomplete. The distance between the facial level of the contact point and the bone crest (Fig. 3-4) was measured by sounding. The measurement thus included not only the epithelium and connective tissue of the papilla but in addition the entire supra-alveolar connective tissue in the inter-proximal area (Fig. 3-5). The authors reported that the papilla was always complete when the distance from the contact point to the crest of the bone was ≤5 mm. When this distance was 6 mm, papilla fill occurred in about 50% of cases and at sites where the distance was ≥7 mm, the papilla fill was incomplete in about 75% of cases. Considering that the supracrestal connective tissue attachment is about 1 mm high, the above data indicate that the papilla height may be limited to about 4 mm in most cases. Interestingly, papillae of similar height (3.2–4.3 mm) were found to reform following surgical denudation procedures (van der Velden 1982; Pontoriero & Carnevale 2001), but to a greater height in patients with a thick (flat) than in those with a thin (pronounced scalloped) biotype.

Summary

- *Flat gingival (periodontal) biotype*: the buccal marginal gingiva is comparatively thick, the papillae are often short, the bone of the buccal cortical wall is thick, and the vertical distance between the interdental bone crest and the buccal bone is short (about 2 mm).
- *Pronounced scalloped gingival (periodontal) biotype*: the buccal marginal gingiva is delicate and may often be located apical of the cemento-enamel junction (receded), the papillae are high and slender, the buccal bone wall is often thin and the vertical distance between the interdental bone crest and the buccal bone is long (>4 mm).

The peri-implant mucosa

The soft tissue that surrounds dental implants is termed *peri-implant mucosa*. Features of the peri-implant mucosa are established during the process of wound healing that occurs subsequent to the closure of mucoperiosteal flaps following implant installation (one-stage procedure) or following abutment connection (two-stage procedure) surgery. Healing of the mucosa results in the establishment of a soft tissue attachment (transmucosal attachment) to the

implant. This attachment serves as a seal that prevents products from the oral cavity reaching the bone tissue, and thus ensures osseointegration and the rigid fixation of the implant.

The peri-implant mucosa and the gingiva have several clinical and histological characteristics in common. Some important differences, however, also exist between the gingiva and the peri-implant mucosa.

Biologic width

The structure of the mucosa that surrounds implants made of titanium has been examined in man and several animal models (for review see Berglundh 1999). In an early study in the dog, Berglundh *et al*. (1991) compared some anatomic features of the gingiva (at teeth) and the mucosa at implants. Since the research protocol from this study was used in subsequent experiments that will be described in this chapter, details regarding the protocol are briefly outlined here.

The mandibular premolars in one side of the mandible were extracted, leaving the corresponding teeth in the contralateral jaw quadrant. After 3 months of healing following tooth extraction (Fig. 3-6) the fixture part of implants (Brånemark system®, Nobel Biocare, Gothenburg, Sweden) were installed (Fig. 3-7) and submerged according to the guidelines given in the manual for the system. Another 3 months later, abutment connection was performed (Fig. 3-8) in a second-stage procedure, and the animals were placed in a carefully monitored plaque-control program. Four months subsequent to abutment connection, the dogs were exposed to a clinical examination following which biopsy specimens of several tooth and all implant sites were harvested.

The clinically healthy gingiva and peri-implant mucosa had a pink color and a firm consistency (Fig. 3-9). In radiographs obtained from the tooth sites it

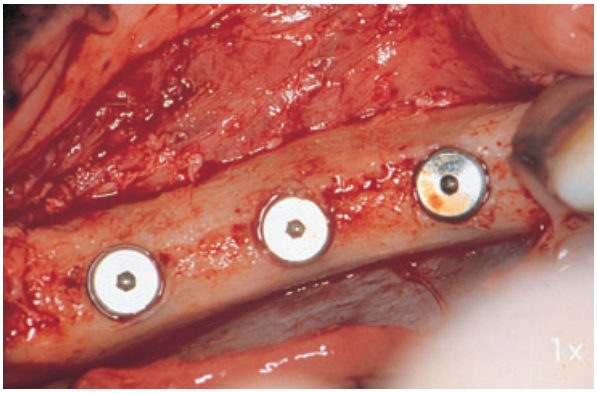

Fig. 3-7 Three titanium implants (i.e. the fixture part and cover screw; Brånemark System®) are installed.

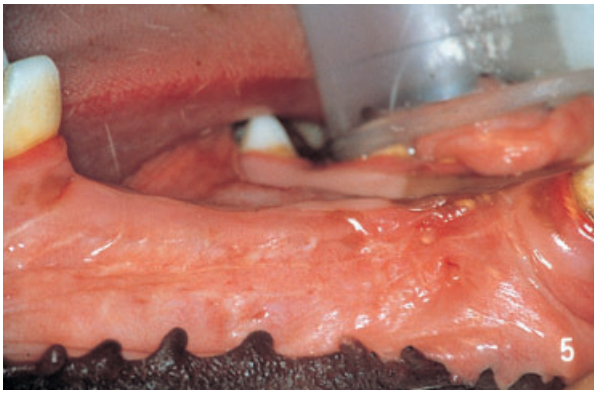

Fig. 3-6 The edentulous mandibular right premolar region 3 months following tooth extraction (from Berglundh *et al*. 1991).

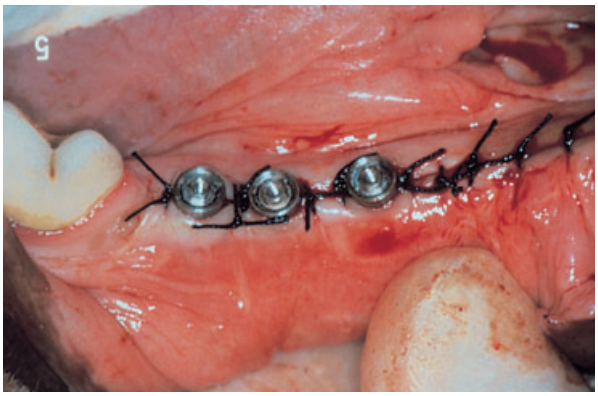

Fig. 3-8 Abutment connection is performed and the mucosa sutured with interrupted sutures.

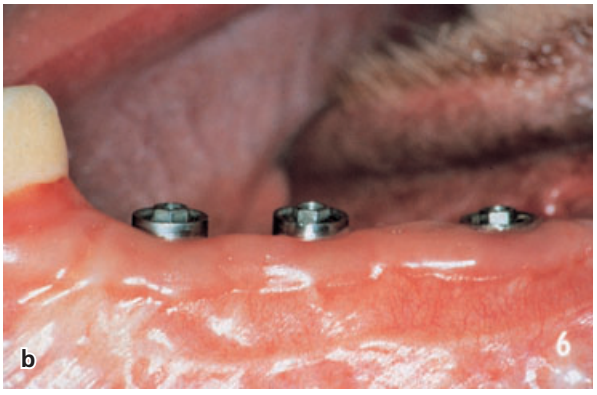

Fig. 3-9 After 4 months of careful plaque control the gingiva (a) and the peri-implant mucosa (b) are clinically healthy.

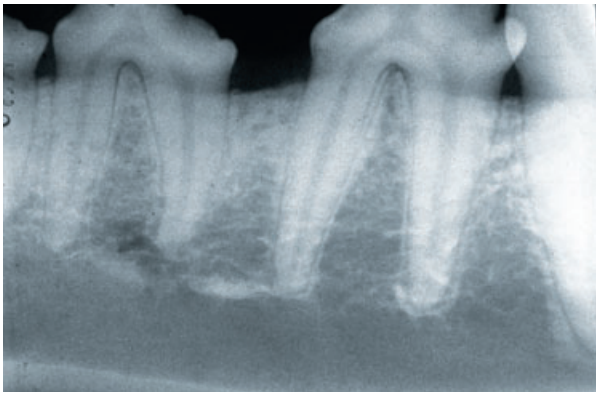

Fig. 3-10 Radiograph obtained from the premolars in the left side of the mandible.

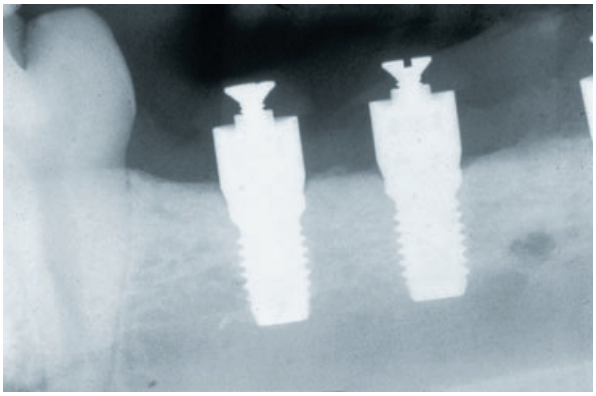

Fig. 3-11 Radiograph obtained from the implants in the right side of the mandible.

was observed that the alveolar bone crest was located about 1 mm apical of a line connecting the cemento-enamel junction of neighboring premolars (Fig. 3-10). The radiographs from the implant sites disclosed that the bone crest was close to the junction between the abutment and the fixture part of the implant (Fig. 3-11).

Histological examination of the sections revealed that the two soft tissue units, the gingiva and the peri-implant mucosa, had several features in common. The oral epithelium of the gingiva was well keratinized and continuous with the thin junctional epithelium that faced the enamel and that ended at the cemento-enamel junction (Fig. 3-12). The supra-alveolar connective tissue was about 1 mm high and the periodontal ligament about 0.2–0.3 mm wide. The principal fibers were observed to extend from the root cementum in a fan-shaped pattern into the soft and hard tissues of the marginal periodontium (Fig. 3-13).

The outer surface of the peri-implant mucosa was also covered by a keratinized oral epithelium, which in the marginal border connected with a thin barrier epithelium (similar to the junctional epithelium at the teeth) that faced the abutment part of the implant (Fig. 3-14). It was observed that the barrier epithelium was only a few cell layers thick (Fig. 3-15) and

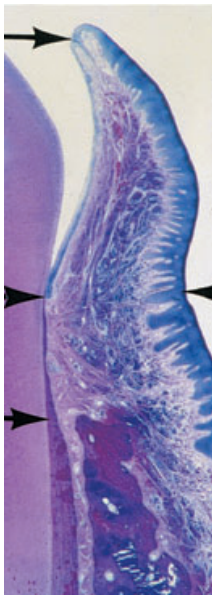

Fig. 3-12 Microphotograph of a cross section of the buccal and coronal part of the periodontium of a mandibular premolar. Note the position of the soft tissue margin (top arrow), the apical cells of the junctional epithelium (center arrow) and the crest of the alveolar bone (bottom arrow). The junctional epithelium is about 2 mm long and the supracrestal connective tissue portion about 1 mm high.

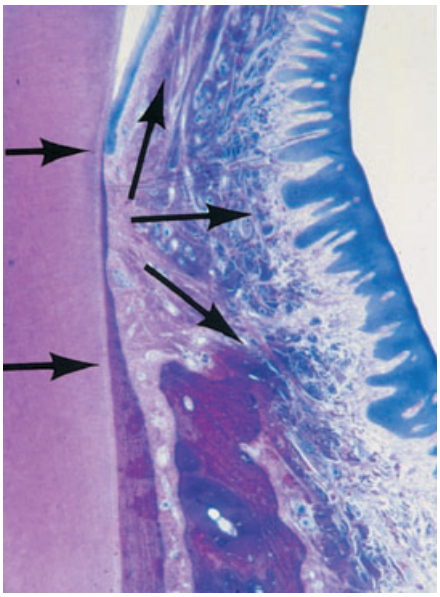

Fig. 3-13 Higher magnification of the supracrestal connective tissue portion seen in Fig. 3-12. Note the direction of the principal fibers (arrows).

that the epithelial structure terminated about 2 mm apical of the soft tissue margin (Fig. 3-14) and 1–1.5 mm from the bone crest. The connective tissue in the compartment above the bone appeared to be in direct contact with the surface (TiO_2) of the implant (Figs. 3-14, 3-15, 3-16). The collagen fibers in this connective tissue apparently originated from the periosteum of the bone crest and extend towards the margin of the soft tissue in directions parallel to the surface of the abutment.

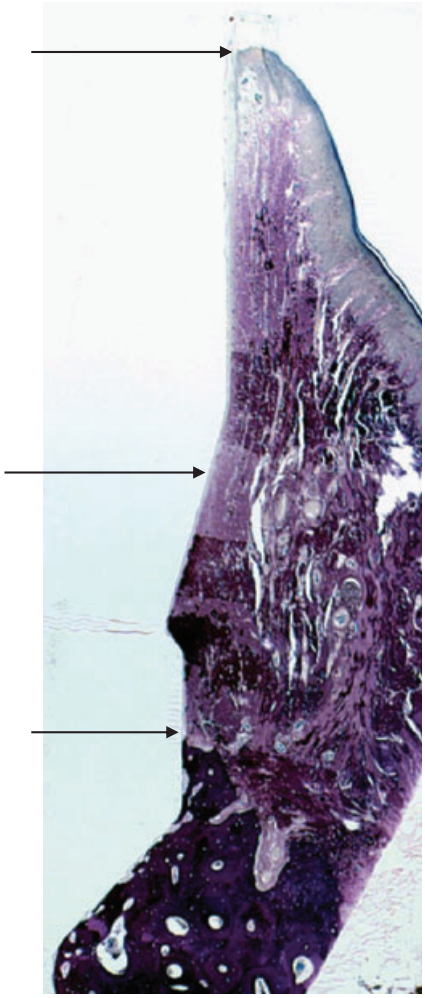

Fig. 3-14 Microphotograph of a buccal–lingual section of the peri-implant mucosa. Note the position of the soft tissue margin (top arrow), the apical cells of the junctional epithelium (center arrow), and the crest of the marginal bone (bottom arrow). The junctional epithelium is about 2 mm long and the implant–connective tissue interface about 1.5 mm high.

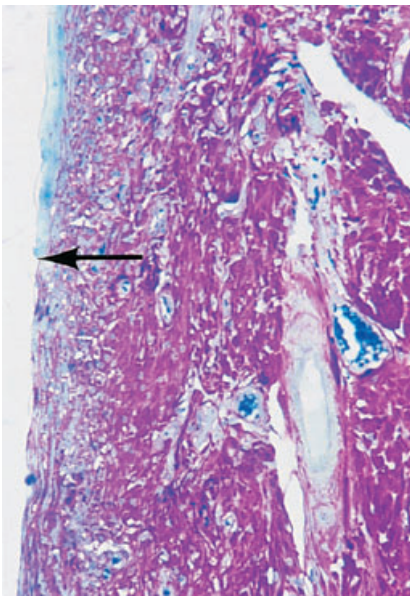

Fig. 3-15 Higher magnification of the apical portion of the barrier epithelium (arrow) in Fig. 3-14.

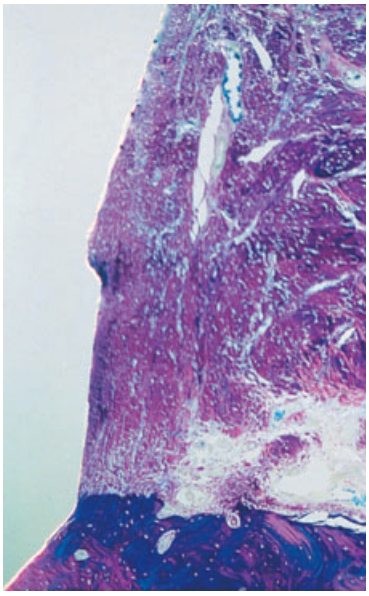

Fig. 3-16 Microphotograph of a section (buccal–lingual) of the implant–connective tissue interface of the peri-implant mucosa. The collagen fibers invest in the periosteum of the bone and project in directions parallel to the implant surface towards the margin of the soft tissue.

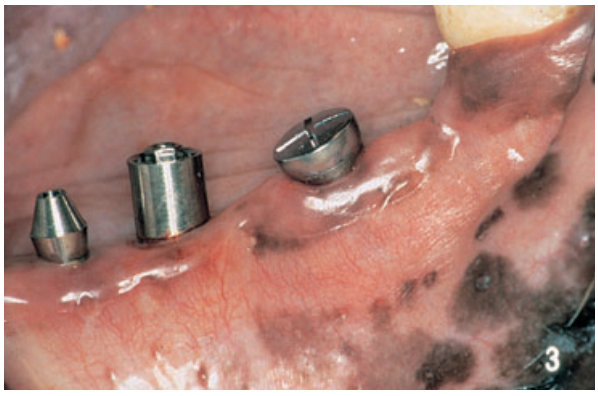

Fig. 3-17 Implants of three systems installed in the mandible of a beagle dog. Astra Tech Implants® Dental System (left), Brånemark System® (center) and ITI® Dental Implant System (right).

The observation that the barrier epithelium of the healthy mucosa consistently ended at a certain distance (1–1.5 mm) from the bone is important. During healing following implant installation surgery, fibroblasts of the connective tissue of the mucosa apparently formed a biological attachment to the TiO_2 layer of the "apical" portion of the abutment portion of the implant. This attachment zone was evidently not recognized as a wound and was therefore not covered with an epithelial lining.

In further dog experiments (Abrahamsson *et al*. 1996, 2002) it was observed that a similar mucosal attachment formed when different types of implant systems were used (e.g. Astra Tech Implant System, Astra Tech Dental, Mölndal, Sweden; Brånemark System®, Nobel Biocare, Göteborg, Sweden; Strau-

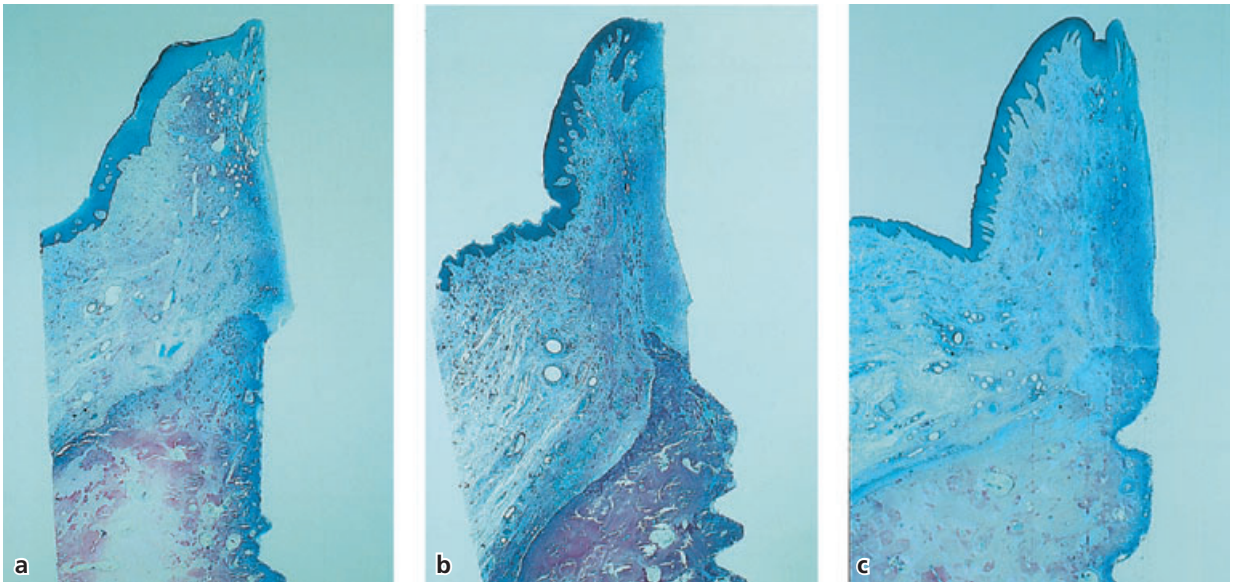

Fig. 3-18 Microphotographs illustrating the mucosa (buccal–lingual view) facing the three implant systems. (a) Astra. (b) Brånemark. (c) ITI.

mann® Dental Implant System, Straumann AG, Basel, Switzerland; 3i® Implant System, Implant Innovation Inc., West Palm Beach, FL, USA). In addition, the formation of the attachment appeared to be independent of whether the implants were initially submerged or not (Figs. 3-17, 3-18).

In another study (Abrahamsson *et al*. 1998), it was demonstrated that the material used in the abutment part of the implant was of decisive importance for the location of the connective tissue portion of the transmucosal attachment. Abutments made of aluminum-based sintered ceramic (Al_2O_3) allowed for the establishment of a mucosal attachment similar to that which occurred at titanium abutments. Abutments made of a gold alloy or dental porcelain, however, provided conditions for inferior mucosal healing. When such materials were used, the connective tissue attachment failed to develop at the abutment level. Instead, the connective tissue attachment occurred in a more apical location. Thus, during healing following the abutment connection surgery, some resorption of the marginal peri-implant bone took place to expose the titanium portion of the fixture (Brånemark System®) to which the connective tissue attachment was eventually formed.

The location and dimensions of the transmucosal attachment were examined in a dog experiment by Berglundh and Lindhe (1996). Implants (fixtures) of the Brånemark System® were installed in edentulous premolar sites and submerged. After 3 months of healing, abutment connection was performed. In the left side of the mandible the volume of the ridge mucosa was maintained while in the right side the vertical dimension of the mucosa was reduced to ≤2 mm (Fig. 3.19) before the flaps were replaced and sutured. In biopsy specimens obtained after another 6 months, it was observed that the transmucosal

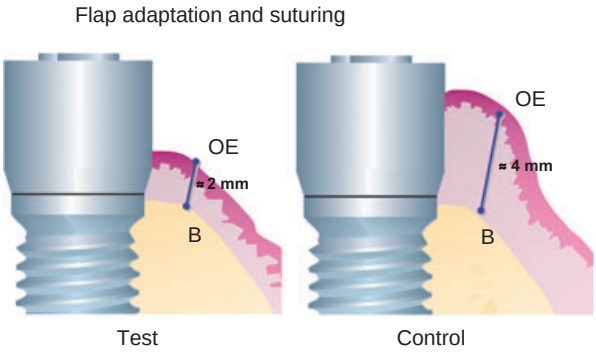

Fig. 3-19 Schematic drawing illustrating that the mucosa at the test site was reduced to about 2 mm. From Berglundh & Lindhe (1996).

attachment at all implants included one barrier epithelium that was about 2 mm long and one zone of connective tissue attachment that was about 1.3–1.8 mm high.

A further examination disclosed that at sites with a thin mucosa, wound healing consistently had included marginal bone resorption to establish space for a mucosa that eventually could harbor both the epithelial and the connective tissue components of the transmucosal attachment (Figs. 3-20, 3-21).

The dimensions of the epithelial and connective tissue components of the transmucosal attachment at implants are established during wound healing following implant surgery. As is the case for bone healing after implant placement (see Chapter 5), the wound healing in the mucosa around implants is a delicate process that requires several weeks of tissue remodeling.

In a recent animal experiment, Berglundh *et al*. (2007) described the morphogenesis of the mucosa attachment to implants made of c.p. titanium. A non-submerged implant installation technique was used and the mucosal tissues were secured to the conical marginal portion of the implants (Straumann® Dental Implant System) with interrupted sutures. The sutures were removed after 2 weeks and a plaque-control program was initiated. Biopsies were performed at various intervals to provide healing periods extending from day 0 (2 hours) to 12 weeks. It was reported that large numbers of neutrophils infiltrated and degraded the coagulum that occupied the compartment between the mucosa and the implant during the initial phase of healing. The first signs of epithelial proliferation were observed in specimens representing 1–2 weeks of healing and a mature barrier epithelium was seen after 6–8 weeks. It was also demonstrated that the collagen fibers of the mucosa were organized after 4–6 weeks of healing. Thus, prior to this time interval, the connective tissue is not properly arranged.

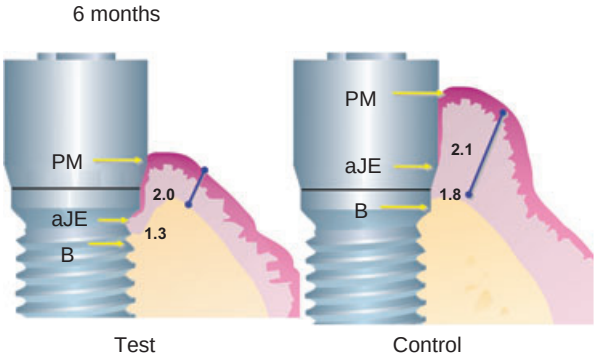

Fig. 3-20 Schematic drawing illustrating that the peri-implant mucosa at both control and test sites contained a 2 mm long barrier epithelium and a zone of connective tissue that was about 1.3–1.8 mm high. Bone resorption occurred in order to accommodate the soft tissue attachment at sites with a thin mucosa. From Berglundh & Lindhe (1996).

Conclusion

The junctional and barrier epithelia are about 2 mm long and the zones of supra-alveolar connective tissue are between 1 and 1.5 mm high. Both epithelia are attached via hemi-desmosomes to the tooth/implant surface (Gould *et al*. 1984). The main attachment fibers (the principal fibers) invest in the root cementum of the tooth, but at the implant site the equivalent fibers run in a direction parallel with the implant and fail to attach to the metal body. The soft tissue attachment to implants is properly established several weeks following surgery.

Quality

The quality of the connective tissue in the supra-alveolar compartments at teeth and implants was examined by Berglundh *et al*. (1991). The authors observed that the main difference between the mesenchymal tissue present at a tooth and at an implant site was the occurrence of a cementum on the root surface. From this cementum (Fig. 3-22), coarse dento-gingival and dento-alveolar collagen fiber bundles projected in lateral, coronal, and apical

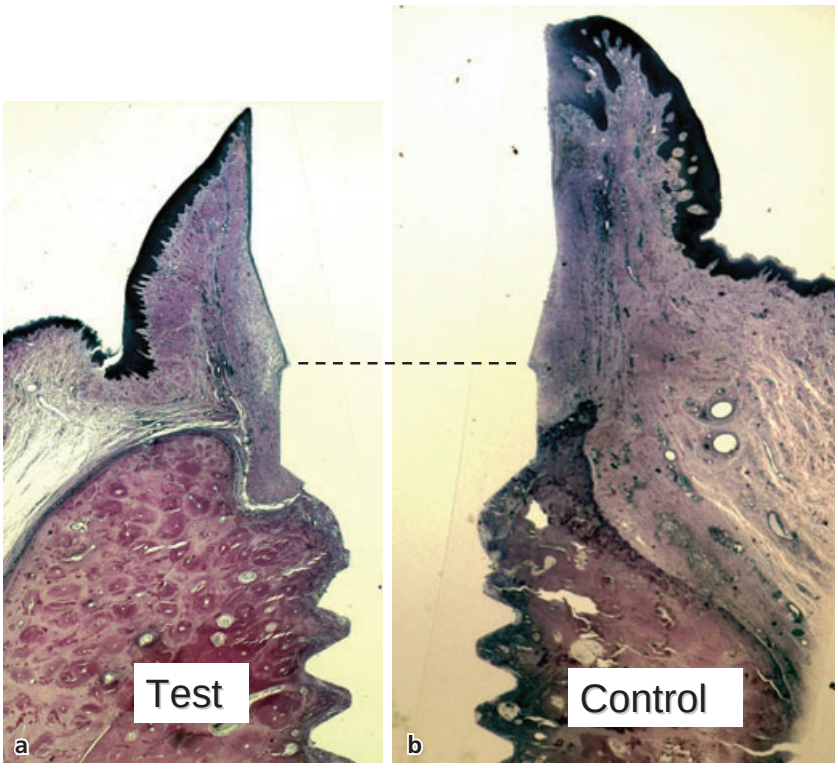

Fig. 3-21 Microphotograph illustrating the peri-implant mucosa of a normal dimension (left) and reduced dimension (right). Note the angular bone loss that had occurred at the site with the thin mucosa.

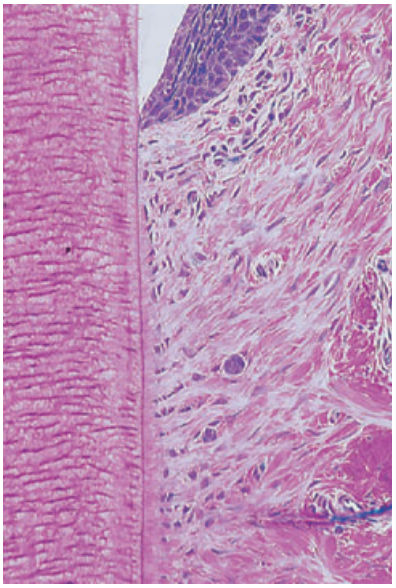

Fig. 3-22 Microphotograph of a tooth with marginal periodontal tissues (buccal–lingual section). Note on the tooth side the presence of an acellular root cementum with inserting collagen fibers. The fibers are orientated more or less perpendicular to the root surface.

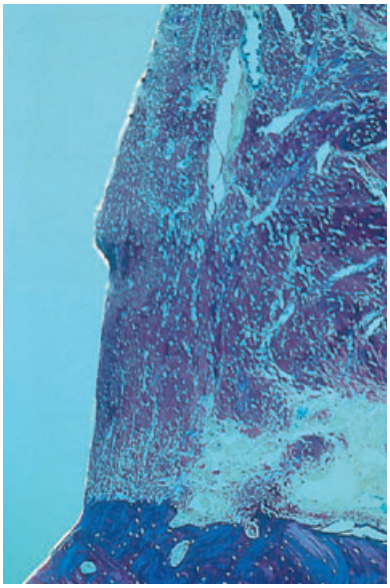

Fig. 3-23 Microphotograph of the peri-implant mucosa and the bone at the tissue/titanium interface. Note that the orientation of the collagen fibers is more or less parallel (not perpendicular) to the titanium surface.

directions (Fig. 3-13). At the implant site, the collagen fiber bundles were orientated in an entirely different manner. Thus, the fibers invested in the periosteum at the bone crest and projected in directions parallel with the implant surface (Fig. 3-23). Some of the fibers became aligned as coarse bundles in areas distant from the implant (Buser *et al*. 1992).

The connective tissue in the supra-crestal area at implants was found to contain more collagen fibers, but fewer fibroblasts and vascular structures, than the tissue in the corresponding location at teeth. Moon *et al*. (1999), in a dog experiment, reported that the attachment tissue close to the implant (Fig. 3-24) contained only few blood vessels but a large number of fibroblasts that were orientated with their long axes parallel with the implant surface (Fig. 3-25). In more lateral compartments, there were fewer fibroblasts but more collagen fibers and more vascular structures. From these and other similar findings it may be concluded that the connective tissue attachment between the titanium surface and the connective tissue is established and maintained by fibroblasts.

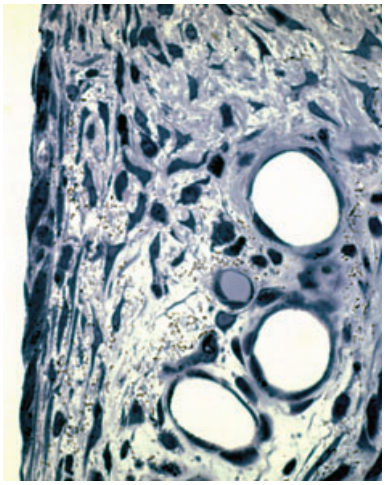

Fig. 3-24 Microphotograph of the implant/connective tissue interface of the peri-implant mucosa. A large number of fibroblasts reside in the tissue next to the implant.

Fig. 3-25 Electron micrograph of the implant–connective tissue interface. Elongated fibroblasts are interposed between thin collagen fibrils (magnification ×24 000).

Vascular supply

The vascular supply to the gingiva comes from two different sources (Fig. 3-26). The first source is represented by the large *supraperiosteal blood vessels*, that put forth branches to form (1) the capillaries of the connective tissue papillae under the oral epithelium and (2) the vascular plexus lateral to the junctional epithelium. The second source is the *vascular plexus of the periodontal ligament*, from which branches run in a coronal direction and terminate in the supra-

alveolar portion of the free gingiva. Thus, the blood supply to the zone of supra-alveolar connective tissue attachment in the periodontium is derived from two apparently independent sources (see also Chapter 1).

Berglundh *et al.* (1994) observed that the vascular system of the peri-implant mucosa of dogs (Fig. 3-27) originated *solely* from the large *supra-periosteal blood vessel* on the outside of the alveolar ridge. This vessel that gave off branches to the supra-alveolar mucosa and formed (1) the capillaries beneath the oral epithelium and (2) the vascular plexus located immediately lateral to the barrier epithelium. The connective tissue part of the transmucosal attachment to titanium implants contained only few vessels, all of which could be identified as terminal branches of the *supra-periosteal blood vessels.*

Fig. 3-26 A buccal–lingual section of a beagle dog gingiva. Cleared section. The vessels have been filled with carbon. Note the presence of a supraperiosteal vessel on the outside of the alveolar bone, the presence of a plexus of vessels within the periodontal ligament, as well as vascular structures in the very marginal portion of the gingiva.

Summary

The gingiva at teeth and the mucosa at dental implants have some characteristics in common, but differ in the composition of the connective tissue, the alignment of the collagen fiber bundles, and the distribution of vascular structures in the compartment apical of the barrier epithelium.

Probing gingiva and peri-implant mucosa

It was assumed for many years that the tip of the probe in a pocket depth measurement identified the most apical cells of the junctional (pocket) epithelium or the marginal level of the connective tissue attachment. This assumption was based on findings by, for example, Waerhaug (1952), who reported that the "epithelial attachment" (e.g. Gottlieb 1921; Orban & Köhler 1924) offered no resistance to probing. Waerhaug (1952) inserted, "with the greatest caution", thin blades of steel or acrylic in the gingival pocket of various teeth of >100 young subjects without signs of periodontal pathology. In several sites the blades were placed in approximal pockets, "in which position radiograms were taken of them". It was concluded that the insertion of the blades could be performed without a resulting bleeding and that the device consistently reached to the cemento-enamel junction (Fig. 3.28). Thus, the epithelium or the epithelial attachment offered no resistance to the insertion of the device.

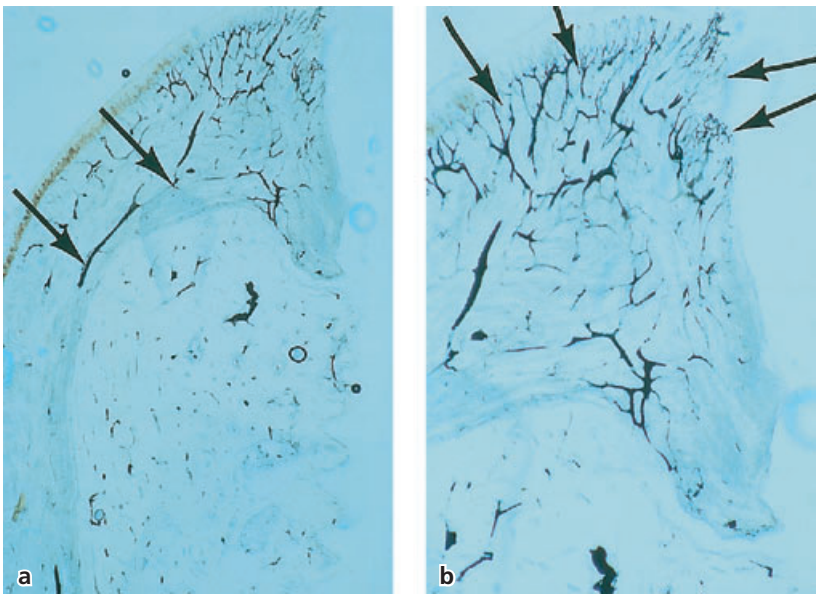

Fig. 3-27 (a) A buccal–lingual cleared section of a beagle dog mucosa facing an implant (the implant was positioned to the right). Note the presence of a supraperiosteal vessel on the outside of the alveolar bone, but also that there is no vasculature that corresponds to the periodontal ligament plexus. (b) Higher magnification (of a) of the peri-implant soft tissue and the bone implant interface. Note the presence of a vascular plexus lateral to the junctional epithelium, but the absence of vessels in the more apical portions of the soft tissue facing the implant and the bone.

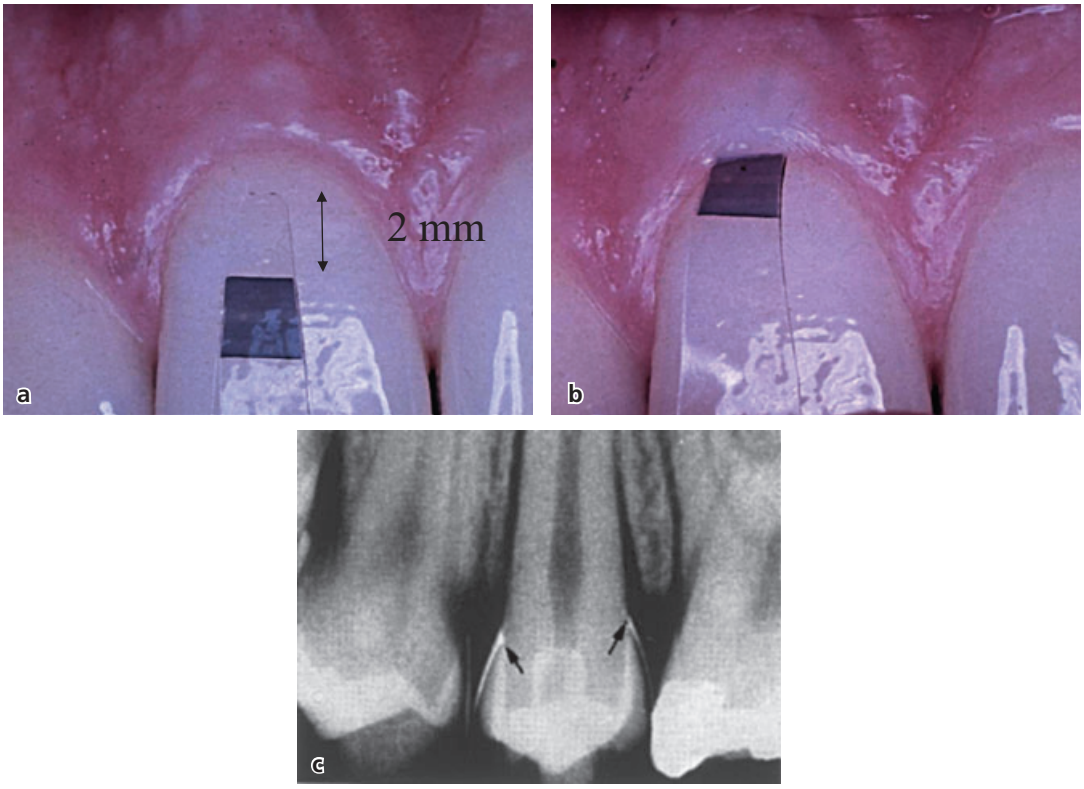

Fig. 3-28 An acrylic strip with a blue zone located 2 mm from the strip margin (a) prior to and (b) after its insertion into a buccal "pocket". The strip could with a light force be inserted 2 mm into the "pocket". (c) Thin blades of steel were inserted in pockets at approximal sites of teeth with healthy periodontal conditions. In radiographs, Waerhaug (1952) could observe that the blades consistently reached the cemento-enamel junction.

In subsequent studies it was observed, however, that the tip of a periodontal probe in a pocket depth measurement only identified the base of the dento-gingival epithelium by chance. In the absence of an inflammatory lesion the probe frequently failed to reach the apical part of the junctional epithelium (e.g. Armitage *et al*. 1977; Magnusson & Listgarten 1980). If an inflammatory lesion, rich in leukocytes and poor in collagen, was present in the gingival connective tissue, however, the probe penetrated beyond the epithelium to reach the apical–lateral border of the infiltrate.

The outcome of probing depth measurements at *implant sites* was examined in various animal models. Ericsson and Lindhe (1993) used the model by Berglundh *et al*. (1991) referred to above and, hence, had both teeth and implants available for examination. The gingiva at mandibular premolars and the mucosa at correspondingly positioned implants (Brånemark System®) were, after extended periods of plaque control, considered clinically healthy. A probe with a tip diameter of 0.5 mm was inserted into the buccal "pocket" using a standardized force of 0.5 N. The probe was anchored to the tooth or to the implant and biopsies from the various sites were performed. The histologic examination of the biopsy material revealed that probing the dento-gingival interface had resulted in a slight compression of the gingival tissue. The tip of the probe was located coronal to the apical cells of the junctional epithelium. At the implant sites, probing caused both compression and a lateral dislocation of the peri-implant mucosa, and the average "histologic" probing depth was markedly deeper than at the tooth site: 2.0 mm versus 0.7 mm. The tip of the probe was consistently positioned deep in the connective tissue/abutment interface and apical of the barrier epithelium. The distance between the probe tip and the bone crest at the tooth sites was about 1.2 mm. The corresponding distance at the implant site was 0.2 mm. The findings presented by Ericsson and Lindhe (1993) regarding the difference in probe penetration in healthy gingiva and peri-implant mucosa are not in agreement with data reported in subsequent animal experiments.

Lang *et al*. (1994) used beagle dogs and prepared the implant (Straumann® Dental Implant System) sites in such a way that at probing some regions were healthy, a few sites exhibited signs of mucositis, and some sites exhibited peri-implantitis. Probes with different geometry were inserted into the pockets using a standardized probing procedure and a force of only 0.2 N. The probes were anchored and block biopsy specimens were harvested. The probe locations were studied in histologic ground sections. The authors reported that the mean "histologic" probing depth at

healthy sites was about 1.8 mm, i.e. similar to the depth (about 2 mm) recorded by Ericsson and Lindhe (1993). The corresponding depth at sites with mucositis and peri-implantitis was about 1.6 mm and 3.8 mm respectively. Lang *et al*. (1994) further stated that at healthy and mucositis sites, the probe tip identified "the connective tissue adhesion level" (i.e. the base of the barrier epithelium) while at peri-implantitis sites, the probe exceeded the base of the ulcerated pocket epithelium by a mean distance of 0.5 mm. At such peri-implantitis sites the probe reached the base of the inflammatory cell infiltrate.

Schou *et al*. (2002) compared probing measurements at implants and teeth in eight cynomolgus monkeys. Ground sections were produced from tooth and implant sites that were (1) clinically healthy, (2) slightly inflamed (mucositis/gingivitis), and (3) severely inflamed (peri-implantitis/periodontitis) and in which probes had been inserted. An electronic probe (Peri-Probe®) with a tip diameter 0.5 mm and a standardized probing force of 0.3–0.4 N was used. It was demonstrated that the probe tip was located at a similar distance from the bone in healthy tooth sites and implant sites. On the other hand, at implants exhibiting mucositis and peri-implantitis, the probe tip was consistently identified at a more apical position than at corresponding sites at teeth (gingivitis and periodontitis). The authors concluded that (1) probing depth measurements at implant and teeth yielded different information, and (2) small alterations in probing depth at implants may reflect changes in soft tissue inflammation rather than loss of supporting tissues.

Recently, Abrahamsson and Soldini (2006) evaluated the location of the probe tip in healthy periodontal and peri-implant tissues in dogs. It was reported that probing with a force of 0.2 N resulted in a probe penetration that was similar at implants and teeth. Furthermore, the tip of the probe was often at or close to the apical cells of the junctional/barrier epithelium. The distance between the tip of the probe and the bone crest was about 1 mm at both teeth and implants (Figs. 3-29, 3-30). Similar observations were reported from clinical studies in which different implant systems were used (Buser *et al*. 1990; Quirynen *et al*. 1991; Mombelli *et al*. 1997). In these studies the distance between the probe tip and the bone was assessed in radiographs and was found to vary between 0.75 and 1.4 mm when a probing force of 0.25–0.45 N was used.

By comparing the findings from the studies reported above, it becomes apparent that probing depth and probing attachment level measurements are also meaningful at implant sites. When a "normal" probing force is applied in healthy tissues the probe seems to reach similar levels at implant and tooth sites. Probing inflamed tissues both at tooth and implant sites will, however, result in a more advanced probe penetration and the tip of the probe may come closer to the bone crest.

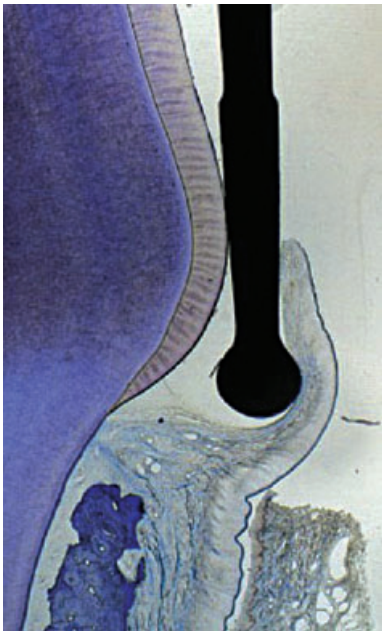

Fig. 3-29 Buccal–lingual ground section from a tooth site illustrating the probe tip position in relation to the bone crest (from Abrahamsson & Soldini 2006).

Fig. 3-30 Buccal–lingual ground section from an implant site illustrating the probe tip position in relation to the bone crest (from Abrahamsson & Soldini 2006).

Dimensions of the buccal soft tissue at implants

Chang *et al*. (1999) compared the dimensions of the periodontal and peri-implant soft tissues of 20 subjects who had been treated with an implant-supported single-tooth restoration in the esthetic zone of the maxilla and had a non-restored natural tooth in the contralateral position (Fig. 3-31). In

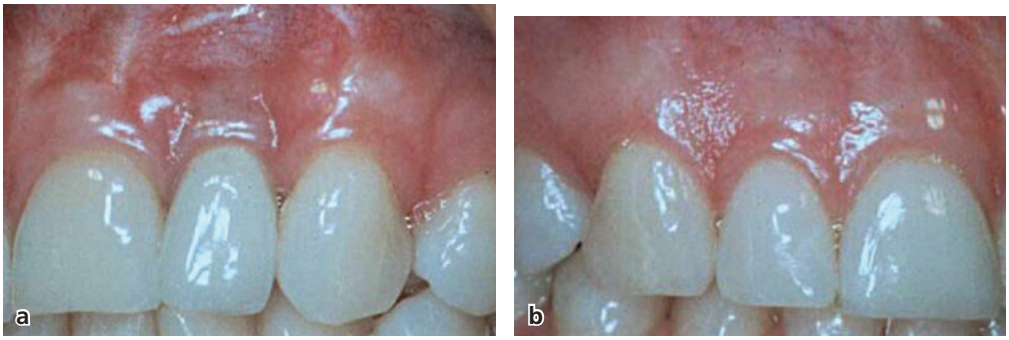

Fig. 3-31 Clinical photographs of (a) an implant-supported single tooth replacement in position 12 and (b) the natural tooth in the contralateral position (from Chang *et al*. 1999).

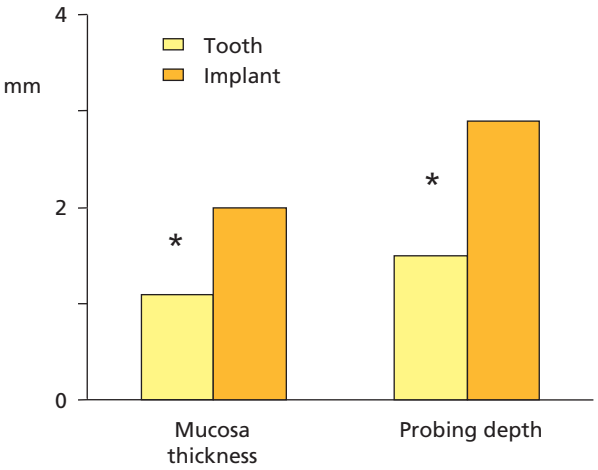

Fig. 3-32 Comparison of mucosa thickness and probing depth at the facial aspect of single-implant restorations and the natural tooth in the contralateral position (from Chang *et al*. 1999).

comparison to the natural tooth, the implant-supported crown was bordered by a thicker buccal mucosa (2.0 mm versus 1.1 mm), as assessed at a level corresponding to the bottom of the probeable pocket, and had a greater probing pocket depth (2.9 mm versus 2.5 mm) (Fig. 3-32). It was further observed that the soft tissue margin at the implant was more apically located (about 1 mm) than the gingival margin at the contralateral tooth.

Kan *et al*. (2003) studied the dimensions of the peri-implant mucosa at 45 single implants placed in the anterior maxilla that had been in function for an average of 33 months. Bone sounding measurements performed at the buccal aspect of the implants showed that the height of the mucosa was 3–4 mm in the majority of the cases. Less than 3 mm of mucosa height was found at only 9% of the implants. It was suggested that implants in this category were (1) found in subjects that belonged to a *thin periodontal biotype*, (2) had been placed too labially, and/or (3) had an overcontoured facial prosthetic emergence. A peri-implant soft tissue dimension of >4 mm was usually associated with a *thick periodontal biotype.*

Dimensions of the papilla between teeth and implants

In a study by Schropp *et al*. (2003) it was demonstrated that following single tooth extraction the height of the papilla at the adjacent teeth was reduced about 1 mm. Concomitant with this reduction (recession) of the papilla height the pocket depth was reduced and some loss of clinical attachment occurred.

Following single tooth extraction and subsequent implant installation, the height of the papilla in the tooth–implant site will be dependent on the attachment level of the tooth. Choquet *et al*. (2001) studied the papilla level adjacent to single-tooth dental implants in 26 patients and in total 27 implant sites. The distance between the apical extension of the contact point between the crowns and the bone crest, as well as the distance between the soft tissue level and the bone crest, was measured in radiographs. The examinations were made 6–75 months after the insertion of the crown restoration. The authors observed that the papilla height consistently was about 4 mm, and, depending on the location of the contact point between adjacent crowns papilla, fill was either complete or incomplete (Fig. 3-33). The closer the contact point was located to the incisal edge of the crowns (restorations) the less complete was the papilla fill.

Chang *et al*. (1999) studied the dimensions of the papillae at implant-supported single-tooth restorations in the anterior region of the maxilla and at non-restored contralateral natural teeth. They found that the papilla height at the implant-supported crown was significantly shorter and showed less fill of the embrasure space than the papillae at the natural tooth (Fig. 3-34). This was particularly evident for the distal papilla of implant-supported restorations in the central incisor position, both in comparison to the distal papilla at the contralateral tooth and to the papilla at the mesial aspect of the implant crown. This indicates that the anatomy of the adjacent natural teeth (e.g. the diameter of the root, the proximal outline/curvature of the cemento-enamel junction/connective tissue attachment

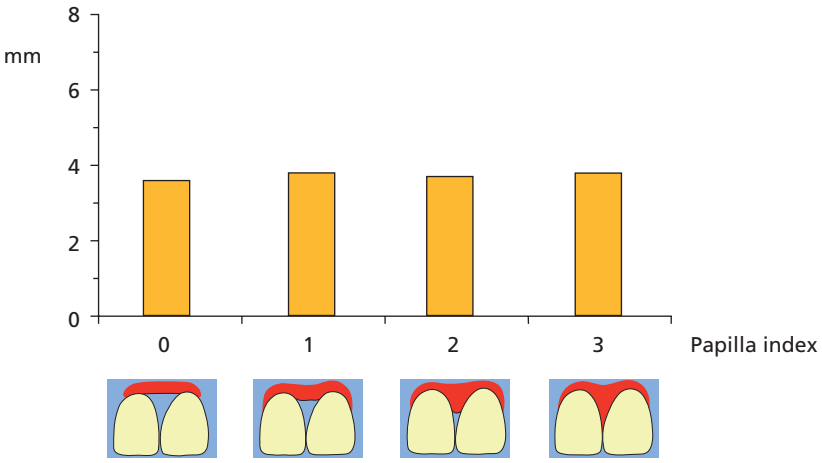

Fig. 3-33 Soft tissue height adjacent to single-tooth dental implants in relation to the degree of papilla fill (from Choquet *et al*. 2001).

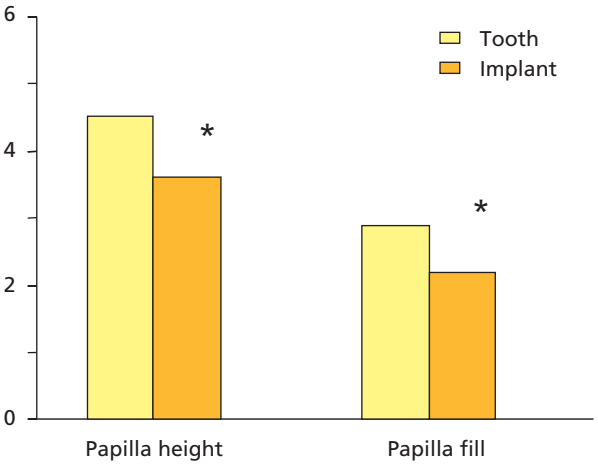

Fig. 3-34 Comparison of papilla height and papilla fill adjacent to single-implant restorations and the natural tooth in the contralateral position (from Chang *et al*. 1999).

level) may have a profound influence on the dimension of the papilla lateral to an implant. Hence, the wider facial–lingual root diameter and the higher proximal curvature of the cemento-enamel junction of the maxillary central incisor – in comparison to corresponding dimensions of the lateral incisor (Wheeler 1966) – may favor the maintenance of the height of the mesial papilla at the single-implant supported restoration.

Kan *et al*. (2003) assessed the dimensions of the peri-implant mucosa lateral to 45 single implants placed in the anterior maxilla and the 90 adjacent teeth using bone sounding measurements. The bone sounding measurements were performed at the mesial and distal aspects of the implants and at the mesial and distal aspects of the teeth. The authors reported that the thickness of the mucosa at the mesial/distal surfaces of the implant sites was on the average 6 mm while the corresponding dimension at the adjacent tooth sites was about 4 mm. It was further observed that the dimensions of the peri-implant mucosa of subjects who belonged to the *thick periodontal biotype* were significantly greater than that of subjects of a *thin biotype*.

The level of the connective tissue attachment on the adjacent tooth surface and the position of the contact point between the crowns are obviously key factors that determine whether or not a complete papilla fill will be obtained at the single-tooth implant-supported restoration (Fig. 3.35). Although there are indications that the dimensions of the approximal soft tissue may vary between individuals having thin and thick periodontal biotypes, the height of the papilla at the single-implant restoration seems to have a biological limit of about 4 mm (compare the dimension of the interdental papilla). Hence, to achieve a complete papilla fill of the embrasure space, a proper location of the contact area between the implant crown and the tooth crown is mandatory. In this respect it must also be recognized that the papilla fill at single-tooth implant restorations is unrelated to whether the implant is inserted according to a one- or two-stage protocol and whether a crown restoration is inserted immediately following surgery or delayed until the soft tissues have healed (Jemt 1999; Ryser *et al*. 2005).

Dimensions of the "papilla" between adjacent implants

When two neighboring teeth are extracted, the papilla at the site will be lost (Fig. 3-36). Hence, at replacement of the extracted teeth with implant-supported restorations the topography of the bone crest and the thickness of the supracrestal soft tissue portion are the factors that determine the position of the soft tissue margin in the inter-implant area ("implant papilla"). Tarnow *et al*. (2003) assessed the height above the bone crest of the inter-implant soft tissue ("implant papilla") by transmucosal probing at 136 anterior and posterior sites in 33 patients who had maintained implant-supported prostheses for at least

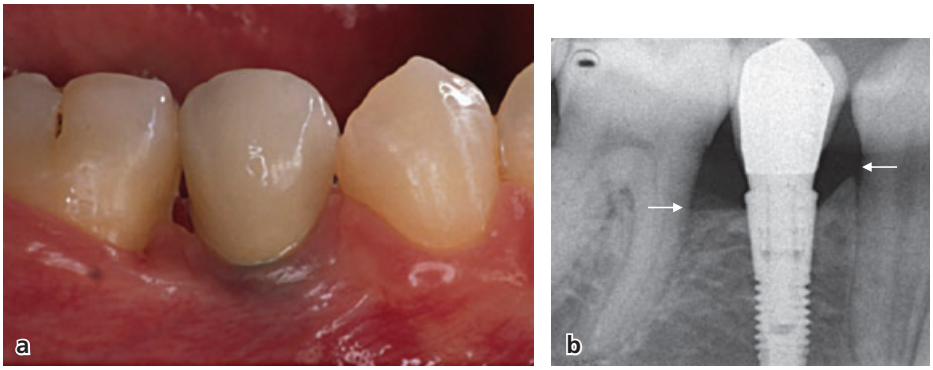

Fig. 3-35 See text for details.

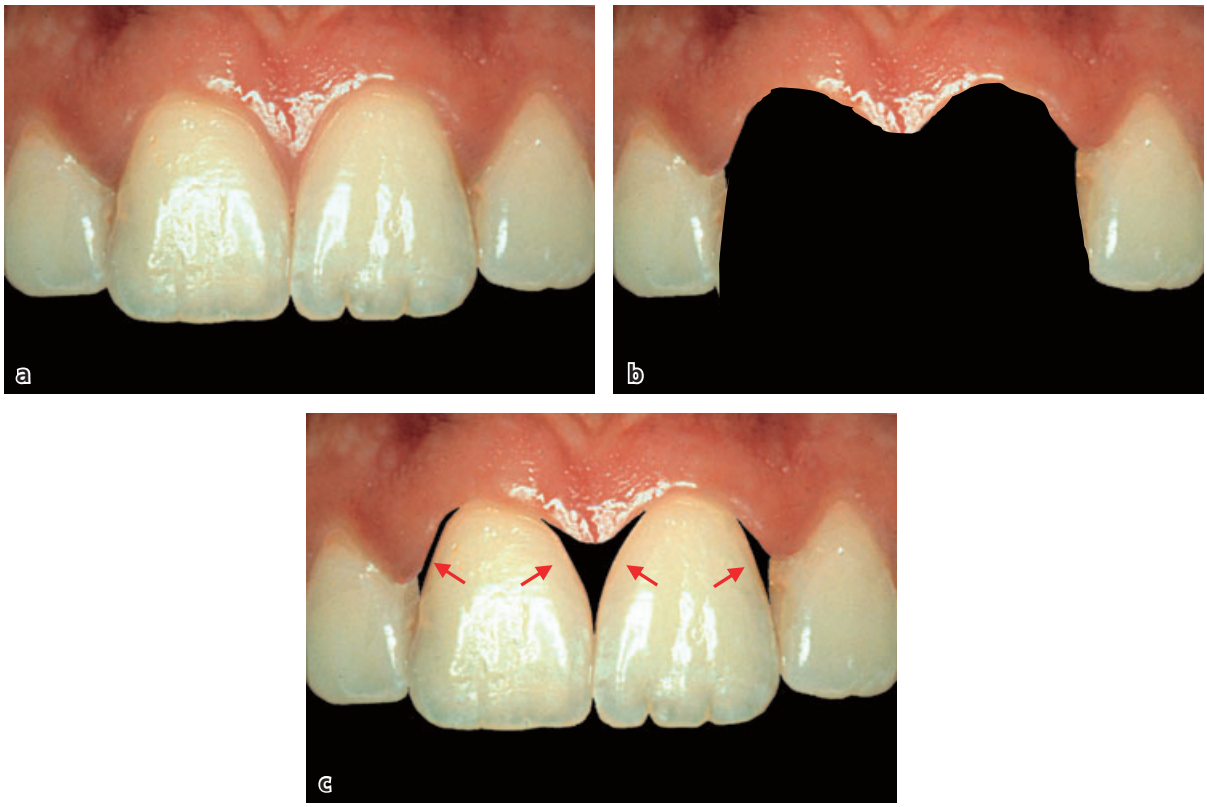

Fig. 3-36 See text for details.

2 months. It was found that the mean height of the "papillae" was 3.4 mm, with 90% of the measurements in the range of 2–4 mm.

The dimension of the soft tissues between adjacent implants seems to be independent of the implant design. Lee *et al.* (2006) examined the soft tissue height between implants of two different systems (Brånemark Implant® and Astra Tech Implant® systems) as well as the potential influence of the horizontal distance between implants. The height of the inter-implant "papilla", i.e. the height of soft tissue coronal to the bone crest measured in radiographs, was about 3.1 mm for both implant systems. No difference was found regarding the "papilla" height for any of the implant systems with regard to sites with <3 mm and ≥3 mm in horizontal distance between the implants. Gastaldo *et al.* (2004) evaluated the presence or absence of "papilla" at 96 inter-implant sites in 58 patients. It was reported that the "papilla" filled the entire space between the implants only when the distance from the bone crest to the base of the contact point between the crown restorations, assessed by sounding, was <4 mm. Thus, taken together these observations indicate that the soft tissue between two implants will have a maximum height of 3–4 mm, and that the location of the contact point between the crown restorations in relation to the bone crest level determines whether a complete soft tissue fill will be obtained in the embrasure space between two implants (Fig. 3-37).

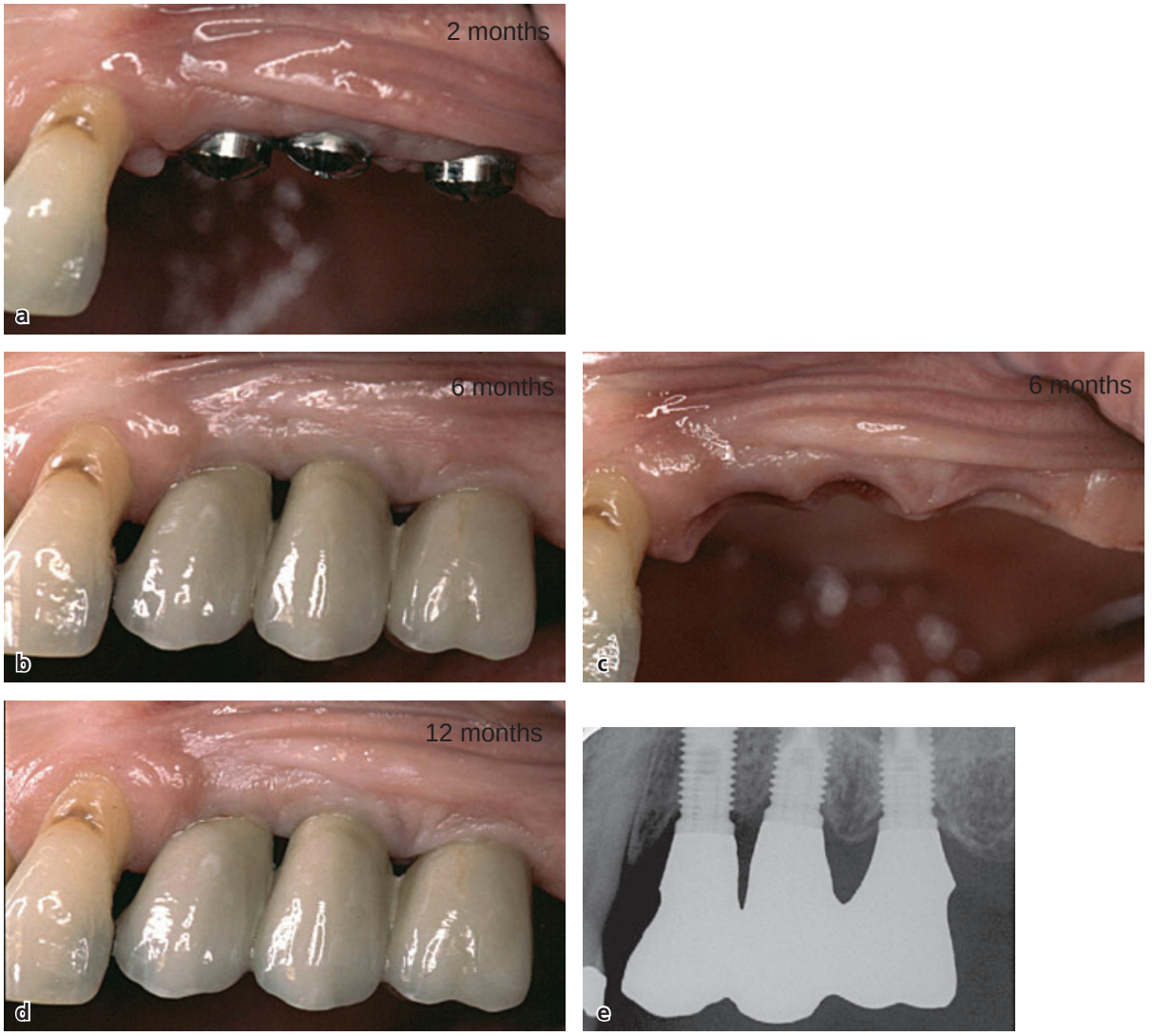

Fig. 3-37 See text for details.

References

Abrahamsson, I., Berglundh, T., Glantz, P.O. & Lindhe, J. (1998). The mucosal attachment at different abutments. An experimental study in dogs. *Journal of Clinical Periodontology* **25**, 721–727.

Abrahamsson, I., Berglundh, T., Wennström, J. & Lindhe, J. (1996). The peri-implant hard and soft tissues at different implant systems. A comparative study in the dog. *Clinical Oral Implants Research* **7**, 212–219.

Abrahamsson, I., Zitzmann, N.U., Berglundh, T., Linder, E., Wennerberg, A. & Lindhe, J. (2002). The mucosal attachment to titanium implants with different surface characteristics: an experimental study in dogs. *Journal of Clinical Periodontology* **29**, 448–455.

Abrahamsson, I. & Soldini, C. (2006). Probe penetration in periodontal and peri-implant tissues: an experimental study in the beagle dog. *Clinical Oral Implants Research* **17**, 601–605.

Andlin-Sobocki, A. & Bodin, L. (1993). Dimensional alterations of the gingiva related to changes of facial/lingual tooth position in permanent anterior teeth of children. A 2-year longitudinal study. *Journal of Clinical Periodontology* **20**, 219–224.

Armitage, G.C., Svanberg, G.K. & Löe, H. (1977). Microscopic evaluation of clinical measurements of connective tissue attachment levels. *Journal of Clinical Periodontology* **4**, 173–190.

Becker, W., Ochenbein, C., Tibbets, L. & Becker, B.E. (1997). Alveolar bone anatomic profiles as measured from dry skulls. *Journal of Clinical Periodontology* **24**, 727–731.

Berglundh, T. (1999). Soft tissue interface and response to microbial challenge. In: Lang, N.P., Lindhe, J. & Karring, T., eds. *Implant Dentistry. Proceedings from 3rd European Workshop on Periodontology*. Berlin: Quintessence, pp. 153–174.

Berglundh, T. & Lindhe, J. (1996). Dimensions of the peri-implant mucosa. Biological width revisited. *Journal of Clinical Periodontology* **23**, 971–973.

Berglundh, T., Lindhe, J., Ericsson, I., Marinello, C.P., Liljenberg, B. & Thomsen, P. (1991). The soft tissue barrier at implants and teeth. *Clinical Oral Implants Research* **2**, 81–90.

Berglundh, T., Lindhe, J., Jonsson, K. & Ericsson, I. (1994). The topography of the vascular systems in the periodontal and peri-implant tissues dog. *Journal of Clinical Periodontology* **21**, 189–193.

Berglundh, T., Abrahamsson, I., Welander, M., Lang, N.P. & Lindhe, J. (2007). Morphogenesis of the periimplant mucosa. An experimental study in dogs. *Clinical Oral Implants Research* (in press).

Buser, D., Weber, H.P. & Lang, N.P. (1990). Tissue integration of non-submerged implants. 1-year results of a prospective

study on 100 ITI-hollow-cylinder and hollow-screw implants. *Clinical Oral Implants Research* **1**, 225–235.

Buser, D., Weber, H.P., Donath, K., Fiorellini, J.P., Paquette, D.W. & Williams, R.C. (1992). Soft tissue reactions to non-submerged unloaded titanium implants in beagle dogs. *Journal of Periodontology* **63**, 226–236.

Chang, M., Wennström, J., Ödman, P. & Andersson, B. (1999). Implant supported single-tooth replacements compared to contralateral natural teeth. *Clinical Oral Implants Research* **10**, 185–194.

Choquet, V., Hermans, M., Adriaenssens, P., Daelemans, P., Tarnow, D. & Malevez, C. (2001). Clincal and radiographic evaluation of the papilla level adjacent to single-tooth dental implants. A retrospective study in the maxillary anterior region. *Journal of Periodontology* **72**, 1364–1371.

Coatoam, G.W., Behrents, R.G. & Bissada, N.F. (1981). The width of keratinized gingiva during orthodontic treatment: its significance and impact on periodontal status. *Journal of Periodontology* **52**, 307–313.

Ericsson, I. & Lindhe, J. (1993). Probing depth at implants and teeth. *Journal of Clinical Periodontology* **20**, 623–627.

Gargiulo, A.W., Wentz, F.M. & Orban, B. (1961). Dimensions and relations of the dentogingival junction in humans. *Journal of Periodontology* **32**, 261–267.

Gastaldo, J.F., Cury, P.R. & Sendyk, W.R. (2004). Effect of the vertical and horizontal distances between adjacent implants and between a tooth and an implant on the incidence of interproximal papilla. *Journal of Periodontology* **75**, 1242–1246.

Gottlieb, B. (1921). Der Epithelansatz am Zahne. *Deutsche monatschrift führ Zahnheilkunde* **39**, 142–147.

Gould, T.R.L., Westbury, L. & Brunette, D.M. (1984). Ultrastructural study of the attachment of human gingiva to titanium in vivo. *Journal of Prosthetic Dentistry* **52**, 418–420.

Jemt, T. (1999). Restoring the gingival contour by means of provisional resin crowns after single-implant treatment. *International Journal of Periodontics and Restorative Dentistry* **19**, 21–29.

Kan, J., Rungcharassaeng, K., Umezu, K. & Kois, J. (2003). Dimensions of the periimplant mucosa: An evaluation of maxillary anterior single implants in humans. *Journal of Periodontology* **74,** 557–562.

Kohl, J. & Zander, H. (1961). Morphology of interdental gingival tissue. *Oral Surgery, Oral Medicine and Oral Pathology* **60**, 287–295.

Lang, N.P., Wetzel, A.C., Stich, H. & Caffesse, R.G. (1994). Histologic probe penetration in healthy and inflamed peri-implant tissues. *Clinical Oral Implants Research* **5**, 191–201.

Lee, D-W., Park, K-H. & Moon, I-S. (2006). Dimension of interproximal soft tissue between adjacent implants in two distinctive implant systems. *Journal of Periodontology* **77**, 1080–1084.

Magnusson, I. & Listgarten, M.A. (1980). Histological evaluation of probing depth following periodontal treatment. *Journal of Clinical Periodontology* **7**, 26–31.

Matherson, D. & Zander, H. (1963). Evaluation of osseous surgery in monkeys. *Journal of Dental Research* **42**, 116.

Mombelli, A., Mühle, T., Brägger, U., Lang, N.P. & Bürgin, W.B. (1997). Comparison of periodontal and peri-implant probing by depth-force pattern analysis. *Clinical Oral Implants Research* **8**, 448–454.

Moon, I-S., Berglundh, T., Abrahamsson, I., Linder, E. & Lindhe, J. (1999). The barrier between the keratinized mucosa and the dental implant. An experimental study in the dog. *Journal of Clinical Periodontology* **26**, 658–663.

Müller, H.P. & Könönen, E. (2005). Variance components of gingival thickness. *Journal of Periodontal Research* **40**, 239–244.

O'Connor, T.W. & Biggs, N. (1964). Interproximal craters. *Journal of Periodontology* **35**, 326–330.

Olsson, M. & Lindhe, J. (1991). Periodontal characteristics in individuals with varying forms of upper central incisors. *Journal of Clinical Periodontology* **18**, 78–82.

Olsson, M., Lindhe, J. & Marinello, C. (1993). On the relationship between crown form and clinical features of the gingiva in adolescents. *Journal of Clinical Periodontology* **20**, 570–577.

Orban, B & Köhler, J. (1924). Die physiologische Zanhfleischetasche, Epithelansatz und Epitheltiefenwucherung. *Zeitschrift für Stomatologie* **22**, 353.

Oschenbein, C. & Ross, S. (1969). A reevaluation of osseous surgery. In: *Dental Clinics of North America*. Philadelphia, PA: W.B. Saunders, pp. 87–102.

Pontoriero, R. & Carnevale, G. (2001). Surgical crown lengthening: A 12-month clinical wound healing study. *Journal of Periodontology* **72**, 841–848.

Quirynen, M., van Steenberge, D., Jacobs, R., Schotte, A. & Darius, P. (1991). The reliability of pocket probing around screw-type implants. *Clinical Oral Implants Research* **2**, 186–192.

Ryser, M.R., Block, M.S. & Mercante, D.E. (2005). Correlation of papilla to crestal bone levels around single tooth implants in immediate or delayed crown protocols. *Journal of Maxillofacial Surgery* **63**, 1184–1195.

Schou, S., Holmstrup, P., Stolze, K., Hjørting-Hansen, E., Fien, N.E. & Skovgaard, L.T. (2002). Probing around implants and teeth with healthy or inflamed marginal tissues. A histologic comparison in cynomolgus monkeys (*Macaca fascicularis). Clinical Oral Implants Research* **13**, 113–126.

Schropp, L., Wenzel, A., Kostopoulos, L. & Karring, T. (2003). Bone healing and soft tissue contour changes following singe-tooth extraction: A clinical and radiographic 12-month prospective study. *International Journal of Periodontics and Restorative Dentistry* **23**, 313–323.

Sicher, H. (1959). Changing concepts of the Supporting Dental Structure. *Oral Surgery, Oral Medicine and Oral Pathology* **12**, 31–35.

Tarnow, D., Elian, N., Fletcher, P., Froum, S., Magner, A., Cho, S-C., Salama, M., Salama, H. & Garber, D.A. (2003). Vertical distance from the crest of bone to the height of the interproximal papilla between adjacent implants. *Journal of Periodontology* **74**, 1785–1788.

Tarnow, D., Magner, A. & Fletcher, P. (1992). The effect of the distance from the contact point to the crest of bone on the presence or absence of the interproximal dental papilla. *Journal of Periodontology* **63**, 995–996.

van der Velden, U. (1982). Regeneration of the interdental soft tissues following denudation procedures. *Journal of Clinical Periodontology* **9**, 455–459.

Weisgold, A. (1977). Contours of the full crown restoration. *Alpha Omegan* **7**, 77–89.

Waerhaug, J. (1952). Gingival pocket: anatomy, pathology, deepening and elimination. *Odontologisk Tidskrift* **60** (Suppl 1).

Wheeler, R.C. (1961). Complete crown form and the periodontium. *Journal of Prosthetic Dentistry* **11**, 722–734.

Wheeler, R. C. (1966). *An Atlas of Tooth Form.* Philadelphia: W.B. Saunders Co, pp. 24–25.

Chapter 4

Bone as a Tissue

William V. Giannobile, Hector F. Rios, and Niklaus P. Lang

During embryogenesis, in the alveolar process of the maxilla and the mandible, bone is formed within a primary connective tissue. This process is termed *intramembranous* bone formation and also occurs at the cranial vault and in the midshaft or diaphysis of the long bones. In contrast, bone formation in the remaining parts of the skeleton occurs via an initial deposition of a cartilage template that is subsequently replaced by bone. This process is called *endochondral* bone formation.

Alveolar bone lost as a result of disease, trauma or extensive post-extraction bone modeling may pose therapeutic problems in periodontal reconstructive and/or implant dentistry. Thus, implant placement both in the maxilla and in the mandible may be hampered by the lack of sufficient volume of alveolar bone at the recipient sites. *De novo* formation of alveolar bone in such compromised sites may be necessary and different regenerative therapies need to be considered to promote new bone. They all, however, have one aspect in common: the compliance with the principles of bone biology. There are several reconstructive modalities for restoration of the alveolar process, such as bone graft replacements and guided bone regeneration (GBR).

Basic bone biology

Bone is a specialized connective tissue that is mainly characterized by its mineralized organic matrix. The bone organic matrix is comprised of collagenous and non-collagenous proteins. Within this matrix, ions of calcium and phosphate are laid down in the ultimate form of hydroxyapatite. This composition allows the bone tissue to: (1) resist load, (2) protect highly sensitive organs (e.g. the central nervous system) from external forces, and (3) participate as a reservoir of minerals that contribute to systemic homeostasis of the body.

Bone cells

Osteoblasts are the primary cells responsible for the formation of bone; they synthesize the organic extracellular matrix (ECM) components and control the mineralization of the matrix. Osteoblasts are located on bone surfaces exhibiting active matrix deposition and may eventually differentiate into two different types of cells: *bone lining cells* and *osteocytes*. Bone lining cells are elongated cells that cover a surface of bone tissue and exhibit no synthetic activity. Osteocytes are stellate-shaped cells that are trapped within the mineralized bone matrix but remain in contact with other bone cells by thin cellular processes. The osteocytes are organized as a syncytium that provides a very large contact area between the cells (and their processes) and the non-cellular part of the bone tissue. This arrangement allows osteocytes to: (1) participate in the regulation of the blood-calcium homeostasis, and (2) sense mechanical loading and to signal this information to other cells within the bone.

The osteoblasts are fully differentiated cells and lack the capacity for migration and proliferation. Thus, in order to allow bone formation to occur at a given site, undifferentiated mesenchymal progenitor cells (*osteoprogenitor cells*) must migrate to the site and proliferate to become osteoblasts. Friedenstein (1973) divided osteoprogenitor cells into *determined* and *inducible osteogenic precursor cells*. The determined osteoprogenitor cells are present in the bone marrow, in the endosteum and in the periosteum that covers the bone surface. Such cells possess an intrinsic capacity to proliferate and differentiate into osteoblasts. Inducible osteogenic precursor cells, on the other hand, represent mesenchymal cells present in other organs and tissues (e.g. myoblasts or adipocytes) that may differentiate into bone-forming cells when exposed to specific stimuli. As osteogenesis is generally closely related to the ingrowth of vascular tissue,

Table 4-1 Effects of growth factors in bone wound healing

Wound healing phase	Growth factor	Cell of origin	Functions
Inflammatory	PDGF	Platelets	Increases chemotaxis of neutrophils and monocytes
	TGF-β	Platelets, leukocytes, fibroblasts	Increases chemotaxis of neutrophils and monocytes Autocrine expression – generation of additional cytokines (TNFα, IL-1β, PDGF, and chemokines)
	VEGF	Platelets, leukocytes, fibroblasts	Increases vascular permeability
Proliferative	EGF	Macrophages, mesenchymal cells, platelets	Stimulates epithelial proliferation and migration
	FGF-2	Macrophages, endothelial cells	Stimulates fibroblast proliferation and ECM synthesis Increases chemotaxis, proliferation, and differentiation of endothelial cells
	KGF (FGF-7)	Keratinocytes, fibroblasts	Stimulates epithelial proliferation and migration
	PDGF	Macrophages, endothelial cells	Stimulates fibroblast proliferation and ECM synthesis Increases chemotaxis, proliferation, and differentiation of endothelial cells
	TGF-β	Macrophages, leukocytes, fibroblast	Stimulates epithelial proliferation and migration Stimulates fibroblasts proliferation and ECM synthesis Inhibits proteases and enhances inhibitor production
	VEGF	Macrophages	Increases chemotaxis of endothelial progenitor cells Stimulates endothelial cell proliferation
Bone remodeling, matrix synthesis	BMPs 2–4	Osteoblasts	Stimulates mesenchymal progenitor cell migration
	BMP-7	Osteoblasts	Stimulates osteoblast and chondroblast differentiation
	FGF-2	Macrophages, endothelial cells	Stimulates mesenchymal progenitor cell migration
	IGF-II	Macrophages, fibroblasts	Stimulates osteoblast proliferation and bone matrix synthesis
	PDGF	Macrophages, osteoblasts	Stimulates differentiation of fibroblasts into myofibroblasts Stimulates proliferation of mesenchymal progenitor cells
	TGF-β	Fibroblasts, osteoblasts	Induces endothelial cell and fibroblast apoptosis Induces differentiation of fibroblasts into myofibroblasts Stimulates chemotaxis and survival of osteoblasts
	VEGF	Macrophages	Chemotaxis of mesenchymal stem cells, antiapoptotic effect on the bone forming cells, angiogenesis promotion

Adapted from: Kaigler, D., Cirelli, J.A. & Giannobile, W.V. (2006). Growth factor delivery for oral and periodontal tissue engineering. *Expert Opinion on Drug Delivery* **3**, 647–662, with permission.
PDGF = platelet-derived growth factor; TGF = transforming growth factor; VEGF = vascular endothelial growth factor; EGF = epidermal growth factor; FGF = fibroblast growth factor; KGF = keratinocyte growth factor; BMP = bone morphogenetic protein; IGF = insulin-like growth factor; TNFα = tumor necrosis factor alpha.

the stellate-shaped perivascular cell (the *pericyte*) is considered to be the main osteoprogenitor cell. The differentiation and development of osteoblasts from osteoprogenitor cells are dependent on the release of osteoinductive or osteopromotive growth factors (GFs) such as bone morphogenetic proteins (BMP) and other growth factors such as insulin-like growth factor (IGF), platelet-derived growth factor (PDGF) and fibroblast growth factor (FGF) (Table 4-1).

The bone formation activity is consistently coupled to bone resorption that is initiated and maintained by *osteoclasts*. Osteoclasts are multinucleated cells that originate from hematopoietic precursor cells.

Modeling and remodeling

Once bone has formed, the new mineralized tissue starts to be reshaped and renewed by processes of resorption and apposition, i.e. through *modeling* and *remodeling*. Modeling represents a process that allows a change in the initial bone architecture. It has been suggested that external demands (such as load) on bone tissue may initiate modeling. Remodeling, on the other hand, represents a change that occurs within the mineralized bone without a concomitant alteration of the architecture of the tissue. The process of remodeling is important (1) during bone formation, and (2) when old bone is replaced with new bone. During bone formation, remodeling enables the substitution of the primary bone (woven bone), which has low load-bearing capacity, with lamellar bone that is more resistant to load.

The bone remodeling that occurs in order to allow replacement of old bone with new bone involves two processes: bone resorption and bone apposition (formation). These processes are coupled in time and are

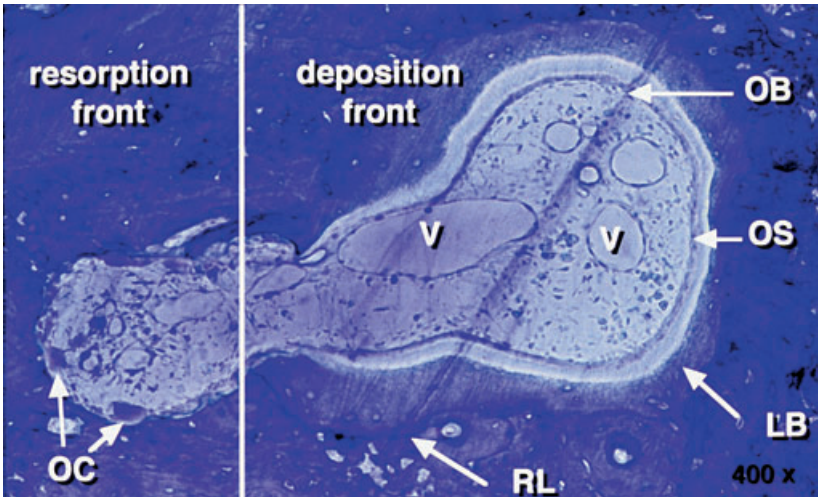

Fig. 4-1 Histological section illustrating a bone multicellular unit (BMU). Note the presence of a resorption front with osteoclast (OC) and a deposition front that contains osteoblasts (OB), and osteoid (OS). Vascular structures (V) occupy the central area of the BMU. RL = reversal line; LB = lamellar bone.

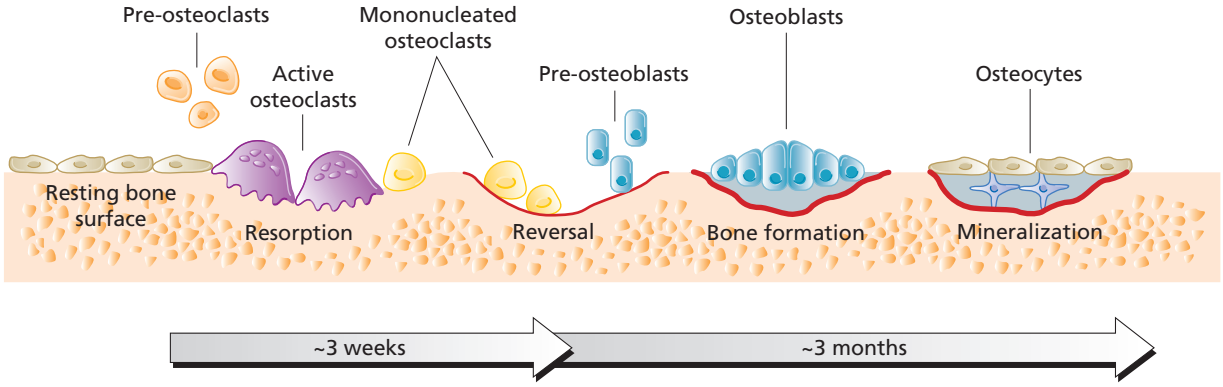

Fig. 4-2 The bone remodeling cycle. Preosteoblasts are recruited to sites of resorption, induced to differentiate into active osteoclasts, and form resoption pits. After their period of active resorption, transient mononuclear cells replace them. Through the process of coupling, preosteoblasts are recruited, differentiate into active matrix-secreting cells, and form bone. Some osteoblasts become entrapped in the matrix and become osteocytes. Adapted from McCauley, L.K. & Nohutcu, R.M. (2002) Mediators of periodontal osseous destruction and remodeling: principles and implications for diagnosis and therapy. *Journal of Periodontology* **73**, 1377–1391, with permission.

characterized by the presence of so called *bone multicellular units* (BMUs). A BMU (Fig. 4-1) is comprised of (1) a front osteoclast residing on a surface of newly resorbed bone (the resorption front), (2) a compartment containing vessels and pericytes, and (3) a layer of osteoblasts present on a newly formed organic matrix (the deposition front). The process of the bone remodeling cycle is shown in Figs. 4-2 and 4-3. Local stimuli and release of hormones, such as parathyroid hormone (PTH), growth hormone, leptin, and calcitonin, are involved in the control of bone remodeling. Modeling and remodeling occur throughout life to allow bone to adapt to external and internal demands.

Growth factors and alveolar bone healing

Understanding the complex processes of wound healing has been a challenge for researchers for many years. Recently, advances in the areas of cellular and molecular biology have allowed the elucidation of functions of GFs and their participation in the different phases of wound healing. Restoration of normal form and function is the ultimate goal of regenerative approaches of alveolar bone disrupted by trauma, surgical resection or infectious disease. However, if the functional integrity of the tissue is not achieved, the process of repair will take place and a fibrous tissue will replace the original tissue (Le *et al.* 2005). Recent studies have confirmed that GFs can improve the capacity of alveolar bone to regenerate, improving cellular chemoattraction, differentiation, and proliferation. GFs are natural biological mediators that regulate important cellular events involved in tissue repair by binding to specific cell surface receptors (Giannobile 1996). After reaching specific target cells, GFs induce intracellular signaling pathways, which result in the activation of genes that change cellular activity and phenotype (Anusaksathien & Giannobile 2002). However, the effect of each GF is regulated through a complex system of feedback loops, which involve other GFs, enzymes, and binding proteins (Schilephake 2002; Ripamonti *et al.* 2005). Recent studies have taken place with the target of defining the proper application for therapeutic purposes of many different growth factors and other cytokines,

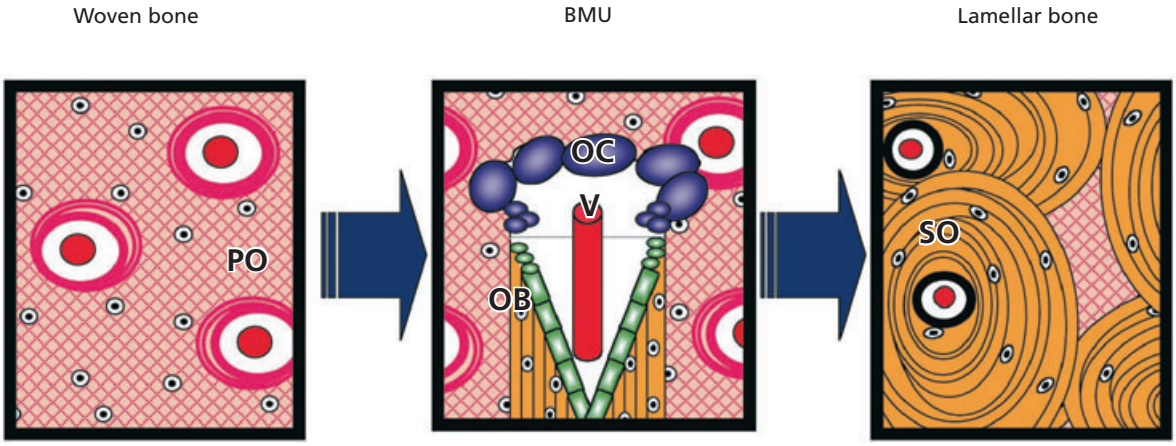

Fig. 4-3 Schematic drawing describing the transition between woven bone and lamellar bone, i.e. remodeling. Woven bone with primary osteons (PO) is transformed into lamellar bone in a process that involves the presence of BMUs. The BMU contains osteoclasts (OC), as well as vascular structures (V) and osteoblasts (OB). Thus, the osteoblasts in the BMU produce bone tissue that has a concentric orientation around the vessel, and secondary osteons (SO) are formed within lamellar bone.

each of which has several functions during the different phases of wound healing (Schilephake 2002; Ripamonti *et al.* 2005).

Healing of osseous tissue is regulated by GFs and other cytokines in a sequence of overlapping events similar to cutaneous wound repair. In ideal circumstances, this process mimics embryonic bone development allowing replacement of damaged bone with new bone, rather than with fibrous scar tissue. This process is driven by cellular and molecular mechanisms controlled by the TGF-β superfamily of genes, which encode a large number of extracellular signaling molecules (Blair *et al.* 2002). Bone morphogenetic proteins (BMPs) are a well studied group of these GFs involved in the processes of bone healing; the human genome encodes at least 20 of these multifunctional polypeptides (Blumenthal *et al.* 2002). Among several functions, BMPs induce the formation of both bone and cartilage by stimulating the cellular events of mesenchymal progenitor cells. However, only a subset of BMPs, most notably BMP-2, -4, -6, -7, and -9, has osteoinductive activity, a property of inducing *de novo* bone formation by themselves (Cheng *et al.* 2003). Studies involving mutations of BMP ligands, receptors, and signaling proteins have shown important roles of BMPs in embryonic and postnatal development. Severe skeletal deformation, development of osteoporosis, reduction in bone mineral density and bone volume are all aberrations associated with disrupted and dysregulated BMP signaling (Chen *et al.* 2004).

Several other GFs produced by osteogenic cells, platelets and inflammatory cells participate in bone healing, including IGF-I and -II, TGFβ-1, PDGF, and FGF-2 (Sykaras & Opperman, 2003). The bone matrix serves as a reservoir for these GFs and BMPs and they are activated during matrix resorption by matrix metalloproteinases (Baylink *et al.* 1993; Janssens *et al.* 2005). Additionally, the acidic environment that develops during the inflammatory process leads to activation of latent GFs (Linkhart *et al.* 1996), which assist in the chemoattraction, migration, proliferation, and differentiation of mesenchymal cells into osteoblasts (Linkhart *et al.* 1996). All of these functions are driven by a complex mechanism of interaction among GFs and other cytokines, which is influenced by several regulatory factors (King & Cochran, 2002).

Local and systemic factors affecting bone volume and healing

Metabolic disorders affecting bone metabolism

A variety of systemic situations can affect local bone density, ultimately influencing tooth support or available bone volume for dental implant installation. Such diseases affecting bone mass include osteopenia, osteoporosis, and diabetes mellitus. The later two will be discussed in detail given their overall prevalence and implications to alveolar bone reconstruction.

Osteoporosis

Osteoporosis is a systemic skeletal disease characterized by low bone mass and microarchitectural deterioration of the bone scaffold that result in increased bone fragility and susceptibility to fracture. In osteoporosis, the *bone mineral density* (BMD) is reduced, bone microarchitecture is disrupted, and the amount and variety of non-collagenous proteins in bone is altered. *Dual energy X-ray absorptiometry* (DXA, formerly DEXA) is considered the gold standard for diagnosis of osteoporosis. Diagnosis is made when the BMD is less than or equal to 2.5 standard deviations below that of a young adult reference population. This is translated as a T-score. The World Health Organization has established diagnostic guidelines as T-score –1.0 or greater is "normal", T-score between –1.0 and –2.5 is osteopenia, and –2.5 or below as osteoporosis (WHO Study Group 1994).

Oral bone loss has been shown to be associated with osteoporosis and low skeletal BMD. In their search for oral radiographic changes associated with osteoporosis, most investigators have focused on measures of jaw bone mass or morphology. The commonly used assessment of oral bone status include radiographic measures of loss of alveolar crestal height (ACH), measures of resorption of the residual ridge after tooth loss (RRR), and assessment of oral BMD. Tools used to measure bone mass include single and dual photon absorptiometry, DXA, quantitative computed tomography (QCT), and film densitometry.

Periodontitis results from pathogenic bacterial infection, which produces factors that destroy collagenous support of the tooth, as well as loss of alveolar bone. Systemic factors can lead to loss of BMD throughout the body, including bone loss in the maxilla and mandible. The resulting local reduction of BMD in the jaw bones could set the stage for more rapid ACH loss because a comparable challenge of bacterial bone-resorbing factors could be expected to result in greater alveolar crestal bone loss than in an individual with good bone mass. In addition to this, there are systemic risk factors such as smoking, diabetes, diet, and hormone levels that affect systemic bone level and may also affect periodontitis (discussed in Chapters 12 and 13). Although periodontal disease has historically been thought to be the result of a local infectious process, others have suggested that periodontal disease may be an early manifestation of generalized osteopenia (Whalen & Krook 1996), which would classify osteoporosis as a risk indicator, rather than a risk factor, for periodontal disease.

Mandibular mineral content is reduced in subjects with osteoporotic fractures (von Wowern *et al.* 1994). Further, the BMD of buccal mandibular bone correlates with osteoporosis (low skeletal BMD) (Klemetti *et al*. 1993; Taguchi *et al*. 1996). Mandibular density also correlates with skeletal BMD (Horner *et al*. 1996). Using film densitometry, the optical density of the mandible has been found to be increased in subjects with osteoporosis compared with controls. Further, mandibular radiographic optical density correlates with vertebral BMD in osteoporotic women (Kribbs 1990), control women (Kribbs 1990), and in women with a history of vertebral fracture (Kribbs *et al*. 1990; Law *et al.* 1996). Reduction in cortical and subcortical alveolar bone density has also been reported to correlate with osteoporosis in longitudinal studies (Payne *et al*. 1997, 1999; Civitelli *et al*. 2002). As concluded by Hildebolt (1997), the preponderance of the evidence indicates that the jaws of subjects with osteoporosis show reduced bone mass with potential implications on dental implant installation.

Several potential mechanisms by which osteoporosis or systemic bone loss may be associated with periodontal attachment loss, loss of alveolar bone height or density, and tooth loss have been proposed. One of these mechanisms states that low BMD or loss of BMD may lead to more rapid resorption of alveolar bone after insult by periodontal bacteria. With less dense oral bone to start with, loss of bone surrounding the teeth may occur more rapidly. Another mechanism proposes that systemic factors affecting bone remodeling may also modify local tissue response to periodontal infection. Persons with systemic bone loss are known to have increased production of cytokines (i.e. interleukin-1, interleukin-6) that may have effects on bone throughout the body, including the bones of the oral cavity. Periodontal infection has been shown to increase local cytokine production that, in turn, increases local osteoclast activity resulting in increased bone resorption. A third mechanism would be related to genetic factors that predispose an individual to systemic bone loss and also influence or predispose an individual to periodontal destruction. Also, certain lifestyle factors such as cigarette smoking and suboptimal calcium intake, among others, may put individuals at risk for development of both systemic osteopenia and oral bone loss (Oh *et al.* 2007).

Recently, long-term use of bone anti-resorptive agents, specifically bisphosphonates, has been associated with osteonecrosis of the jaw (ONJ) (Marx 2003; Ruggiero *et al*. 2004). According to a web-based survey conducted by the International Myeloma Foundation (Durie *et al.* 2005), an increased incidence of ONJ has been observed after 36 months from the start of therapy in patients receiving zoledronic acid or pamidronate for the treatment of myeloma or breast cancer. This data also indicated that patients with prior dental problems might have a higher risk of ONJ. As the bisphosphonates are potent osteoclast inhibitors, their long-term use may suppress bone turnover and compromise healing of even physiological micro-injuries within bone (Odvina *et al*. 2005). Despite the encouraging therapeutic results, further long-term studies are warranted to determine the relative risk : benefit ratio of bisphosphonate therapy. See Fig. 4-4 for therapies used to treat bone loss.

With regard to osseointegration, preclinical animal studies note the influence of osteoporosis on bone–implant contact as suggesting a negative effect (Mori *et al*. 1997; Duarte *et al*. 2003; Cho *et al*. 2004). For instance, Cho *et al*. (2004), using an osteoporotic animal model, found a bone contact reduction of 50%. Lugero *et al*. (2000), using an induced osteoporosis rabbit model, also found that integration was impaired, although they pointed out that cortical thickness was decreased as well.

Some early clinical reports have difficulties demonstrating an increased loss of implants during early stages of implant therapy (Becker *et al*. 2000; Friberg *et al*. 2001), mostly because osteopenia is treated at the time of placement. Yet early implant failure is often correlated with local lack of bone density or volume (van Steenberghe *et al*. 2002). For instance, Esposito *et al*. (2005) in a recent systematic review,

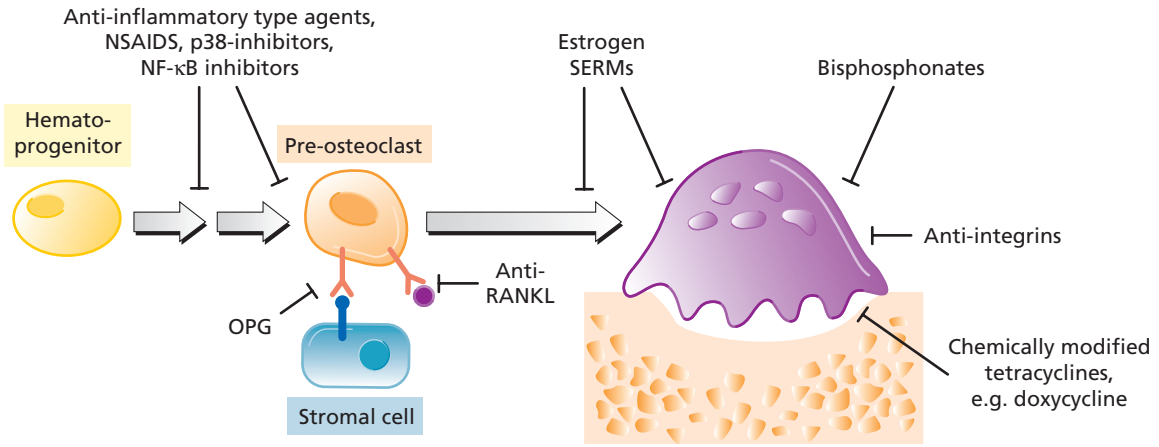

Fig. 4-4 Potential therapeutic strategies to treat bone resorption: agents that block the differentiation or activity of osteoclasts are potential therapeutic agents. Osteoprotegrin (OPG) inhibits the differentiation of osteoclasts through its action as a decoy receptor that blocks RANK (receptor activator of nuclear factor-kappa beta) and RANKL (RANK ligand) juxtacrine interaction. Non-steroidal anti-inflammatory drugs (NSAIDs) and other anti-inflammatory type molecules can inhibit the formation of hematoprogenitor cells to pre-osteoclasts. Antibodies to RANKL can also block this interaction. Estrogen and selective estrogen receptor modulators (SERMs) may inhibit the activity of osteoclasts but also promote apoptosis of osteoclasts, thus reducing their active lifespan. Bisphosphonates also promote osteoclast apoptosis. Chemically modified tetracylines reduce the protease degradation of the organic matrix, and anti-integrins block the initial osteoclast adhesion to the matrix. Adapted with permission from Kirkwood, K.L., Taba, M. Jr., Rossa, C., Preshaw, P. & Giannobile, W.V. (2006). Molecular biology concepts in host-microbe interaction in periodontal diseases. In: Newman M.G. *et al*. (eds). *Carranza's Clinical Periodontology*, 10th Edn. Elsevier Publishing, St. Louis, MO, pp. 259–274.

reported that implant failure is three times greater in the posterior maxilla, where bone density is less, than in the mandible. On the other hand, clinical evaluation or resistance during surgical osteotomy creation for implant installation may be indicative of osteopenia or osteoporosis (Friberg *et al*. 2001). It has also been reported that dental radiography and clinical evaluation at the time of surgery can suggest the presence of osteopenia, but early implant survival is not affected (Becker *et al*. 2000). Although the influence of bone density on early failure is unclear, mostly because bone volume is often a confounding factor, this suggests that it is more critical to study long-term consequences. There is, however, little information available on long-term maintenance of implants in the presence of osteoporosis. Thus, based on the available data, there is evidence to interpret an association between osteoporosis and bone density that exists around teeth and dental implant fixtures. There is also some information to suggest that decreased bone mass may place dental implants at a greater risk to failure or to decreased ability to handle load over the long term.

Diabetes mellitus

Diabetes mellitus is associated with a variety of metabolic sequlae including effects on bone maintenance and healing. There are three main types of diabetes mellitus. Type 1 is caused by damage or destruction of the beta cells of the pancreas which leads to production of insufficient amounts of insulin. Type 2 is caused by resistance to insulin with failure to produce enough additional insulin to compensate for the insulin resistance (see also Chapter 12). Type 2 diabetes constitutes 90–95% of the individuals suffering from diabetes mellitus in the US (Kahn & Flier 2000). There is a third type of diabetes that is gestational and occurs when there is a glucose intolerance of variable severity that starts or is first recognized during pregnancy (Novak *et al*. 2006).

The liver, the skeletal muscles, and the adipose tissue are the main insulin-responsive tissues, yet insulin also influences the physiology of other tissues, including bone and cartilage. In conditions of hypoinsulinemia (e.g. type 1 diabetes) or hyperinsulinemia with or without glucose intolerance or fasting hyperglycemia (type 2 diabetes), endochondral bone growth and bone remodeling show significant alterations.

Type 1 diabetes

Although bone histomorphometry data are lacking, results from biochemical markers of bone formation studies reveal unequivocal evidence that bone formation is decreased in diabetes mellitus. Serum osteocalcin concentrations are about 25% lower in diabetic children, adolescents and adults (Bouillon *et al*. 1995). Several relatively small studies that have investigated the effect of type 1 diabetes on axial bone density have found that the BMD Z score (age-matched BMD) from the lumbar spine or the femoral neck of diabetic patients is either not significantly different from that of the control groups or that there is a small decrease in cortical bone density but no difference in trabecular bone density (Roe *et al*. 1991; Ponder *et al*. 1992;

Gallacher *et al*. 1993; Olmos *et al*. 1994). The conclusion from these studies is that type 1 diabetic subjects have a mean Z score below, but generally within 1 SD of, reference values (Lunt *et al*. 1998; Miazgowski & Czekalski 1998; Rix *et al.* 1999). This effect can be seen within a few years after diagnosis and is not progressive.

Type 2 diabetes

Bone formation and bone mineralization are also decreased in type 2 diabetes. Histomorphometry results showed a significant decrease in the osteoid thickness and in the dynamic bone formation rate of a human bone biopsy specimen of a type 2 diabetic patient with a low BMD Z score at the radius. However, low bone turnover in type 2 diabetes does not cause bone loss (Krakauer *et al*. 1995).

In support of these data, hyperinsulinemia, which is a marker of insulin resistance and the central mechanism in the pathogenesis of type 2 diabetes, has been found to be linked with higher cortical thickness and a small but significant increase in BMD (Wakasugi *et al*. 1993; Rishaug *et al*. 1995; Bauer *et al.* 2002).

Insulin stimulates endochondral bone growth and osteoblast proliferation and function *in vitro* and *in vivo* at physiological concentrations. Severe diabetes in animal models typically induces reduction in bone blood flow, bone growth, periosteal bone apposition, and bone remodeling (both resorption and formation). Consequently, bone size and bone mass are reduced. However, no effect on bone mineral density has been identified when adjusted for bone size. Less apparent changes are observed in (insulin-treated) human type 1 diabetes, although many studies report a mild reduction in growth velocity in pubertal children with this condition, a mild deficit in BMD area (maximum 10%) which does not deteriorate with longer diabetes duration, and significantly reduced bone remodeling parameters. On the other hand, individuals with hyperinsulinemia and/or type 2 diabetes have a mild increase (3–5%) in BMD area.

Apart from insulin deficiency, there are likely to be other causative factors in the development of diabetes bone disease such as alterations in the IGF-IGFBP system and hypercorticolism. The cellular and molecular mechanisms by which diabetes affects chondrocyte, (pre)osteoblast, and (pre)-osteoclast proliferation and function still need to be elucidated.

In conclusion, diabetes is associated with an increased risk of periodontitis and progressive bone loss of the alveolus; however, this risk may vary depending on differences in susceptibility to periodontitis among populations (Kinane *et al.* 2006).

Diabetes as a risk factor for alveolar bone loss around implants

Studies investigating dental implants in the presence of diabetes mellitus are limited, but there is evidence that this disease is not a contra-indication for placement (Shernoff *et al.* 1994). In fact, there is evidence that early implant survival in well controlled patients is similar to that in non-diabetic patients. It is also noticeable that this may be true for all indications (Abdulwassie & Dhanrajani 2002), as well as for more advanced surgical techniques, such as bone grafting (Farzad *et al.* 2002). However, animal experiments have shown that bone–implant contact is affected (Nevins *et al*. 1998), suggesting that clinical consequences in long-term maintenance may arise. In a large prospective 5-year clinical study, Olson *et al*. (2000) found that duration of diabetes was an important factor in implant survival. Other retrospective or observational studies have also concluded that diabetes contributes to an increase in failure rates (Moy *et al*. 2005). In a 4-year retrospective clinical analysis of 215 implants of controlled diabetes mellitus patients, Fiorellini *et al*. (2000) reported an overall success rate of 85.6%, with some variation with regard to implant location and cumulative time in function. They concluded that the implant failure rate was significantly greater than in non-diabetic patients. However, there is controversy as to whether this is due to initial failure (Fiorellini *et al*. 2000).

In contrast to the previous studies where early implant loss was greater in diagnosed patients, Peled *et al*. (2003), in a clinical evaluation of well controlled edentulous patients who had received two implants, found that there was no difference in initial osseointegration. Van Steenberghe *et al*. (2002), in a large clinical evaluation exploring various systemic parameters, found that diabetes was not a detrimental factor during initial phases of integration and prosthesis fabrication, again supporting the importance of long-term studies. The influence of underlying elevated glucose levels on osseointegration is also supported by animal studies (Ottoni & Chopard 2004). For instance, using a diabetic rat model, Siqueira *et al*. (2003) reported a 50% decrease of osseointegration when animals did not receive insulin therapy, suggesting that an association exists. Kopman *et al*. (2005), using a similar model, also reported that bone–implant contact was significantly reduced. Interestingly, these previous studies also found that treatment of the condition did not improve osseointegration, when compared to uncontrolled diabetic animals, suggesting that treated individuals may have impaired implant healing regardless of their disease stability. Furthermore, there are suggestions that poorly controlled conditions could lead to loss of bone–implant contact, resulting in a weaker bone–implant interface (Kwon *et al*. 1997). Therefore, it is likely that long-term risks for complications are greater in the presence of diabetes mellitus. This hypothesis can only be reinforced when diabetes is poorly controlled or undiagnosed.

Diabetes has been reported to adversely affect bone repair by decreasing expression of genes that induce osteoblast differentiation, and diminishing

growth factor and ECM production (Bouillon 1991; Kawaguchi *et al*. 1994; Lu *et al*. 2003). One proposed mechanism for these adverse effects is through the contribution of advanced glycation end-products (AGEs) to decreased extracellular matrix production and inhibition of osteoblast differentiation (McCarthy *et al*. 2001; Cortizo *et al*. 2003; Santana *et al*. 2003). AGEs may also delay wound healing by inducing apoptosis of ECM-producing cells. This enhanced apoptosis would reduce the number of osteoblastic and fibroblastic cells available for the repair of resorbed alveolar bone (Graves *et al*. 2006). In addition to promoting apoptosis, AGEs could affect oral tissue healing by reducing expression of collagen and promoting inflammation. The mechanisms suggested for AGE-enhanced apoptosis include the direct activation of caspase activity, and indirect pathways that increase oxidative stress or the expression of pro-apoptotic genes that regulate apoptosis (Graves *et al*. 2006).

Bone healing

Healing of an injured tissue usually leads to the formation of a tissue that differs in morphology or function from the original tissue. This type of healing is termed *repair*. Tissue *regeneration*, on the other hand, is a term used to describe a healing that leads to complete restoration of morphology and function.

The healing of bone tissue includes both regeneration and repair phenomena depending on the nature of the injury. For example, a properly stabililized, narrow bone fracture (e.g. greenstick fracture) will heal by regeneration, while a larger defect (e.g. segmental bone defect) will often heal with repair. There are certain factors that may interfere with the bone tissue formation following injury, such as:

1. Failure of vessels to proliferate into the wound
2. Improper stabilization of the coagulum and granulation tissue in the defect
3. Ingrowth of "non-osseous" or fibrous tissues with a high proliferative activity
4. Bacterial contamination.

The healing of a wound includes four phases:

1. Blood clotting
2. Wound cleansing
3. Tissue formation
4. Tissue modeling and remodeling.

These phases occur in an orderly sequence but, in a given site, may overlap in such a way that in some areas of the wound, tissue formation may be in progress, while in other areas tissue modeling is the dominating event. Examples of bone remodeling can be also seen in Chapter 2 on the edentulous ridge and Chapter 49 on ridge augmentation procedures.

Bone grafting

Although bone tissue exhibits a large regeneration potential and may restore its original structure and function completely, bony defects may often fail to heal with bone tissue. In order to facilitate and/or promote healing, bone grafting materials have been placed into bony defects. It is generally accepted that the biologic mechanisms forming the basis for bone grafting include three basic processes: *osteogenesis*, *osteoconduction*, and *osteoinduction*.

Osteogenesis occurs when viable osteoblasts and precursor osteoblasts are transplanted with the grafting material into the defects, where they may establish centers of bone formation. Autogenous iliac bone and marrow grafts are examples of transplants with osteogenic properties (see Chapter 49).

Osteoconduction occurs when non-vital implant material serves as a scaffold for the ingrowth of precursor osteoblasts into the defect. This process is usually followed by a gradual resorption of the implant material. Autogenous cortical bone or banked bone allografts may be examples of grafting materials with osteoconductive properties (Fig. 4-5). Such grafting materials, as well as bone-derived or synthetic bone substitutes, have similar osteoconductive properties. However, degradation and substitution by viable bone is often poor. If the implanted material is not resorbable, which is the case for most porous hydroxylapatite implants, the incorporation is restricted to bone apposition to the material surface, but no substitution occurs during the remodeling phase.

Osteoinduction involves new bone formation by the differentiation of local uncommitted connective tissue cells into bone-forming cells under the influence of one or more inducing agents. *Demineralized bone matrix* (DMB) or *bone morphogenetic proteins* (BMP) are examples of such grafting materials (Giannobile & Somerman 2003; Reynolds *et al*. 2003).

It often occurs that all three basic bone-forming mechanisms are involved in bone regeneration. In fact, osteogenesis without osteoconduction and osteoinduction is unlikely to occur, since almost none of the transmitted cells of autogenous cancellous bone grafts survive the transplantation. Thus, the grafting material predominantly functions as a scaffold for invading cells of the host. In addition, the osteoblasts and osteocytes of the surrounding bone lack the ability to migrate and divide which, in turn, means that the transplant is invaded by uncommitted mesenchymal cells that later differentiate into osteoblasts.

On that basis, it is appropriate to define three basic conditions as prerequisites for bone regeneration:

1. The *supply of bone-forming cells* or cells with the capacity to differentiate into bone-forming cells

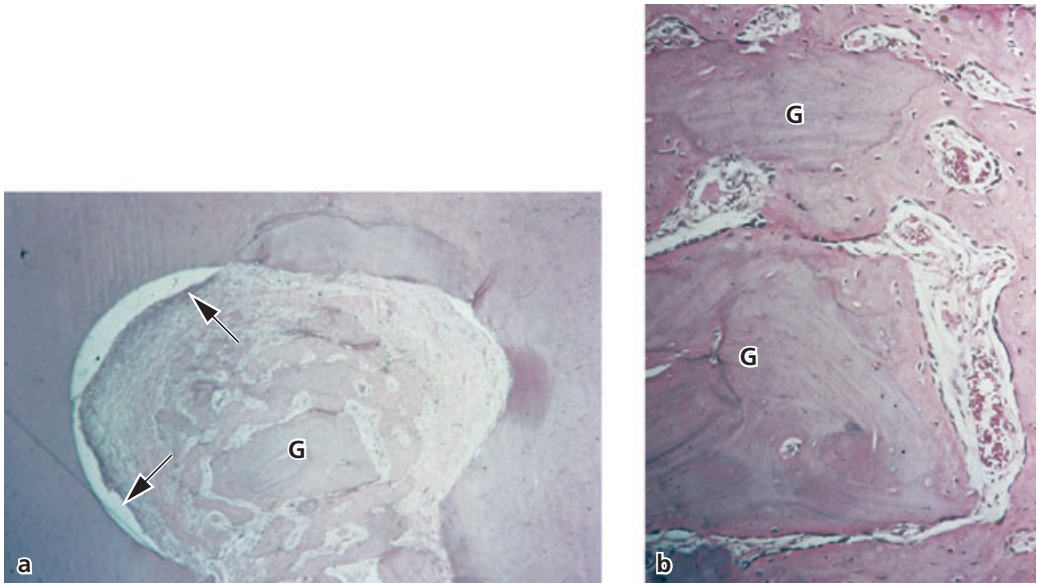

Fig. 4-5 (a) Microphotograph demonstrating bifurcation defect 3 weeks after grafting with autogenous cancellous jaw bone (G). New bone has invaded the defect, and the bone grafts have exerted an osteoconductive function. Epithelium (arrows) has migrated into one side of the defect. (b) Higher magnification of (a) showing that new bone has formed around the bone grafts (G), which have lost their vitality, indicated by the empty osteocyte lacunae.

2. The presence of *osteoinductive stimuli* to initiate the differentiation of mesenchymal cells into osteoblasts
3. The presence of an *osteoconductive environment* forming a scaffold upon which invading tissue can proliferate and in which the stimulated osteoprogenitor cells can differentiate into osteoblasts and form bone.

The placement of bone-grafting materials to favor healing in osseous defects or to augment atrophic alveolar ridges has been evaluated in a number of experimental and clinical studies (Boyne 1970; Thompson & Casson 1970; Steinhauser & Hardt 1977; Fazili *et al*. 1978; Baker *et al*. 1979; Mulliken & Glowacki 1980; Swart & Allard 1985; Block *et al*. 1987; Cullum *et al*. 1988; Hupp & McKenna 1988) (also see Chapter 49). However, there are several reports indicating that this type of treatment fails predictably to produce bone fill and augment alveolar ridges (Korlof *et al.* 1973; Curtis & Ware 1977; Steinhauser & Hardt 1977; Taylor 1983; Davis *et al.* 1984; Jackson *et al.* 1986; Hupp & McKenna 1988). Often the bone grafts do not attach to the graft site through bony attachment and there is bone resorption and bone loss associated with grafting procedures. As a consequence, much of the intended volume is lost, and frequently the defects heal with a fibrous connective tissue instead of bone.

Human experimental studies on alveolar bone repair

At present, most of the information regarding the biologic events which lead to new bone formation is derived from animal studies. Results regarding bone formation collected in animal studies have to be applied with proper caution in humans. In particular, the time sequence of the various steps ultimately leading to the formation of mineralized mature bone in man is different from that in all experimental animal systems known. A few human specimens, often harvested under poorly controlled conditions, contribute relatively little to the understanding of the biologic events of bone regeneration in humans.

A model system was designed to obtain human specimens of regenerated and also newly generated alveolar bone for the study of the biologic events under a variety of conditions (Hämmerle *et al*. 1996). A mucoperiosteal flap was raised in the retromolar area of the mandible of nine healthy volunteers. Following flap reflection, a standardized hole was drilled through the cortical bone into the bone marrow. Congruent test cylinders were firmly placed into the prepared bony bed, yielding primary stability; 1.5–2 mm of the test device were submerged below the level of the surrounding bone, leaving 2–3 mm above the bone surface. The bone-facing end of the cylinder was left open, while the coronal soft tissue-facing end was closed by an expanded polytetrafluoroethylene (ePTFE) membrane. The flap was sutured to obtain primary wound closure. In order to prevent infection, penicillin was prescribed systemically and oral rinses of chlorhexidine were administered. After 2, 7, and 12 weeks, one test device, including the regenerated tissue, was surgically harvested, while after 16, 24, and 36 weeks, respectively, two devices were harvested and processed for soft or hard tissue histology or immunohistochemistry. The tissue generated after 2 and 7 weeks (Fig. 4-6) presented with a cylindrical shape, whereas the specimens harvested at 12 weeks and thereafter resembled the form of an hourglass.

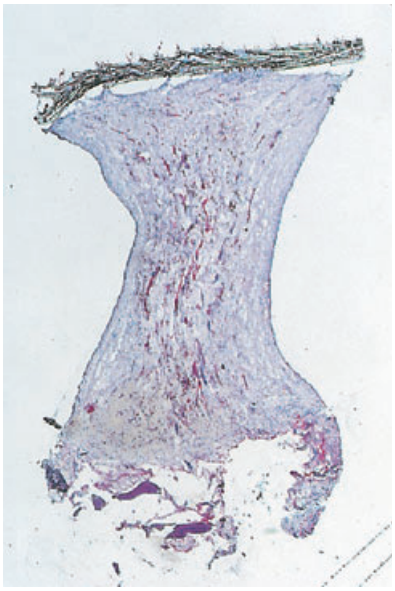

Fig. 4-6 Histological section of a 7-week specimen, comprising non-mineralized connective tissue in the shape of an hourglass. Note the covering e-PTFE membrane.

Fig. 4-7 Histological section of a 9-month specimen. The height of the mineralized tissue has reached the top 20% of the cylinder space area.

Specimens of 12 weeks and less regeneration time were almost entirely composed of soft tissue, while specimens with a regeneration time of 4 months and more were composed of both soft and increasing amounts of mineralized tissue (Fig. 4-7). It was concluded that the model system is suitable for studying temporal dynamics and tissue physiology of bone regeneration in humans with minimal risk of complications or adverse effects for the volunteers.

In a retrospective re-entry study (Lang *et al.* 1994), the bone volume regenerated using non-bioresorbable membrane barriers was assessed. Nineteen patients with jaw bone defects of various sizes and configurations were included. Combined split-thickness/full-thickness mucosal flaps were elevated in the area of missing bone. The size of the defects was assessed geometrically. Following the placement of Gore-Tex® augmentation material as a barrier, the maximum possible volume for bone regeneration was calculated. At the time of membrane removal (3–8 months later), the same measurements were performed and the percentages of regenerated bone in relation to the possible volume for regeneration determined. In six patients in whom the membranes had to be removed early, between 3 and 5 months, due to an increased risk of infection, bone regeneration varied between 0 and 60%. In 13 patients in whom the membranes were left for 6–8 months, regenerated bone filled 90–100% of the possible volume. It was concluded that successful bone regeneration consistently occurred with an undisturbed healing period of at least 6 months.

Conclusion: In summary, the bone of the alveolar process is of critical importance to maintain the structure and function of the jaws and subsequently the housing of teeth or tooth replacements. The physiological and biomechanical influences on bone by local and systemic mediators of bone homeostasis are important in the maintenance of alveolus. Reconstructive modalities aimed at the repair of bone tissues as a result of disease or injury utilize fundamental principles of bone biology. These regenerative biology approaches have been exploited in implant dentistry and periodontology with the use of bone grafting biomaterials, guided bone regeneration approaches, and more recently with polypeptide growth factors. Future work in this area will focus on the implications of systemic disease on bone maintenance during function as well as more predictable modalities for alveolar bone reconstruction.

References

Abdulwassie, H. & Dhanrajani, P.J. (2002). Diabetes mellitus and dental implants: a clinical study. *Implant Dentistry* **11**, 83–86.

Anusaksathien, O. & Giannobile, W.V. (2002). Growth factor delivery to re-engineer periodontal tissues. *Current Pharmaceutical Biotechnology* **3**, 129–139.

Baker, R.D., Terry, B.C., Davis, W.H. & Connole, P.W. (1979). Long-term results of alveolar ridge augmentation. *Journal of Oral Surgery* **37**, 486–489.

Bauer, D.C., Bauer, D.C., Palermo, L., Black, D. & Cauley, J.A. (2002). Quantitative ultrasound and mortality: a prospective study. *Osteoporosis International* **13**, 606–612.

Baylink, D.J., Finkelman, R.D. & Mohan, S. (1993). Growth factors to stimulate bone formation. *Journal of Bone and Mineral Research* **8** (Suppl 2), S565–572.

Becker, W., Hujoel, P.P., Becker, B.E. & Willingham, H. (2000). Osteoporosis and implant failure: an exploratory case-control study. *Journal of Periodontology* **71**, 625–631.

Blair, H.C., Zaidi, M. & Schlesinger, P.H. (2002). Mechanisms balancing skeletal matrix synthesis and degradation. *Biochemical Journal* **364**, 329–341.

Block, M.S., Kent, J.N., Ardoin, R.C. & Davenport, W. (1987). Mandibular augmentation in dogs with hydroxylapatite combined with demineralized bone. *Journal of Oral and Maxillofacial Surgery* **45**, 414–420.

Blumenthal, N.M., Koh-Kunst, G., Alves, M.E., Miranda, D., Sorensen, R.G., Wozney, J.M. & Wikesjo, U. M. (2002). Effect of surgical implantation of recombinant human bone morphogenetic protein-2 in a bioabsorbable collagen sponge or calcium phosphate putty carrier in intrabony periodontal defects in the baboon. *Journal of Periodontology* **73**, 1494–1506.

Bouillon, R. (1991). Diabetic bone disease. *Calcified Tissue International* **49**, 155–160.

Bouillon, R., Bex, M., Van Herck, E., Laureys, J., Dooms, L., Lesaffre, E. & Ravussin, E. (1995). Influence of age, sex, and insulin on osteoblast function: osteoblast dysfunction in diabetes mellitus. *Journal of Clinical Endocrinology and Metabolism* **80**, 1194–1202.

Boyne, P.J. (1970). Autogenous cancellous bone and marrow transplants. *Clinical Orthopaedics and Related Research* **73**, 199–209.

Chen, D., Zhao, M. & Mundy, G.R. (2004). Bone morphogenetic proteins. *Growth Factors* **22**, 233–241.

Cheng, H., Jiang, W., Phillips, F.M., Haydon, R.C., Peng, Y., Zhou, L., Luu, H.H., An, N., Breyer, B., Vanichakarn, P., Szatkowski, J.P., Park, J.Y. & He, T.C. (2003). Osteogenic activity of the fourteen types of human bone morphogenetic proteins (BMPs). *Journal of Bone and Joint Surgery. American Volume* **85-A**, 1544–1552.

Cho, P., Schneider, G.B., Krizan, K. & Keller, J.C. (2004). Examination of the bone-implant interface in experimentally induced osteoporotic bone. *Implant Dentistry*, **13**, 79–87.

Civitelli, R., Pilgram, T.K., Dotson, M., Muckerman, J., Lewandowski, N., Armamento-Villareal, R., Yokoyama-Crothers, N., Kardaris, E.E., Hauser, J., Cohen, S. & Hildebolt, C.F. (2002). Alveolar and postcranial bone density in postmenopausal women receiving hormone/estrogen replacement therapy: a randomized, double-blind, placebo-controlled trial. *Archives of Internal Medicine* **162**, 1409–1415.

Cortizo, A.M., Lettieri, M.G., Barrio, D.A., Mercer, N., Etcheverry, S.B. & McCarthy, A.D. (2003). Advanced glycation end-products (AGEs) induce concerted changes in the osteoblastic expression of their receptor RAGE and in the activation of extracellular signal-regulated kinases (ERK). *Molecular and Cellular Biochemistry* **250**, 1–10.

Cullum, P.E., Frost, D.E., Newland, T.B., Keane, T.M. & Ehler, W.J. (1988). Evaluation of hydroxylapatite particles in repair of alveolar clefts in dogs. *Journal of Oral and Maxillofacial Surgery* **46**, 290–296.

Curtis, T.A. & Ware, W.H. (1977). Autogenous bone graft procedures for atrophic edentulous mandibles. *Journal of Prosthetic Dentistry* **38**, 366–379.

Davis, W.H., Martinoff, J.T. & Kaminishi, R.M. (1984). Long-term follow up of transoral rib grafts for mandibular atrophy. *Journal of Oral and Maxillofacial Surgery* **42**, 606–609.

Duarte, P.M., Cesar Neto, J.B., Goncalves, P.F., Sallum, E.A. & Nociti, F.H. (2003). Estrogen deficiency affects bone healing around titanium implants: a histometric study in rats. *Implant Dentistry* **12**, 340–346.

Durie, B.G., Katz, M. & Crowley, J. (2005). Osteonecrosis of the jaw and bisphosphonates. *New England Journal of Medicine* **353**, 99–102.

Esposito, M., Coulthard, P., Thomsen, P. & Worthington, H. V. (2005). The role of implant surface modifications, shape and material on the success of osseointegrated dental implants. A Cochrane systematic review. *European Journal of Prosthodontics & Restorative Dentistry* **13**, 15–31.

Farzad, P., Andersson, L. & Nyberg, J. (2002). Dental implant treatment in diabetic patients. *Implant Dentistry* **11**, 262–267.

Fazili, M., von Overvest-Eerdmans, G.R., Vernooy, A.M., Visser, W.J. & von Waas, M.A. (1978). Follow-up investigation of reconstruction of the alveolar process in the atrophic mandible. *International Journal of Oral Surgery* **7**, 400–404.

Fiorellini, J.P., Chen, P.K., Nevins, M. & Nevins, M.L. (2000). A retrospective study of dental implants in diabetic patients. *International Journal of Periodontics and Restorative Dentistry* **20**, 366–373.

Friberg, B., Ekestubbe, A., Mellstrom, D. & Sennerby, L. (2001). Branemark implants and osteoporosis: a clinical exploratory study. *Clinical Implant Dentistry & Related Research* **3**, 50–56.

Friedenstein, A.J. (1973). Determined and inducible osteogenic precursor cells. In: *Hand Tissue Growth Repair and Remineralisation. Ciba Foundation Symposium. New series* **11**, 169–181.

Gallacher, S.J., Fenner, J.A., Fisher, B.M., Quin, J.D., Fraser, W.D., Logue, F.C., Cowan, R.A., Boyle, I.T. & MacCuish, A.C. (1993). An evaluation of bone density and turnover in premenopausal women with type 1 diabetes mellitus. *Diabetic Medicine* **10**, 129–133.

Giannobile, W.V. (1996). Periodontal tissue engineering by growth factors. *Bone* **19**, 23S-37S.

Giannobile, W.V. & Somerman, M.J. (2003). Growth and amelogenin-like factors in periodontal wound healing. A systematic review. *Annals of Periodontology* **8**, 193–204.

Graves, D.T., Liu, R., Alikhani, M., Al-Mashat, H. & Trackman, P.C. (2006). Diabetes-enhanced inflammation and apoptosis–impact on periodontal pathology. *Journal of Dental Research* **85**, 15–21.

Hämmerle, C.H., Schmid, J., Olah, A.J. & Lang, N.P. (1996). A novel model system for the study of experimental guided bone formation in humans. *Clinical Oral Implants Research* **7**, 38–47.

Hildebolt, C.F. (1997). Osteoporosis and oral bone loss. *Dentomaxillofacial Radiology* **26**, 3–15.

Horner, K., Devlin, H., Alsop, C.W., Hodgkinson, I.M. & Adams, J.E. (1996). Mandibular bone mineral density as a predictor of skeletal osteoporosis. *British Journal of Radiology* **69**, 1019–1025.

Hupp, J.R. & McKenna, S.J. (1988). Use of porous hydroxylapatite blocks for augmentation of atrophic mandibles. *Journal of Oral and Maxillofacial Surgery* **46**, 538–545.

Jackson, I.T., Helden, G. & Marx, R. (1986). Skull bone grafts in maxillofacial and craniofacial surgery. *Journal of Oral and Maxillofacial Surgery* **44**, 949–955.

Janssens, K., ten Dijke, P., Janssens, S. & Van Hul, W. (2005). Transforming growth factor-beta1 to the bone. *Endocrine Reviews* **26**, 743–774.

Kahn, B.B. & Flier, J.S. (2000). Obesity and insulin resistance. *Journal of Clinical Investigation* **106**, 473–481.

Kawaguchi, H., Kurokawa, T., Hanada, K., Hiyama, Y., Tamura, M., Ogata, E. & Matsumoto, T. (1994). Stimulation of fracture repair by recombinant human basic fibroblast growth factor in normal and streptozotocin-diabetic rats. *Endocrinology*, **135**, 774–781.

Kinane, D.F., Peterson, M. & Stathopoulou, P.G. (2006). Environmental and other modifying factors of the periodontal diseases. *Periodontology 2000* **40**, 107–119.

King, G.N. & Cochran, D.L. (2002). Factors that modulate the effects of bone morphogenetic protein-induced periodontal regeneration: a critical review. *Journal of Periodontology* **73**, 925–936.

Klemetti, E., Vainio, P., Lassila, V. & Alhava, E. (1993). Cortical bone mineral density in the mandible and osteoporosis status in postmenopausal women. *Scandinavian Journal of Dental Research* **101**, 219–223.

Kopman, J.A., Kim, D.M., Rahman, S.S., Arandia, J.A., Karimbux, N.Y. & Fiorellini, J.P. (2005). Modulating the

effects of diabetes on osseointegration with aminoguanidine and doxycycline. *Journal of Periodontology* **76**, 614–620.
Korlof, B., Nylen, B. & Rietz, K.A. (1973). Bone grafting of skull defects. A report on 55 cases. *Plastic and Reconstructive Surgery* **52**, 378–383.
Krakauer, J.C., McKenna, M.J., Buderer, N.F., Rao, D.S., Whitehouse, F.W. & Parfitt, A.M. (1995). Bone loss and bone turnover in diabetes. *Diabetes* **44**, 775–782.
Kribbs, P.J. (1990). Comparison of mandibular bone in normal and osteoporotic women. *Journal of Prosthetic Dentistry* **63**, 218–222.
Kribbs, P.J., Chesnut, C.H., 3rd, Ott, S.M. & Kilcoyne, R.F. (1990). Relationships between mandibular and skeletal bone in a population of normal women. *Journal of Prosthetic Dentistry* **63**, 86–89.
Kwon, Y.K., Bhattacharyya, A., Alberta, J.A., Giannobile, W.V., Cheon, K., Stiles, C.D. & Pomeroy, S.L. (1997). Activation of ErbB2 during wallerian degeneration of sciatic nerve. *Journal of Neuroscience* **17**, 8293–8299.
Lang, N.P., Hammerle, C.H., Bragger, U., Lehmann, B. & Nyman, S.R. (1994). Guided tissue regeneration in jawbone defects prior to implant placement. *Clinical Oral Implants Research* **5**, 92–97.
Law, A.N., Bollen, A.M. & Chen, S.K. (1996). Detecting osteoporosis using dental radiographs: a comparison of four methods. *Journal of the American Dental Association* **127**, 1734–1742.
Le, A.D., Basi, D.L. & Abubaker, A.O. (2005). Wound healing: findings of the 2005 AAOMS Research Summit. *Journal of Oral and Maxillofacial Surgery* **63**, 1426–1435.
Linkhart, T.A., Mohan, S. & Baylink, D.J. (1996). Growth factors for bone growth and repair: IGF, TGF beta and BMP. *Bone* **19**, 1S-12S.
Lu, H., Kraut, D., Gerstenfeld, L.C. & Graves, D.T. (2003). Diabetes interferes with the bone formation by affecting the expression of transcription factors that regulate osteoblast differentiation. *Endocrinology* **144**, 346–352.
Lugero, G.G., de Falco Caparbo, V., Guzzo, M.L., Konig, B., Jr. & Jorgetti, V. (2000). Histomorphometric evaluation of titanium implants in osteoporotic rabbits. *Implant Dentistry* **9**, 303–309.
Lunt, H., Florkowski, C.M., Cundy, T., Kendall, D., Brown, L. J., Elliot, J.R., Wells, J.E. & Turner, J.G. (1998). A population-based study of bone mineral density in women with long-standing type 1 (insulin dependent) diabetes. *Diabetes Research and Clinical Practice* **40**, 31–38.
Marx, R.E. (2003). Pamidronate (Aredia) and zoledronate (Zometa) induced avascular necrosis of the jaws: a growing epidemic. *Journal of Oral and Maxillofacial Surgery* **61**, 1115–1117.
McCarthy, A.D., Etcheverry, S.B. & Cortizo, A.M. (2001). Effect of advanced glycation endproducts on the secretion of insulin-like growth factor-I and its binding proteins: role in osteoblast development. *Acta Diabetologica* **38**, 113–122.
Miazgowski, T. & Czekalski, S. (1998). A 2-year follow-up study on bone mineral density and markers of bone turnover in patients with long-standing insulin-dependent diabetes mellitus. *Osteoporosis International* **8**, 399–403.
Mori, H., Manabe, M., Kurachi, Y. & Nagumo, M. (1997). Osseointegration of dental implants in rabbit bone with low mineral density. *Journal of Oral & Maxillofacial Surgery* **55**, 351–361; discussion 362.
Moy, P.K., Medina, D., Shetty, V. & Aghaloo, T.L. (2005). Dental implant failure rates and associated risk factors. *International Journal of Oral & Maxillofacial Implants* **20**, 569–577.
Mulliken, J.B. & Glowacki, J. (1980). Induced osteogenesis for repair and construction in the craniofacial region. *Plastic and Reconstructive Surgery* **65**, 553–560.
Nevins, M.L., Karimbux, N.Y., Weber, H.P., Giannobile, W.V. & Fiorellini, J.P. (1998). Wound healing around endosseous implants in experimental diabetes. *International Journal of Oral & Maxillofacial Implants* **13**, 620–629.
Novak, K.F., Taylor, G.W., Dawson, D.R., Ferguson, J.E., 2nd & Novak, M.J. (2006). Periodontitis and gestational diabetes mellitus: exploring the link in NHANES III. *Journal of Public Health Dentistry* **66**, 163–168.
Odvina, C.V., Zerwekh, J.E., Rao, D.S., Maalouf, N., Gottschalk, F.A. & Pak, C.Y. (2005). Severely suppressed bone turnover: a potential complication of alendronate therapy. *Journal of Clinical Endocrinology and Metabolism* **90**, 1294–1301.
Oh, T.J., Bashutski, J. & Giannobile, W.V. (2007). Interrelationship between osteoporosis and oral bone loss. *Grand Rounds in Oral Systemic Medicine*, **2**, 10–21.
Olmos, J.M., Perez-Castrillon, J.L., Garcia, M.T., Garrido, J.C., Amado, J.A. & Gonzalez-Macias, J. (1994). Bone densitometry and biochemical bone remodeling markers in type 1 diabetes mellitus. *Bone and Mineral* **26**, 1–8.
Olson, J.W., Shernoff, A.F., Tarlow, J.L., Colwell, J.A., Scheetz, J.P. & Bingham, S.F. (2000). Dental endosseous implant assessments in a type 2 diabetic population: a prospective study. *International Journal of Oral & Maxillofacial Implants* **15**, 811–818.
Ottoni, C.E. & Chopard, R.P. (2004). Histomorphometric evaluation of new bone formation in diabetic rats submitted to insertion of temporary implants. *Brazilian Dental Journal* **15**, 87–92.
Payne, J.B., Reinhardt, R.A., Nummikoski, P.V. & Patil, K.D. (1999). Longitudinal alveolar bone loss in postmenopausal osteoporotic/osteopenic women. *Osteoporosis International* **10**, 34–40.
Payne, J.B., Zachs, N.R., Reinhardt, R.A., Nummikoski, P.V. & Patil, K. (1997). The association between estrogen status and alveolar bone density changes in postmenopausal women with a history of periodontitis. *Journal of Periodontology* **68**, 24–31.
Peled, M., Ardekian, L., Tagger-Green, N., Gutmacher, Z. & Machtei, E.E. (2003). Dental implants in patients with type 2 diabetes mellitus: a clinical study. *Implant Dentistry* **12**, 116–122.
Ponder, S.W., McCormick, D.P., Fawcett, H.D., Tran, A.D., Ogelsby, G.W., Brouhard, B.H. & Travis, L.B. (1992). Bone mineral density of the lumbar vertebrae in children and adolescents with insulin-dependent diabetes mellitus. *Journal of Pediatrics* **120**, 541–545.
Reynolds, M.A., Aichelmann-Reidy, M.E., Branch-Mays, G.L. & Gunsolley, J.C. (2003). The efficacy of bone replacement grafts in the treatment of periodontal osseous defects. A systematic review. *Annals of Periodontology* **8**, 227–265.
Ripamonti, U., Herbst, N.N. & Ramoshebi, L.N. (2005). Bone morphogenetic proteins in craniofacial and periodontal tissue engineering: experimental studies in the non-human primate Papio ursinus. *Cytokine and Growth Factor Review* **16**, 357–368.
Rishaug, U., Birkeland, K.I., Falch, J.A. & Vaaler, S. (1995). Bone mass in non-insulin-dependent diabetes mellitus. *Scandinavian Journal of Clinical and Laboratory Investigation* **55**, 257–262.
Rix, M., Andreassen, H. & Eskildsen, P. (1999). Impact of peripheral neuropathy on bone density in patients with type 1 diabetes. *Diabetes Care* **22**, 827–831.
Roe, T.F., Mora, S., Costin, G., Kaufman, F., Carlson, M.E. & Gilsanz, V. (1991). Vertebral bone density in insulin-dependent diabetic children. *Metabolism* **40**, 967–971.
Ruggiero, S.L., Mehrotra, B., Rosenberg, T.J. & Engroff, S.L. (2004). Osteonecrosis of the jaws associated with the use of bisphosphonates: a review of 63 cases. *Journal of Oral and Maxillofacial Surgery* **62**, 527–534.
Santana, R.B., Xu, L., Chase, H.B., Amar, S., Graves, D.T. & Trackman, P.C. (2003). A role for advanced glycation end products in diminished bone healing in type 1 diabetes. *Diabetes* **52**, 1502–1510.

Schilephake, H. (2002). Bone growth factors in maxillofacial skeletal reconstruction. *International Journal of Oral & Maxillofacial Surgery* **31**, 469–484.

Shernoff, A.F., Colwell, J.A. & Bingham, S.F. (1994). Implants for type II diabetic patients: interim report. VA Implants in Diabetes Study Group. *Implant Dentistry* **3**, 183–185.

Siqueira, J.T., Cavalher-Machado, S.C., Arana-Chavez, V.E. & Sannomiya, P. (2003). Bone formation around titanium implants in the rat tibia: role of insulin. *Implant Dentistry* **12**, 242–251.

Steinhauser, E.W. & Hardt, N. (1977). Secondary reconstruction of cranial defects. *Journal of Maxillofacial Surgery* **5**, 192–198.

Swart, J.G. & Allard, R.H. (1985). Subperiosteal onlay augmentation of the mandible: a clinical and radiographic survey. *Journal of Oral and Maxillofacial Surgery* **43**, 183–187.

Sykaras, N. & Opperman, L.A. (2003). Bone morphogenetic proteins (BMPs): how do they function and what can they offer the clinician? *Journal of Oral Science* **45**, 57–73.

Taguchi, A., Tanimoto, K., Suei, Y., Ohama, K. & Wada, T. (1996). Relationship between the mandibular and lumbar vertebral bone mineral density at different postmenopausal stages. *Dentomaxillofacial Radiology* **25**, 130–135.

Taylor, G.I. (1983). The current status of free vascularized bone grafts. *Clinical Plastic Surgery* **10**, 185–209.

Thompson, N. & Casson, J.A. (1970). Experimental onlay bone grafts to the jaws. A preliminary study in dogs. *Plastic and Reconstructive Surgery* **46**, 341–349.

van Steenberghe, D., Jacobs, R., Desnyder, M., Maffei, G. & Quirynen, M. (2002). The relative impact of local and endogenous patient-related factors on implant failure up to the abutment stage. *Clinical Oral Implants Research* **13**, 617–622.

von Wowern, N., Klausen, B. & Kollerup, G. (1994). Osteoporosis: a risk factor in periodontal disease. *Journal of Periodontology* **65**, 1134–1138.

Wakasugi, M., Wakao, R., Tawata, M., Gan, N., Koizumi, K. & Onaya, T. (1993). Bone mineral density measured by dual energy x-ray absorptiometry in patients with non-insulin-dependent diabetes mellitus. *Bone* **14**, 29–33.

Whalen, J.P. & Krook, L. (1996). Periodontal disease as the early manifestation of osteoporosis. *Nutrition* **12**, 53–54.

Chapter 5

Osseointegration

Jan Lindhe, Tord Berglundh, and Niklaus P. Lang

The edentulous site

The fully healed, edentulous site of the alveolar ridge (see Fig. 2-23 and Chapter 2) is most often covered by a masticatory mucosa that is about 2–3 mm thick. This type of mucosa is covered by a keratinized epithelium and includes a connective tissue, rich in collagen fibers and fibroblasts, that is firmly attached to the bone via the periosteum. The outer walls of the alveolar process, the cortical plates, are comprised of lamellar bone and enclose the spongy or cancellous bone that contains bone trabeculae (lamellar bone) embedded in marrow. The bone marrow contains numerous vascular structures as well as adipocytes and pluripotent mesenchymal cells.

Osseointegration

Different types of implant systems have been used to replace missing teeth, including subperiosteal implants, endosseous implants with fibrous encapsulation, and endosseous implants with direct bone contact (*osseointegrated*). One definition of *osseointegration* (a term originally proposed by Brånemark *et al*. 1969) was provided by Albrektsson *et al*. (1981) who suggested that this was "a direct functional and structural connection between living bone and the surface of a load carrying implant". Another, clinical definition was provided by Zarb and Albrektsson (1991) who proposed that *osseointegration* was "a process whereby clinically asymptomatic rigid fixation of alloplastic materials is achieved and maintained in bone during functional loading".

Schroeder *et al*. (1976, 1981, 1995) used the term *"functional ankylosis"* to describe the rigid fixation of the implant to the jaw bone, and stated that "new bone is laid down directly upon the implant surface, provided that the rules for atraumatic implant placement are followed (rotation of the cutting instrument and less than 800 rpm, cooling with sterile physiologic saline solution) and the implant exhibits primary stability".

Thus, in order to acquire proper conditions for osseointegration (or functional ankylosis), the implant must exhibit proper initial fixation (stability) following installation in the recipient site. This initial (primary) stability is the result of the contact relationship or friction that is established following insertion of the implant, between mineralized bone (often the cortical bone) at the recipient site and the metal device.

Implant installation

Tissue injury

Basic rule: the less traumatic the surgical procedure is and the smaller the tissue injury (the damage) becomes in the recipient site during implant installation, the more expeditious is the process through which new bone is formed and laid down on the implant surface.

The various steps used in the implant installation procedure, such as (1) *incision* of the mucosa, often but not always followed by (2) the elevation of *mucosal flaps* and the separation of the periosteum from the cortical plates, (3) the preparation of the *canal* in the cortical and spongy bone of the recipient site, and (4) the insertion of the titanium device (the implant) in this canal, bring to bear a series of mechanical insults and injury to both the mucosa and the bone tissue. The host responds to this injury with an inflammatory reaction, the main objective of which is to eliminate the damaged portions of the tissues and prepare the site for regeneration or repair. To the above described hard tissue injury must be added the effect of the so-called "press fit", i.e. when the inserted implant is slightly wider than the canal prepared in the host bone at the recipient site. In such situations, (1) the mineralized bone tissue in the periphery of the

implant is compressed, (2) the blood vessels particularly in the cortical portion of the canal are collapsed, (3) the nutrition to this portion of the bone compromised, and (4) the affected tissues most often become non-vital.

The damage or injury to the soft and hard tissues of the recipient site initiates the process of wound healing that ultimately ensures that (1) the implant becomes "ankylotic" with the bone, i.e. osseointegrated, and (2) a delicate mucosal attachment (see Chapter 3) is established and a soft tissue seal formed that protects the bone tissue from substances in the oral cavity.

Wound healing

The healing of the severed bone following implant installation is a complex process that apparently involves different events in the cortical and in the spongy (cancellous) compartments of the surgical site.

In the *cortical bone compartment*, the non-vital mineralized tissue must first be removed (resorbed) before new bone can form. In the *spongy compartment* of the recipient site, on the other hand, the surgically inflicted damage (preparation of the canal and the installation of the implant) results mainly in soft tissue (marrow) injury that initially is characterized by localized bleeding and clot (coagulum) formation. The coagulum is gradually resorbed and the compartment thus becomes occupied by proliferating blood vessels and mesenchymal cells; granulation tissue. As result of the continuous migration of mesenchymal cells from the surrounding marrow, the young granulation tissue becomes replaced with provisional connective tissue and eventually with osteoid. In the osteoid, deposition of hydroxyapatite will occur around the newly formed vascular structures. Hereby, immature bone, most often woven bone, is formed (for detail see Chapter 2) and sequentially osseointegration, a direct connection between the newly formed bone and the metal device, takes place.

In summary: in the initial phase of the process that results in osseointegration, the non-vital lamellar bone in the cortical compartment is of importance for the initial fixation of the implant. Osseointegration, however, is often first established in areas occupied by cancellous bone.

Cutting and non-cutting implants

In this chapter only screw-shaped implants made of c.p. titanium will be discussed. The design of the metal device and the installation protocol followed may influence the speed of the process that leads to osseointegration.

"*Non-cutting*" implants (Fig. 5-1) require meticulous handling of the recipient site including the preparation of a standardized track (thread) on the inside

Fig. 5-1 A "non-cutting" implant (solid screw: Straumann® Implant System).

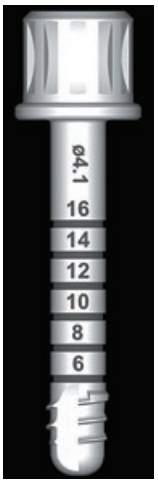

Fig. 5-2 A thread-tap (Straumann® Implant System) that is used to cut a track in the walls of the hard tissue canal. Following this preparation the cavity in the host tissue and the implant are congruent.

of the hard tissue canal. This preparation (precutting) of the track (thread) is made by the use of a thread-tap that is fitted with cutting edges (Fig. 5-2).

Figure 5.1 illustrates a "non-cutting" implant (solid screw, 4.1 mm: Straumann® implant system) that is designed as a cylinder with a rounded "apical" base. The diameter of the cylinder is 3.5 mm. Pilot and twist drills of gradually increasing dimension are used to prepare the hard tissue canal of the recipient site to a final diameter of 3.5 mm. On the surface of the cylinder the implant is designed with a helix-shaped pitch that is 0.3 mm high. The diameter of the entire screw shaped device therefore becomes 4.1 mm.

In sites with a high bone density a thread-tap (Fig. 5-2) is used to cut a 4.1 mm wide helix-shaped track in the walls of the hard tissue canal. The implant and the cavity prepared in the hard tissues of the recipient site are now congruent. When the implant is installed, the pitch on the device will capture and follow the helix-shaped track on the walls of the hard tissue canal and hereby guide the implant with a minimum of force into the pre-prepared position (Fig. 5-3).

Fig. 5-3 Ground section with a "non-cutting" implant and surrounding tissues obtained from a biopsy performed 24 hours after implant installation.

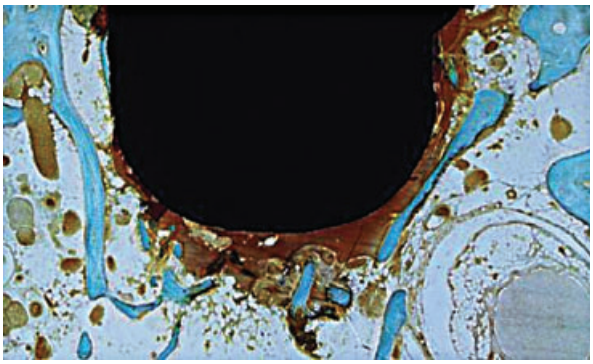

Fig. 5-4 Detail from the apical region of the implant described in Fig. 5-3. Note the presence of a coagulum in the bone marrow.

Figure 5-3 illustrates a "non-cutting" Straumann® solid screw with surrounding tissues in a biopsy sampled 24 hours after implant installation. The implant had proper initial fixation (stability) obtained by the large contact area that was achieved between the metal screw and the buccal and lingual bone walls in the cortical compartment of the recipient site. During site preparation and placement of the implant, bone trabeculae in the spongy compartment of the site were obviously dislocated into the bone marrow. Blood vessels in the marrow compartment were severed, bleeding provoked and a coagulum formed (Fig. 5-4).

After 16 weeks of healing (Fig. 5-5) the marginal portions of the "non-cutting" implant are surrounded by dense lamellar bone that is in direct contact with the rough surface of the metal device. Also in the apical portion of the implant, a thin coat of mature bone can be seen to contact the implant surface and

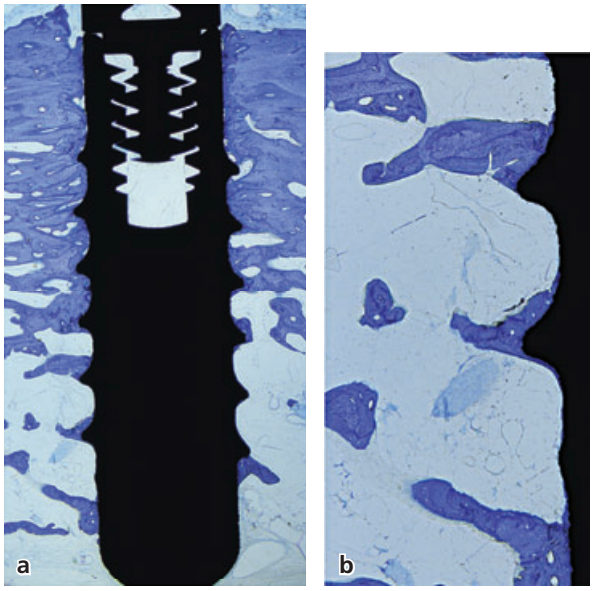

Fig. 5-5 (a) Ground section illustrating a "non-cutting" implant and surrounding bone after 16 weeks of healing. In the cortical portion of the recipient site, the bone density is high. (b) Detail of (a). In more apical areas a thin coat of bone is present on the implant surface. Note also the presence of trabeculae of lamellar bone that extend from the implant into the bone marrow.

Fig. 5-6 A "cutting" implant (Astra Tech® Implant System). Note the presence of cutting edges in the "apical" portion of the implant. During insertion this implant will cut a 0.3 mm wide chip from the lateral border of the canal prepared in the recipient site.

to separate the titanium screw from the bone marrow.

Cutting or self-tapping implants (e.g. Astra Tech® implants, diameter 4.0 mm) (Fig. 5-6) are designed with cutting edges placed in the "apical" portion of the screw-shaped device. The threads of the screw are prepared during manufacturing by cutting a continuous groove into the body of the titanium

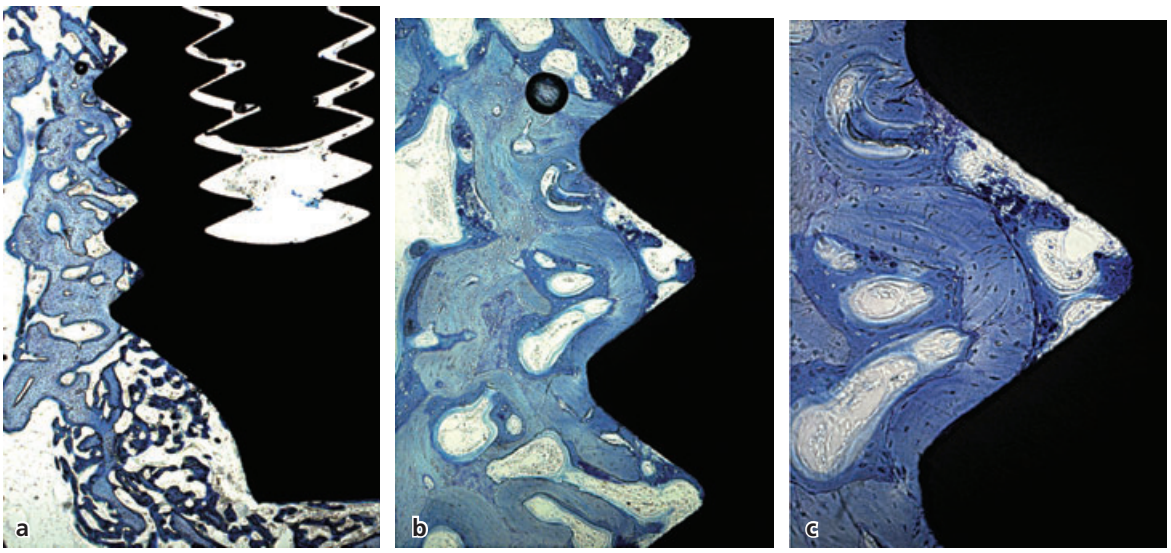

Fig. 5-7 (a) Ground section of an implant (Astra Tech®) site from a biopsy sampled after 2 weeks of healing. In the apical area large amounts of woven bone has formed. (b) Detail of (a). In the threaded region, newly formed bone can be seen to reach contact with the implant surface. (c) Higher magnification of (b). Newly formed bone extends from the old bone and reaches the titanium surface in the invagination between two consecutive "threads".

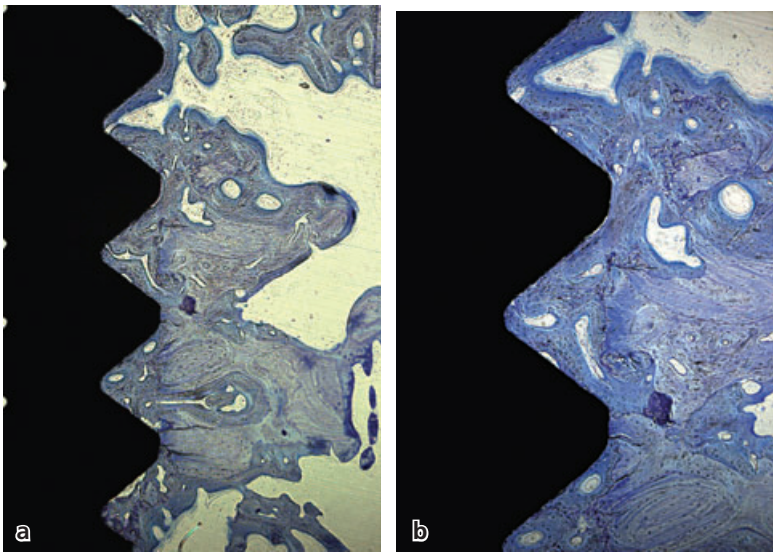

Fig. 5-8 Ground section of an implant site (Astra Tech® self-tapping implant) from a biopsy specimen obtained after 6 weeks of healing. (a) In the marginal area a continuous layer of bone covers most of the TiOblast® surface. (b) Higher magnification. Note the zone of newly formed (darker stained) bone that is in direct contact with the implant surface.

cylinder. When a self-tapping 4.0 mm wide implant is to be placed, the recipient site is first prepared with pilot and twist drills to establish a hard tissue canal that most often has a final diameter of 3.7 mm. During the insertion the cutting edges in the "apical" portion of the implant create a 0.15 mm wide track in the walls of the canal and thereby establish the final 4.0 mm dimension. When the implant has reached its insertion depth, contact has been established between the outer portions of the threads and the mineralized bone in the cortical compartment (initial or primary fixation is hereby secured) and with the severed bone marrow tissue in the spongy compartment.

Figure 5-7 illustrates a recipient site with a self-tapping implant (Astra Tech® implant). This implant is designed with a TiOblast® surface modification. The biopsy was harvested 2 weeks after installation surgery. The outer portion of the thread is in contact with the parent "old" bone, while bone formation is the dominant feature in the invaginations between the threads and in areas lateral to the "apical" portions of the implant. Thus, discrete areas of newly formed bone can be seen also in direct contact with the implant surface. In sections representing 6 weeks of healing (Fig. 5-8), it was observed that a continuous layer of newly formed bone covers most of the TiOblast® surface. This newly formed bone is also in contact with the old, mature bone that is present in the periphery of the recipient site. After 16 months of healing (Fig. 5-9), the bone tissue in the zone of osseointegration has remodeled and the entire hard tissue bed for the implant is comprised of lamellar bone including both concentric and interstitial lamella.

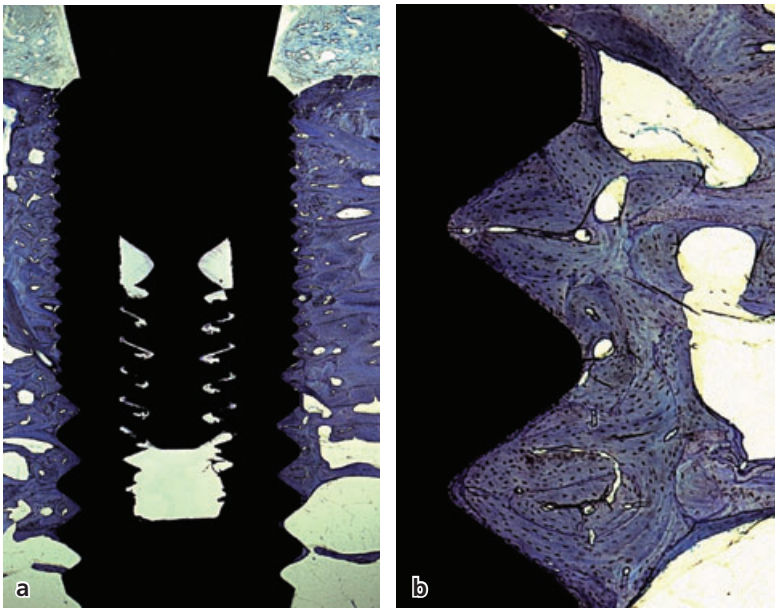

Fig. 5-9 Ground section of an implant site representing 16 months of healing. (a) The implant is surrounded by dense lamellar bone. (b) Higher magnification.

Fig. 5-10 The device used in the dog experiment. The implant is a modification of a solid screw (Straumann® Implant System). The distance between two consecutive threads is 1.25 mm. The depth of the trough is 0.4 mm.

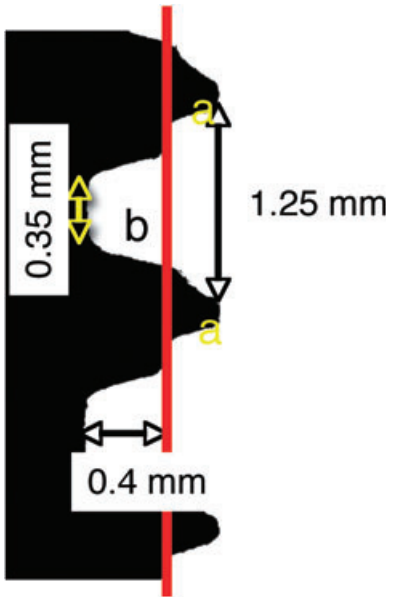

Fig. 5-11 The device. Schematic drawing illustrating the dimensions of the "wound chamber".

The process of osseointegration

De novo bone formation in the severed alveolar ridge following implant placement was studied in experiments in various experimental animal models (for review see Schroeder *et al*. 1995).

Recently Berglundh *et al*. (2003) and Abrahamsson *et al*. (2004) described various steps involved in bone formation and osseointegration to implants placed in the mandible of dogs.

The device: Custom-made implants that had the shape of a solid screw (Straumann® implant), that were made of c.p. titanium and configured with a rough surface topography (SLA®; Straumann) were utilized (Fig. 5-10). In the implant device the distance between two consecutive profiles of the pitch (i.e. the threads in a vertical cross section) was 1.25 mm. A 0.4 mm deep U-shaped circumferential trough had been prepared within the thread region during manufacturing (Fig. 5-11). The tip of the pitch was left untouched. Following the installation of the non-cutting device (Fig. 5-12) the pitch was engaged in the hard tissue walls prepared by the cutting tapping device. This provided intitial or primary fixation of the device. The void between the pitch and the body of the implant established a geometrically well defined wound chamber (Fig. 5-13). Biopsies were performed to provide healing periods extending from 2 hours following implant insertion to 12 weeks of healing. The biopsy specimens were prepared for ground sectioning as well as for decalcification and embedding in epon.

The wound chamber: Figure 5.13 illustrates a cross section (ground section) of an implant with surrounding soft and hard tissues from a biopsy specimen sampled 2 hours after installation of the metal device. The peripheral portions of the pitch were in

contact with the invaginations of the track prepared by the tap in the cortical bone. The wound chambers (Fig. 5-14a) were occupied with a blood clot in which erythrocytes, neutrophils, and monocytes/macrophages occurred in a network of fibrin (Fig. 5-14b). The leukocytes were apparently engaged in the wound cleansing process.

Fibroplasia: Figure 5-15a illustrates a device with surrounding tissues after 4 days of healing. The coagulum had in part been replaced with granulation tissue that contained numerous mesenchymal cells, matrix components, and newly formed vascular structures (angiogenesis) (Fig. 5-15b). A *provisional connective tissue* had been established.

Bone modeling: After 1 week of healing the wound chambers were occupied by a provisional connective tissue that was rich in vascular structures and contained numerous mesenchymal cells (Fig 5-16a). The number of remaining inflammatory cells was relatively small. In large compartments of the chamber, a cell-rich immature bone (woven bone) was seen in the mesenchymal tissues that surrounded the blood vessels. Such areas of woven bone formation occurred in the center of the chamber as well as in discrete locations that apparently were in direct contact with the surface of the titanium device (Fig. 5-16b). This

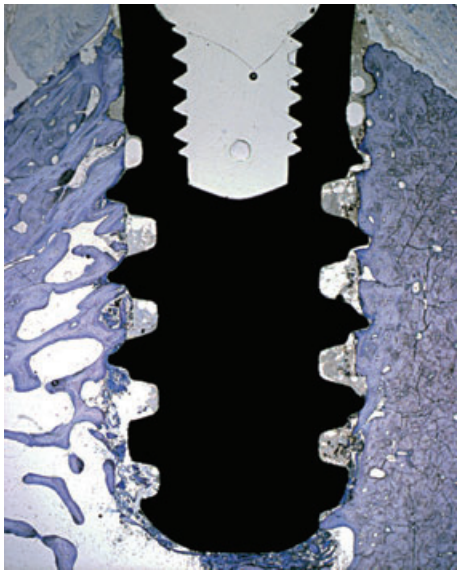

Fig. 5-12 Ground section showing the implant and adjacent tissues immediately after implant installation. The pitch region is engaged in the hard tissue walls. The void between two consecutive pitch profiles includes the wound chamber.

Fig. 5-13 Detail of Fig. 5-12. The wound chamber was filled with blood and a coagulum has formed.

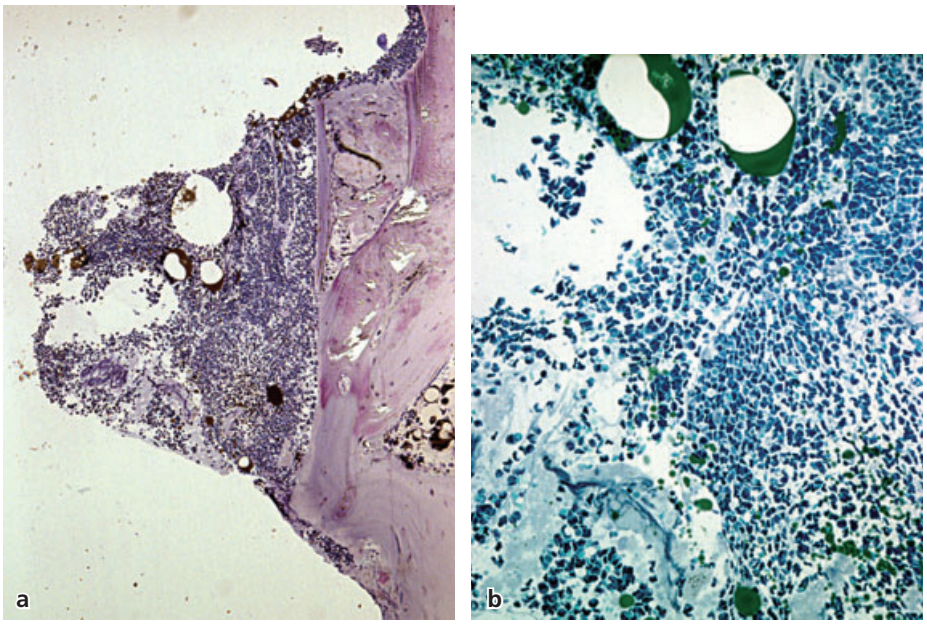

Fig. 5-14 The wound chamber 2 hours after implant installation. Decalcified sections. (a) The wound chamber is filled with blood. (b) Erythrocytes, neutrophils, and macrophages are trapped in a fibrin network.

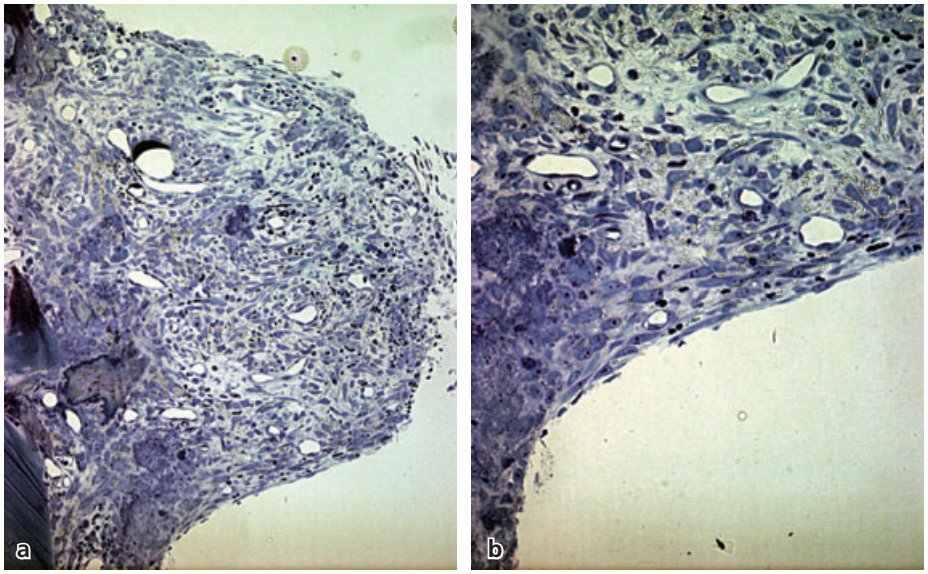

Fig. 5-15 The wound chamber after 4 days of healing (decalcified sctions). (a) Most portions of the wound chamber are occupied by granulation tissue (fibroplasia). (b) In some areas of the chamber provisional connective tissue (matrix) is present. This tissue includes large numbers of mesenchymal cells.

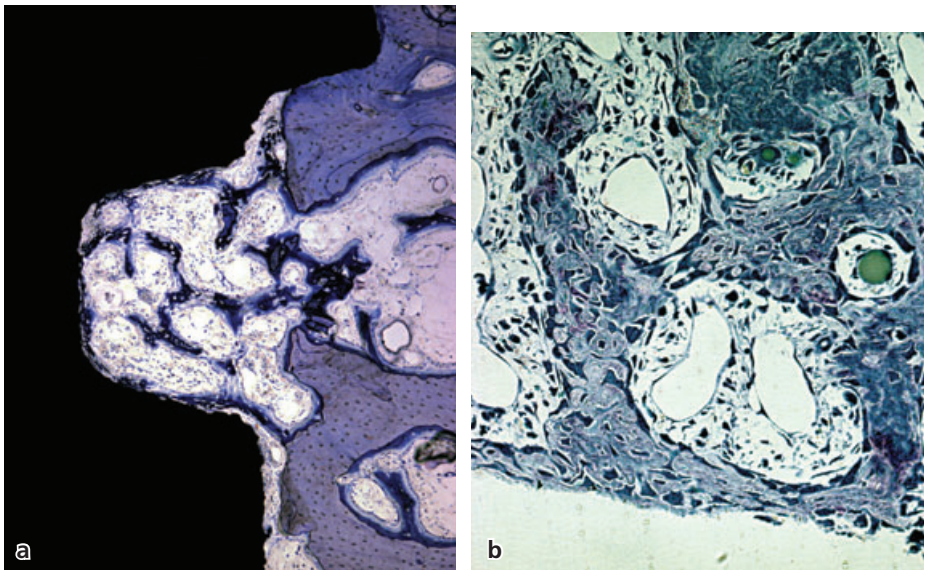

Fig. 5-16 (a) Ground section representing 1 week of healing. Note the presence of newly formed woven bone in the wound chamber. (b) Decalcified section. The woven bone is in direct contact with the implant surface.

was considered to represent the very first phase of osseointegration; contact between the implant surface and newly formed woven bone.

After 2 weeks of healing, woven bone formation appeared to be pronounced in all compartments, apical as well as lateral, surrounding the implant (Fig. 5-17a). Large areas of woven bone were found in the bone marrow regions "apical" of the implant. In the wound chamber, portions of the newly formed woven bone apparently extended from the parent bone into the provisional connective tissue (Fig. 5-17b) and had in many regions reached the surface of the titanium device. At this interval most of the implant surface was occupied by newly formed bone and a more comprehensive and mature osseointegration had been established (Fig. 5-17c). In the pitch regions there were signs of ongoing new bone formation (Fig. 5-17d). Thus, areas of the recipient site located lateral to the device, that were in direct contact with the host bone immediately following installation surgery and provided initial fixation for the implant, had undergone tissue resorption and were also involved in new bone formation after 2 weeks of healing.

At 4 weeks (Fig. 5-18a), the newly formed mineralized bone extended from the cut bone surface into the chamber and a continuous layer of cell-rich, woven bone covered most of the titanium wall of the

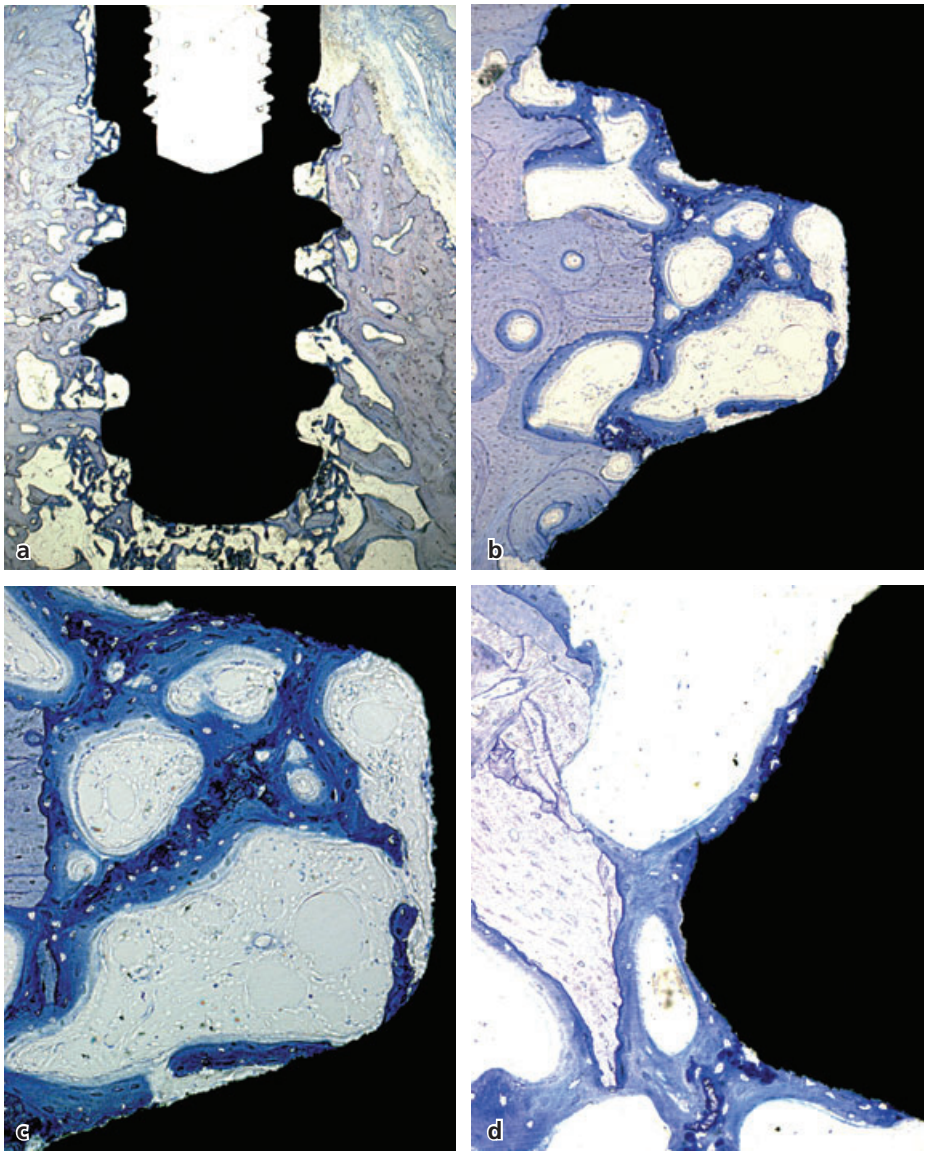

Fig. 5-17 Ground sections illustrating, in various magnifications, the tissues in the wound chamber after 2 weeks of healing. (a) Darker stained woven bone is observed in the apical area of the metal device. (b, c, d) Most portions of the implant surface are coated with bone.

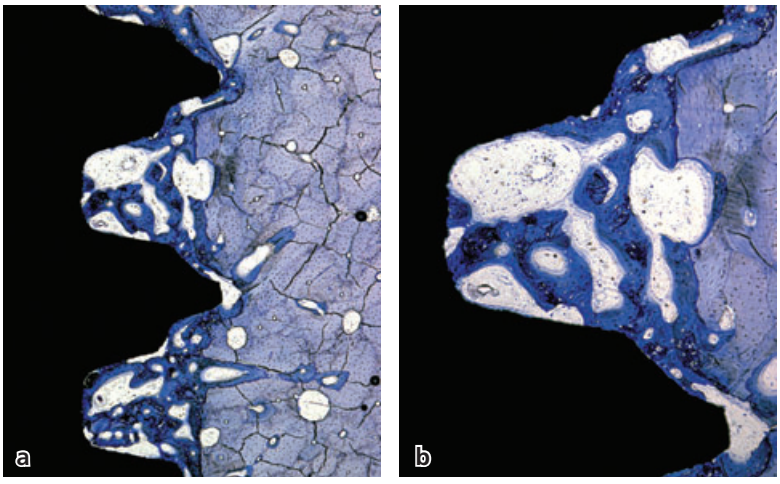

Fig. 5-18 Ground sections representing 4 weeks of healing. (a) The newly formed bone (dark blue) extends from the "old" bone into the wound chamber. (b) Appositional growth. Note the presence of primary osteons.

chamber. The central portion of the chamber was filled with a primary spongiosa (Fig. 5-18b), rich in vascular structures and a multitude of mesenchymal cells.

Remodeling: After 6–12 weeks of healing most of the wound chambers were filled with mineralized bone (Fig. 5-19). Bone tissue, including primary and secondary osteons, could be seen in the newly formed tissue and in the mineralized bone that made contact with the implant surface. Bone marrow that contained blood vessels, adipocytes, and mesenchymal cells was observed to surround the trabeculae of mineralized bone.

Summary: The wound chambers were first occupied with a coagulum. With the ingrowth of vessels and migration of leukocytes and mesenchymal cells, the coagulum was replaced with granulation tissue. The migration of mesenchymal cells continued and the granulation tissue was replaced with a provisional matrix, rich in vessels, mesenchymal cells, and fibers. The process of *fibroplasia* and angiogenesis had started. Formations of newly formed bone could be recognized already during the first week of healing; the newly formed woven bone projected from the lateral wall of the cut bony bed (appositional bone formation; distance osteogenesis) (Davies 1998) but *de novo* formation of new bone could also be seen on the implant surface, i.e. at a distance from the parent bone (contact osteogenesis) (Davies 1998). During subsequent weeks the trabeculae of woven bone were replaced with mature bone, i.e. lamellar bone and marrow (bone remodeling).

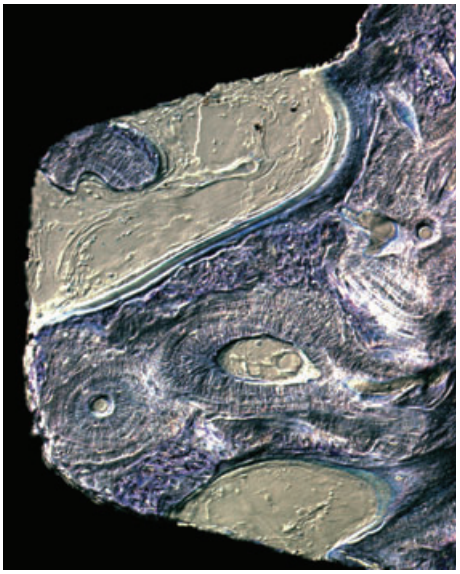

Fig. 5-19 Ground section representing 12 weeks of healing. The woven bone is being replaced with lamellar bone and marrow. Note the formation of secondary osteons.

References

Abrahamsson, I., Berglundh, T., Linder, E., Lang, N.P. & Lindhe, J. (2004). Early bone formation adjacent to rough and turned endosseous implant surfaces. An experimental study in the dog. *Clinical Oral Implants Research* **15**, 381–392.

Albrektsson, T., Brånemark, P-I., Hansson, H-A. & Lindström, J. (1981). Osseointegrated titanium implants. Requirements for ensuring a long-lasting, direct bone anchorage in man. *Acta Orthopaedica Scandinavica* **52**, 155–170.

Berglundh, T., Abrahamsson, I., Lang, N.P. & Lindhe, J. (2003). De novo alveolar bone formation adjacent to endosseous implants. a model study in the dog. *Clinical Oral Implants Research* **14**, 251–262.

Brånemark, P.I., Adell, R., Breine, U., Hansson, B.O., Lindström, J. & Ohlsson, Å. (1969). Intra-osseous anchorage of dental prostheses I. Experimental studies. *Scandinavian Journal of Plastic Reconstructive Surgery* **3**, 81–100.

Davies, J.E. (1998). Mechanisms of endosseous integration. *International Journal of Prosthodontics* **11**, 391–401.

Schroeder, A., Pohler, O. & Sutter, F. (1976). Gewebsreaktion auf ein Titan-Hohlzylinderimplant mit Titan-Spritzschichtoberfläche. *Schweizerisches Monatsschrift für Zahnheilkunde* **86**, 713–727.

Schroeder, A., van der Zypen, E., Stich, H. & Sutter, F. (1981). The reactions of bone, connective tissue, and epithelium to endosteal implants with titanium-sprayed surfaces. *Journal of Maxillofacial Surgery* **9**, 15–25.

Schroeder, A., Buser, D. & Stich, H. (1995) Tissue response. In: Schroeder, A., Sutter, F., Buser, D. & Krekeler, G., eds. *Oral Implantology. Basics, ITI Hollow Cylinder System.* New York: Thieme, pp. 80–111.

Zarb, G.A. & Albrektsson, T. (1991). Osseointegration – a requiem for the periodontal ligament? Editorial. *International Journal of Periodontology and Restorative Dentistry* **11**, 88–91.

Chapter 6

Periodontal Tactile Perception and Peri-implant Osseoperception

Reinhilde Jacobs

Introduction

Perception is the ability to detect external stimuli. In man, several kinds of sensory systems enable perception (vision, audition, balance, somatic function, taste, and smell) (Martin 1991). In all sensory systems, the initial contact with the external world is made through special neural structures called sensory receptors, endings or organs. A distinction is needed between nociceptors, chemo-, photo-, thermo-, and mechanoreceptors, each responding to a particular stimulus. In the oral cavity, taste and somatic sensory systems predominate. The former are sensitive to chemical stimuli while the latter respond to mechanical, thermal, and nociceptive stimuli. In this chapter, only the somatic sensory system is explored. The preponderance of the oral somatosensory system is illustrated by its major representation, besides that of the hand, on the sensory homunculus proposed by Penfield (Penfield and Rasmussen 1950). In general, the somatosensory function is essential for fine-tuning of limb movements. In analogy with the rest of the skeleton, the tactile function of teeth plays a crucial role in refinement of jaw motor control. Periodontal mechanoreceptors, especially those located in the periodontal ligament, are extremely sensitive to external mechanical stimuli. The periodontal ligament can thus be considered as a keystone for masticatory and other oral motor behaviours. Any condition that may influence periodontal mechanoreceptors, may alter the sensory feedback pathway and thus affect tactile function and fine-tuning of jaw motor control (e.g. periodontal breakdown, bruxism, re-implantation, anesthesia).

The most dramatic change may occur after extraction of teeth, as this eliminates all periodontal ligament receptors. This condition may persist after implant placement as functional re-innervation has

not yet been proven in humans. Surprisingly enough, patients with implant-supported prostheses often seem to function quite well. The underlying mechanism of this so-called "osseoperception" phenomenon remains a matter of debate, but the response of assumed peri-implant receptors might help to restore the proper peripheral feedback pathway. This hypothesized physiological integration might thus lead to better acceptance, improved psychological integration, and more natural functioning.

This chapter will unravel periodontal tactile function and guide the reader through the mysteries of peri-implant osseoperception in order to find neuroanatomical, histological, physiological, and psychophysical evidence to confirm the hypothesis.

Neurophysiological background

Afferent nerve fibres and receptors

When considering the human somatic sensory system, four types of afferent nerve fibers can be distinguished in association with sensation: Aα, Aβ, Aδ and C. Some types of afferent nerve fibers exist in specific tissues only, while others are widely distributed throughout the body. Based on the structure or signalling properties, receptors may be divided into several classes or categories (Birder & Perl 1994). Three different groups of receptors are associated with thermal and (vibro)tactile sensation: thermoreceptors, nociceptors and mechanoreceptors.

Thermoreceptors and nociceptors

Thermal sensations are divided into warm and cold and are perceived by specific receptors. There are indeed separate spots on skin and mucosal surface where thermal stimulation elicits either warm or cold sensation. Cold-sensitive spots are more numerous than warm-sensitive with the highest density of both cold and warm spots on the face (Bradley 1995). Unmyelinated neurite complexes are responsible for cold sensation and some free nerve endings for warm sensation (Bradley 1995). Receptors which can induce pain feeling are referred to as nociceptors and mostly supplied by Aδ and C fibers. In the periodontal ligament, one can identify free nerve endings which may be responsive to pain, but not thermal receptors. The majority of the receptors located within the periodontal ligament are of the mechanoreceptive type.

Mechanoreceptors

Mechanoreceptors are responsive to mechanical stimuli. These can be classified on the basis of their morphology, receptive field, and adaptation characteristics. In man, four receptor structures have been associated with mechanoperception: Meissner corpuscles, Pacinian corpuscles, Merkel cells, and Ruffini endings (Martin & Jessell 1991). These structural elements do determine, to some extent, the physiological characteristics of the peripheral receptors. On the basis of their receptive field, two subgroups of mechanoreceptors have been identified: receptors with small and distinct receptive fields (type I) and receptors with large and diffuse receptive fields (type II). Mechanoreceptors can also be subdivided based on their adaptation properties: rapidly adapting (RA) and slowly adapting (SA) receptors. The RA receptors, also called fast adapting receptors, only respond during the dynamic phase of stimulus application. In contrast, the SA receptors respond to both dynamic and static force applications (Iggo 1985). A relationship has been established between the aforementioned receptor morphologies and their adaptation characteristics. Rapidly adapting receptors include Meissner corpuscles (RA I) and Pacinian corpuscles (RA II) while SA receptors include Merkel cells (SA I) and Ruffini endings (SA II).

Trigeminal neurophysiology

Trigeminal neurosensory pathway

The trigeminal nerve is the largest cranial nerve, including a motor root supplying the masticatory muscles, and a predominant sensory root supplying the oral cavity, head, and face. The trigeminal nerve has three divisions (ophthalmic, maxillary, mandibular). The ophthalmic nerve is a sensory nerve and the smallest division. The maxillary nerve is a sensory nerve and intermediate, both in position and size, between ophthalmic and mandibular divisions. The mandibular nerve is the largest and made up of two roots: a large, sensory root and a small motor root.

The sensory inputs of the oral region are carried by the mandibular and maxillary divisions of the trigeminal nerve via the trigeminal ganglion to the brainstem. This is part of an important sensory feedback pathway, involved in refinement of jaw movements. The afferent signals are transmitted either to the main sensory nucleus of the trigeminal nerve (responsive to discriminate tactile senses, light touch and pressure) or to the descending spinal tract nuclei, including: (1) nucleus oralis, responsive to cutaneous sensation of oral mucosa; (2) nucleus interpolaris, responsive to tooth pulp pain; and (3) nucleus caudalis, responsive to pain, temperature, and crude touch.

From there, signals are transferred across the midline and sent to the thalamus and, via thalamocortical projections, to the respective cortical areas involved in orofacial sensation where they can result in conscious perception.

Neurovascularization of the jaw bones

The jaws are richly supplied by neurovascular structures, and it is thus of utmost important to identify vital anatomic structures before carrying out a

Fig. 6-1 These human dry mandibular bone sections illustrate the presence and dimensional importance of the mandibular incisive nerve, even in edentulism. The middle section is actually visualizing the mandibular midline, confirming that there is no true connection between the left and right sections.

surgical procedure. During a radiographic preoperative planning procedure, neurovascular structures need to be precisely localized to attempt avoiding interference. Particular attention should be paid to the anterior jaw bones, which are often considered as relatively safe surgical areas. The increasing rate of surgical interventions in the anterior jaw bone, such as oral implant placement and bone grafting, has indeed highlighted potential risks and raised the number of reported complications. Recent studies reveal that edentulous and dentate anterior jaws present significant variation in the occurrence of the mandibular incisive canal and genial spinal foramina as well as the maxillary nasopalatine canal (for review see Jacobs *et al*. 2007). All these canal structures contain a neurovascular bundle, whose diameter may be large enough to cause clinically significant trauma. While surgeons need to avoid the nervous structures, these critical structures may afterwards become essential to potentially reinnervate peri-implant bone. Indeed, the existence of remaining neurovascular bundles in the edentulous jaw bone may support the idea that nerves may regenerate after tooth extraction and implant placement. This particular assumption is the basis of the so-called osseoperception phenomenon and will be further outlined below.

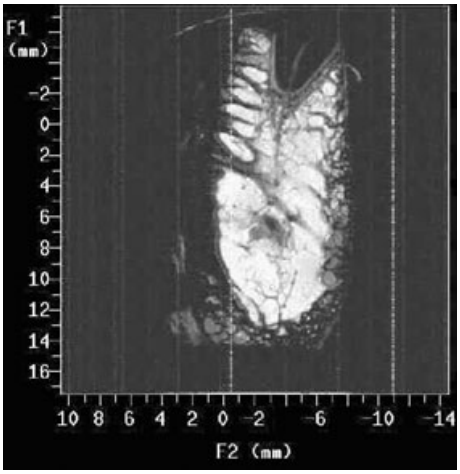

Fig. 6-2 Single cross-sectional slice of an high resolution MRI dataset localized at the incisor region of a dentate anterior human mandible, with the fatty marrow colored white. A black root-form structure corresponds to the root of an incisor tooth. It is surrounded by a small band of intermediate signal intensity, representing the periodontal ligament. The dental neurovascular supply is seen as a line of intermediate signal intensity in the middle of the root. The latter descends to the level of a larger structure of intermediate signal intensity (incisive nerve) with a black oval area on top (vascular structure). (Reprinted from Jacobs *et al*. 2007, Copyright 2006, with permission from Elsevier.)

Mandibular neuroanatomy

The mandibular nerve is the largest of the three divisions of the fifth cranial nerve and gives off the inferior alveolar nerve. The latter enters the mandible through the mandibular foramen and continues to run forward through the mandibular canal. At the mental foramen it gives off an important branch, called the mental nerve. It should not be considered as the only terminal branch of the inferior alveolar nerve. The mandibular incisive nerve is often detected as a second terminal branch with an intraosseous course in a so-called mandibular incisive canal, located anterior to the mental foramen (Mraiwa *et al*. 2003a,b) (Fig. 6-1). Conventional intraoral and panoramic radiographs often fail to show this canal (Jacobs *et al*. 2004). Cross-sectional imaging may however be used to locate the canal and as such avoid any risk for neurovascular damage (Jacobs *et al*. 2002a) The mandibular incisive canal contains a true neurovascular bundle with nervous sensory structures (Fig. 6-2). Its existence in edentulous patients is underlined by reported surgical complications. Indeed, sensory disturbances, caused by direct trauma to the mandibular incisive canal bundle have been reported after implant placement in the interforaminal region (Jacobs & van Steenberghe 2006; Jacobs *et al*. 2007) (Fig. 6-3).

A sensory disorder might also be related to indirect trauma caused by a hematoma in the canal, which acts as a closed chamber; this will affect the mandibular incisive canal bundle and spread to the main mental branch (Mraiwa *et al.* 2003b).

Other anatomic landmarks to be noted are superior and inferior genial spinal foramina and their bony canals, situated in the midline of the mandible in 85–99% of people (Liang *et al*. 2005a,b; Jacobs *et al*. 2007). The superior one is at the level of, or superior to, the genial spine; the inferior one is below the genial spine (Fig. 6-4). The superior genial spinal foramen has been found to contain a branch of the lingual artery, vein and nerve. Furthermore, a branch of the mylohyoid nerve together with branches or anastomoses of sublingual and/or submental arteries and veins have been identified upon entering the inferior genial spinal foramen. This artery could be of sufficient size to provoke hemorrhage intraosseously or in the connective soft tissue, which might be difficult to control (Darriba & Mendonca-Cardad 1997; Liang *et al*. 2005a,b) (Fig. 6-5).

The observation that immediate loading of implants in the anterior mandible results in a significant reduction of tactile function using the Brånemark Novum® concept rather than a conventional implant-supported overdenture might be explained by contact with the aforementioned neurovascular bundles in the anterior mandible (Abarca *et al*. 2006).

Fig. 6-3 Cross-sectional slice of a cone beam dataset showing an osseointegrated implant placed in an edentulous lateral incisor region, on top of a prominent incisive canal lumen. Chronic pressure on the incisive nerve resulted in a neuropathic pain problem. (Reprinted from Jacobs & van Steenberghe 2006, Copyright 2006, with permission from Blackwell Publishing.)

Maxillary neuroanatomy

The maxillary nerve is a sensory nerve, with its superior nasal and alveolar branches supplying the maxilla, including the palate, nasal and maxillary sinus mucosa, upper teeth and their periodontium. One of the superior nasal branches is named the nasopalatine nerve. It descends to the roof of the mouth through the nasopalatine canal and communicates with the corresponding nerve of the opposite side and with the anterior palatine nerve. The nasopalatine foramen and canals are situated at the maxillary midline, posterior to the central incisor teeth (Mraiwa *et al*. 2004). Typically, it has been described as having a Y-shape with the orifices of two lateral canals, terminating at the nasal floor level in the foramina of Stenson (Fig. 6-6). The nasopalatine nerve and the terminal branch of the descending palatine artery pass through these canals. Occasionally, two additional minor canals are seen (foramina of Scarpa), which may carry the nasopalatine nerves (Fig. 6-7). Mraiwa *et al*. (2004) point out a significant variability both regarding dimensions and morphological appearance of the nasopalatine canal.

To avoid disturbing neurovascular bundles and further complications, this important variability should be taken into account when dealing with surgical procedures such as implant placement in the maxillary incisor region.

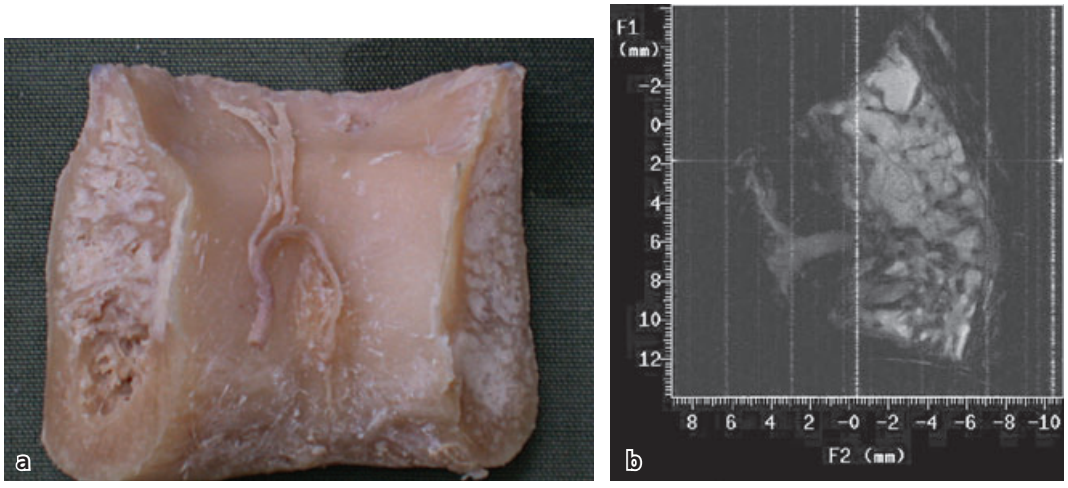

Fig. 6-4 (a) A macroanatomical view of a human anterior mandible showing a clear neurovascular bundle entering the superior genial spinal foramen. (b) A matching horizontal slice acquired through high-resolution MRI confirms the entry of a neurovascular bundle into the superior genial spinal foramen. (Courtesy of Professor I. Lambrichts, University of Hasselt.)

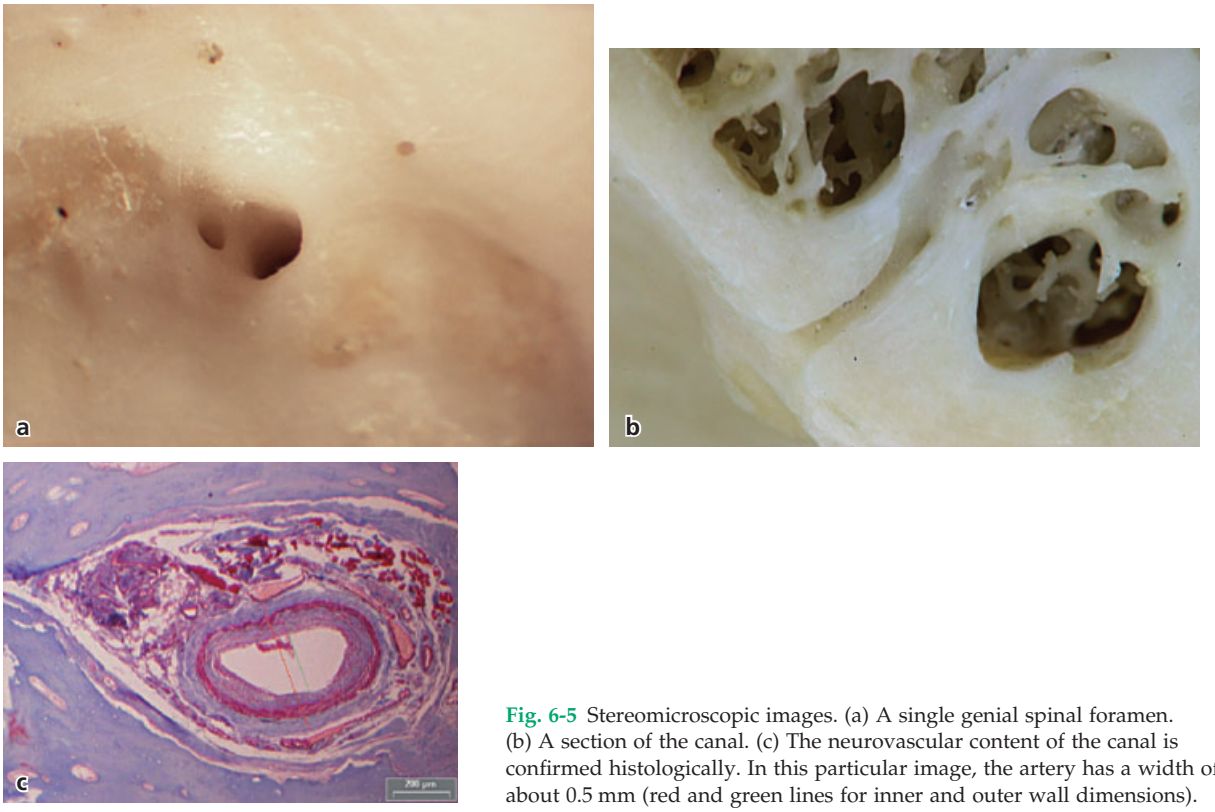

Fig. 6-5 Stereomicroscopic images. (a) A single genial spinal foramen. (b) A section of the canal. (c) The neurovascular content of the canal is confirmed histologically. In this particular image, the artery has a width of about 0.5 mm (red and green lines for inner and outer wall dimensions).

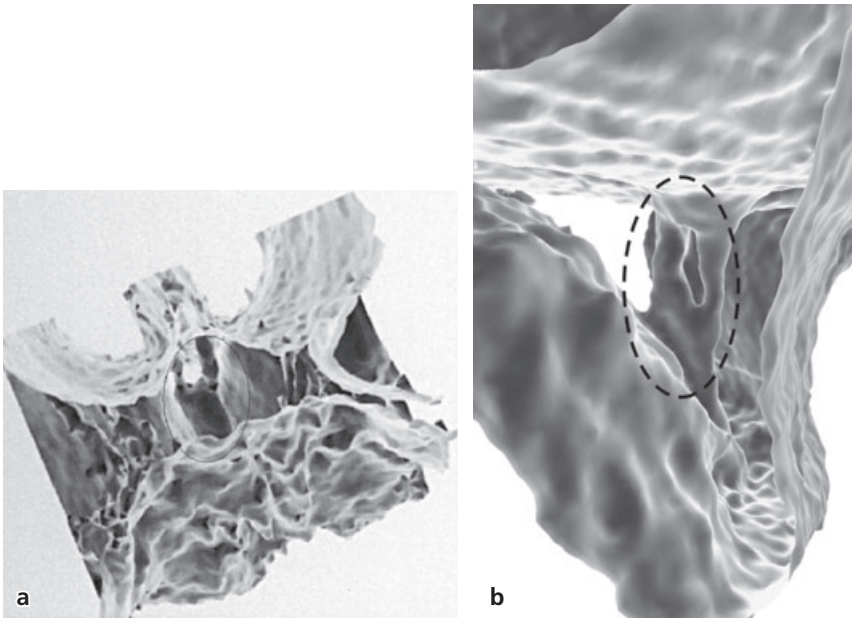

Fig. 6-6 Outline of the common Y-morphology of the nasopalatine canal (seen in black oval) on a three-dimensional reconstruction of the palate and the floor of the nose, seen from a posterior viewing angle (a) and a side view (b).

Periodontal innervation

Periodontal receptors are located within the gingiva, jaw bone, periosteum, and periodontal ligament. Most receptors seem to have mechanoreceptive characteristics, contributing to a sophisticated exteroceptive tactile function. This tactile information is not primarily used for protective purposes, but rather applied by the human brain to improve oral motor behavior and fine-tuning of biting and chewing (Trulsson 2006).

It is clear that the periodontal ligament plays a predominant role in this dedicated mechanoreceptive function. It has an extremely rich sensory nerve supply, especially in those locations that are more prone to displacement (peri-apical, buccal, and lingual periodontal ligament). It contains three types of nerve endings: free nerve endings, Ruffini-like endings, and lamellated corpuscles (Lambrichts *et al*. 1992). Free nerve endings stem from both unmyelinated and myelinated nerve fibers. Lamellated corpuscules are found in close contact to each other. Most

Fig. 6-7 View from the palate of an edentulous dry skull, showing the nasopalatine foramen, formed at the articulation of both maxillae, behind the incisor teeth. In the depth of the canal, the orifices of two lateral canals are seen. As an anatomic variant, two minor canals can be observed on the midline, one anterior and one posterior to the major nasopalatine canals.

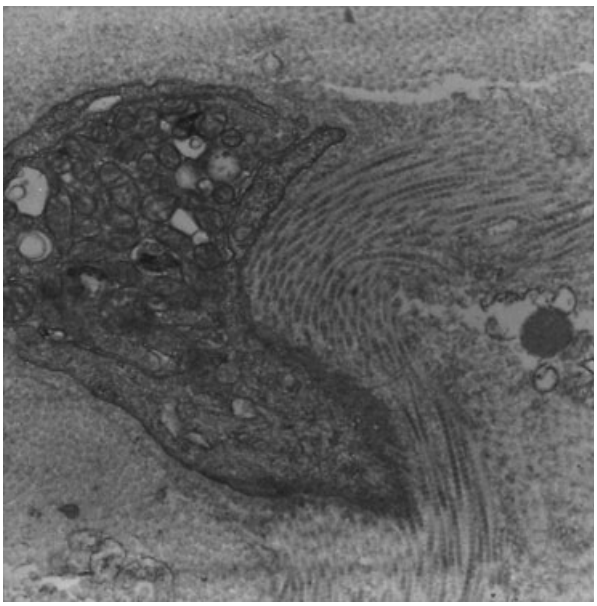

Fig. 6-8 Electron microscope image at the level of the human periodontal ligament, showing collagen fibrils inserted into the basal lamina of an ensheating cell in a Ruffini-like receptor. (Reprinted from Lambrichts *et al.* 1992, Copyright 2006, with permission from Ivo Lambrichts, University of Hasselt and Blackwell Publishing.)

mechanoreceptive endings are, however, Ruffini-like, and are predominantly present in the apical part of the periodontal ligament. Morphologic studies indicate that these endings are in close contact with collagen fibres of the surrounding tissues (Lambrichts *et al.* 1992) (Fig. 6-8). This particular association may explain their extremely high sensitivity upon loading a tooth. This results in low threshold levels for periodontal tactile function, and is considered as the basis of an elaborate sensory apparatus that may be linked to a number of clinical phenomena.

Recordings from the inferior alveolar nerve reveal that human periodontal mechanoreceptors discharge continuously during sustained loading of teeth (Trulsson *et al.*, 1992). Like the slowly adapting type II receptors in the human skin, most periodontal ligament mechanoreceptors are spontaneously active with a regular discharge in response to forces applied to teeth.

The mechanoreceptive function of the periodontal ligament allows it to signal differential information about the mechanical events that occur when manipulating and biting food with anterior teeth and chewing food with the posterior teeth (Trulsson 2006). The detailed differential signalling allows the brain to analyze and characterize the specific mechanical events enabling further processing for fine-tuning, resulting in an optimized masticatory sequence (Trulsson 2006). Considering this crucial role, it is clear that some sensory–motor interactions are impaired or even lost when altering or damaging the periodontal ligament. When teeth are extracted and thus ligament receptors eliminated, tactile functioning may be hampered. Indeed, Haraldson (1983) describes a similar muscle activity during the entire masticatory sequence in patients with implant-supported fixed prosthesis. This finding contrasts to subjects with natural teeth, having a chewing pattern that gradually changes with altering food bolus properties. Jacobs and van Steenberghe (1994) identify a silent period in muscle activity (reflex response) when tapping teeth or implanting neighboring teeth. A reflex response remains absent, however, when tapping implants in a fully edentulous jaw bone. Both findings may illustrate the modulatory role of periodontal ligament input in jaw muscle activity.

Testing tactile function

Neurophysiological assessment

Information on the exteroceptive function can be examined by neurophysiological as well as psychophysical methods. Neurophysiological investigations on the sensory function of the human trigeminal system are scarce. Afferent nerve recordings of the human trigeminal nerve require skilful performance. Only few studies have been performed so far (Johansson *et al.* 1988a,b; Trulsson *et al.* 1992). Alternatively, non-invasive approaches may be considered to evaluate oral tactile function. The first approach is the recording of the so-called trigeminal somatosensory evoked potentials (TSEP) after stimulation of receptors in the oral cavity (Van Loven *et al.* 2000, 2001). This set-up has the advantage of obtaining information on the cortical response of the trigeminal afferent system upon non-invasive stimulation of oral receptors. Unfortunately, SEPs from the trigeminal branches are, in contrast to those recorded from limbs, weak and difficult to discriminate from

the background noise; advanced signal analysis is required to gain reliable information (Swinnen *et al*. 2000; van Loven *et al*. 2000, 2001). Another non-invasive method to assess sensory function is to visualize brain activity by functional magnetic resonance imaging (fMRI) (Borsook *et al*. 2004, 2006). This is a complex but most promising method, which has received hardly any attention in relation to tactile function of teeth and implants (Lundborg *et al*. 2006; Miyamoto *et al*. 2006).

The main drawbacks of fMRI include complexity of the signal, relatively long imaging time, potential hazard imposed by the presence of ferromagnetic material in the vicinity of the imaging magnet, potential risk for claustrophobia, and costs. The technique is most promising, however. When combined with other techniques, such as psychophysics and TSEPs, it may offer a new non-invasive approach to evaluate how the human oral somatosensory system functions (Ducreux *et al*. 2006; Lundborg *et al*. 2006).

Psychophysical assessment

Sensory function can also be evaluated by psychophysical testing, relying on the patient's response. This technique has often been applied for testing oral tactile function (Jacobs & van Steenberghe 1994; Jacobs *et al*. 2002b,c,d). When carried out in a strictly standardized condition, the psychophysical response can be directly linked to the neural receptor activation (Vallbo & Johansson 1984).

Psychophysical studies on the oral sensory function are numerous. A major advantage of this type of study is that they are simple non-invasive techniques that can be performed in a clinical environment. Psychophysics include a series of well defined methodologies to help determine the threshold level of sensory receptors in man. Psychophysical methods allow connection between the psychological response of the patient to the physiological functions of the receptors involved. The methods should be carried out in a standardized and accurate manner, to enable one to draw conclusions about their outcome with regard to sensory function (Jacobs *et al*. 2002b,c,d).

Regardless of the tests used, one must keep in mind that many variables contribute to the subjective nature of psychophysical sensory testing. Some variables are manageable, others are more difficult to deal with. Influencing factors exist in various components of the experiment set-up (environmental influence, psychophysical approach, patient-related factors) (Jacobs *et al.* 2002b).

Environmental factors should be well controlled, as background noise is distracting to patient and examiner. To minimize the effect of noise, testing should be done in a quiet room with stable background illumination.

Patient-related variables may contribute greatly to the outcome of the testing. Psychological and/or physical factors may lead to an inter- and intra-subject variability, making the expression of a threshold level more obvious than assessment of an absolute value. Psychological factors include motivation, level of concentration, and anxiety level. The psychophysical approach may attempt to control such variability.

Different psychophysical procedures have been described in order to assess tactile function reliably (Falmagne 1985). Adaptive methods are generally recommended for threshold level determination, as these seem very effective and consistent. Such approaches are termed adaptive, as the subsequent stimulus value depends on the subject's response in preceding trials. In the staircase method, the stimulus value is changed by a constant amount. When the response shifts from one answer to another, the stimulus direction is reversed. Afterwards, the threshold is determined by averaging peaks and valleys throughout all runs. Some patients may imagine a stimulus when there is none. Others admit feeling a sensation, only if they are absolutely positive that it was felt. The inclusion of false alarms (implying that no stimulus is presented in the specified time interval) may exclude response bias and a guessing strategy of the subject. A thorough and standardized instruction to all subjects is important in this respect.

Other patient-related factors that should be considered are of physical origin and include age, gender, dental status and dexterity. Age is an important variable with respect to implant physiology, considering the fact that edentulous patients are usually found amongst the elderly. Age-related impairment is seen, both of motor function and most sensory modalities in the extremities (Masoro 1986). A decline in oral sensory function is also established. After the age of 80, the ability to differentiate tactile and vibratory stimuli on the lip decreases and two-point discrimination deteriorates on the upper lip, on the cheeks, and on the lower lip, but not on the tongue and the palate (Calhoun *et al*. 1992). Stereognostic ability also declines with age (Müller *et al*. 1995). It is clear that this age effect should be considered in experimental studies.

In contrast to age, the influence of gender on tactile function remains a matter of debate. Taking into account the important inter-individual variability, clear-cut gender differences are not easily discerned with regard to oral sensory function. There is no marked gender effect on stereognostic ability or vibrotactile function (Jacobs *et al*. 1992, 2002b). The tactile sensory systems of men and women seem to operate similarly at both threshold and suprathreshold levels of stimulation (Chen *et al*. 1995). However, females seem to have greater ability to discern subtle changes in lip, cheek, and chin position than males (Chen *et al*. 1995). Dexterity is another patient-related variable. Although there is some relation between masticatory performance and dexterity (Hoogmartens & Caubergh 1987), this is not the case

for either tactile function or stereognosis (Jacobs *et al*. 1992, 2002b).

Periodontal tactile function

A variety of psychophysical tests has been used to evaluate oral exteroceptive function by assessment of threshold levels. Although some of the methods designed for functional psychophysical testing are unable to identify the specific receptor groups involved in the mechanisms of oral sensation, the tests may clearly reflect periodontal tactile function. Assessing light touch or the tactile function of teeth is performed by determination of the threshold levels for active and passive detection and discrimination tasks (Jacobs *et al*. 1992, 2002b,d). The distinction between detection and discrimination is based on the fact that, in a detection task, the subject has to indicate the presence or absence of a stimulus ("yes" or "no" strategy) while in a discrimination task, the subject has to compare two stimuli ("smaller" or "larger" strategy). A further division is made between active and passive tasks. In the passive task, forces are applied to a tooth in the upper jaw. The active tactile function of teeth is evaluated by inserting an object, mostly a foil of a certain thickness, in between two antagonistic teeth. The latter rather reflects daily functioning and automatically involves other than periodontal receptors (e.g. joint, muscle and inner ear receptors), while the passive test involves solely activation of periodontal ligament mechanoreceptors.

Active threshold determination

The active absolute threshold level is determined by the interocclusal detection of small objects such as foils of varying thicknesses (Fig. 6-9). This may involve the activation of mechanoreceptors, mainly originating from the periodontium but also from the muscles, inner ear, and temporomandibular joints (TMJs). It should, however, be realized that the foil materials used may have different thermal and mechanical properties, resulting in conflicting results (Jacobs *et al*. 1992). Foil materials with high thermal conductivity (e.g. steel, aluminium) may lower the threshold level by activation of thermal receptors.

Fig. 6-9 Active threshold determination by interocclusal thickness perception yields superior results for teeth than for implant-supported prostheses, with fixed prostheses being more sensitive than removable ones.

Another factor that may affect the active tactile function is chewing activity, because this involves progressive intrusion of the tooth after each chewing cycle. The latter leads to adaptation of the periodontal mechanoreceptive inputs. Chewing or bruxism may thus lead to an increase in threshold levels up to 60 times the normal values (Kiliaridis *et al*. 1990). An interocclusal discrimination task of small objects determines the differential threshold level. The active threshold level varies according to the experiment set-up, but the most important variable is test stick dimension (Jacobs & van Steenberghe 1994). For size discrimination with a mouth opening of less than 5 mm, periodontal mechanoreceptive input plays the primary role. For increased mouth opening, the response of muscle spindles predominates.

Passive threshold determination

The most common device used in clinical neurology to measure light touch sensation is a set of Semmes-Weinstein monofilaments (Semmes-Weinstein Aesthesiometer®, Stoelting, Illinois, USA). The original idea dates back from the nineteenth century when von Frey suggested testing cutaneous light touch by using calibrated hairs of different stiffness by changing their length and hardness. Later on, the so-called von Frey hairs were replaced by nylon monofilaments mounted into a plastic handle (Fig. 6-10). This technique has also been applied intraorally for assessment of light touch thresholds for teeth, implants or oral mucosa (Jacobs & van Steenberghe 1994; Jacobs *et al*. 2002d). The drawback remains the variation caused by the hand-held and thus variable nature of stimulation application. Other stimulators have therefore been developed, enabling a controlled force level under more standardized stimulation conditions for measuring both manual and oral light touch (Jacobs *et al*. 2002b,d).

The passive discrimination task allows testing of the ability to differentiate between intensities of forces applied to a tooth. It depends on the force characteristics such as the rate of force application and the range of forces presented. When comparing teeth and implants, passive threshold levels are much lower for teeth but at suprathreshold force levels, implants and teeth become equally sensitive. For the passive detection of forces applied to a tooth, different stimulating devices have been developed. In order to avoid tapping and subsequent transmission of the waves through the jaw bone with activation of other receptors, such as in the inner ear, pushing forces are recommended (Fig. 6-11). This is done by placement of the stimulating rod in contact with the tissue under investigation (Jacobs & van Steenberghe 1993).

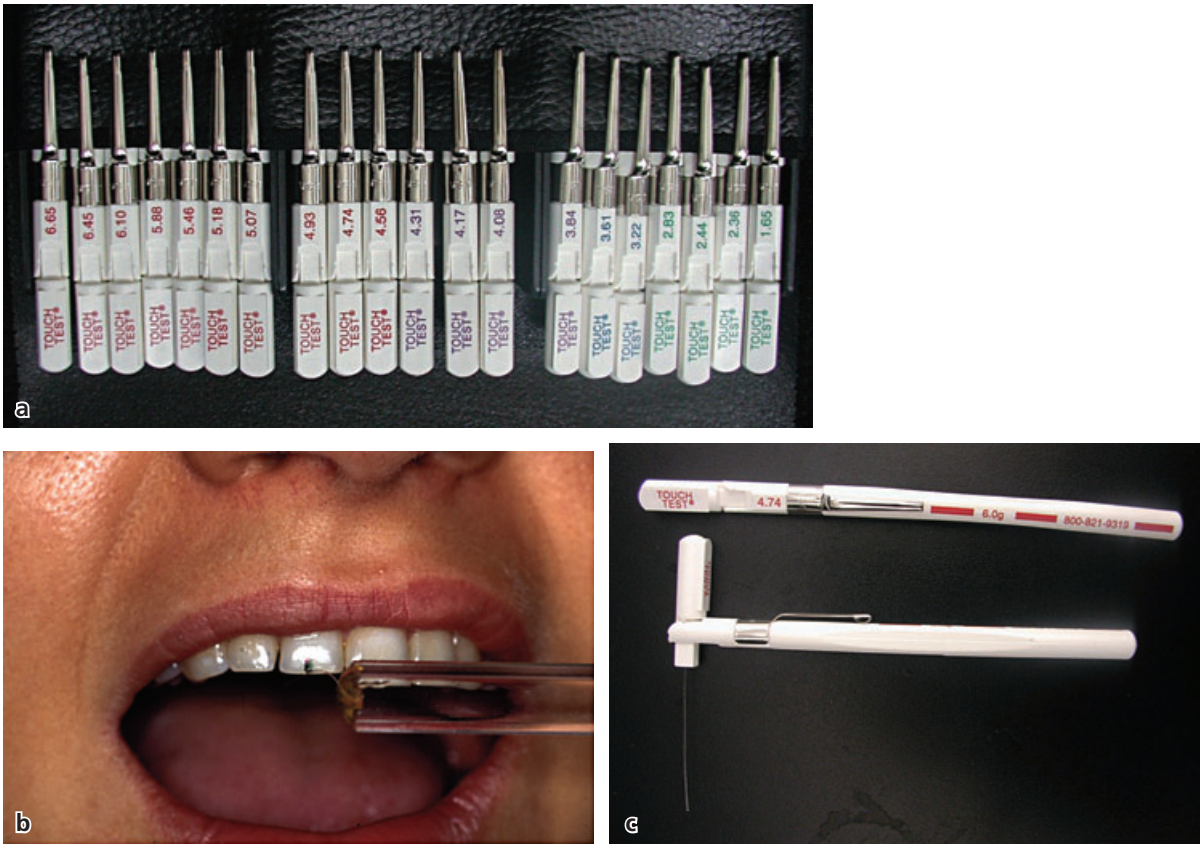

Fig. 6-10 Passive threshold determination. (a) Using a kit of pressure esthesiometers of increasing loads. (b) From determination of the absolute detection threshold upon tooth loading. (c) Using the individual hand-held stimulation rod.

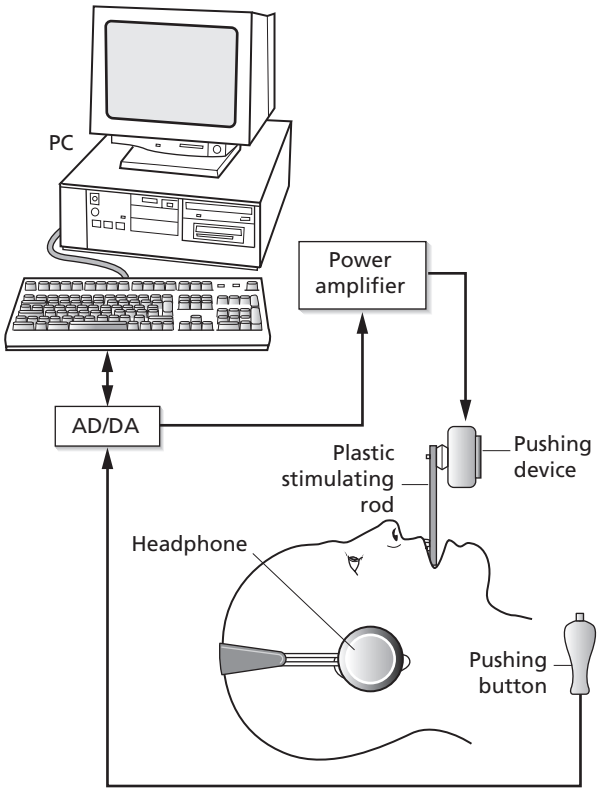

Fig. 6-11 Set-up of passive threshold determination of a maxillary front tooth by applying axial pushing forces against the tooth.

Influence of dental status on tactile function

From several psychophysical studies, it has been established that the oral tactile function is influenced by tooth position and dental status (Jacobs *et al.* 2002b). The tactile function of teeth is primarily determined by the presence of periodontal ligament receptors. Vital or non-vital teeth may show a comparable tactile function. However, when periodontal ligament receptors are reduced or eliminated (e.g. periodontitis, bruxism, chewing, extraction, anesthesia, etc.), tactile function is impaired (Table 6-1). This clinically implies that a patient's ability to detect occlusal inaccuracies (e.g. induced by restorative treatment) is decreased in these situations. Indeed, exteroceptors inform the nervous system on the characteristics of the stimulus, which then allows modulation of the motoneuron pool to optimize jaw motor activity and avoid overloading. Elimination of these exteroceptors by tooth extraction may reduce the tactile function to an important extent (Jacobs *et al.* 2001; Jacobs & van Steenberghe 1991, 1994, 2006; Mericske-Stern 1994; Mericske-Stern *et al.* 1995; Jacobs 1998). Even after rehabilitation with a prosthesis, tactile function remains impaired and inappropriate exteroceptive feedback may thus present a risk for overloading the prosthesis (Jacobs & van Steenberghe 2006). In comparison to the tactile function of a natural dentition, the active threshold is seven to

Table 6-1 Factors influencing the tactile function of teeth (for review see Jacobs *et al*. 2002b; Jacobs & van Steenberghe 2006)

Influencing factors	Active threshold (thickness detection)	Passive threshold (force detection)
Vital tooth	20 µm	2 g
Non-vital tooth	20 µm	2 g
Anesthesia	↑	↑
Periodontitis	↑	↑ (> 5 g)
Chewing	↑	↑
Bruxism	↑	↑
Extraction	↑	↑
Reimplantation	↑	↑
Denture	150 µm	150 g
Implant-supported prosthesis	50 µm	100 g
Ageing	↑	↑
Polyneuropathy	↑	↑

↑: increase in threshold level implying a decrease in tactile function and hampered feedback.

eight times higher for dentures but only three to five times higher for implants (see Table 6-1). For the passive detection of forces applied to upper teeth, thresholds are increased 75 times for dentures and 50 times for implants (see Table 6-1). The large discrepancies between active and passive thresholds can be explained by the fact that several receptor groups may respond to active testing, while the passive method selectively activates periodontal ligament receptors. The latter are eliminated after extraction, which may explain the reduced tactile function in edentulous patients.

After rehabilitation with a bone-anchored prosthesis, however, edentulous patients seem to function quite well. These patients perceive mechanical stimuli exerted on osseointegrated implants in the jaw bone. Some of them even note a special sensory awareness with the bone-anchored prosthesis, coined "osseoperception". It can be defined as a perception of external stimuli transmitted via the implant through the bone by activation of receptors located in peri-implant environment, periosteum, skin, muscles, and/or joints (Jacobs 1998). The existence of this phenomenon could imply that the feedback pathway to the sensory cortex is partly restored with a hypothetical representation of the prosthesis in the sensory cortex; this may allow an adjusted modulation of the motoneuron pool leading to more natural functioning and avoiding overload.

Activation of oral mechanoreceptors during oral tactile function

When performing psychophysical testing, various types of oral mechanoreceptors may be activated. Mechanoreceptors in the oral region may be located in the periodontal ligament, oral mucosa, gingiva, bone, periosteum, and tongue. Mechanoreceptors in the periodontal ligament contribute to the very high sensitivity of teeth to mechanical stimuli (Jacobs & van Steenberghe 1994). The periodontal ligament is richly supplied with mechanoreceptors, with the majority being identified histologically as Ruffini-like endings (Lambrichts *et al*. 1992). During passive threshold determination, these receptors will be activated. The assessment of the active tactile threshold level is, however, not solely based on activation of periodontal mechanoreceptors. Temporomandibular joint receptors are found to only play a minor role, but muscular receptors are important in the discriminatory ability for mouth openings of 5 mm and more (Broekhuijsen & Van Willigen 1983).

Considering that mechanoreceptors in the periodontal ligament largely contribute to tactile function, one can question what happens after tooth extraction. It can be assumed that remaining receptors in the peri-implant environment (gingiva, alveolar mucosa, periosteum, and bone) may take over part of the normal exteroceptive function.

In the oral mucosa, different types of mechanoreceptors can be identified including lamellar organs, Ruffini-like endings, and free nerve endings (Lambrichts *et al*. 1992). The number of nerve fibers per unit area is greater in the anterior areas of the oral cavity, making this region the most sensitive part of the oral mucosa (Mason 1967).

The gingiva contains round and oval lamellar corpuscles. These receptors respond to mechanical stimuli for coordination of the lip and buccal muscles during mastication (Johansson *et al*. 1988a,b). Cutaneous mechanoreceptors in the facial skin are activated by skin stretching or contraction of facial muscles and may operate as proprioceptors involved in facial kinesthesia and motor control (Nordin & Hagbarth 1989).

The periosteum contains free nerve endings, complex unencapsulated, and encapsulated endings. The free nerve endings are activated by pressure or stretching of the periosteum through the action of masticatory muscles and the skin (Sakada 1974). Periosteal innervation has been suggested to play a role in peri-implant tactile function (Jacobs 1998). Indeed, when applying forces to osseointegrated implants in the jaw bone, pressure build-up in the bone is sometimes large enough to allow deformation of the bone and its surrounding periosteum (Jacobs 1998). The involvement of bone innervation in mechanoreception and peri-implant osseoperception remains a matter of debate, however (Jacobs & van Steenberghe 2006).

Functional testing of the oral somatosensory system

Functional testing of the oral somatosensory system may include two-point and size discrimination as

well as stereognosis. Two-point discrimination is the ability to differentiate between two points of simultaneous contact. A traditional disk for two-point discrimination is divided into equal triangles containing two points placed at standard distances, usually between 2 and 25 mm (Fig. 6-12). This kind of test can be applied on different areas of the skin or the oral mucosa (Jacobs *et al*. 2002b,c,d). Size discrimination consists in holding a stick between two antagonistic teeth or fingers. This discriminatory ability is better for antagonistic teeth than for fingers (Morimoto 1990). The most documented and relevant test for the oral cavity is, however, stereognosis, which is considered as a complex functional test, evaluating the ability to recognize and discriminate different forms (Jacobs *et al*. 1997).

Oral stereognosis

While touch may obtain information on the mechanoreceptors activated by simple detection or discrimination of mechanical stimuli, stereognosis is a more complex process. It is a function of both peripheral receptors (touch and kinesthetic) and central integrating processes (Jacobs *et al*. 1998). It may give an idea on daily functioning and may be applied to measure sensory impairment due to the presence of general or local pathology (speech pathology, blindness, deafness, cleft lip and palate, temporary sensory ablations, etc.).

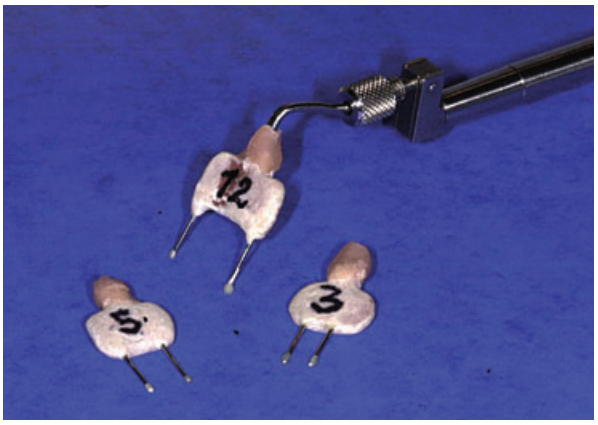

Fig. 6-12 Intraoral two-point discrimination testing device based on a constant pressure probe to compensate for the variability induced by hand-held equipment.

Influence of dental status on stereognostic ability

A change in the oral cavity by means of partial or complete loss of the dentition certainly creates certain changes to the oral sensory function. The roles of periodontal neural receptors and of the tongue seem essential in dentate subjects. After bilateral mandibular block, the stereognostic ability decreases by about 20% (Mason 1967). When comparing teeth with full dentures, a far better stereognostic ability is noted for natural teeth when freely manipulating the test pieces (Litvak *et al*. 1971). When removing the denture(s) in complete denture wearers, a considerable reduction in stereognostic ability is noted (Jacobs *et al*. 1998).

Lundqvist (1993) demonstrated that stereognostic ability improved after rehabilitation with oral implants. Jacobs *et al*. (1997) compared different prosthetic superstructures and noted no significantly different stereognostic ability with implant-supported fixed or removable prostheses, even when eliminating the involvement of tongue and lip receptors (Fig. 6-13).

Other compromising factors for oral stereognosis

Stutterers and speakers with articulation problems have an impaired stereognostic ability in comparison to normal speakers (Moser *et al*. 1967). They require more time to identify objects than normal speakers. Speakers with cerebral palsy also have an impaired stereognostic ability (Moser *et al*. 1967). Hemiplegic

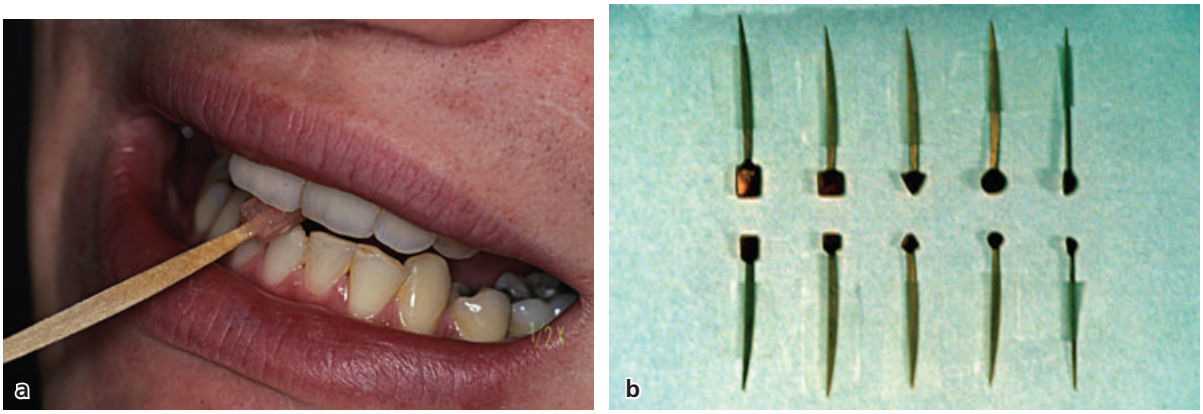

Fig. 6-13 (a) Stereognostic detection of objects in between teeth is better than for implant-supported prostheses. (b) The use of toothpicks to which the forms are attached and manipulated may avoid direct lip and tongue contact.